UNIVERSITY OF SOUTHAMPTON

FACULTY OF MEDICINE, HEALTH AND LIFE SCIENCES

SCHOOL OF MEDICINE

Characterisation of Myeloid-Derived Suppressor Cells in Chronic Inflammatory Diseases

by

Delphine LABROUSSE

Thesis for the degree of Doctor of Philosophy

September 2010

UNIVERSITY OF SOUTHAMPTON

ABSTRACT

FACULTY OF MEDICINE, HEALTH AND LIFE SCIENCES - SCHOOL OF MEDICINE

Doctor of Philosophy

CHARACTERISATION OF MYELOID-DERIVED SUPPRESSOR CELLS IN CHRONIC INFLAMMATORY DISEASES

by Delphine LABROUSSE

Myeloid Derived Suppressor Cells (MDSC) are cells of the myelomonocytic lineage consisting of myeloid progenitors and immature myeloid cells that have the ability to differentiate into mature myeloid cells such as granulocytes, dendritic cells and macrophages depending on the nature of the microenvironment. While MDSC play an important role in the replenishment of the pool of short-lived APC in lymphoid organs, they also have a crucial role in controlling the activation and function of self-reactive T cells. The failure of the mechanisms of peripheral tolerance to control the activation of self-reactive T cells is associated with the occurrence of autoimmune diseases (AID). The aim of this project is to characterize and investigate the role of MDSC in chronic inflammation. I have used the humanised TAZ10 transgenic mouse model that spontaneously develops autoimmune thyroiditis. T cells from TAZ10 mice (TAZ10-T) express a human TCR specific for a cryptic epitope generated upon endogenous processing of the main thyroid autoantigen (thyroid peroxidase; TPO) by thyroid epithelial cells (TEC). TAZ10-T also recognise the naturally occurring Altered Peptide Ligand of the cryptic TPO epitope generated upon exogenous processing of TPO by DC.

I showed that the sole activation and proliferation of self-reactive TAZ10-T at the onset of thyroiditis was sufficient to promote the differentiation of MDSC into immunostimulatory APC that contribute to the pathogenesis of the disease. Despite displaying strong inhibitory activity on T cells, MDSC could not prevent the activation of self-reactive TAZ10-T. As the inflammatory process amplifies, the recruitment of MDSC to peripheral tissues was exacerbated leading to their accumulation in the thyroid and DLN of TAZ10 mice. MDSC also exerted stronger suppressive functions on T cells. Despite this gain in inhibitory function, MDSC failed to control the strong activation of self-reactive TAZ10-T that mediate the destruction of the thyroid thus leading to the amplification of inflammation and the exacerbation of the disease.

The detrimental role of MDSC in cancer models once the tumour is established has been extensively studied. Considering the importance of the fate of MDSC at the onset of the disease in TAZ10 mice, I next investigated whether MDSC had any role in the generation of anti-tumour immune responses in the CT26 tumour model. As they naturally give rise to APC, MDSC were crucial in promoting the generation of an efficient anti-tumour response to CT26 observed after depletion of Tregs *in-vivo*.

TABLE OF CONTENTS

LIST OF FIGURES

Chapter 1

Chapter 3

Chapter 4

Chapter 5

Chapter 6

LIST OF TABLES

DECLARATION OF AUTHORSHIP

I, Delphine LABROUSSE, declare that this thesis and the work presented in it are my own and have been generated by me as a result of my own original research.

Characterisation of Myeloid-Derived Suppressor Cells in Chronic Inflammatory Diseases

I confirm that:

1. This work was done wholly or mainly while in candidature for a research degree at this University;

2. Where any part of this thesis has previously been submitted for a degree or any other qualification at this University or any other institution, this has been clearly stated;

3. Where I have consulted the published work of others, this is always clearly attributed;

4. Where I have quoted form the work of others, the source is always given. With the exception of such quotations, this thesis is entirely my work;

5. I have acknowledged all main sources of help;

6. Where the thesis is based on work done by myself jointly with others, I have made clear exactly what was done by others and what I have contributed myself;

7. None of this work has been published before submission

- *"Suppressive $Gr1^+CD11b^+$ Myeloid Derived Suppressor Cells (MDSC) fail to control the development of spontaneous autoimmunity"* - Cexus ON., **Labrousse D.**, Badami E., Tan LA., Londei M., Quaratino S and Elliott T. (First co-author - submission end 09/2010)

- *"Defect in $CD34^+$ cells in patients with rheumatoid arthritis and Sytemic Lupus Erythematosus"* - Cexus ON., **Labrousse D.**, Goulston L., Quaratino S., Edward C., and Elliott T. (submission end 10/2010)

Signed: .....

Date: .....

ACKNOWLEDGEMENTS

First and foremost, a massive MERCI to Dr Olivier Cexus for his continued support and invaluable contribution that have made the completion of this thesis possible. There is no word strong enough to express how grateful I am for the excellent guidance he gave me throughout these past 4 years and his patience when correcting my thesis. It has been a long process with some ups and many downs but his endless enthusiasm and exciting ideas always kept me motivated and gave me the strength to carry on when times were hard. I have thoroughly enjoyed working under his supervision and I am honoured to be his first ever PhD student, hopefully one of many to come.

I would also like to thank Professor Tim Elliott for his constant support and guidance throughout this project and for giving me the opportunity of undertaking this PhD.

Many thanks to Dr Edd James for his helpful advice and interest in my project, Dr Antony Antoniou and Alexander Potocnik for their precious input in the acquisition of the B6.eYFP mouse strain, Dr Sonya Martin and Dr Alexandra Mant for their hard work and valuable knowledge in confocal microscopy and histology and finally a big Thank You to Richard Reid and his staff (Lisa, Mel, Vicky, Myriam, Sam and Kerry) for their support and technical assistance with the mouse work.

Of the many friends and colleagues I have met during the course of my PhD, I must first acknowledge Nasia Kontouli for displaying the patience of Saints when asked the same question 100 times and for always providing a reassuring ear and being so supportive over the years. To past and present members of the lab, Lena, Karwan, Chris, Emma, Edd, Ian, Yifang, Ali, Sharon, Paul and Rahila: You made this experience enjoyable and brought some much needed laughter, even when “understably” making fun of my French accent and slight “wonkiness”!!! I owe you all...big time!

Last but by no means least, I would like to thank my parents who have always been really supportive of everything I aimed to achieve and a special thank you to my dear uncle Christian (Kiki!) who has given me tremendous comfort over the past four years...

I would also like to acknowledge Cancer Research UK for funding this project.

ABBREVIATIONS

AICD	Antigen-Induced Cell Death
AID	Autoimmune Diseases
AIRE	Autoimmune regulator
APC	Antigen Presenting Cells
APL	Altered peptide ligands
Arg-1	Arginase 1
AT	Adoptive Transfer
ATRA	All-*trans*-retinoic acid
β-gal	β-galactosidase
BM	Bone marrow
BM-DC	Bone Marrow Derived Dendritic cells
cTEC	cortical thymic epithelial cells
CCIA	Chronic Collagen Induced Arthritis
CFA	Complete Freund's Adjuvant
CFSE	Carboxyfluorescein Succinimidyl Ester
CID	Chronic Inflammatory Diseases
CD	Cluster of Differentiation
CLIP	Class-II invariant chain peptide
CPRG	Chlorophenolred-β-D-Galactoside
CTL	Cytotoxic T lymphocytes
CTLA-4	Cytotoxic T lymphocyte antigen 4
DC	Dendritic Cells
DLN	Draining Lymph Nodes
DN	Double negative
DP	Double positive
EAE	Experimental Autoimmune Encephalitis
EAU	Experimental Autoimmune Uveoretinitis
ECM	Extracellular Matrix
ER	Endoplasmic Reticulum
ERAP	Endoplasmic Reticulum Aminopeptidase
FACS	Fluorescence Activated Cell Sorting

FCS	Foetal Calf Serum
FITC	Fluorescein Isothiocyanate
FSC	Forward Scatter
GITR	Glucocorticoid-induced TNF-receptor
GM-CSF	Granulocyte/macrophage colony stimulating factor
HLA	Human Leucocyte Antigen
Hsp	Heat shock proteins
iDC	Immature dendritic cells
IDO	Indoleamine 2,3- dioxygenase
IFNγ	Interferon gamma
iNOS	Inducible Nitric Oxide Synthase
LFA.1	Lymphocyte Function-associated Antigen 1
LN	Lymph Nodes
L-NMMA	NG-Monomethyl-L-Arginine
LPS	Lipopolysaccharide
mAb	Monoclonal antibody
mDC	Mature dendritic cells
MDSC	Myeloid Derived Suppressor Cells
MFI	Mean Fluorescence Intensity
MHC	Major Histocompatibility Complex
MHC-I	MHC class I molecules
MHC-II	MHC class II molecules
MTEC	Medullary thymic epithelial cells
NDLN	Non-Draining Lymph Nodes
NF-κB	Nuclear factor κB
NK	Natural Killer cells
NKT	Natural Killer T cells
NO	Nitric Oxide
NOD	Nonobese diabetic mouse
NOHA	NG-Hydroxy-L-arginine
OVA	Ovalbumin
PAMP	Pathogen Associated Molecular Patterns
PBS	Phosphate Buffered Saline

PE	Phycoerythrin
PerCp	Peridin Chlorophyll Protein
PFA	Paraformaldehyde
PGE2	Prostaglandin E2
PI-NOD	Proinsulin nonobese diabetic mouse
PLC	Peptide Loading Complex
PRR	Pattern recognition receptors
Rag	Recombinant activating gene
RNOS	Reactive Nitrogen Oxide Species
ROS	Reactive oxygen species
RT	Room Temperature
RT-PCR	Reverse transcription-polymerase chain reaction
SCID	Severe Combined Immunodeficiencies
SCF	Stem Cell Factor
SN	Spleen
SSC	Side Scatter
STAT	Signal Transducer and Activator of Transcription
TAA	Tumour-Associated Antigens
TAM	Tumour-Associated Macrophages
TAP	Transporter associated with antigen processing
TAZ10-T	T cells from TAZ10 mice
TAZ10-T_N	Naive T cells from TAZ10 mice
TCR	T cell Receptor
TEC	Thyroid Epithelial cells
T_{EFF}	Effector T cells
TLR	Toll-like Receptor
T_N	Naive T cells
TNFα	Tumour Necrosis Factor alpha
TGFβ	Transforming Growth Factor beta
TPO	Thyroid Peroxidase
Tregs	Regulatory T cells
TSA	Tissue-restricted self antigens
VLA.4	Very Late Antigen 4

VEGF	Vascular Endothelial Growth Factor
WT	Wild-Type
WT-T_N	Naive T cells from WT mice
eYFP	Enhanced Yellow fluorescent protein

1 – Introduction

1.1– The immune response

The immune system is designed to protect an individual from a variety of pathogens, such as bacteria, parasites or viruses but also from its own altered cells. Several systems designed to keep these insults at bay have been shaped throughout evolution when pathogens have developed efficient methods to escape these immune mechanisms (Finlay et al. 2006). Two components can be distinguished characterized by their specificity to the infectious agents. The innate immune response present in nearly all forms of life provides an immediate first line of defence against infection in a non-specific manner. By contrast, the immune system has evolved in vertebrates to develop an adaptive immune system composed of highly specialised cells which are pathogen-specific and lead to the development of an immunological memory.

1.1.1 – The innate immune response

First lines of defence, epithelia such as the epithelium of the skin, the gut or the airway represent physical barriers that prevent pathogens from invading adjacent tissues. If a pathogen breaches these barriers, it could cause infection/inflammation and induce the development of disease. The innate immune system must therefore react quickly in order to provide an immediate but non-specific response that will lead to the complete or partial clearance of the pathogens while initiating the activation of the adaptive immune system. This process includes the recruitment of immune cells, such as macrophages, dendritic cells, neutrophils or natural killer cells, to the site of infection. These cells express Pattern Recognition Receptors (PRR) which recognise Pathogens Associated Molecular Patterns (PAMP) present in foreign pathogens but not expressed by the host (Janeway et al. 2002). This recognition triggers an inflammatory response associated with the production of various soluble mediators such as histamine, cytokines (e.g. chemokines, interleukins) and eicosanoids (e.g. prostaglandins) that promote the recruitment of cells of the immune system to the site of inflammation such as phagocytic cells that engulf pathogens or infected cells through phagocytosis.

Impaired innate immunity has been linked with chronic inflammatory disorders. Indeed a reduced accumulation of neutrophils and an impaired production of IL-8 initiate a cascade of events resulting in the development of Crohn's disease affecting the gastrointestinal tract (Marks et al. 2006).

Although highly effective, if first physical barriers are broken, the innate immune system will be activated allowing for the efficient activation and coordination of the acquired or adaptive immune system. At this point cells of the innate immune system will shape the adaptive immune response according to the nature of the soluble factors present in the microenvironment to mount an immune response adapted to the nature of the infection/inflammation.

1.1.2 – The adaptive immune response

The importance of the acquired or adaptive immune system is well established and has been extensively demonstrated. The adaptive immune system amplifies and arms the innate immune system to provide the best response against pathogens while also feeding back on itself through cytokines and other mediators. The activation of the two arms of the immune system (innate and adaptive immune systems) and the subsequent amplification of the response resulting from their cross-talk lead to the efficient and specific clearance of the pathogens over time (Zhao et al. 2009). An immunological memory will also be generated so that a second encounter with the same antigen prompts a rapid and robust response (Lanier et al. 2009).

The crucial role played by the adaptive immune response in clearing infections is further highlighted in individuals with primary immunodeficiency that are more susceptible to viral and bacterial infections (Fischer 2004). Gene therapy aimed at restoring the immune system has been highly successful in patients with X-linked Severe-Combined Immunodeficiency (SCID-X1) disease and has opened new horizons for the treatment of primary immunodeficiencies (Gaspar et al. 2005; Cavazzana-calvo et al. 2000).

A fundamental feature of the adaptive immune system is its ability to recognise non-self antigens from pathogens while avoiding the recognition of self-antigens that could potentially lead to autoimmune diseases (AID) or "horror autotoxicus" (Paul Elrich Theory exposed in Steinman et al. 2002). It is therefore crucial for a clear distinction to be made between "self"

and “non-self”. Jerne proposed the “natural selection theory” where he suggested the existence of a repertoire of antibodies from which the antigens select. Antigen-antibody complexes are taken up into the cells where the antibody replicated (Jerne et al. 1955). In contrast, Burnet proposed the “clonal selection theory” where the immune system only mounts an immune response against “non-self” while avoiding any attack against “self”. This work was based on experiments on skin grafts: an individual will reject a graft from another donor while his own graft will be accepted (Burnet 1961; Burnet 1976). However, this theory failed to explain the emergence of AID. To address this issue, Matzinger proposed the “Danger model” where the immune system triggers an immune response when confronted to “Danger signals”, regardless of self/non-self discrimination (Matzinger 2001; Matzinger 2002). An immune response could therefore be mounted against self or non-self as long as danger signals are present.

The nature of the “Danger” modulates dendritic cell differentiation to polarise different T cell responses triggering the adaptive immune response (Germain et al. 2004).

1.2 – Dendritic cells at the interface between innate and adaptive immunity

Dendritic cells (DC) play a major role in the generation of immune responses by bridging the innate and the adaptive immune systems. DC sense signals from pathogens at the site of inflammation/infection to subsequently promote both B and T cell responses thus leading to the initiation of specific adaptive immune responses. While critical for the induction of primary immune responses, DC can also tolerize T cells to self-antigens to induce immunological peripheral tolerance and prevent the occurrence of AID (Banchereau et al. 1998).

At the resting state, DC are immature and patrol the tissues until activated by “Danger signals” which can result from the recognition of pathogens by cells of the innate immune system. Immature DC display a highly phagocytic activity enabling the capture of antigens shed in the microenvironment. Maturing and migrating to secondary lymphoid organs, mature DC (mDC) present immunogenic epitopes to lymphocytes promoting their activation and differentiation into effector cells (Schuurhuis et al. 2006).

The "Danger signals" from pathogens sensed by the cells of the innate immune system, are responsible for the induction of DC maturation and the subsequent induction of an appropriate adaptive immune response (Banchereau et al. 2000; Rossi et al. 2005).

1.2.1 – Maturation of dendritic cells

In an inflammatory context, professional antigen presenting cells (APC) such as DC sample the microenvironment for the presence of antigens (Figure 1.1). These antigens are then processed following the endogenous or exogenous processing pathways and the resulting epitopes are presented in the context of Major Histocompatibility Molecule Complex (MHC) Class I or II molecules. These antigen/MHC complexes are then recognised by $CD8^+$ and $CD4^+$ T cells: this is known as the "first activation signal" (Banchereau et al. 2000). The ability of DC to provide costimulatory signals to T cells via costimulatory molecules (such as the proteins of the B7 family on DC and CD28 on T cells) is essential for the efficient activation of T cells (Greenfield et al. 1998). This costimulatory signal (or "second activation signal") between DC and T cells leads to the release of DC- derived cytokines and the engagement of other costimulatory molecules newly expressed by T cells and mDC. This provides the "third activation signal" necessary to fully activate T cells (Anderton et al. 2002).

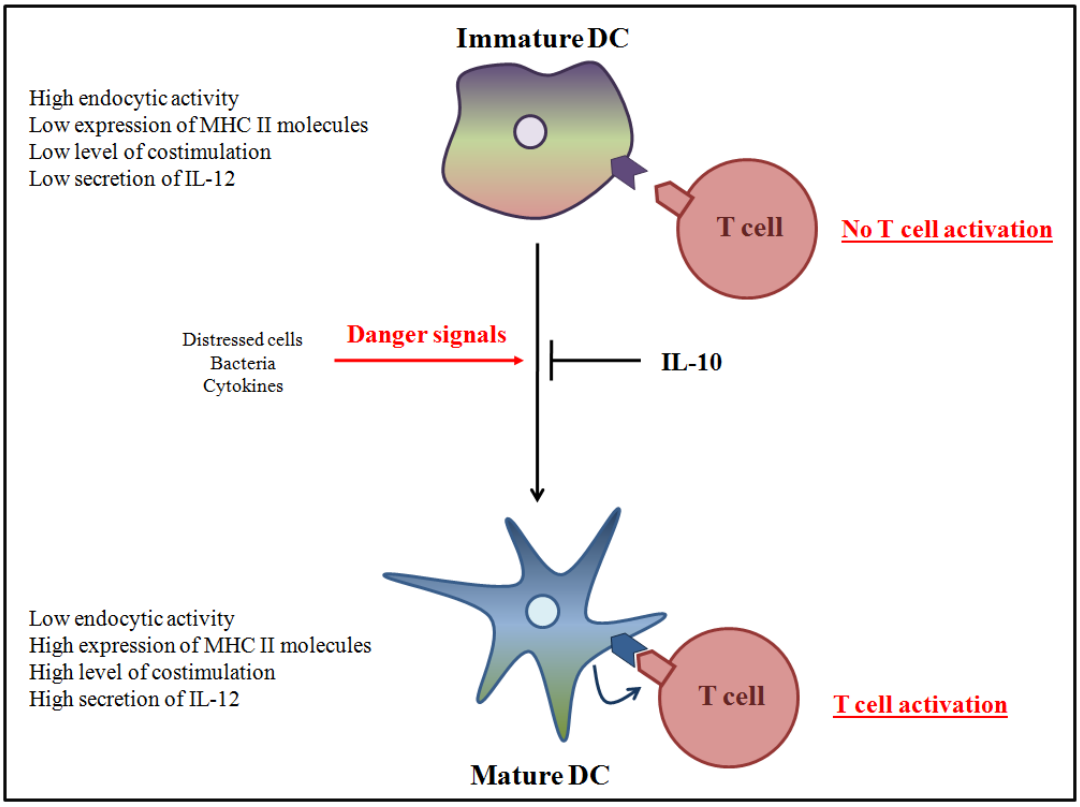

Figure 1.1: Activation of dendritic cells by danger signals
"Dangers signals" released by pathogens or distressed cells undergoing necrosis promote the maturation of immature dendritic cells (iDC). While iDC possess high endocytic capacity enabling them to capture antigens present in the microenvironment, terminally differentiated mature DC express high levels of costimulation and MHC-II molecules that allow antigenic peptides to be presented to T cells for priming. IL-10 blocks the maturation of DC.

1.2.1.1 – Nature of danger signals

Present in different forms, "Danger signals" originate from pathogens or the host upon stress. Within these signals specific structures/motifs also called pathogen-associated molecular patterns (PAMPs) are recognised by a limited number of germline-encoded pattern recognition receptors (PRRs). The recognition of a specific PAMP by given PRR activates specific intracellular signalling pathways leading to the induction of pro-inflammatory cytokines, chemokines and the maturation of DC that promotes the activation of a specific adaptive immune responses (Kawai et al. 2005). The diversity of "Danger signals" and the wide range of specific receptors on DC therefore allow the immune response to be finely tuned.

Among the PRRs, the Toll-like receptor (TLR) family is the most studied (Beutler et al. 2004, Kapsenberg et al. 2003). TLRs are type 1 integral membrane glycoproteins that

possess amino-terminal leucine-rich repeats responsible for the recognition of PAMPs and a carboxy-terminal Toll-interleukin-1 receptor (TIR) domain required for the initiation of intracellular signalling (Takeda et al. 2003). At present, thirteen mammalian TLRs have been identified and are divided into two subgroups depending on their cellular localization and the nature of the ligands. The first group composed of TLR1, TLR2, TLR4, TLR5, TLR6 and TLR9 expressed at the cell surface mainly recognises components of the microbial membrane such as lipids and lipoproteins. The second group is constituted by TLR3, TLR7, TLR8 and TLR9 that are expressed exclusively in endolysosomal compartments (Table 1.1). Their ligands are mainly microbial and viral nucleic acids and require their internalization for their recognition (Kawai et al. 2010, Akira et al. 2006). While TLR4 binds the bacterial product lipopolysaccharide (LPS), TLR2 binds bacterial lipoproteins and TLR5 recognises flagellin. TLR3 binds double stranded RNA derived from viruses as they replicate in the cell (Guermonprez et al. 2002, Akira et al. 2006).

The recognition of PAMPs by TLRs triggers a signalling cascade that begins with the translocation to the cell membrane of the myeloid differentiation factor 88 (MyD88). Subsequent activation of the nuclear factor κB transcription factor (NF-κB) promotes the expression of inflammatory genes. Alternative signalling pathways may occur through the induction of MyD88-independent signalling cascades leading to the expression of interferon-inducible genes (Netea et al. 2002, Akira et al. 2006). While ligands for TLR4, TLR5 and TLR9 favours the synthesis of Th1-associated cytokines such as IL-12p70, TLR2 ligands induce the release of IL-10 thus favouring Th2-biased immune responses (Dillon et al. 2004, Kawai et al. 2010). This demonstrates that APC can finely tune and shape the immune response after engagement of a specific TLR.

Receptors	Ligands
TLR1 / TLR2	Lipoproteins: e.g. OspA Triacylated Lipopeptides
TLR2	Bacterial lipoproteins Glycosylphosphatidyl-inositol Glycolipids Porins
TLR3	Double-stranded RNA Poly I:C mRNA/tRNA
TLR4	Lipopolysaccharides Monophosphoryl lipid A Flavolipin Glycoinositolphospholipids
TLR5	Flagellin
TLR7	Single-stranded RNA Polyuridylic acid
TLR8	Single-stranded RNA Polyuridylic acid
TLR9	Unmethylated CpG DNA

Table 1.1: Members of the Toll-like receptor (TLR) family bind to a wide range of ligands
Description of the ligands recognized by the different members of the toll-like receptor family (Adapted from Akira et al. 2006).

To avoid recognition by the immune system, certain pathogens have acquired the capacity to modulate the structure of LPS by promoting a different degree of acetylation of the lipid A recognised by TLR molecules. Lipid A composing LPS from *Pseudomonas aeruginosa* is hexa-acylated in cystic fibrosis and penta-acylated in chronic lung

bronchiectasis and conventional bacterial culture (Ernst et al. 1999). Interestingly, hexa-acylated LPS binding TLR4 promotes a robust production of pro-inflammatory factors which is not observed with penta-acylated LPS (Hajjar et al. 2004).

In the "Dander model" proposed by Matzinger (Matzinger 2001; Matzinger 2002), the nature of the Danger is prevalent to the self/non-self nature of the antigenic peptide. Although components of foreign infectious pathogens are able to trigger an immune response, cells or tissues from the host can also release "Danger signals" in a situation of stress. By contrast to apoptosis, necrosis leads to the release of various endogenous molecules that are sensed as "Danger signals" by the immune system (Matzinger 2002, Matzinger 2007) (Figure 1.1). Most of these "Danger signals" resulting from the death and injury of normal or tumour cells, include degradation products of the extracellular matrix (ECM), heat-shock proteins (e.g. heat-shock protein 70, HSP70) or high-mobility group box 1 (HMGB1) proteins (Kawai et al. 2010). HMGB1 is a nuclear non-histone protein that has been shown to be released by dying tumour cells following chemotherapy. By binding to TLR4, HMGB1 leads to the transduction of signals through MyD88 and the generation of an immune response (Apetoh et al. 2007, Yang et al. 2009). Endogenous molecules can therefore activate innate immune response through TLRs even in the absence of pathogens.

1.2.1.2 – Activation of the adoptive immune response by dendritic cells

The maturation of APC induced by "Danger signals" results in fundamental morphological and functional changes. While a loss of endocytic activity and a reduced antigen-processing capacity can be observed upon maturation, the expression of costimulatory (CD80, CD86, CD40) and MHC-II molecules is increased. As they mature, DC migrate from peripheral to lymphoid tissues where they present antigenic peptides in the context of MHC-I and MHC-II molecules (Schuurhuis et al. 2006) (Figure 1.2).

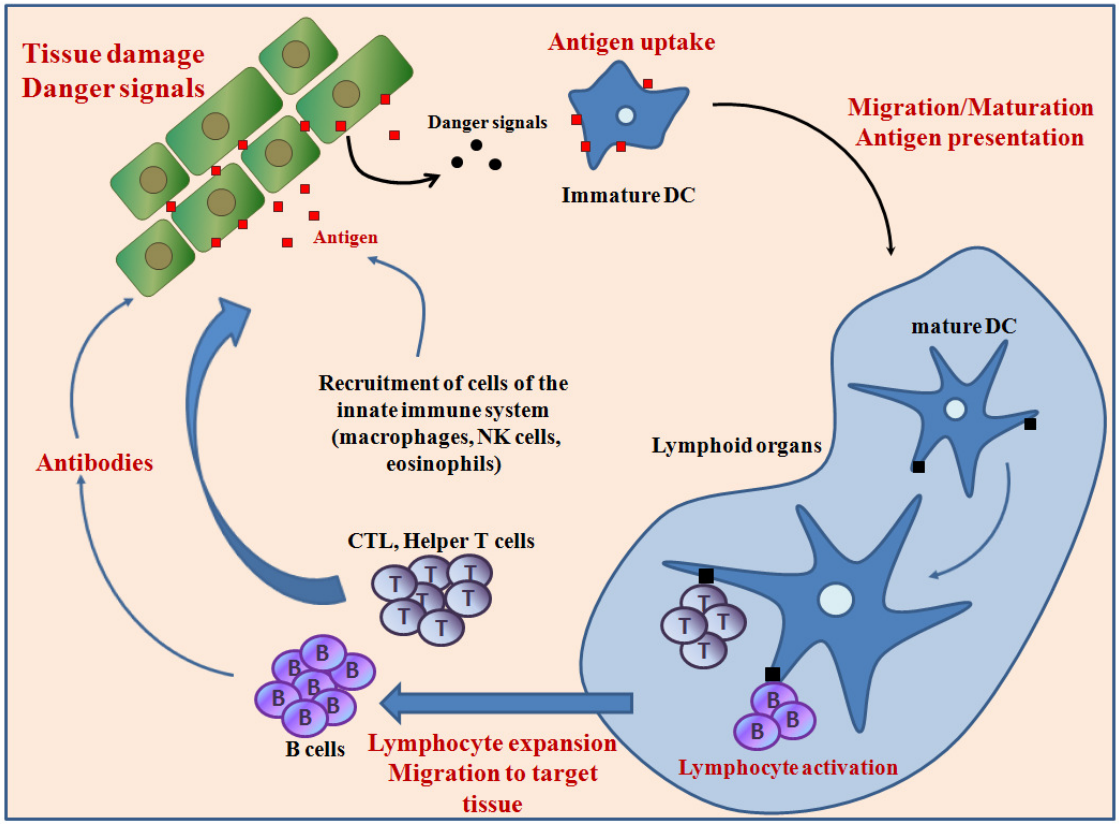

Figure 1.2: Dendritic cells play a pivotal role in the cooperation between the innate and the adaptive immune systems

Following activation by "Danger signals", immature DC uptake antigens present in the microenvironment and migrate to lymphoid organs while undergoing their complete maturation. In lymphoid organs, mDC present antigens to B and T cells. Activated lymphocytes are recruited to the site of inflammation where they interact with cells of the innate immune system to mount an effective immune response. NK: Natural Killer cells; DC: Dendritic cells; CTL: Cytotoxic T cells; T: T lymphocytes; B: B cells (Adapted from Banchereau et al. 2000).

The complete activation of T cells by mDC requires several signals (Figure 1.3). Activation signal 1 is represented by the recognition of MHC:peptide complexes on mDC by the TCR on T cells. The sole activation of T cells through this signal leads to T cell anergy unless full T cell activation is provided by "activation signals 2 and 3" (Mueller et al. 1995). Indeed, T cell activation can only be efficient if sustained by the engagement of costimulatory molecules expressed on DC and their ligands on T cells (proteins of the B7 family on mDC interacting with CD28 on T cells). This second signal, or "costimulatory signal", is very important to overcome tolerance (Kapsenberg et al. 2003). Recent studies have also highlighted the importance of a "third activation signal" resulting from the communication between mDC and T cells. Upon encounter with T cells, mDC receive additional maturation signals through for example CD40-CD40L (Banchereau et al. 2000) leading to the upregulation of costimulatory molecules, the secretion of IL-12 and the release

of chemokines (IL-8, MIPα, etc.) and cytokines (IL-6, IL-10, etc.). This "third activation signal" is crucial to fully activate T cells and finely shape the adaptive immune response (Schmidt et al. 2002; Curtsinger et al. 2003).

The nature of the interactions between DC and T cells plays a major role in the activation of T cells. While stable and prolonged DC-T contacts result in an efficient T cell priming and therefore immunity, brief contacts have been associated with the induction of T cell tolerance (Hugues et al. 2004).

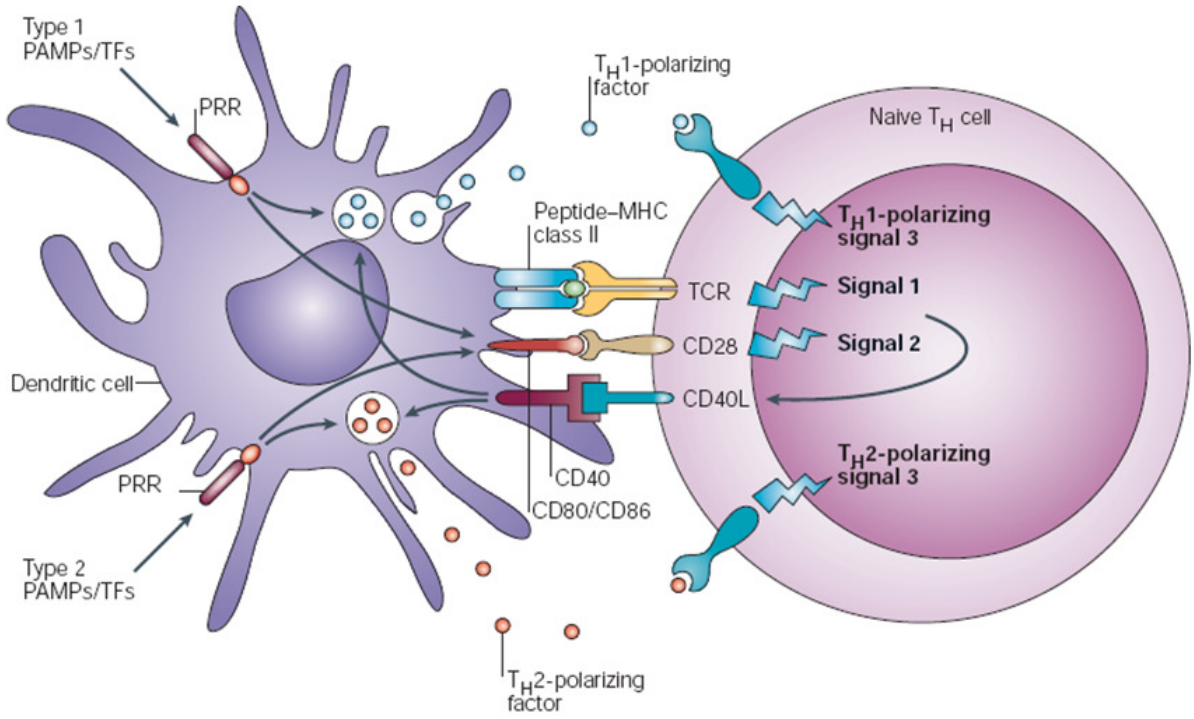

Figure 1.3: T cell simulation requires three signals provided by dendritic cells
Signal 1 is mediated when the T cell receptor (TCR) recognises MHC-peptide complexes. Signal 2 corresponds to costimulatory signals between mDC and T cells such as the interaction between CD80 and CD86 on DC and CD28 on T cells. Signal 3 is mediated through various cytokines and their nature depend on the activation of particular pattern recognition receptors (PPRs) and dictate the fate of T cells (Adapted from Kapsenberg et al. 2003)

Not all mature DC are however able to generate an efficient adaptive immune response characterised by the proliferation, differentiation and acquisition by T cells of effector functions. Indeed, while DC can be activated as a result of the direct recognition of PAMP by PRR, they can also sense inflammation and infections indirectly through inflammation-associated factors such as TNFα, IL-6 or $TGF_β$, released by cells/tissues following an

infection. DC activated with these bystander inflammatory molecules are not fully licensed to promote the complete activation of $CD4^+$ T cells. While these inflammatory signals promote the functional maturation of DC (upregulation of MHC-II and costimulatory molecules), $CD4^+$ T cells undergo clonal expansion but are defective in their effector functions. In contrast, iDC directly stimulated by pathogens through TLRs induce the differentiation and the acquisition of effector functions by $CD4^+$ T cells (Sporri and Reis e Sousa, 2005).

Several soluble factors such as IL-10 have been shown to impair the ability of mDC to activate T cells. IL-10 inhibits the maturation of DC by preventing the up-regulation of activation markers such as MHC-II and costimulatory molecules. These DC remaining in an immature state promote T cell anergy or the generation of Tregs (Steinbrink et al. 1997). A recent study has also shown that IL-10 does not prevent maturation but controls the kinetics and the quality of DC activation. DC activated in the presence of IL-10 show functional and phenotypic maturation, but this activation is transient compared with DC matured with LPS; they secrete little IL-12 and fail to induce T cell proliferation (Perona-wright et al. 2007).

Once activated by mDC in peripheral lymphoid organs, B and T cells migrate to the site of inflammation where they coordinate with the cells of the innate immune system (natural killer cells, macrophages, eosinophils...) to clear the source of danger. As the source of Danger is disappearing, most of the T cells die by apoptosis while a few undergo further differentiation and become memory T cells. These memory cells will trigger an immediate and robust immune response should they encounter again the cognate antigen (Banchereau et al. 2000).

1.2.2 – Antigen processing and presentation

Dendritic cells are efficient stimulators of B and T lymphocytes. While B cells recognise the naive antigen directly through their B cell receptors, T cells recognise the cognate peptide presented by DC in the context of MHC-I and MHC-II molecules. There are three main mechanisms for the processing and presentation of antigens: the endogenous pathway (processing and presentation of endogenous antigens onto MHC-I molecules), the exogenous pathway (processing and presentation of exogenous antigens onto MHC-II

molecules) and the cross-presentation of endogenous and exogenous antigens onto MHC-II and MHC-I molecules respectively.

1.2.2.1 – Processing of endogenous antigens and presentation onto MHC class I molecules

The presentation by all nucleated cells of their pool of proteins or foreign proteins (from viral and bacterial origin) in the context of MHC-I molecules is important to allow the immunosurveillance mediated by $CD8^+$ T cells (Figure 1.4).

Antigens are ubiquitinated by 3 different enzymes (U1, U2 and U3 ubiquitin ligases) in the cytosol before being directed to the proteasome, an ATP-dependent multisubunit proteolytic complex. The proteasome cleaves ubiquitinated antigens into 8 to 10 amino acid long peptides. Once generated, these peptides are translocated into the ER by an ATP-dependent transporter, the transporter associated with antigen processing (TAP). Once in the ER, they can be further trimmed by ER-residing proteases such as the Endoplasmic Reticulum Aminopeptidase (ERAP) (Cresswell 2005). MHC-I molecules are composed of a transmembrane heavy chain non-covalently associated with the β2-microglobulin (β2m) subunit. The heavy chain has an extracellular domain divided into 3 domains (α1, α2 and α3), 2 of which forming the peptide binding groove (α1 and α2 subunits). Once synthesized, this heavy chain associates with chaperones such as calnexin and ERp57 that facilitate its binding with β2m. At this stage, the calnexin-ERp57 complex is replaced by calreticulin-ERp57 until a peptide is loaded onto MHC-I molecule (Saveanu et al. 2002; Elliott et al.2005). The association of TAP proteins (Transporter associated with Antigen Processing composed of two subunits: TAP1 and TAP2), the different chaperones and the empty MHC-I molecule forms the Peptide Loading Complex (PLC) that allows the binding of peptides with the correct affinity onto MHC-I molecules. Stabilised MHC:peptide complexes are then freed from the different protein chaperones and migrate via the Golgi to the plasma membrane where they can prime MHC-I restricted $CD8^+$ T cells (Banchereau 2000).

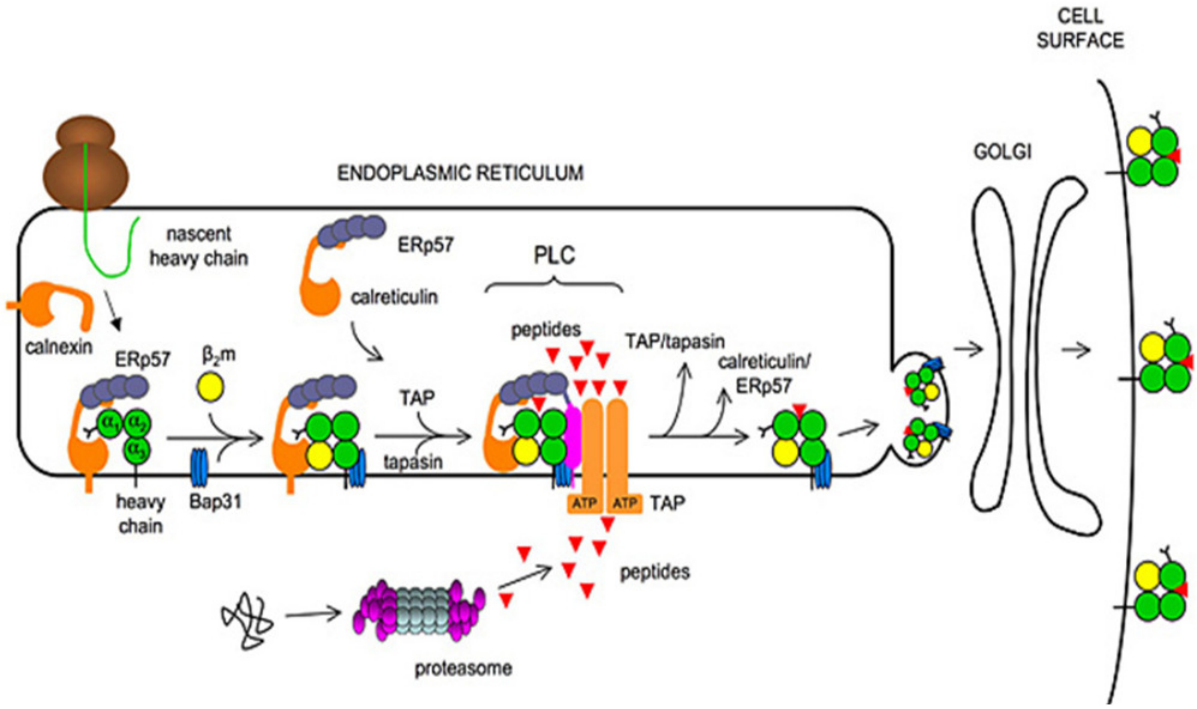

Figure 1.4: Processing of endogenous proteins and presentation in the context of MHC class I molecules
Nascent heavy α chain bound to the β2-microglobulin (β2-m) subunit associates with chaperones (ERp57, calreticulin, TAP) to form the peptide loading complex (PLC). Misfolded proteins or proteins at the end of their life are ubiquitinated and degraded by the proteasome into peptides. These peptides are translocated in the endoplasmic reticulum (ER) via TAP and loaded onto MHC-I molecules. Stabilised MHC:peptide complexes migrate to the cell surface to be recognised by $CD8^+$ T cells.

After their synthesis, nascent proteins associate with chaperones such as Hsp70 and undergo complex folding to acquire the tridimensional structure required to perform their function. The binding of chaperones prevent the premature misfolding and aggregation of nascent proteins (Hartl et al. 2002). This system is not efficient as cells favour high speed protein synthesis and therefore increase the probability of producing large amounts of misfolded proteins. These defective ribosomal products (DRiPs) are ubiquitinated and rapidly degraded by the proteasome to avoid their accumulation in the ER (Yewdell et al. 2006). The accumulation of misfolded proteins within the ER is indeed associated with cellular stress such as the unfolded protein response (UPR) that can be potentially toxic to the cells. UPR is associated with numerous neurological pathologies such as Alzheimer's disease (Kim et al. 2008).

It has been estimated that for one protein, about 30% are DRiPs that are targeted to the ubiquitin-proteasome pathway for degradation. These DRiPs have important immunological functions as they represent the major source of peptides binding MHC-I molecules. This mechanism where peptides are quickly generated allows the rapid presentation of peptides

from pathogens and mainly viruses for the immediate recognition by patrolling $CD8^+$ T cells that mediate the clearance of the infected cells (Schubert et al. 2000).

1.2.2.2 – Processing of exogenous antigens and presentation onto MHC class II molecules

Exogenous antigens are taken up by endocytosis through the endocytic pathway to be directed to the lysosomes where they are proteolytically degraded into 12 to 15 amino acids long fragments by acid-dependent proteases such as cathepsins (Figure 1.5).

Although all nucleated cells express MHC-I molecules, professional APC such as dendritic cells, macrophages and B cells are capable of expressing MHC-II molecules. This is not only restricted to professional APC as epithelial cells have been shown to upregulate the expression of MHC-II molecules when challenged with pro-inflammatory cytokines such as interferon γ (IFNγ). These non-professionals APC can then present self-antigens to self-reactive T cells that have not been eliminated by mechanisms of central tolerance in the thymus (Chan et al. 2006, Quaratino et al. 2000). Central tolerance will be discussed Paragraph 1.4.1.

The α and β chains forming MHC-II molecules are synthesized and associate in the ER. In the ER, newly formed MHC-II molecules associate with invariant chain (Ii) before the αβIi complex associated with the MHC-II like molecule HLA-DM (H-2M in mice) is transported to the lysosomes and MHC-II rich compartments (MIIC). The Ii chain is gradually degraded by cathepsin-S leaving only a small fragment. The class II-associated invariant-chain peptide (CLIP) remains therefore in the peptide-binding groove of MHC-II molecules formed by the α1 and β1 subunits. HLA-DM then catalyses the exchange of CLIP for a peptide with high affinity. Stable peptide:MHC-II complexes are transported to the cell surface to be recognized by $CD4^+$ T cells (Watts. 2004; Banchereau. 1998)

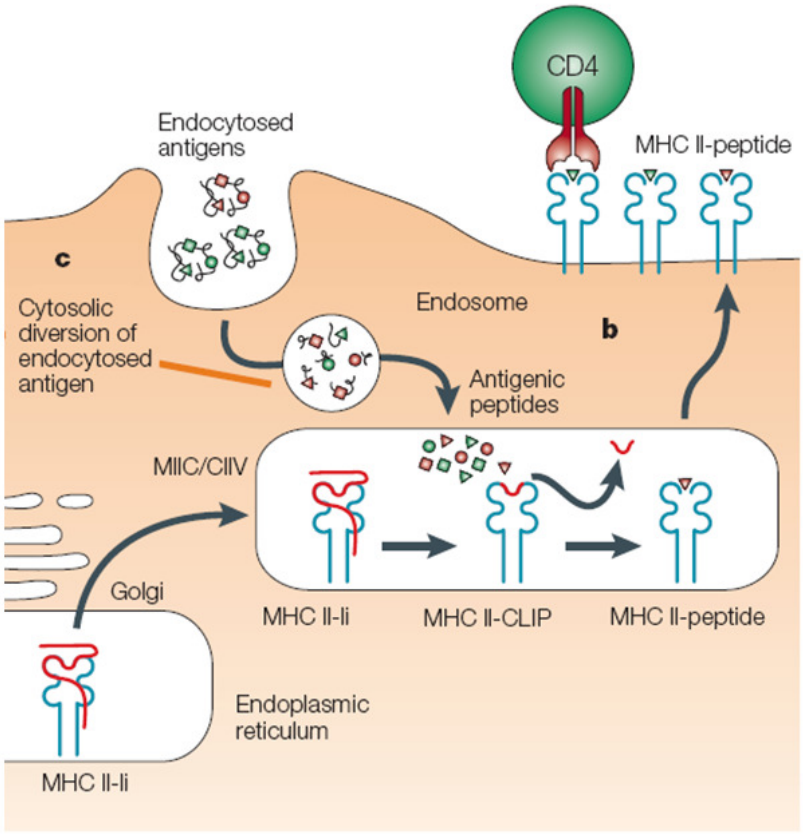

Figure 1.5: Processing of exogenous proteins and presentation in the context of MHC class II molecules
Exogenous antigens are taken up by the cells through endocytosis and are degraded in the lysosomes by acid-dependent proteases. MHC-II molecules are synthesized in the endoplasmic reticulum (ER) and are dimeric consisting of an α and β chains. Associated with the invariant chain Ii, they are transported to MHC-II rich compartments (MIIC). This invariant chain is degraded and the class II-associated invariant-chain peptide CLIP remains in the peptide-binding groove. Under the influence of HLA-DM, the CLIP peptide is exchanged for higher affinity peptides. Peptide loaded MHC-II molecules are then transported at the cell surface for the priming of $CD4^+$ T cells (Adapted from Heath et al. 2001).

By binding MHC-II molecules, Ii and therefore CLIP have the ability to regulate and optimize the loading of high-affinity peptides in the peptide-binding groove of MHC-II molecules. Different MHC-II alleles exhibit distinct affinities for CLIP. Alleles with high affinity for CLIP ($I\text{-}A^b$ in mice) rely on H2-M to exchange CLIP with MHC-II restricted peptides (Gautam et al. 1995). In contrast, alleles with a low affinity for CLIP ($I\text{-}A^k$, $I\text{-}A^d$ and $I\text{-}E^k$ in mice) are less dependent on H-2M for the loading of MHC-II peptides. It has been suggested that a decreased affinity for CLIP facilitates the loading of peptides onto MHC-II molecules, therefore escaping the editing process mediated by H-2M. This leads to the generation of a larger repertoire of MHC-II restricted peptides presented to $CD4^+$ T cells thus increasing the probability to develop AID (Honey et al. 2004, Lovitch et al. 2003).

In addition to its impact on the peptide repertoire presented in the context of MHC-II molecules, Ii plays an important role in regulating the transport of newly synthesized MHC-II molecules from the ER to the lysosomes/MIIC compartments. Phosphorylation of Ii has indeed a direct effect on the trafficking of MHC-II as an impaired transport is observed when the phosphorylation of Ii is inhibited (Anderson et al. 1999). Ii also plays a role in the regulation of the motility of mDCs. While mDC alternate between episodes of high and low motility, Ii deficient DC move in a faster and uniform manner (Faure-Andre et al. 2008). The pleiotropic role of Ii in the presentation of peptides in the context of MHC-II molecules, the trafficking of newly synthesized MHC-II molecules and the motility of DC suggest that Ii enhances the ability of mDC to uptake, process and present antigens for the generation of an efficient $CD4^+$ T cell response.

1.2.2.3 – Cross presentation of endogenous antigens onto MHC class II molecules and of exogenous antigens onto MHC class I molecules

A characteristic of some professional APC is their ability to cross-present exogenous antigens onto MHC-I molecules (Bevan et al. 1976, Kurts et al. 1996). If endocytosed antigens can be directly loaded onto recycling MHC-I molecules, various routes of cross-presentation of exogenous antigens onto MHC-I molecules have been characterised:

• Endocytosed antigens can be degraded in the lysosomes in a TAP-independent manner and then loaded onto recycling MHC-I molecules present in these compartments (Guermonprez et al. 2002).

• The phagosome-to-cytosol pathway is proteasome and TAP-dependent. Antigens internalized into phagosomes are hydrolysed by the proteasome and the resulting peptides enter the ER via TAP before being loaded onto MHC-I molecules (Guermonprez et al. 2002; Kovacsovics-Bankowski et al. 1995).

• By fusing with the ER, phagosomes acquire MHC-I, TAP and other ER proteins. Exogenous antigens released from ER-phagosomes to the cytosol are degraded by proteasomes before being re-imported into the ER-phagosome by TAP where they bind MHC-I molecules (Guermonprez et al. 2003; Shen et al. 2006). This last pathway remains

however controversial as the concept of fusion of the ER with the phagosomes has been challenged by various groups (Touret et al. 2005).

Although endogenous proteins are presented in the context of MHC-I molecules, cross-presentation onto MHC-II molecules can naturally occur. Cytosolic proteins degraded in the cytosol can be translocated into the lysosome for loading onto MHC-II molecules (Dani et al. 2004). The cross-presentation of endogenous antigens onto MHC-II molecules has an important role in immunosurveillance by allowing the rapid presentation of antigens from viruses and pathogens that have infected the cells. This allows for the efficient recognition by $CD4^+$ T cells and rapid clearance of the infected cells (Wan et al. 2005; Strawbridge et al. 2007).

1.3 – The polarization of the T cell response is mediated by dendritic cells

Professional APC such as DC are critical for the induction of an efficient adaptive immune response. Following antigen recognition and upon appropriate costimulation, naive T cells differentiate into specific effector cells according to the cytokine environment.

1.3.1 – T cell priming: recognition of MHC:peptide complexes by TCR

T cells recognize the cognate peptide presented in the context of MHC molecules through the TCR. Although important in promoting T cell tolerance or stimulation, this interaction characterised as activation signal 1 also dictates the fate of thymocytes. Indeed, their selection in the thymus based on their ability to recognize self-MHC molecules but not self-antigens ensures the elimination of self-reactive T cells thus preventing the development of AID (Mechanisms of thymic selection will be discussed paragraph 1.4).

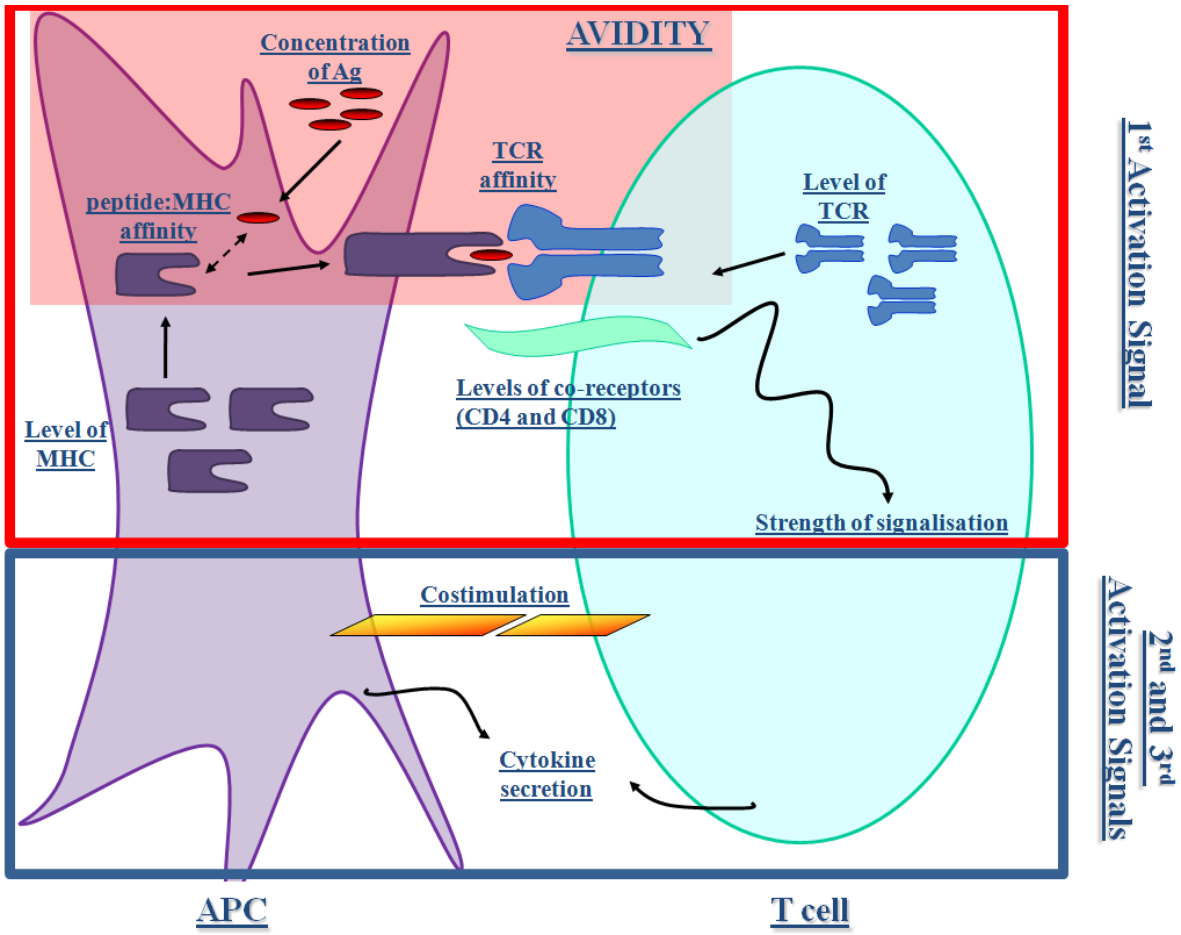

Figure 1.6: Factors dictating DC-T cell interactions and T cell response
The interaction between a T cell receptor (TCR) and a peptide bound to an MHC molecule presented by antigen presenting cells (APC) depends on numerous factors. The avidity of the complex MHC:peptide/TCR is defined by the affinity between a peptide and the MHC molecule, the affinity of the TCR for the MHC:peptide complex and the concentration of the antigen (Ag) (Red-filled area). The first activation signal based on the recognition of the MHC:peptide complex by the TCR depends on the avidity of the MHC:peptide/TCR complex, the level of expression of MHC molecules, TCR and co-receptor (CD4 and CD8α) but also the strength of the signal after T cell engagement (red rectangle). A successful T cell activation will require the engagement of costimulatory molecules and the presence of cytokines secreted by DCs and T cells (blue rectangle) (Olivier Cexus, 2009, University of Southampton - PhD thesis).

The interaction of a TCR with a peptide:MHC complex depends on the overall avidity of a specific MHC:peptide/TCR complex (Figure 1.6). This notion relies on the affinity of the MHC molecule for a specific antigen, the affinity of the TCR for a specific MHC:peptide complex but also on the concentration of the antigen (Anderton et al. 2002). The avidity of the TCR for a specific peptide:MHC complex is defined by the concentration of peptide required for the activation of 50% of the pool of antigen-specific T cells. This in turn defines a threshold of activation that has to be reached for T cells to be activated (Van den Broon et al. 2006). The level of expression of MHC:peptide complexes on DC and the level of TCR

expressed on T cells are important as they dictate the fate of T cells towards the state of anergy or activation.

Peptides bind to an MHC molecule via a few anchoring points in the peptide-binding groove. The binding off-rate of a peptide to an MHC molecule depends on the affinity and the strength of the interaction between a specific peptide and the peptide binding-groove. Low-affinity peptides have a fast off-rate while high-affinity peptides display a low off-rate.

The definition of anchor residues has introduced the concept of T cell cross-reactivity which highlighted the fact that one TCR is not specific to only one peptide but that one TCR can bind different epitopes with different strength (Kersh et al. 1996). The generation of Altered Peptide Ligands (APL) that naturally occurs *in-vivo* has been shown to be important in the induction/control of immune responses in cancer and AID. Indeed, peptides with post-translational modifications (such as phosphorylation or glycosylation) and peptides with modified anchor residues can display an increased affinity for MHC molecules and therefore an enhanced immunogenicity (Vertuani et al. 2004, Mohammed et al. 2008). TCR can bind different peptides with different strength thus highlighting that the nature of the processed peptide rather than the type of APC dictates the outcome of T cell activation: anergy or stimulation.

1.3.2 – Different pathways for the generation of T cell responses

I have previously highlighted how the source of "Danger signals" affects the maturation of DC and the subsequent generation of an efficient T cell response. According to the nature of the pathogen or inflammation, DC have the ability to polarize naive $CD4^+$ T cells into different $CD4^+$ effector T cells after recognition of the cognate peptide and depending on the cytokines secreted by mDC and T cells (Kapsenberg et al. 2003).

Indeed, different LPS can bind different TLRs and therefore trigger different T cell responses. The ligation of TLR4 by LPS from *Escherichia coli* results in the production of IL-12 and IL-18 by DC, which in turn promotes the development of Th1 cells (Palucka et al. 2002). Th1 cells producing IFNγ are responsible for the stimulation of macrophages and Cytotoxic T Lymphocytes (CTL) that will mediate the clearance of cells infected by a

pathogen. By binding TLR2, LPS from *Porphytomonas gingivalis* promotes the release of IL-5, IL-10 and IL-13 by DC (Netea et al. 2002). Such cytokines will favour a Th2-like response and the subsequent generation of an humoral immune response via B cells (O'Garra et al 1998). In contrast, the production of IL-10 by DC following the ligation of TLR2 by LPS from *Schistosoma mansoni* leads to the expansion of Tregs that inhibit the function of T cells via the release of IL-10 and TGF_{β} (Van der Kleij et al. 2002).

1.3.2.1 – The different subsets of $CD4^+$ helper T cells

In a specific cytokine environment and upon recognition of the appropriate cognate peptide, naive T cells differentiate into different subsets such as Th1, Th2, Tregs or the newly described Th17 and Th9 (Figure 1.7):

Th1 cells are generated in the presence of cytokines such as IL-12, IFNγ, IL-2, IL-1β and TNFα. This cytokine environment induces the expression of Signal Transducer and Activator of Transcription 1 (STAT1) and the expression of the transcription factor T-BET by naive $CD4^+$ T cells (Afkarian et al. 2002). Further stimulation with IL-12 and IL-18 leads to the expression of STAT4 (Kalinski et al. 1999). Mature Th1 cells secrete various cytokines such as IL-2, TNFα and high amounts of IFNγ (Murphy et al. 2002) and are responsible for directing cellular-mediated immunity in response to intracellular infections such as mycobacteria or viruses.

Other cytokines are playing a role in the induction of Th1. IL-23 activates STAT4 and cooperates with IL-18 to promote the production of IFNγ by Th1 while IL-27 produced by APC alters the generation of Th1 cells at the early stages of differentiation (Murphy et al. 2002).

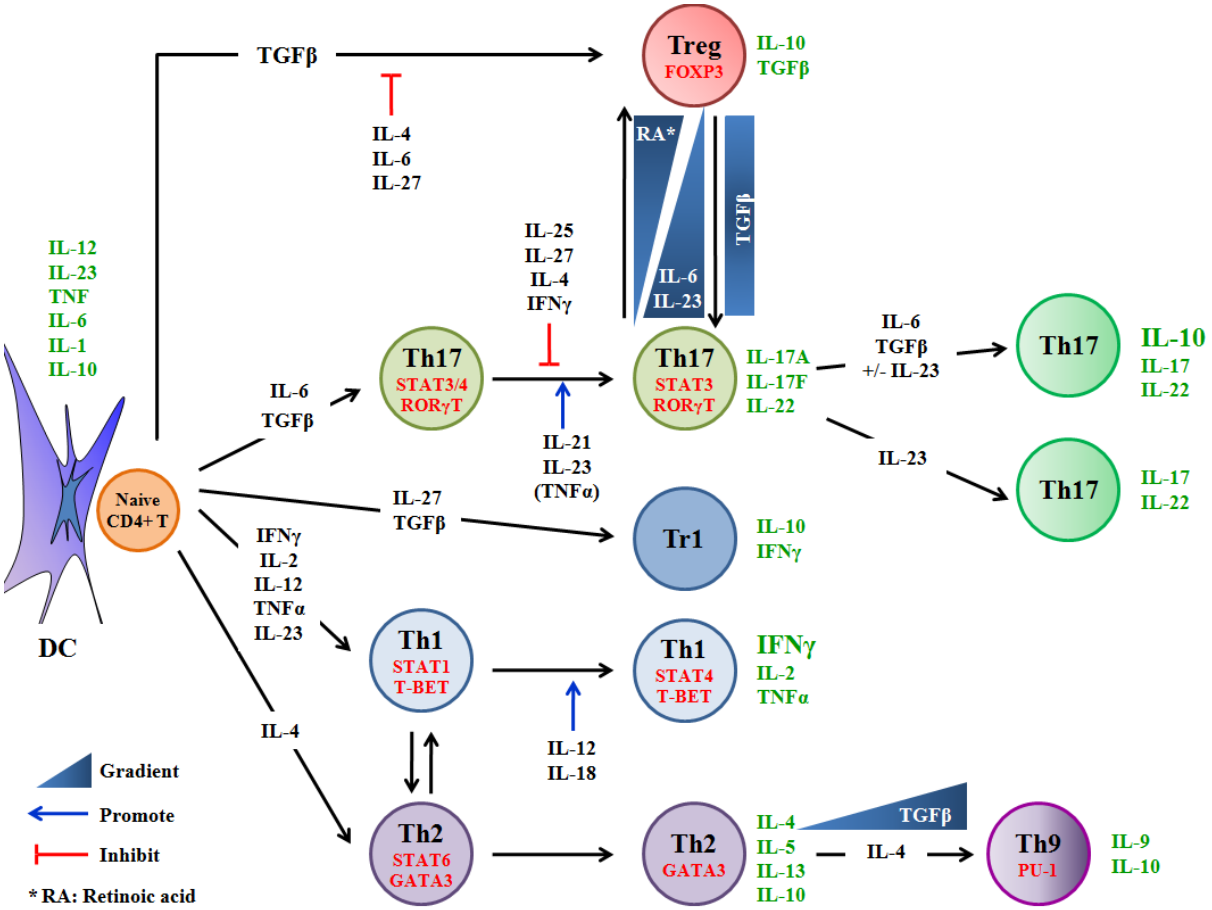

Figure 1.7: Control of the T cell polarization by dendritic cells and the cytokine environment
Dendritic cells induce the development of various $CD4^+$ T cell subsets such as Th1, Th2, Th9, Th17, Tr1 and Tregs. The generation of $Foxp3^+$ **Tregs** is promoted by TFG_β but inhibited by IL-6, IL-4 and IL-27. These cells inhibit T cell function via the release of TFG_β and IL-10. In synergy with TFG_β, IL-6 induces the generation of IL-17 and IL-22 secreting $ROR\gamma t^+$ **Th17** T cells. While IL-27 inhibits the generation of Th17 T cells, it favours the generation of IL-10 producing **Tr1** cells when associated with TFG_β. In an environment rich in IL-2, IFNγ and IL-12, naive T cells differentiate into **Th1** T cells that express STAT1 and T-BET and secrete high amounts of IFNγ. In contrast, naive T cells stimulated with IL-4 differentiate into **Th2** T cells expressing GATA3 and secreting IL-4, IL-5, IL-10 and IL-13 cytokines.

Upon stimulation with TFG_β and IL-4, Th2 cells differentiate into IL-9 and IL-10 producing **Th9** T cells. Depending on the inflammatory nature of the microenvironment, Th17 can adjust their phenotype. They release high amounts of IL-10 in an environment rich in IL-6 and TFG_β thus adopting a more regulatory phenotype. In the absence of these two cytokines, Th17 become more pathogenic.

In green are represented the cytokines secreted by the various T cell subsets. In red are represented the transcription factors while in black are the cytokines promoting the differentiation/generation of the different T cell subsets (Figure adapted from Olivier Cexus, 2009, University of Southampton - PhD thesis).

Th2 cells are generated in an environment rich in IL-4, IL-10, IL-5 and IL-13. The expression of the transcription factor GATA3 by naive T cells is rapidly induced through the previous activation of STAT6 by IL-4 (Ouyang et al. 1998). The Th2 cells generated secrete IL-4, IL-5, IL-10 (low amounts) and IL-13 and stimulate the production of IgE by B cells to

promote the clearance of extracellular pathogens. Th2 cells favour the recruitment and functions of mast cells and eosinophils to play a major role in the immunology of mucosal barriers such as the trachea or the gut (Dong et al. 2006).

A third subset of $CD4^+$ T cells has recently been described (Harrington et al. 2005). The development of **Th17 cells** under the influence of both TGF_β and IL-6 (or IL-21) leads to the the expression of STAT1 and the retinoic acid-related orphan nuclear hormone receptor γt (RORγt) (Korn et al. 2007). Also secreted by NK and NKT cells, IL-21 is produced by Th17 cells that express the receptor for IL-21 (IL-21R). This cytokine is required for the amplification of the Th17 proliferation and response which leads to the expression of a functional receptor for IL-23 by Th17 cells. IL-23 secreted by APC promote the full maturation of Th17 that produce various cytokines such as IL-17A, IL-17F, IL-21 and IL-22 (Betelli et al. 2006). While their pathogenic role in the induction of AID has been described, Th17 are involved in the clearance of pathogens (Ogura et al. 2008; Hirota et al. 2007).

Similarly to Th17 cells, TGF_β promotes the development of inducible regulatory T cells (**Tregs**) while IL-6 prevents their induction (Zhu et al. 2008). Tregs express the transcription factor Foxp3 which is essential for the maintenance of their phenotype and function (Hori et al. 2003). Tregs have been shown to inhibit T cell proliferation and function through the neutralization of IL-2 (Pandiyan et al. 2007) and the secretion of anti-inflammatory cytokines such as IL-10 and TGF_β. By aggregating on DC, Tregs also downregulate the expression of costimulatory molecules and proinflammatory cytokines thus actively inhibiting the maturation of DC that is also achieved through the release of IL-10 (Onishi et al. 2008). $Foxp3^+$ Tregs play a critical role in maintaining tolerance to self-antigens and a deficiency in Tregs has been associated with the development of multiple AID (Sakaguchi et al. 1995).

1.3.2.2 – Plasticity of the T cell response

The ability of mDC to dictate the differentiation of T cells into different T cell subsets must allow a certain degree of plasticity to finely tune the T cell response to the inflammation over time.

The first line of evidence of functional plasticity is the relative flexibility of Th1 and Th2 cells to interconvert. Previous work has shown that ongoing Th2 responses to *Leishmania major* can revert to Th1 responses in Balb/c mice treated with IL-12 (Nabors et al. 1995). Early Th1 cells can be reversed by the addition of IL-4 while Th2 cells can be converted into Th1 cells upon stimulation with IL-12 (Murphy et al. 1996). This is however controversial as previous studies have described that Th2 cells are resistant to phenotype reversal as they rapidly become unresponsive to IL-12 (Perez et al.1994, Szabo et al. 1995). Th1 and Th2 cells seem to be rapidly stabilized thus justifying why the reversibility is lost in fully differentiated Th1 and Th2 cells (Murphy et al.1996).

TGF_{β} and IL-6 (or IL-21) are cytokines crucial for the generation of Th17 cells whose involvement in the pathogenesis of AID such as experimental autoimmune encephalomyelitis (EAE) is established (Betteli et al. 2006). While continued exposure of Th17 to TGF_{β} and IL-6 stabilises their phenotype *in-vitro*, it abrogates their pathogenic function *in-vivo*. Under these conditions, Th17 produce high amounts of IL-10 and fail to upregulate proinflammatory chemokines thus suggesting a more regulatory phenotype (Figure 1.7). In contrast, the stimulation of Th17 with IL-23 in absence of TGF_{β} and IL-6 preserves their pathogenic functions. These observations highlight the dual role of TGF_{β} and IL-6 as promoting the differentiation of Th17 cells while restraining their functions over time (McGeachy et al. 2007).

The conversion between Tregs and Th17 cells results from the direct interaction between Foxp3 and RORγt. TGF_{β} upregulates Foxp3 which in turn binds to RORγt to inhibit its activity. However, in the presence of proinflammatory cytokines such as IL-6, IL-21 and IL-23, the inhibition of RORγt mediated by Foxp3 is relieved thereby promoting the generation of Th17 cells (Zhou et al. 2008). In addition to the balance of local amounts of IL-6, IL-23 and TGF_{β}, this conversion process is regulated by retinoic acids (RA). In the absence of IL-6 and IL-23 and in the presence of TGF_{β}, increased concentration of RA favours the differentiation of Th17 into Tregs. RA inhibits Th17 cell development *in-vitro* and *in-vivo* by reducing the expression of RORγt while promoting the expression of Foxp3. Th17 cells cultured with RA in the presence of IL-6 and TGF_{β} convert to $Foxp3^{+}$ cells (Mucida et al. 2007) (Figure 1.7).

The stimulation of Th2 cells in the presence of both IL-4 and increasing concentrations of TGF_{β} results in the inhibition of the expression of Foxp3 and the generation of **Th9** cells characterised by the secretion of IL-9 and IL-10. Like Th2, Th9 require the expression of STAT6 and GATA3 for their generation while they secrete low levels of Th2 cytokines such as IL4, IL-5 and IL-13 (Tato et al. 2008). A recent study has identified PU.1 as a transcription factor that promotes Th9 by repressing the production of Th2-specific cytokines while promoting the expression of IL-9 (Chang et al. 2010). Despite their abundant production of IL-10, Th9 promote tissue inflammation and do not possess any regulatory functions. Indeed, Th9 cells do not inhibit the proliferation and functions of effector T cells in a mouse model of autoimmune colitis. The adoptive-transfer of Th9 cells in these mice led to a more severe inflammation of the guts (Dardalhon et al. 2008). Interestingly, Th9 cells provide protection to infections by the helminth *Trichuris muris* potentially via the recruitment of mast cells (Veldhoen et al. 2008). Th9 cells are therefore beneficial in host-pathogen infections while being detrimental in autoimmune diseases.

The immune system is therefore carefully balanced so that it drives immunity against pathogens while promoting tolerance to self-antigens. The shaping of the T cell repertoire is therefore crucial to achieve this balance. Mechanisms are in place to eliminate T cells that recognise self-peptide:self-MHC complexes.

1.4 – Shaping of the T cell repertoire – Role of central and peripheral tolerance

The shaping of the T cell repertoire is a prerequisite for the efficient activity of the immune system. Two systems exist to prevent the generation and activation of self reactive T cells: **central** and **peripheral tolerance**. The different mechanisms governing these two systems will be discussed in this paragraph.

1.4.1 – Central tolerance

Mammals have developed throughout evolution the mechanism of central tolerance by which T cells are selected on their ability not to recognize self antigens. By contrast to peripheral tolerance, central tolerance occurs while T cell precursors mature in the thymus before being released in the blood.

The thymus supports the development of T cells and athymic patients develop severe immunodeficiencies resulting from a lack of mature T cells in the periphery (Zuniga-pflucker et al. 2004). Thymocytes derived from hematopoietic stem cells in the bone marrow enter the thymus through the cortico-medullary junction. Thymocytes present in the outer cortex do not express CD4 or CD8α co-receptors but a pre-TCRβ chain that drives their expansion (Von Boehmer et al. 2003). Only those double negative cells (DN) that have successfully rearranged their pre-TCRβ chain with an endogenous α chain, upregulate the expression of CD4 and CD8α to become double positive (DP) thymocytes. A wide repertoire of T cells is therefore generated and DP thymocytes go through a stringent selection process within the thymus that will result in the death of about 95% of thymocyte precursors by apoptosis (Kyewski et al. 2006). During the mechanism of **positive selection**, DP thymocytes are selected on the overall affinity of self MHC:TCR complexes, where self-MHC molecules are expressed by cortical thymic epithelial cells (cTEC). DP thymocytes unable to bind self-MHC molecules do not receive the signals necessary for their survival and undergo apoptosis (death by neglect). By contrast, if the TCR binds to self-MHC molecules, thymocytes receive survival signals and migrate to the medulla (Figure 1.8). Among the high and low affinity DP thymocytes positively selected, some can recognize “self” antigens and their migration in the periphery could result in the induction of AID.

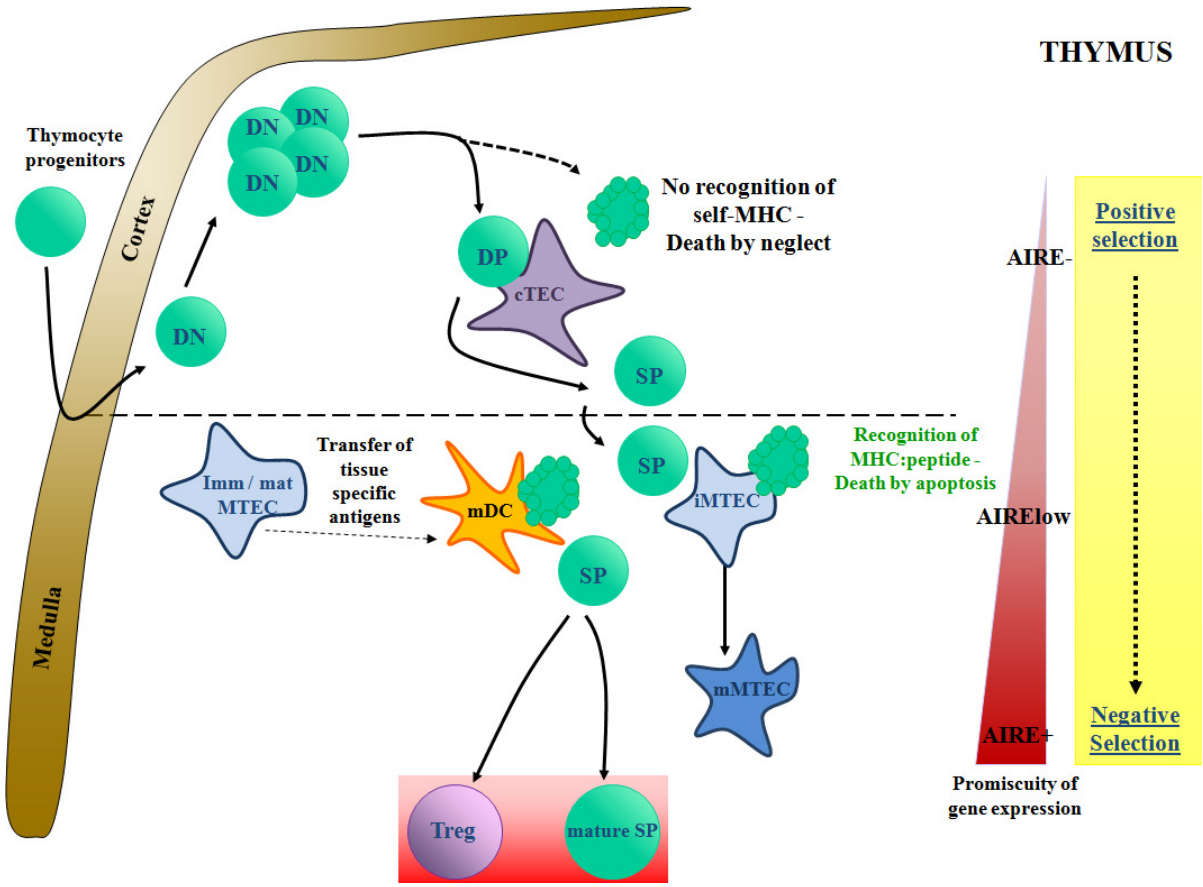

Figure 1.8: Central tolerance: positive and negative selection
Thymocyte progenitors enter the thymus where they differentiate into double negative (DN) cells. In the cortex of the thymus, double positive (DP) thymocytes undergo positive selection mediated by cortical thymic epithelial cells (cTEC). Positively selected thymocytes migrate towards the medulla and go through negative selection via the binding of their TCR to self-antigen:self MHC complexes. Depending on their affinity for the complex, they are either deleted by negative selection or positively selected to become mature single positive (mature SP) effector naive T cells or regulatory T cells. Immature medullary thymic epithelial cells (iMTEC) express low level of AIRE. As they mature (m MTEC), they upregulate the expression of AIRE after engagement of LTβR present at the surface of thymocytes. Tissue specific antigens from iMTEC or mMTEC can be transferred to mature DCs (mDCs) thus enhancing the process of negative selection (Adapted from Ladi et al. 2006).

Thymocytes that have been selected for during the positive selection enter the medulla of the thymus. The clonal deletion of thymocytes recognising self-antigen:self-MHC complexes will occur during the **negative selection** (Palmer et al. 2003). As they enter the medulla, positively selected DP thymocytes differentiate into $CD4^+CD8^-$ or $CD4^-CD8^+$ single positive (SP) thymocytes. The recognition of a peptide:MHC-I / II complex by a DP thymocyte induces their differentiation into $CD8^+$ and $CD4^+$ T cells respectively (Palmer et al. 2003). While the presentation of tissue-restricted self-antigens (TSA) by MTEC is restricted to MHC-II molecules, DC can present them on MHC-I and class II molecules, thus ensuring the thymic selection of both $CD4^+$ and $CD8^+$ self-reactive T cells.

Thymocytes bearing a TCR with a very high affinity for a self-antigen:self-MHC complex die by apoptosis. Thymocytes with an intermediate affinity for a self-antigen:self-MHC complex will become Tregs while those with a low affinity will be selected to become naive T cells that leave the thymus into the bloodstream. This is thought to be the fate of most thymocytes as it leads to the removal of 80-90% thymocytes ocurring during thymic selection (Ladi et al. 2006, Klein et al. 2009) (Figure 1.9). This selection is finely tuned as small differences in the affinity of the interaction between a TCR and self-peptide:self-MHC complex are sufficient to alter the fate of the thymocytes (Alam et al. 1996).

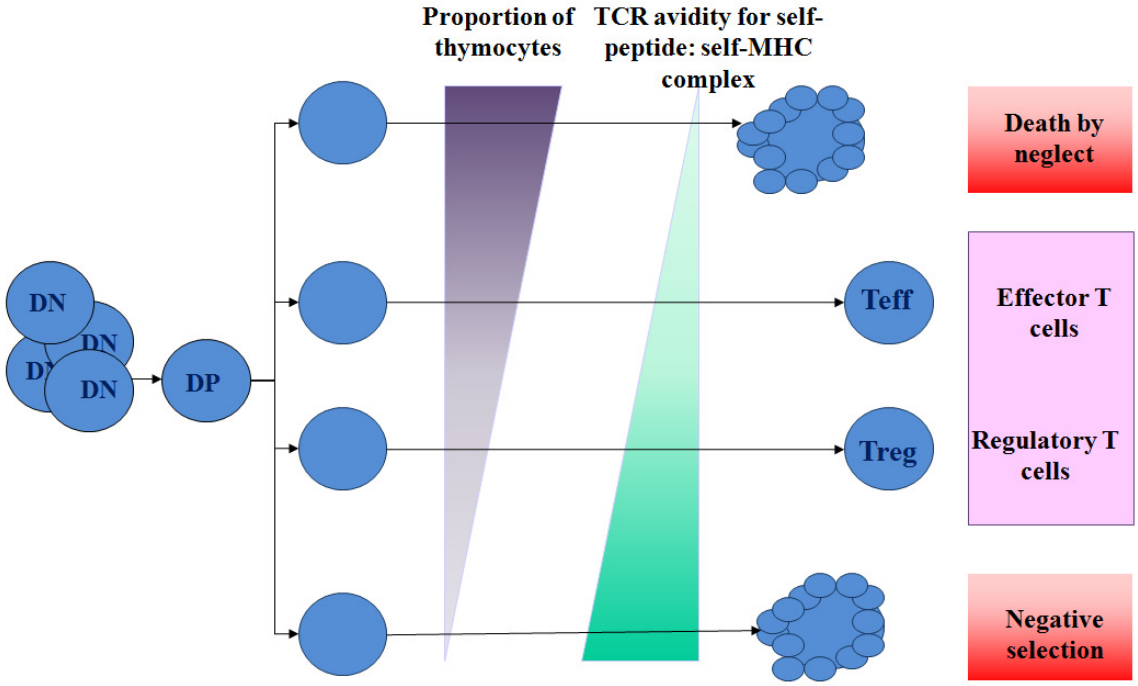

Figure 1.9: The affinity of a TCR for a self-peptide:self-MHC complex determines the fate of thymocytes
The affinity of the TCR for self-peptide:self-MHC complexes is crucial to determine the fate of thymocytes in the thymus. DP thymocytes that have no affinity or very low affinity die by neglect. Thymocytes with a TCR exhibiting a high affinity for self-peptide:self-MHC complexes are eliminated by negative selection. Thymocytes with intermediate affinity are positively selected and differentiate into effector mature naive T cells or regulatory T cells (Adapted from Hogquist et al. 2005).

Medullary thymic epithelial cells (MTEC) play a crucial role in mediating negative selection. These cells are able to transcribe a highly diverse set of genes that are normally expressed in peripheral tissues to express a vast array of TSA (Derbinski et al. 2005). The pool of genes expressed consists of up to 3,000 or 5-10% of all the genes currently known with diverse ontology. This process called promiscuous gene expression is unique to MTEC

and is under the influence of the autoimmune regulator (AIRE) transcription factor (Anderson et al. 2005; Su et al. 2004).

cTEC do not express AIRE and are therefore not able to mediate negative selection. Immature MTEC (iMTEC) express low levels of AIRE whose expression is upregulated under the action of thymic medullary chemokines and after engagement of lymphotoxin-β receptor (LTβR) promoting the maturation of iMTEC to mMTEC (Zhu et al. 2007; Venanzi et al. 2007). Stimulation of LTβR with an agonist antibody leads to an increased expression of AIRE and of TSA presented (Kyewski et al. 2004; Chin et al. 2003). LTβR deficient mice have a reduced number of MTEC and a defective T cell selection leading to the development of AID (Boehm et al. 2003).

AIRE has a crucial role in negative selection and AIRE-deficient mice or humans are unable to effectively present self-antigens in the thymus and therefore fail to deplete self-antigens specific thymocytes (Su et al. 2004). If AIRE knock-out mice show evidence of spontaneous organ-specific autoimmunity (Anderson et al. 2002), patients with rare autosomal disorders leading to the expression of defective AIRE proteins suffer from Autoimmune Polyendocrinopathy-Candidiasis-Ectodermal Dystrophy (APECED) (Betterle et al.1998; Peterson et al. 1998). While MTEC efficiently mediate negative selection, thymic DC also play an important role by cross-presenting antigens from dying immature and mature MTEC (Merkenschlager et al. 1999). The maturation state of MTEC is also crucial as a deficiency in the levels of expression of MHC or costimulatory molecules will allow high avidity self-reactive T cells to reach the periphery by escaping negative selection (Van den Boorn et al. 2006). Overall, this shows that the heterogenous APC population in the thymus (MTEC and thymic DC) drives the negative selection of thymocytes by the large spectrum of TSA presented (Kyewski et al. 2004).

This selection process is however not perfect and some self-reactive T cells are not eliminated. This occurs if the TCR has a high affinity for a TSA whose expression is not dependent on AIRE or if this expression occurs later in life when the T cell repertoire has already been formed. Other mechanisms have therefore been put in place throughout evolution to keep these self-reactive T cells at bay and prevent the occurrence of AID; these are the mechanisms of peripheral tolerance.

1.4.2 – Peripheral tolerance

Peripheral tolerance involves various mechanisms aimed at controlling the activation and function of self-reactive T cells in the periphery. These mechanisms can be divided into two groups: intrinsic depending on the antigen and the level of costimulation and extrinsic relying on regulatory cells of the innate and adaptive immune systems.

1.4.2.1 – Mechanisms of intrinsic peripheral tolerance

Mechanisms of intrinsic T cell peripheral tolerance depend on the level of antigen:MHC complexes as well as the nature and amount of costimulatory signals provided to T cells upon TCR engagement. Four different cases can be considered:

- Self-reactive T cells might never encounter the self-antigens, either because they are not accessible to T cells or simply because the amount is not sufficient to reach the threshold of activation to trigger a T cell response. These T cells are therefore **ignorant** (Walker et al. 2002).

- Antigen recognition by T cells might lead to **anergy**. Although anergy was first thought to be the result of a lack of costimulation, it became clear that other receptors are also involved. Indeed, the ligation of CD80/86 on APC by cytotoxic T-lymphocytes associated antigen 4 (CTLA-4) on T cells results in the functional inactivation of T cells (Perez et al. 1997). The Programmed Cell Death-1 (PD-1) molecule is also important as it is expressed in high levels by all anergic T cells and mice lacking this receptor develop multiple AID (Fife et al. 2008).

- As previously described, T cell activation results from the recognition of an antigen presented by an APC in a context of "danger". However, variants of an antigenic peptide or **Altered Peptide Ligands** (APL) can be recognised by the same TCR leading to T cell anergy rather than T cell activation (Quaratino et al. 2000).

- Finally, high concentration of self-antigens and/or a highly inflammatory environment can lead to T cell deletion by apoptosis. This **activation-induced cell death** (AICD) involves the upregulation of Fas ligand (FasL) on T cells (Zhang et al. 2004).

1.4.2.2 – Mechanisms of extrinsic peripheral tolerance

Extrinsic mechanisms of T cells tolerance involve different cell subsets of the innate and adaptive immune system.

- **$CD4^+$ $CD25^+$ $Foxp3^+$ regulatory T cells** have been described to play a crucial role in maintaining peripheral self-tolerance. Two subsets of Tregs can be described: naturally arising (generated in the thymus during central tolerance) and peripherally induced Tregs. Tregs have been shown to inhibit T cell function and proliferation via the secretion of TGF_β and IL-10 while Tregs can also induce the apoptosis of T cells by depleting the microenvironment of IL-2 (Pandiyan et al. 2007; Sakaguchi et al. 2008).

- Both IL-27 and TGF_β have been shown to play an important role in promoting the generation of **Tr1 cells** (Battaglia et al. 2006). Tr1 cells suppress effector T cells and tissue inflammation via the release of high levels of IL-10. Recent work has also highlighted the role of TGF_β-producing **Th3 cells** in maintaining peripheral tolerance by driving the differentiation of antigen-specific $Foxp3^+$ Tregs in the periphery (Carrier et al. 2007) while double negative T cells (**DN T cells**) also promote the inhibition of T cell responses (Zhang et al. 2007).

- Precursor cells of the myeloid lineage, **Myeloid derived suppressor cells (MDSC)** have been shown to inhibit T cell proliferation and function (This will be discussed in detail in paragraph 1.5).

- Finally, in addition to their key role in promoting efficient adaptive immune responses, **DC** are also involved in the induction and maintenance of peripheral tolerance.

Uptake of antigens or apoptotic bodies via DEC-205 on DC mediates the uptake and presentation of antigens without further inducing the maturation of DC. iDC presenting antigens to T cells can induce T cell anergy or T cell death by apoptosis. It has been shown that targeting antigens to DC via the DEC-205 endocytic pathway results in the induction of peripheral tolerance to the antigen while the combination with αCD40 mAb leads to strong $CD8^+$ and $CD4^+$ T cell responses (Figure 1.10/A).

There is accumulating evidence that interactions between DC and Tregs play a crucial role in the balance between immune response and tolerance. Both iDC and mDC have been shown to promote the conversion of naive $CD4^+$ $CD25^-$ T cells into antigen-specific $Foxp3^+$ Treg; a phenomenon mediated by TGF_β and IL-2 (Luo et al. 2007) (Figure 1.10/B).

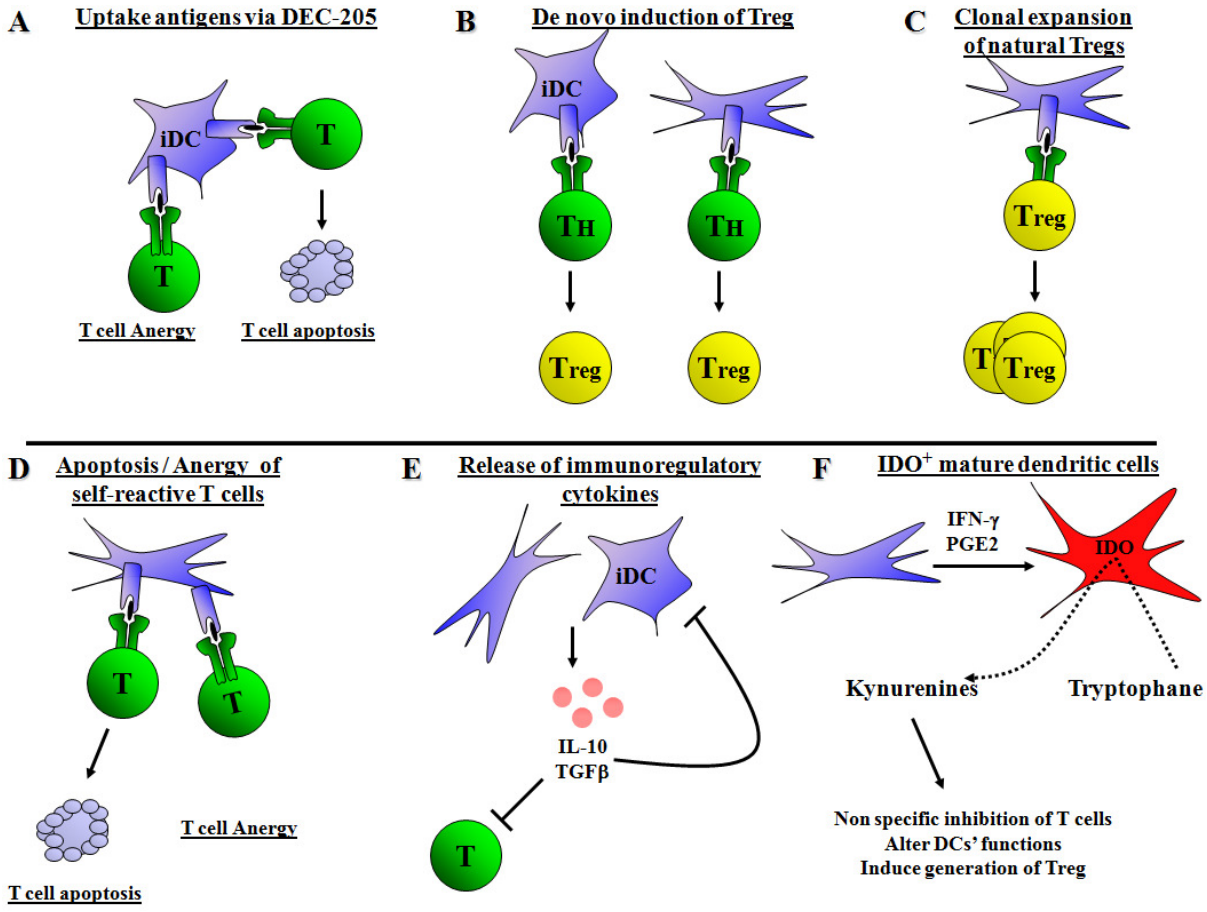

Figure 1.10: Mechanisms of peripheral tolerance mediated by DC
(A) Uptake of antigens via the DEC-205 mannose receptor does not induce the maturation of DC. iDC presenting antigens to T cell can lead to T cell anergy or T cell death. **(B)** Both immature and mature DC can induce the generation of functional regulatory T cells. **(C)** DC can promote the expansion of Tregs. **(D)** mDC presenting peptides in the context of MHC molecules can lead to either T cell anergy or T cell death via different mechanisms such as Fas/FasL pathway. **(E)** DC can produce immunoregulatory cytokines that affect the function of DC and T cells. **(F)** Under stimulation with various factors such as PGE2, mDC upregulate the expression of IDO, leading to a tryptophan-deprived environment and the inhibition of T cells (Figure from Olivier Cexus, 2009, University of Southampton - PhD thesis).

Some studies have also shown that DC promote the expansion of pre-existing functional Tregs (Yamazaki et al. 2003) (Figure 1.10/C) thus suppressing AID as it has been described in the nonobese mouse model of type 1 diabetes (Tarbell et al. 2004). DC can also

lead to the effective expansion of alloantigen-specific Tregs while promoting the high expression of Foxp3. These DC-expanded Tregs can then exert a more potent and antigen-specific suppression of immune responses (Yamazaki et al. 2006).

DC presenting peptides in the context of MHC molecules can lead to either T cell anergy (involvement of CTLA-4 and PD-1) or T cell death (involvement of the Fas/FasL pathway) (Figure 1.10/D). The nature of the peptide presented by DC has also been shown to determine the fate of T cells (Paragraph 1.4.2.1; Quaratino et al. 2000).

In a tumour microenvironment, myeloid DC can be converted into TGF_{β} and IL-10-secreting DC promoting the generation of $Foxp3^{+}$ Tregs (Figure 1.10/B) while inhibiting T cells (Figure 1.10/E) (Ghiringhelli et al. 2005). The production of immunosuppressive cytokines by DC can therefore be crucial in inducing the differentiation of other regulatory T cells such as Tr1 cells while also altering the function of both DC and T cells (Rutella et al. 2006) (Figure 1.10/E). Upon stimulation with IFNγ or prostaglandin E2 (PGE2), DC upregulate the expression of indoleamine 2,3-dioxygenase (IDO) (Figure 1.10/F). This enzyme degrades the essential amino acid tryptophan into kynurenines leading to the inhibition of T cells and the alteration of DC's functions while favouring the generation of Tregs (Steinman et al. 2003; Puccetti et al. 2007).

1.5 – Myeloid Derived Suppressor cells (MDSC)

Myeloid Derived Suppressor Cells (MDSC) have been described 20 years ago because of their widespread presence in cancer patients but their functional importance has only been recently appreciated. Initially called "natural suppressor cells" (Strober et al. 1984), "Immature suppressor cells" (Kusmartsev et al. 2002) or "myeloid suppressor cells" (Serafini et al. 2004) from their ability to block the activation of T cells, MDSC is a heterogeneous population of cells of the myelomonocytic lineage originating from Common Myeloid Precursor cells in the bone marrow (Bronte et al. 1998; Bronte et al. 2000) (Figure 1.11). Although MDSC are present in healthy individuals, these cells accumulate in pathological conditions such as cancer, bacterial or viral infections, traumatic stress where they differentiate into macrophages, granulocytes or DC according to the pro- versus anti-

inflammatory nature of the microenvironment (Delano et al. 2007, Makarenkova et al. 2006, Zhu et al. 2007a).

MDSC were first characterised in tumour-bearing mice and cancer patients (Bronte et al. 2000; Almand et al. 2000). In the peripheral blood of patients with head and neck cell-squamous carcinomas and breast cancers, a significant decrease in the number of myeloid DC is associated with an increased number of MDSC (Almand et al. 2000). Similarly, this accumulation is observed in various tumour models where MDSC accumulate at the tumour site and in the bone marrow, blood and secondary lymphoid organs such as spleen where they can represent up to 30% of the splenocytes (Melani et al. 2003).

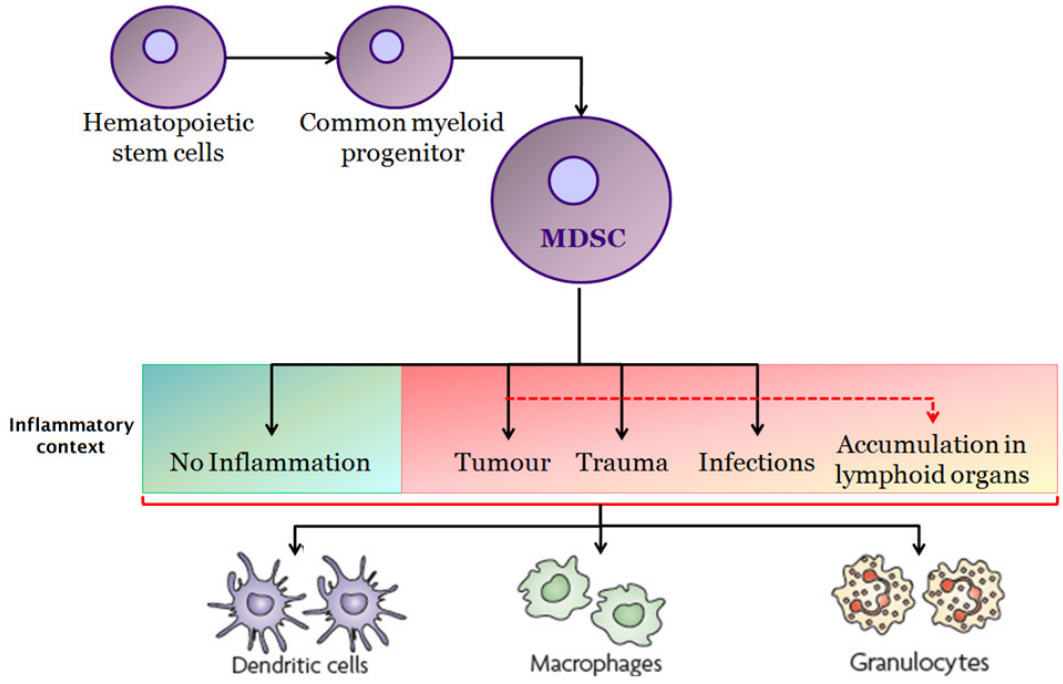

Figure 1.11: Origin and accumulation of MDSC upon inflammation
MDSC are present in multiple tissues in healthy individuals. However, in a specific inflammatory context such as cancer or infections, MDSC accumulate in lymphoid organs and the tissues affected by the inflammation. At this stage and depending on the nature of the inflammation, MDSC can differentiate into mature myeloid cells such as DC, macrophages and granulocytes (Adapted from Gabrilovich et al. 2009).

Two major subsets of MDSC have been described on the basis of the differential espression of the Ly6C and Ly6G markers. Granulocytic MDSC are polymorphonuclear leukocytes expressing high levels of Ly6G while containing high levels of arginase 1 (Arg-1). In contrast, monocytic MDSC are mononuclear and express high levels of Ly6C, Arg-1 and

inducible nitric oxide synthase (iNOS) (Peranzoni et al. 2010, Youn et al. 2008). If polymorphonuclear MDSC suppress CTLs mainly through the generation of Reactive Oxygen Species (ROS), monocytic MDSC exert their inhibition through the degradation of L-arginine by iNOS and the subsequent release of NO (Mohavedi et al. 2008).

The inhibition mediated by MDSC can target antigen-specific or antigen non-specific T cells (Gabrilovich et al. 2001, Bronte et al. 2000) in an MHC restricted and unrestricted manner (Nagaraj et al. 2007, Sinha et al. 2005). In addition to their ability to inhibit adaptive immune responses, MDSC have a direct impact on the innate immune system by altering the functions and proliferation of natural killer (NK) cells, macrophages and Natural Killer T cells (NKT). The cross-talk between MDSC and macrophages results in an increased production of IL-10 by MDSC but a decreased production of IL-12 by macrophages. This promotes the polarization of macrophages to an alternatively activated "M2" phenotype that favours tumour progression (Sinha et al. 2007). MDSC have also been shown to inhibit NK cell cytotoxicity. Indeed, by affecting the activation of STAT5, MDSC suppress the IL-2 – dependent production of perforin (Liu et al. 2007). MDSC can also induce the anergy of NK cells via membrane-bound TGF_{β} in liver cancer-bearing mice (Li et al. 2009). In contrast, MDSC have the ability to activate the production of high amounts of IFNγ by NK cells after engagement of NKG2D on NK cells. These activated NK cells then promote anti-tumour responses in RMA-S tumour-bearing mice by eliminating MDSC (Nausch et al. 2008). Finally, NKT cells also control the ability of MDSC to expand. Indeed, type II NKT cells producing IL-13 drive the accumulation of MDSC thus facilitating tumour progression (Sinha et al. 2005). However, type I NKT cells (or invariant NKT cells) abolish the suppressive activity of MDSC in a CD1d-dependent manner (De Santo et al. 2008).

The recruitment of MDSC to the site of inflammation is under the influence of several factors with most of them being pro-inflammatory (Serafini et al. 2005). IL-6 and IL-1β present in the microenvironment of many tumours dramatically increase the rate of accumulation of MDSC while enhancing their suppressive activity on T cells (Bunt et al. 2006, Song et al. 2005). Produced by almost all tumour cells and involved in tumour angiogenesis, Vascular Endothelial Growth Factor (VEGF) has also been directly linked to the recruitment of MDSC (Gabrilovich et al. 1998). In BALB-neuT mice that spontaneously develop mammary carcinomas, an increased level of VEGF directly correlates with the

progressive accumulation of MDSC in the blood and the spleen (Melani et al. 2003). Driving the differentiation of DC, Granulocyte/macrophage Colony Stimulating Factor (GM-CSF) is another inflammation-associated molecule capable of promoting the accumulation of MDSC. Indeed, the administration of GM-CSF elicited the expansion of MDSC in CT26.WT and TS/A tumour bearing mice thus causing the impairment of $CD8^+$ T cell functions (Bronte et al. 1999). The bioactive lipid prostaglandin E2 present in inflammatory environments also induces the accumulation and retention of immunosuppressive MDSC in mice inoculated with the BALB/c-derived 4T1 mammary carcinoma cell line (Sinha et al. 2007a). Similarly, pro-inflammatory S100A8/A9 proteins and C5a complement can play a pivotal role in the accumulation and activation of MDSC through the activation of the NF-κB signalling pathway (Sinha et al. 2008; Markiewski et al. 2008).

All these factors target the signalling pathways in MDSC leading to the activation of STAT3 that stimulates myelopoiesis while inhibiting the differentiation of MDSC into mature myeloid cells. The inhibition of the expression of STAT3 is associated with a reduced expansion of MDSC leading to the restoration of anti-tumour responses in tumour-bearing mice (Nefedova et al. 2004).

Attracted at the tumour site, MDSC play a detrimental role in cancer by inhibiting the proliferation and function of tumour specific T cells (Pak et al. 1995; Kusmartsev et al. 2000; Bronte et al. 2000) in part via the modulation of the metabolism of L-arginine by inducible nitric oxide synthase (iNOS) and/or Arg-1.

The activity of these two enzymes is regulated by Th1- and Th2-like cytokines respectively (Figure 1.12). Th1-like cytokines (IFNγ, TNFα) and bacterial products such as LPS lead to an increased production of nitric oxide (NO) via the activation of STAT1, the upregulation of iNOS and the inhibition of Arg-1 (Mazzoni et al. 2002). Indeed, MDSC from $STAT1^{-/-}$ mice have a low expression of iNOS and do not display any suppressive function on T cells (Kusmartsev et al. 2005). NO interferes with the IL-2R signalling pathway by blocking the phosphorylation of several signalling molecules such as Jak1, Jak3, STAT5 and ERK. The inability of T cells to respond to IL-2 can ultimately lead to their death by apoptosis (Bingisser et al. 1998; Mazzoni et al. 2002).

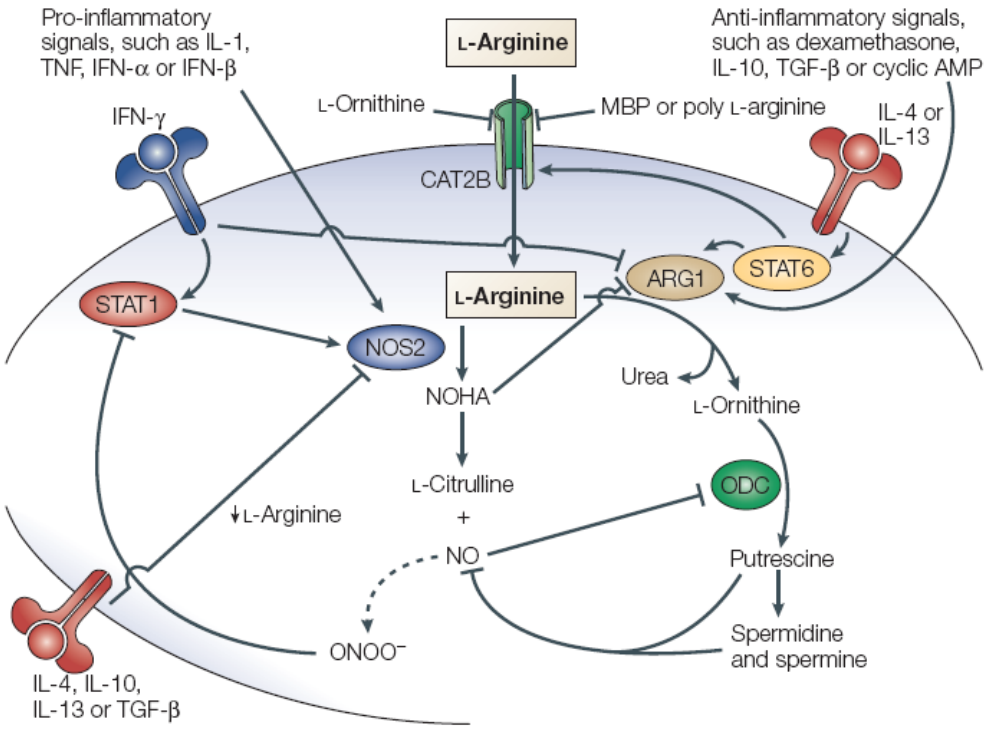

Figure 1.12: The immune suppression mediated by MDSC involves the metabolism of L-arginine
In a Th1-like cytokine environment, MDSC upregulate the expression of inducible nitric oxide synthase (iNOS). This enzyme oxidizes L-arginine to generate L-citrulline and nitric oxide (NO). By contrast, in a Th2-like cytokine environment, the expression of arginase-1 is upregulated, resulting in the depletion of arginine from the milieu and the production of urea and L-ornithine. The resultant L-ornithine can be used by ornithine decarboxilase to form polyamines (i.e. putrescine, spermidine and spermine). Arg-1 and iNOS activate different biological pathways that negatively regulate and feedback on each other. Low extracellular concentration of arginine or the overexpression of Arg-1 can reduce iNOS activity while NG-hydroxy-L-arginine (NOHA) released by macrophages during intense iNOS activity can inhibit Arg-1 (Adapted from Bronte et al. 2005).

By contrast, Th2-like cytokines (such as IL-4, IL-10 and IL-13) inhibit iNOS activity and induce the upregulation of Arg-1 and the cationic amino-acid transporter 2B (CAT2B) favouring the uptake of L-arginine (Figure 1.12). This is mediated by the activation of STAT6 and a deficiency in this transcription factor prevents the signalling through IL-4Rα and the synthesis of Arg-1 by MDSC (Sinha et al. 2005a). Arg-1 hydrolyzes L-arginine into urea and L-ornithine (Yeramian et al. 2006; Bronte et al. 2005). As MDSC deprive the surrounding microenvironment of L-arginine, T cells have an impaired expression of CD3ζ and are stopped at the G0-G1 phase of the cell-cycle (Rodriguez et al. 2004, Rodriguez et al. 2007) while the products of degradation of L-arginine also alter T cell functions by tampering with the translation of various mRNA (Bronte et al. 2005).

Finally, when both enzymes are induced together, iNOS generate superoxide ions (O_2^-) which reacts with other molecules to produce Reactive Nitrogen Oxide Species (RNOS) and

ROS (Bronte et al. 2003). The nitrosylation of tyrosine residues by peroxynitrites affect intracellular signalling pathways and can lead to T cell apoptosis (Bronte et al. 2005) while nitrated TCR renders T cells unable to bind peptide/MHC complexes (Nagaraj et al. 2007).

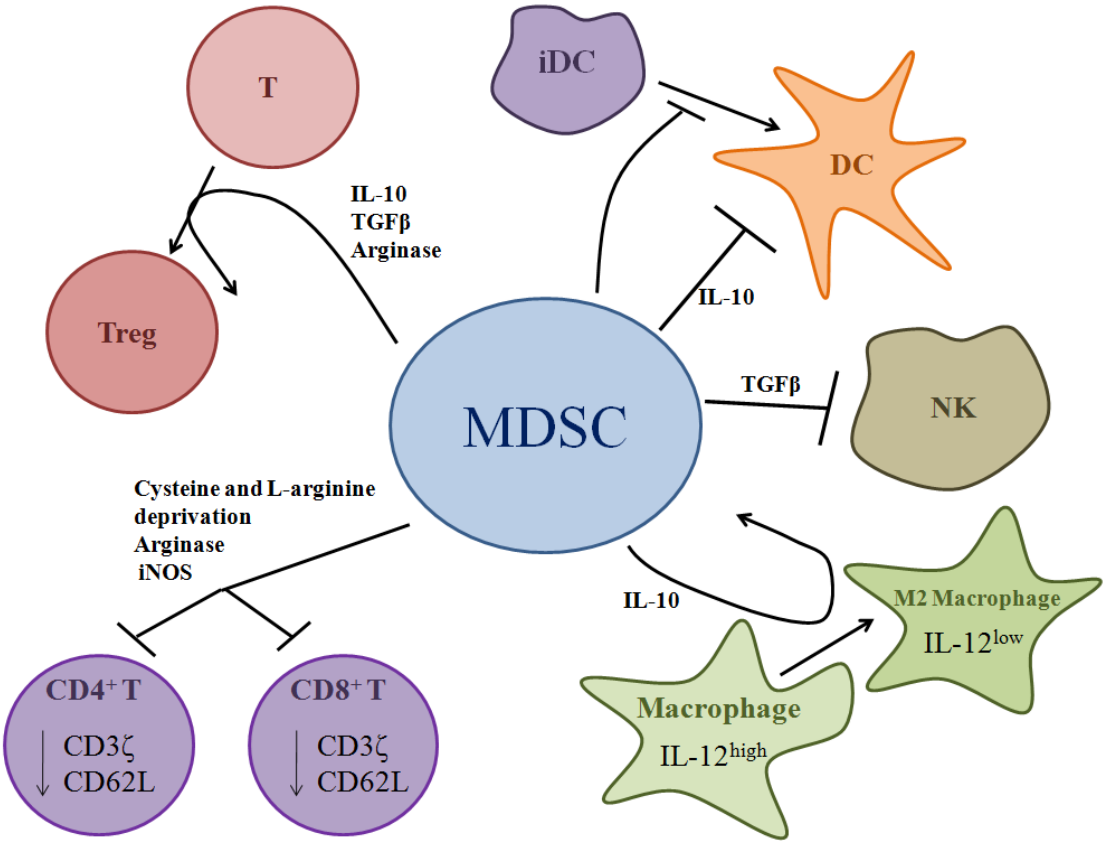

Figure 1.13: MDSC use a diversity of mechanisms to suppress the innate and the adaptive immune responses
MDSC suppress T cell activation via the products of degradation of L-arginine by iNOS and Arg-1 leading to the impaired expression of CD3ζ, the nitration of the TCR, the induction of Tregs, the deprivation of the milieu of L-arginine and/or the induction of T cell apoptosis. They direcly impact on cells of the innate immune system by preventing the maturation of iDC to mDC while altering the function of mDC. MDSC secreting high levels of IL-10 favours the polarization of pro-inflammatory macrophages into M2 type macrophages producing low levels of IL-12. Finally, MDSC suppress NK cell cytotoxicity (Adapted from Ostrand-Rosenberg et al. 2009).

MDSC also mediate their immunosuppressive activity via the induction of Tregs *in-vitro* and in tumour-bearing mice (Figure 1.13). Indeed, $Gr1^+$ $CD115^+$ MDSC induce the development of $Foxp3^+$ Tregs in the presence of IFNγ and IL-10 (Huang et al. 2006). In the A20 mouse model of B cell lymphoma, MDSC mediate the expansion of antigen-specific $Foxp3^+$ Tregs through the activation of Arg-1 activity while TGF_β was not required (Serafini et al. 2008).

Two additional mechanisms have also been recently described. MDSC can block T cell activation by sequestering cysteine, an amino acid necessary for the efficient activation of T cells (Figure 1.13). Indeed, T cells lack the enzyme cystathionase which converts methionine to cysteine and the membrane transporter Xc^- required to import cystine that can then be reduced to cysteine. T cells therefore rely only on extracellular sources of cysteine. T cells are deprived of cysteine by MDSC as they express the Xc^- transporter and import cysteine but lack the ASC transporter required to export cysteine (Srivastava et al. 2010). MDSC also down-regulate the expression of L-selectin (CD62L) on naive $CD4^+$ and $CD8^+$ T cells that cannot home to lymph nodes thus preventing their activation (Hanson et al. 2009).

Because the successes of cancer immunotherapy are hindered by the presence of cells suppressing the generation of an efficient anti-tumour response, different strategies have been explored to reduce or eliminate the immune suppression mediated by MDSC.

Phosphodiesterase-5 (PDE5) inhibitors such as sildenafil, have been shown to target the suppressive activity of MDSC by inducing the down-regulation of Arg-1 and iNOS. Sildenafil treatment in myeloma patients restores T cell proliferation, enhances intratumoral infiltration of T cells and reduces tumour outgrowth (Serafini et al. 2006). Cyclooxygenase 2 inhibitors are also associated with the downregulation of Arg-1 and improved anti-tumour immune responses *in-vivo* (Talmadge et al. 2007). Other strategies are aimed at promoting the depletion of MDSC. Indeed, the administration of gemcitabine to tumour-bearing mice results in a dramatic reduction in the number of MDSC in the spleen leading to the improvement of anti-tumour responses (Suzuki et al. 2005).

In contrast, some strategies have been used to promote the differentiation of MDSC. Administration of all-*trans*-retinoic acid (ATRA) resulted in the reduction of the number of MDSC in cancer patients (Mirza et al. 2006) and tumour-bearing mice (Kusmartsev et al. 2003) by promoting their differentiation into DC, macrophages or granulocytes leading to enhanced anti-tumour responses. This differentiation only involved the neutralization of ROS production by MDSC through the upregulation of glutathione synthase (Nefedova et al. 2007).

Other strategies have been developed to neutralize tumour-derived factors responsible for the expansion of MDSC (e.g. stem cell factor (SCF) or VEGF) (Gabrilovich et al. 2009). Most recently, the use of a selective inhibitor of colony-stimulating factor-1 receptor (CSF1-R) has been shown to directly alter the recruitment of $CD11b^+$ $Gr1^{low}$ $Ly6C^{high}$ MDSC from

peripheral blood. Indeed, the blockade of CSF1-R signalling suppresses the expansion of monocytic MDSC in the bone marrow and reduced their accumulation in the spleens of 3LL tumour-bearing mice (Priceman et al. 2009).

While the mechanisms involved in central tolerance are very efficient, some self-reactive T cells can escape the stringent thymic selection. Peripheral tolerance provides an additional mechanism to protect against the activation of these self-reactive T cells in the periphery and therefore prevent the emergence of AID. However a breakdown of tolerance that will trigger AID can occur in certain conditions.

1.6 – Breakdown of tolerance and emergence of autoimmune diseases

The breakdown of tolerance can be linked to **genetic susceptibility**. Genetic analyses in patients affected by AID indicate that multiple genetic loci are linked with increased risks in developing AID. Indeed, the expression of specific Histocompatibility Leukocytes Antigen (HLA) molecules more prone to binding some self-antigens is associated with increased risk in developing some specific autoimmune disorders. For example, type 1 diabetes is strongly linked to the expression of HLA-DR3, HLA-DR4 and HLA-DQ8 while HLA-DR2 is protective (Aly et al. 2006). Likewise, patients expressing HLA-DR3, HLA-DR5 and HLA-DQ6 are predisposed to develop autoimmune thyroiditis (Kong et al. 2003). The polymorphisms of certain specific genes such as CTLA-4 have also been linked to some AID (Ueda et al. 2003).

Beyond this genetic susceptibility, other factors can lead to the activation of self-reactive T cells that have escaped the central selection in the thymus. The failure of the various mechanisms of peripheral tolerance in keeping these self-reactive T cells at bay leads to the development of AID. This implies that the TCR has been able to recognize some epitopes in the context of MHC molecules that are either hidden or non-existent in normal conditions.

External factors leading to the breakdown of tolerance and the emergence of AID are factors that cause tissue damage and therefore the dissemination of self-antigens. A break of tolerance can occur in persistent viral or microbial infections via different mechanisms:

- Following tissue destruction during an infection, self-antigens released by dying cells can mimic foreign antigens derived from pathogens. Due to this similarity, immune response can eventually be directed against the self-peptide, leading to the cross-activation of pathogen-specific and/or self-reactive T cells. This **molecular mimicry** is only possible if foreign and self-epitopes share a similar antigenic surface (Vanderlugt et al. 2002, Lang et al. 2002) (Figure 1.14/A). Molecular mimicry has been linked with the development of systemic lupus erythematosus (Doria et al. 2008).

  Shape mimicry is an alternative situation when peptides are shifting within the MHC peptide binding groove (Bankovich et al. 2004). Two peptides from thyroid peroxidase ($TPO_{536-547}$ and $TPO_{539-550}$) can stimulate the same T cell clone. Although they have different sequences and anchor residues within MHC-II molecules, molecular models revealed that they shared a similar antigenic surface (Quaratino et al. 1995)

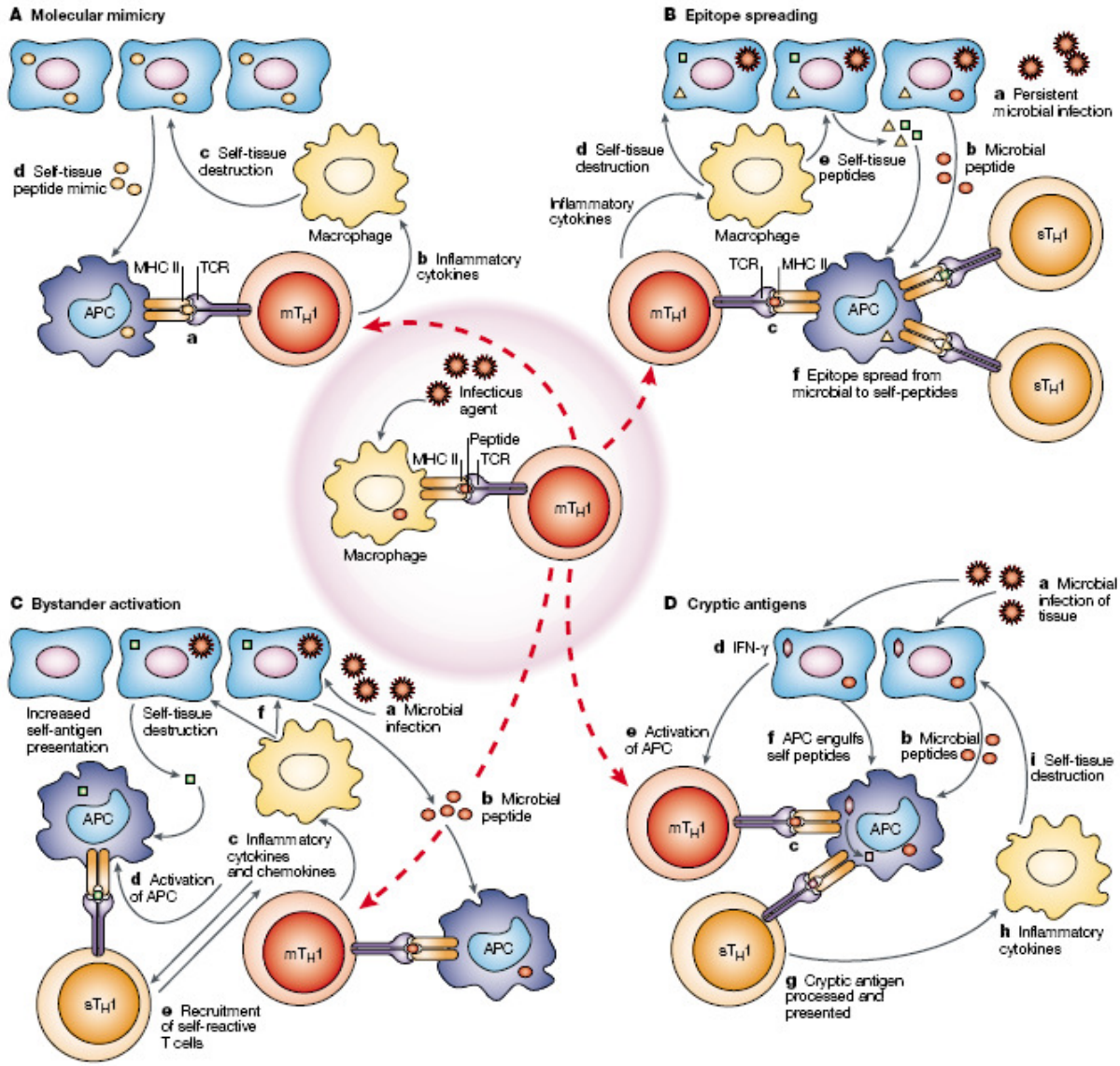

Figure 1.14: Mechanisms of breakdown of tolerance leading to the emergence of autoimmune diseases
Upon bacterial or viral infection, immunological tolerance can be broken via several mechanisms: **(A)** Molecular mimicry: self-antigens released share similar antigenic surfaces than foreign antigens leading to the activation of pathogen-specific and self-reactive T cells. **(B)** Epitope spreading: Tissue damage promoted during inflammatory responses results in the release of self-antigens that in turn activate self-reactive T cells. **(C)** Bystander activation: The pro-inflammatory environment caused by microbial infections leads to the activation of self-reactive T cells through a mechanism that is not antigen-dependent. **(D)** Cryptic epitope: During inflammation, high levels of pro-inflammatory cytokines increase the level of expression of MHC-I and MHC-II molecules as well as the protease content of the cells. Upon these changes, APCs can generate or unmask cryptic epitopes capable of activating self-reactive T cells. (Adapted from Vanderlugt et al. 2002).

- In the context of a persistent microbial infection/inflammation where T cells are continuously activated, tissue damage can occur resulting in the release of self-antigens. These self-antigens loaded by APC recruited to the site of inflammation cause the activation of self-reactive T cells. This **intermolecular epitope spreading** can also result in more self-antigens being released by the damaged tissue thus promoting the

stimulation of a wider range of self-reactive T cells (Figure 1.14/B). As the inflammation persists, more self-antigens are shed and multiple epitopes generated from the same antigen can be presented by APC to be recognised by other self-reactive T cells, thereby amplifying the extent of the inflammatory process (**intramolecular epitope spreading**) (Sercarz et al. 2000; Vandergult et al. 2002).

- Inflammatory and pathogen-specific T cells attracted to the site of inflammation release high levels of pro-inflammatory cytokines thus creating a powerful pro-inflammatory environment that mediates the **bystander activation** or non-specific activation of self-reactive T cells. This in turn increases tissue damage and can lead to the development of AID in other tissues not affected by the original infection/inflammation (Bangs et al. 2006) (Figure 1.14/C).

- Following an infection, high amounts of IFNγ released by pathogen-specific T cells and microbe-infected cells induce the upregulation of MHC-II and MHC-I molecules on APC as well as an increased production of proteases involved in antigen processing and presentation. Upon those changes, APC engulfing self-antigens can generate or unmask **cryptic epitopes** capable of promoting the activation of self-reactive T cells (Lanzavecchia 1995) (Figure 1.14/D).

1.7 – The TAZ10 transgenic mouse model of spontaneous autoimmune thyroiditis

TAZ10 transgenic mice express the human TCR ($V_\beta1/V_\alpha15$) from the thyroid infiltrating T cell clone 37 of a patient with Hashimoto's thyroid disease (Quaratino et al. 2004). Half of the T cell clones generated from the thyroid of this patient were specific for the main thyroid autoantigen: thyroid peroxidase (TPO). Among these, 18% were specific for the immunodominant TPO peptide $TPO_{535-551}$ (N-LDPLIRGLLARPAKLQ-C).

T cell clone 37 is specific for $TPO_{536-547}$ (N-DPLIRGLLARPA-C), identified as the cryptic TPO epitope preferentially generated from the endogenous processing of TPO by TEC and presented in the context of MHC-II molecules upon inflammation (Quaratino et al. 1996). By contrast, DCs pulsed with exogenous TPO presented a natural APL of $TPO_{536-547}$

($TPO_{537-548,}$ N-PLIRGLLARPAK-C) that induces the anergy of T cell clone 37. Although $TPO_{537-548}$ and $TPO_{536-547}$ induce a similar down-regulation of the TCR, $TPO_{537-548}$ does not lead to T cell proliferation and IL-2 secretion while $TPO_{536-547}$ induces a powerful proliferation of T cell clone 37 (Quaratino et al. 2000).

Interestingly, two peptides generated from $TPO_{535-551}$ could induce the proliferation of T cell clone 37: $TPO_{536-547}$ and $TPO_{539-550}$ (N-IRGLLARPAKLQ-C). Although they had different anchor residues for HLA-DQ6, they shared a similar antigenic surface rather than identical sequences (Quaratino et al. 1995).

From these studies, it appeared that human T cell clone 37 presented intriguing features and further *in-vivo* studies were needed to ascertain its major role in autoimmune thyroiditis. Therefore, the generation of TAZ10 transgenic mice expressing the TCR of clone 37 was essential to understand the development of autoimmune thyroiditis and the role played by pathogenic self-reactive T cells. The extracellular domain of the human TCR$V_\beta1/V_\alpha15$ of T cell clone 37 was ligated to the intracellular domain of a mouse TCR and cloned in the TCR expression cassette VAhCD2 under the hCD2 promoter. The TCR DNA was then injected into fertilized eggs from C57BL/6 x CBA-F2 offspring females. Extensive backcrossing resulted in the generation of TAZ10 transgenic mice. Interestingly, the dual expression of the transgenic TCR by $CD4^+$ and $CD8^+$ T cells meant that they could both recognise the TPO cryptic epitope presented by APC in the context of the human HLA-DQ6 and the murine H-$2A^k$ MHC-II molecules. Transgenic T cells from TAZ10 mice recognise the human TPO cryptic epitope ($TPO_{536-547}$) and the murine equivalent ($TPO_{524-535}$, N-DPIVRGLLARAA-C) when presented in the context of murine H2-A^k MHC-II molecules. Molecular modelling of human $TPO_{536-547}$:HLA-DQ6 and human $TPO_{536-547}$:H-$2A^k$ compared with molecular modelling of human $TPO_{536-547}$:H-$2A^k$ and mouse $TPO_{524-535}$:H-$2A^k$ revealed that H-$2A^k$ and HLA-DQ6 molecules display a close similar antigenic surface of $TPO_{536-547}$ that is recognized by the same TCR $V_\beta1/V_\alpha15$. It also showed that murine $TPO_{524-535}$ and human $TPO_{536-547}$ cryptic epitope presented a similar antigenic surface despite the residue differences (amino-acids at position 3 and 11) (Quaratino et al. 2004)

TAZ10 transgenic mice spontaneously develop autoimmune thyroiditis sharing the same clinical signs of disease (gain of body weight), hormonal changes (elevated amounts of thyroid-stimulating hormone (TSH) and decreased levels of T4) and histological

modifications (destruction of the thyroid associated with mononuclear cellular infiltrates) as patients with Hashimoto's thyroiditis. Transgenic T cells from TAZ10 $Rag^{-/-}$ mice were spontaneously activated as they lacked the expression of CD62L but expressed high levels of CD44 and CD25. At 4 months of age, almost 100% of TAZ10 $Rag^{-/-}$ mice develop severe autoimmune thyroiditis (Quaratino et al. 2004). In contrast to other models of autoimmune thyroiditis (Ng et al. 2004), TAZ10 transgenic mice spontaneously develop autoimmune thyroiditis without the need for any immunization or use of adjuvant.

1.8 – Colon carcinoma CT26 mouse model

CT26 is a murine tumour of colorectal origin which is poorly immunogenic since Balb/c mice succumb to the tumour 30 days following challenge. Early experiments have shown that the vaccination of mice with CT26 tumour cells (either irradiated or transduced with GM-CSF) induces long lasting immunity in mice even in the presence of $CD25^+$ regulatory cells (Dranoff et al. 1993). This tumour immunity was mediated by $CD8^+$ CTLs specific for a single immunodominant MHC-I restricted epitope. This peptide known as AH1 (N-SPSYVYHQF-C), was identified as a non-mutated nonamer derived from the envelope protein gp70 of an endogenous ecotropic murine leukemia virus (MuLV), *emv-1*. Interestingly, gp70-specific $CD8^+$ T cells were able to lyse CT26 tumour *in-vitro* and cause tumour rejection when adoptively transferred *in-vivo* (Huang et al. 1996).

Subsequent work has shown that CT26 tumour cells are rejected in Balb/c mice following *in-vivo* depletion of $CD25^+$ Tregs using PC61 mAb. This depletion of $CD25^+$ cells conferred immunity to CT26 and also induced long-lived immunity, since the majority of CT26 immune mice were able to reject a second challenge despite the repopulation of $CD25^+$ Tregs. Most importantly, the immunity was found to be cross-protective against tumours of different histological origins such as RENCA (renal cell carcinoma), BCL-1 and A20 (B cell lymphomas) (Golgher et al. 2002). The cross-protective immunity induced in the absence of Tregs is mediated by both $CD4^+$ and $CD8^+$ T cells.

Since, in the presence of Tregs, immunisation with CT26/GM-CSF did not result in cross-protective immunity, it was suggested that the depletion of $CD25^+$ Tregs uncovers

responses to cryptic epitopes that are shared among the various tumour cell lines. GSW11 (N-GGPESFYCASW-C) was identified as the naturally processed cross-protective tumour antigen and is derived from the *gp90* gene of the endogenous ecotropic murine leukemia virus, *emv-1*. While GSW11 was generated in various tumour cell lines, the amount produced differed significantly with, for example, CT26 generating 50 times more GSW11 than A20 (James et al. 2010).

	PC61	T cell responses		Tumour rejection
		AH1	GSW11	
CT26/GM-CSF	-	++	-	YES
CT26	-	+	-	NO
	+	+++	+++	YES

Table 1.2: Summary of $CD8^+$ T cells responses to AH1 and GSW11
Although AH1-specific CTLs mediated tumour rejection in CT26/GM-CSF challenged mice, they were unable to eradicate tumour cells in CT26 challenged mice. In absence of Tregs, equivalent number of AH1 and GSW11 specific T cells could be observed in CT26 challenged mice. While the tumour was rejected, it was difficult to ascertain whether the rejection was the focus of AH1-specific or GSW11-specific CTLs.

In contrast to AH1-specific T cell responses present in both naive and Tregs depleted mice, GSW11-specific T cell responses are only observed when Tregs are depleted prior to CT26 challenge (Table 1.2). The appearance of GSW11-specific T cell responses indicated the broadening of the anti-tumour responses in the absence of Tregs rather than the acquisition of a more potent effector function (James et al. 2010). In addition, GSW11-specific T cells were shown to be more dependent on IL-2 for their growth and activation than AH1-specific T cells. As Tregs are known as a "cytokine sink" due to their high consumption of IL-2 (Scheffold et al. 2005), this could explain why GSW11-specific responses are only revealed in absence of Tregs.

AIMS:

The aim of this project was to characterize the impact of Myeloid Derived Suppressor Cells (MDSC) in the TAZ10 mouse model of autoimmune thyroiditis. I have assessed the mechanisms displayed by MDSC to inhibit T cell responses and determined whether inhibitory MDSC could be used *in-vivo* as a therapeutic tool in TAZ10 mice to control the progression of the disease. I have also investigated why this regulatory network fails to prevent the development of AID. Finally, I evaluated the impact of MDSC on the generation of anti-tumour responses in the CT26 tumour model.

2 - Material and Methods

2.1 - Mice and Cell lines

Wild-type (WT) C57Bl/6 (H-2K^b background), BALB/c (H-2K^d background), Rag2-deficient (Rag$^{-/-}$, H-2K^b background), TAZ10 Rag$^{+/+}$ and Rag-deficient transgenic mice (H-2K^b background), CCIA transgenic mice (H-2K^q DBA/1 background), B6.eYFP and TAZ10 Rag$^{+/+}$ x B6eYFP (H-2K^b background) mice were housed and bred in the Tenovus animal facility in accordance with Home Office institutional guidelines for animal welfare.

B6.eYFP mice with ubiquitous expression of eYFP were a generous gift from Dr Alexander Potocnik (National Institute for Medical Research, London, UK) and were generated as described in Belyaev et al. 2010. CCIA mice (DBA/1 human TCR-V$_\beta$12) develop chronic arthritis upon immunization with collagen type II in Complete Freund's Adjuvant (CFA). 16 to 20 days after immunization, CCIA mice develop arthritis showing similar clinical signs of disease than patients with rheumatoid arthritis (Mauri et al. 1997). All mice were used between 4 to 30 weeks of age. TAZ10 Rag$^{-/-}$ and Rag$^{-/-}$ mice were maintained under specific pathogen-free conditions.

The CT26-GM cell line used in this study for the production of GM-CSF is derived from the CT26 colon carcinoma genetically modified to secrete GM-CSF (Dranoff et al. 1993). Culture supernatant was spun down, filtered and the resulting cell-conditioned medium was used as a source of GM-CSF. The concentration of GM-CSF was assessed by ELISA (Biosource, UK) and ranged from 200 to 400 ng/mL. The B3Z hybridoma cell line is a lacZ inducible CD8$^+$ T cell hybrid specific for OVA$_{257-264}$ peptide (SIINFEKL or SL8) in the context of H-2K^b MHC-I molecules. The CCD2Z hybridoma cell line is also a lacZ inducible CD8$^+$ T cell hybrid specific for GSW11 peptide (GGPESFYCASW) in the context of H-2D^d MHC-I molecules. The K89 cell line is L cells stably transfected with H-2K^b. Cell lines were maintained in culture media consisting of RPMI-1640 medium (Cambrex, UK) supplemented with 10% heat-inactivated Foetal Calf Serum (FCS) (Globepharm, UK), 0.3 mg/mL L-glutamine (Cambrex, UK), 100 U/mL Penicillin/streptomycin, 1mM non essential amino-acids and 1 mM sodium pyruvate (All from Lonza, UK).

2.2 – Tumour cells

The B16 melanoma and CT26 murine colon carcinoma cell lines were maintained in RPMI-1640 medium (Cambrex, UK) supplemented with 10% heat-inactivated Foetal Calf Serum (FCS) (Globepharm, UK), 0.3 mg/mL L-glutamine (Cambrex, UK), 100 U/mL Penicillin/streptomycin, 1mM non essential amino-acids and 1 mM sodium pyruvate (All from Lonza, UK). In all experiments, mice were injected subcutaneously with 1 x 10^5 tumour cells in 1X PBS. Mice were sacrified when mean tumour diameter was >15mm in accordance with Humane end-point Guidelines. Mice showing any signs of distress before reaching the end point were humanly culled following methods stated in schedule 1 of the project licence.

2.3 – Flow Cytometry and Antibodies

Cells were collected in cold FACS buffer (1X PBS supplemented with 1% FSC and 0.05% sodium azide) and stained using antibodies conjugated to fluorescein isothiocyanate (FITC), phycoerythrin (PE), peridinin chlorophyll protein (PerCp) and allophycocyanin (APC). Tandem conjugates were also used: cyanin dye (Cy7, Cy5 and Cy5.5) combined to phycoerythrin (Pe-Cy7 and Pe-Cy5), to allophycocyanin (APC-Cy7) or peridinin chlorophyll protein (PerCpCy5.5). Cells were stained for MHC class-I (**H-2K^b**, mouse IgG2b, clone AF6-88.5, BD Pharmingen), MHC class-II (**I-A^b**, Rat IgG2b, clone M5/114.15.2, BD Pharmingen), **CD4** (rat IgG2b, clone RM4-5, BD Pharmingen), **CD11b** (rat IgG2b, clone M1/70, eBiosciences), **CD11c** (N418, Hamster IgG, BD Pharmingen), **CD25** (rat IgM, clone PC61.5, eBiosciences), **CD62L** (mouse IgG1, clone DREG-56, eBiosciences), **CD86** (rat IgG2a, clone GL1, eBiosciences), **Gr1** (rat IgG2b, clone RB6-8C5, eBiosciences), **F4/80** (rat IgG2a, clone BM8, eBiosciences), **Foxp3** (rat IgG2a, clone FJK-16s, eBiosciences) and human **TCR-V$_\beta$1** (rat IgG1, clone BL37.2, Beckham Coulter). Detection of Foxp3 was performed by intracellular staining using the Foxp3 staining kit (eBiosciences, UK) according to the manufacturer's instructions. Briefly, cells were stained for cell surface markers before being fixed and permeabilised using the Fixation/Permeabilisation buffer for one hour at 4ºC in the dark. Cells were washed with Permeabilisation buffer and incubated with the relevant

antibody for 30 minutes at 4ºC in the dark. Cells were then washed twice in Permeabilisation buffer before being analysed.

Samples were run through a FACSCanto II flow cytometer and data were analysed using the FACS Diva (BD Biosciences, USA) and FlowJo software (Treestar, USA) softwares. In some experiments, cells were sorted on FacsAria (BD Biosciences, USA) according to their expression of eYFP or H2-K^b molecules.

2.4 – Antibody production and *in-vivo* depletion

Hybridomas secreting αCD25 (PC61, rat IgG1), αCD4 (YTA 3.1.2, rat IgG2b), αGITR (DTA.1, rat IgG2b) and αGr1 (RB6-8C5, rat IgG2b) monoclonal antibodies (mAb) were cultured in CL-1000 Integra cell line flasks (Integra Biosciences, UK) in RPMI-1640 medium (Cambrex, UK) supplemented with 10% heat-inactivated IgG depleted Foetal Calf Serum (FCS) (Autogen-Bioclear, UK), 0.3 mg/mL L-glutamine (Cambrex, UK), 100 U/mL Penicillin/streptomycin, 1mM non essential amino-acids and 1 mM sodium pyruvate (All from Lonza, UK). Cells were split twice a week and supernatants were collected.

αCD25, αCD4 and αGITR mAb were purified by precipitation in saturated ammonium sulphate in endotoxin-free conditions and extensively dialysed against endotoxin-free 1X PBS. αGr1 mAb was purified by affinity chromatography on protein G columns (Sigma, UK). For depletion, mice were given two intraperitoneal (i.p) injections of 300µg mAb in 100µl 1X PBS. The antibodies were administered 3 and 1 day prior to the injection of tumour cells, adoptive transfer of cells or the sacrifice of mice.

2.5 – Isolation of T cells and $Gr1^+$ cells from WT and TAZ10 mice

Where indicated, $Gr1^+$ cells and T lymphocytes and were enriched from spleens or bone-marrow of WT, B6.eYFP, TAZ10 $Rag^{+/+}$ or $Rag^{-/-}$ transgenic mice using the MACS magnetic technology (Myltenyi Biotech, Germany). Briefly, single-cell suspensions were obtained by passing the tissues through a 70µM cell strainer (BD Pharmingen, UK). Red

blood cells were lysed by treating the cell suspension in ACK red blood cell lysis buffer (155 mM NH_4Cl, 10 mM $KHCO_3$ and 0.1 mM EDTA in 1X PBS, pH 7.4). Splenocytes and bone-marrow cells were resuspended in cold MACS buffer (2mM EDTA and 0.5% BSA in 1X PBS).

To isolate $CD4^+$ and $CD8^+$ T cells, cells were incubated with magnetic microbeads coated with mAb to CD4 (clone L3T4) and CD8 (clone Ly-2) for 15 minutes at 4ºC. Excess of free microbeads was washed away with MACS buffer and labelled cells were passed through a separating column on a magnetic field. In all experiments, purity was assessed by flow cytometry analysis and exceeded 90%.

The isolation of $CD4^+$ $CD62L^+$ naive T cells was performed using the mouse $CD4^+$ $CD62L^+$ T cell isolation kit II according to the manufacturer's instructions (Myltenyi Biotech, Germany). Briefly, non-$CD4^+$ T cells were depleted by indirect magnetic labelling with a cocktail of biotin-conjugated antibodies and anti-biotin microbeads. The labelled cells were subsequently depleted over a MACS column. In the second step, $CD4^+$ $CD62L^+$ T cells are directly labelled with CD62L microbeads and isolated by positive selection from the pre-enriched $CD4^+$ T cell fraction. Purity of the fraction was assessed by flow cytometry and was above 90%.

To isolate $Gr1^+$ cells, single-cell suspensions from the spleen or bone-marrow were incubated with magnetic particles conjugated with mAb to Gr1 (clone RB6-8C5, BD Biosciences, USA) for 30 minutes at 4ºC. Cells were run through a separating column (Myltenyi Biotech, Germany) on a magnetic field and the purity of the isolation was above 80% - 90% as evaluated by flow cytometry analysis

2.6 – Generation of bone-marrow derived dendritic cells

Bone-marrow derived dendritic cells (BM-DC) from 4 to 12 week old WT mice were generated following Lutz method (Lutz et al. 1999) with modifications. Marrow from femurs and tibiae was flushed-out and red blood cells lysed in ACK buffer. DC were generated in DC-medium: RPMI-1640 medium (Cambrex, UK) supplemented with 10% low-endotoxin FCS (Autogen-Bioclear, UK), 0.3 mg/mL L-glutamine (Cambrex, UK), 100 U/mL

penicillin/streptomycin, 1mM non essential amino-acids and 1 mM sodium pyruvate (Lonza, UK).

At Day 0, 2 x 10^6 cells were seeded in 100 mm petri-dishes in 10 mL DC medium supplemented with 25% of CT26-GM cell-conditioned medium as a source of GM-CSF to give a final concentration of GM-CSF of 20ng/ml. At Day 3, 10 mL of fresh DC-medium supplemented with GM-CSF was added to each culture dish. At Day 6 and 8, 10 mL of the culture medium was collected, centrifuged, the cell pellet resuspended in 10mL of fresh GM-CSF containing DC-medium and seeded back into the original petri-dishes. Immature DC obtained at Day 10 were harvested and seeded at 2 x 10^6 cells per well of a 6 well-plate.

For complete maturation, lipopolysaccharide (LPS) from *Escherichia Coli E26:B6* (Sigma, UK) was added at 1µg/ml per well on Day 11 and the cells cultured for a further 18 hours.

2.7 – T cell proliferation assay by (^{3}H) thymidine incorporation

The ability of myeloid derived suppressor cells (MDSC) to inhibit T cell proliferation was assessed by (^{3}H) thymidine incorporation. Briefly, freshly isolated splenocytes were cultured in triplicate in 96 well plates at 2.5 x 10^5 or 4 x 10^5 cells per well in culture medium containing soluble αCD3 (clone RC5-4C11, CRUK) at 10µg/mL with or without soluble αCD28 (clone 37.51, made in house) and/or $TPO_{536-547}$ (N-DPLIRGLLARPA-C) peptide (P3 peptide) at 0.1µg/mL. Where indicated mature BM-DC were used as antigen presenting cells and seeded at a DC:T ratio of 1:30 while $Gr1^+$ MDSC were added at a T:MDSC ratio of 1:1 or 5:1.

Cells were co-cultured for 72 hours at 37°C in 5% CO_2. Each well was then pulsed with 1 µCi (^{3}H) thymidine for the last 18 hours of culture. Plates were harvested onto filtermate (Perkin Elmer, UK) and (^{3}H) thymidine incorporation was measured using a microplate scintillation counter (Packard, USA). Data are expressed in cpm (count per minute) and were plotted as mean average of the triplicates.

2.8 – Measurement of intracellular nitric oxide (NO) by flow cytometry

Intracellular NO concentration was measured using the DAF-FM diacetate probe (Molecular Probes, USA). DAF-FM diacetate is cell-permeant and passively diffuses across cellular membranes. Once inside cells, it is deacetylated by intracellular esterases to DAF-FM. This compound is virtually nonfluorescent until it reacts with NO to form a fluorescent benzotrizole with an excitation/emission maxima of 495/515 nm detectable by flow cytometry analysis.

10^6 splenocytes were incubated for 1 hour at 37°C in phenol-red free RPMI medium (Sigma, UK) containing 5µM DAF-FM diacetate. Cells were washed in medium to remove excess probe and incubated for an additional 20 minutes to allow complete de-esterification of the intracellular diacetates. Cells were then washed in cold 1X PBS and stained for Gr1 and CD11b markers to allow for the analysis of $Gr1^+$ $CD11b^+$ MDSC. Samples were analysed by flow cytometry.

2.9 – Determination of NO production using the Griess method

Concentration of NO was measured using the Griess reaction. Nitrites resulting from the breakdown of NO react with sulfanilic acid in acidic solution to form an intermediate diazonium salt. This intermediate salt coupled to N-(1-naphthyl)ethylenediamine (NED) forms a purple azo derivative that can be monitored by reading the absorbance at 550 nm.

Briefly, cells were seeded at 4 x 10^5 in 100µL in 96 well U-bottom plates in the presence of αCD3 and αCD28 antibodies. After 72 hours, the amount of NO released in the medium was measured using the Griess reagent system (Promega, UK). Briefly, 50µL of culture supernatant was incubated in the dark with 50µL sulfamilamide solution (1% sulfamilamide in 5 % phosphoric acid) for 10 minutes at room temperature (RT). The same volume of NED solution (0.1% N-1-napthylethylenediamine dihydrochloride in water) was added to the reaction and the plate incubated for a further 20 minutes in the dark. The absorbance at 550 nm was read on Biorad model 680 plate reader using Microplate manager software (BioRad, UK). Measurements were performed in duplicate and NO concentrations

were determined by comparing the absorbance values obtained for the sample to the standard curve generated by the serial dilution of a 0.1M nitrite sodium solution.

To investigate the role of NO in the MDSC mediated inhibition of T cell response, the NG-Monomethyl-L-arginine (L-NMMA) (Calbiochem, UK) inhibitor of the inducible nitric oxide synthase (iNOS) was added to the cells at 500µM. An arginase inhibitor, NG-Hydroxy-L-arginine (NOHA) (Calbiochem, UK) was also used when mentioned at the same concentration.

2.10 – Adoptive transfer of purified $Gr1^+$ cells

Purified $Gr1^+$ cells were purified from the spleens and bone-marrows of WT or TAZ10 $Rag^{+/+}$ mice. Cells were resuspended in 1X PBS and injected intravenously into the lateral vein at the basis of the tail of $Rag^{-/-}$ and $Rag^{+/+}$ TAZ10 mice. Weight and survival were recorded on a weekly basis as a readout of hypothyroidism (Quaratino et al. 2004). Mice were culled at the end of the experiment and their thyroid was cryopreserved in OCT (RA Lamb, Thermo Fisher Scientific) for further histological analysis.

For *in-vivo* differentiation experiments, $Gr1^+$ cells were purified from the spleens of B6.eYFP mice. Cells were resuspended in 1X PBS and injected intravenously into the lateral vein at the basis of the tail of the $Rag^{-/-}$ and TAZ10 $Rag^{-/-}$ mice. Mice were sacrified 7 days after adoptive transfer and tissues harvested. Cells were stained for specific markers and analysed by flow cytometry. In some experiments, cells were sorted on FACSAria (BD Biosciences, USA) according to their expression of eYFP and then used in (^3H) thymidine incorporation assays (Chapter 2, paragraph 2.7).

For the experiments of the *in-vivo* differentiation of MDSC at the onset of the disease, $Gr1^+$ cells were purified from the bone-marrow of B6.eYFP mice. Cells were resuspended in 1X PBS and injected intravenously into the lateral vein at the basis of the tail of the $Rag^{-/-}$ mice. 2 days later, mice were adoptively transferred with naive T cells purified from the spleen of WT and TAZ10 $Rag^{-/-}$ mice as described paragraph 2.13. Mice were then sacrified

3, 5, 7 and 21 days after adoptive transfer and tissues harvested. Cells were stained for specific markers and analysed by flow cytometry.

2.11 – Induction of Foxp3$^+$ Tregs by MDSC

The ability of MDSC to induce the *de-novo* development of Foxp3$^+$ Tregs was investigated. Briefly, freshly isolated splenocytes from TAZ10 Rag$^{-/-}$ mice were cultured in 96 well plates at 4 x 10^5 cells per well in culture medium in absence or presence of $TPO_{536-547}$ (N-DPLIRGLLARPA-C) peptide (P3 peptide) at 2μg/mL. Where indicated Gr1$^+$ MDSC purified from the spleen of CD4 depleted TAZ10 Rag$^{+/+}$ mice were added at a SN:MDSC ratio of 1:1 or 5:1. Cells were co-cultured for 72 hours at 37°C in 5% CO_2. The level of expression of the transcription factor Foxp3 was then investigated by flow cytometry using the Foxp3 staining kit (eBiosciences, UK) according to the manufacturer's instructions and as described in 2.3.

To investigate the role of TGF_β in the MDSC-mediated induction of Tregs, a monoclonal anti-$TGF_{\beta1}$ neutralizing antibody was added to the cells at 1μg/ml (R&D systems, UK) as well as recombinant human $TGF_{\beta1}$ used at 2ng/ml and 10ng/ml (eBiosciences, UK). The requirement for cell-cell contact was assessed using HTS Transwell-24 well permeable supports (Corning Life Sciences, US)

2.12 – Peptide extraction

The following protocol was used to extract peptides from cells and their subsequent use in immunological assays. Briefly, MDSC and BM-DC (1 x 10^6 or 2 x 10^6) were pulsed with 1mg/ml ovalbumin (OVA, albumin from chicken egg white grade VI, Sigma, UK) for 8 hours. After the incubation, cells were washed twice in 1X PBS and lysed in 10% acetic acid for 10 minutes at 95ºC. Samples were then centrifuged at maximum speed for 15 minutes to pellet the cell debris. Extracts were passed through a 10kDa cutoff filter (Millipore, USA)

and the filtrate was dried in a vacuum centrifuge (Thermo Scientific, USA). The pH of the extracts was adjusted to pH 7 using phenol red and left on ice for 30 minutes to allow the peptides to enter solution. Peptide extracts were used in T cell activation assays using B3Z T cells and the presence of SL8 peptide in MDSC or DC assessed.

For the detection of P3 peptide, thyroids, spleens, cervical and inguinal lymph nodes were isolated from up to 80 WT mice. Tissues were processed and passed through a cell strainer. Cells were then lysed in 10% formic acid for 10 minutes at 95ºC and centrifuged to pellet the membranes. Supernatants were passed through a 30kDa cutoff filter (Millipore, USA) by centrifugation and the pH of the extracts adjusted as previously described. The different peptide extracts were then tested for their ability to promote the proliferation of TAZ10 T cells cultured with mature DC.

2.13 – T cell activation assay

The processing of OVA and presentation of the H-2K^b MHC-I restricted OVA$_{257-264}$ peptide (SIINFEKL or SL8) was assessed using the B3Z T cell hybridoma. B3Z is a lacZ inducible CD8$^+$ T cell hybridoma specific for SL8 peptide presented by murine H-2K^b (K^b) MHC-I molecules. The recognition of the K^b/SL8 complex by B3Z cells results in the IL-2 dependent induction of β-galactosidase (β-gal) synthesis and its intracellular accumulation. The amount of β-gal produced by B3Z cells can be measured by the hydrolysis of the chromogenic substrate chlorophenolred-β-D-galactoside (CPRG) and gives a qualitative indication of the amount of SL8/K^b complexes presented at the surface of the cells of interest.

The assay was performed in 96-well U-bottom plates. Used as antigen presenting cells in the assay, K89, mature DC or MDSC were plated at 5 x 10^4 cells per well and pulsed with the SL8 synthetic peptide or the specific peptide extract. In some experiments, MDSC and DC were pulsed for 8 hours with OVA at 1mg/ml prior to the experiment being performed. After overnight co-incubation with B3Z T cell hybridoma (1 x 10^5 cells per well), cells were washed and lysed by the addition of 100µL of a solution containing 100mM 2-mercaptoethanol, 9mM $MgCl_2$, 0.125% NP40 and 0.15mM CPRG in 1X PBS. The amount of lacZ enzyme was quantified by the hydrolysis of CPRG, which produces chlorophenol red

with an absorbance at 595nm. The absorbance of each well was read using a Biorad model 680 plate reader using Microplate manager software (Biorad, UK).

2.14 – CSFE labelling of T cells for *in-vivo* tracking

Purified naive T cells from WT or TAZ10 $Rag^{-/-}$ mice were washed twice in 1X PBS and resuspended at 1 x 10^7 cells/ml. Cells were incubated with 5μM of CFSE at 37ºC in the dark for 15 minutes and then washed three times in 1X PBS. Cells were resuspended in 1X PBS and 2 x 10^6 cells were injected into $Rag^{-/-}$ mice intravenously into the lateral vein at the base of the tail. After 1, 2, 3, 4 or 7 days depending on the experiment, cardiac blood samples were collected from mice under anaesthesia in accordance with Home Office institutional guidelines for animal welfare. Mice were culled and spleen, bone marrow, cervical and inguinal lymph nodes, and thyroids were harvested. Thyroids were cryopreserved in OCT (RA Lamb, Thermo Fisher Scientific) for further histological analysis. Tissues were processed and cells were stained for specific cell-surface markers and analysed by flow cytometry.

2.15 – CSFE labelling of proteins

Carboxyfluorescein succinimidyl ester (CFSE, Invitrogen, UK) was used to label 1mg OVA. Succinimidyl esters are preferred reagents for the conjugation to proteins because they form a very stable amide bond between the dye and the protein. Briefly, 1.5mg/ml CFSE in anhydrous DMSO was added to 1mg OVA in 1X PBS and the solution was incubated overnight in the dark at 4ºC with continuous gentle agitation. Labelled proteins were separated from free fluorescein compound by extensive dialysis versus 1X PBS. Protein concentration was determined using Micro BCA ProteinAssay kit (Thermo Scientific, UK

2.16 – Opsonisation of latex beads for use in phagocytosis assay

Surfactant-free 3.0μM sulphate white polystyrene latex beads (Interfacial Dynamics Corporation, UK) were opsonised with non-specific mouse IgG (Dako, UK) for Fc-mediated phagocytosis.

After two washes in 1X PBS, beads were resuspended in 1X PBS with 100 μg IgG for 2 hours at RT before being washed in 1X PBS and added immediately to purified MDSC or BM-DC for phagocytosis assay. 100μL IgG-opsonized latex beads were immediately added to the cells (MDSC or BM-DC) and incubated for 45 minutes at 37ºC to allow the cells to phagocytose the beads. Free latex beads were washed away and cells were assessed for beads internalization by confocal microscopy.

2.17 – ELISA

Production of cytokines was assessed by ELISA. Supernatants were tested for cytokine content such as IL-10 and GM-CSF (All purchased from R&D Systems, UK). Flat-bottom 96-well maxisorp plates (Nunc, UK) were coated overnight at RT with capture antibody diluted in 1X PBS (100μL per well). Capture antibody was discarded and plate was washed three times with washing-buffer (0.05% Tween-20 in 1X PBS, pH 7.2-7.4) by inverting the plate onto clean paper towels. Plate was blocked for a minimum of 1 hour with 300μL of blocking-buffer (1% BSA in 1X PBS, pH 7.2-7.4) per well at RT. Plate was washed three times as previously described and 100μL of standard or sample diluted in blocking-buffer was added per well and the plate incubated at RT for 2 hours. Plate was washed as previously described and biotinylated detecting antibody diluted in blocking-buffer was added (100μL per well) and incubated for 2 hours at RT. Wells were washed 3 times with washing-buffer and 100μL/well of a 1:1000 dilution of avidin alkaline-phosphatase (Sigma, UK) in blocking-buffer. Plate was incubated for a further 40 minutes at AT. After 3 washes, 100μL Sigmafast pNPP substrate (Sigma, UK) was added per well and colour development was assessed. Absorbance was read on Biorad model 680 plate reader using Microplate manager software (BioRad, UK) at 405 nm. Results were analysed and graphs plotted using Prism 4 (GraphPad

2.18 – Fluorescence microscopy

When fluorescent microscopy was performed on MDSC and DC, coverslips were pre-coated with poly-L-lysine (Sigma, UK) for 10 minutes at RT and washed three times with 1X PBS.

Cells were washed 3 times with 1X PBS and stain for extracellular markers before being fixed using 4% paraformaldehyde (PFA) in 1X PBS for 7 minutes at RT. PFA was washed off by rinsing the cells 3 times in 1X PBS. Cells were permeabilised in 0.1% Triton X-100 in 1X PBS for 7 minutes at RT and then washed 3 times in 1X PBS before being incubated in 3% BSA in 1X PBS for 45 minutes at RT. Specific antibodies were added at the appropriate concentration in 1X PBS containing 1% BSA (Sigma, UK) to the cells and incubated for 20 minutes at RT in the dark. Coverslips were washed 3 times in 1X PBS and the secondary antibody added in 1X PBS with 1% BSA for a further 20 minutes at RT in the dark. Cells were washed three times and the nucleus was counterstained with DAPI (Molecular Probe, UK) added at 1 μg/mL in 1X PBS with 1% BSA for 10 minutes at RT in the dark. Coverslips were washed 4 times in 1X PBS and mounted on a slide with mounting medium (Vector Laboratories, Burlingham, CA). Slides left overnight in the dark at 4° C to allow the mounting medium to harden were then read on a confocal microscope (Leica, Germany) at x40 magnification and data analysed using Leica Microsystems LAS software (Leica, Germany)

For the detection of calnexin, rabbit mAb to canine calnexin (Stressgen, USA) and cross reactive with mouse calnexin was used. Secondary antibody was a goat anti-rabbit Alexa-Fluor 488 conjugate (Molecular Probes, USA). Cells were stained for MDSC specific marker using αCD11b biotinylated antibody (rat IgG2a,κ, clone M1/70, eBiosciences) associated with streptavidin Alexa-Fluor 546 conjugate (Molecular Probes, USA) and anti-Gr1 Alexa-Fluor 647 (rat IgG2a,κ, clone RB6-8C5, eBiosciences).

2.19 – Histology

Thyroids were frozen embedded by immersion in OCT (RA Lamb, Thermo Fisher Scientific) and placed on top of vapours of liquid nitrogen. 10 μm frozen sections were fixed in dry acetone for 10 minutes at RT, washed 3 times with 1X PBS for 5 minutes. Sections were then blocked for 30 minutes with 5% normal goat serum in 1X PBS and incubated for 2 hours with FITC-conjugated rat αGr1 (clone RB6-8C5, eBiosciences) and APC-conjugated rat αCD11b (clone M1/70, eBiosciences). For cytokeratin detection, mouse mAb to human cytokeratin 5, 6, 8, 17 and probably 19 (clone MNF116; Dako-Denmark) and cross reactive with mouse cytokeratin was used. Secondary antibody was a FITC-labelled rabbit antibody to mouse F(ab)'2 (DakoCytomation). Sections were washed 3 times with 1X PBS, counterstained with Sytox Orange (Molecular Probes, USA) for 20 minutes and mounted in Vectashield (Vector Laboratories, Burlingham, CA). Images were collected sequentially with a Leica SP5 CLSM using 488 nm, 543 nm and 633nm lasers and a pinhole equivalent to 1 Airy disc with HCX PL APO lambda blue 20.0x0.70 IMM UV and HCX PL APO CS 40.0x1.25 OIL UV objective lenses. Images (TIFF) files were transferred to Adobe Photoshop (CS4, Version 11.0.2) and contrast stretched to use the whole grey scale.

2.20 – Quantitative PCR

Total RNA was isolated from CT26 cells, MDSC and $Gr1^-$ $CD11b^-$ cells purified from the spleen of Balb/c mice using Tri reagent (Sigma). Cells were lysed and total RNA obtained by extraction in phenol/chloroform and precipitation in isopropanol. RNA was washed twice in 75% ethanol diluted in DEPC-treated water and resuspended in 30μl DEPC-treated water.
cDNA synthesis was then performed using 1μg RNA and the reverse transcriptase reaction mix containing M-MLV RT buffer 5X, 10 units ribonuclease inhibitor, 0.025mM Oligo dT, 1.25mM NTPs and 200 units M-MLV reverse transcriptase (Promega, UK).
The level of expression of gp90 gene (forward primer: 5'-ATA GGG CCA AAC CCC GTC-3'; reverse primer: 5'-GGA GAT CTG GTG GGT CTA GGC-3'; probe: 5'-FAM TGT CAG ACC GAC GAC CAC CTT CCC TAMRA-3') and Foxp3 (forward primer: 5'-CCC AGG

AAAA GAC AGC AAC CTT-3'; reverse primer: 5'-TTC TCA CAA CCA GGC CAC TTG-3'; probe: 5' –FAM ATC CTA CCC ACT GCT GGC AAA TGG AGT C TAMRA-3') were quantified by real-time PCR and normalised against βactin gene (forward primer: 5'-GCA ACG AGC GGT TCC G-3'; reverse primer: 5'-CAG GAT TCC ATA CCC AAG AAG G-3'; probe: 5'- FAM TGC CCT GAG GCT CTT TTC CAG CC TAMRA-3'). Real-time PCR was performed using 7500 real time PCR system (Applied Biosystems).

2.21 - Statistical analysis

Statistical differences between groups were determined with the unpaired Student's t-test using Prism software (GraphPad, USA). Values of probability were considered as significant when $p < 0.05$.

3 – Characterisation of Myeloid Derived Suppressor Cells (MDSC) in TAZ10 transgenic mice

3.1 – Introduction

Autoimmune diseases (AID) are chronic inflammatory diseases associated with the infiltration of tissues by monocytic cells and the release of soluble factors such as chemokines and cytokines (IFN-γ, TNFα and IL-1β) (Vanderlugt and Miller, 2002). One explanation for the occurrence of AID is the failure of physiological mechanisms responsible for the maintenance of peripheral tolerance to self-antigens (paragraph 1.4.2), thus favouring the activation and expansion of autoreactive T and B cells leading to tissue destruction. Key components of this regulatory network, $CD25^+$ $Foxp3^+$ Tregs contribute to the maintenance of tolerance to self-antigens and their depletion, functional or quantitative deficiency has been linked to the development of various organ-specific AID (Sakaguchi et al. 1995; Suri-Payer et al. 1998). In recent years, another cell subset playing an important role in maintaining peripheral tolerance has been described. Myeloid-Derived Suppressor Cells (MDSC) are a heterogeneous cell population of myelomonocytic lineage, comprising cells at various stages of differentiation that can give rise to macrophages, granulocytes and/or dendritic cells depending on the nature of the microenvironment characterised by the balance between pro- versus anti-inflammatory factors.

The expansion of MDSC has been largely described in cancer patients and tumour-bearing mice where MDSC accumulate in the tumour and peripheral lymphoid tissues (Almand et al. 2001; Bronte et al. 1999). Primarily released by tumour cells, various factors such as VEGF, GM-CSF, IL-6 and IL-1β promote the recruitment of MDSC at the tumour site while preventing their ability to differentiate into mature myeloid cells (Melani et al. 2003; Serafini et al. 2004; Gabrilovich et al. 2004). Mainly characterised by the expression of the myelomonocytic markers Gr1 and CD11b in mouse, MDSC have been shown to inhibit the activity of anti-tumour specific T cells thus promoting tumour growth (Kusmartsev et al. 2000; Bronte et al. 2003). As a consequence, various therapeutic strategies targeting MDSC have been developed by either inhibiting their expansion and function (Talmadge et al. 2007), favouring their differentiation into mature myeloid cells (Kusmartsev et al. 2003) or promoting their depletion *in-vivo* (Ko et al. 2007; Suzuki et al. 2005).

It is now evident that there is a correlation between anti-tumour responses and AID. Indeed, if the development of vitiligo is a good prognostic factor in patients with melanoma

(Yee et al. 2000), the frequency of Hashimoto's thyroiditis is increased in patients with thyroid carcinoma (Roberts et al. 2004). While the inhibitory function and detrimental role of MDSC in cancer has been largely studied (Marigo et al. 2008), it remains unclear whether MDSC have any regulatory activity in autoimmunity. To address their role in AID, I used the TAZ10 humanised TCR transgenic mouse model of autoimmune thyroiditis. In this model, T cells express a human TCR isolated from a thyroid infiltrating T cell clone from a patient with Hashimoto's thyroiditis. TAZ10 transgenic mice spontaneously develop autoimmune hypothyroiditis sharing the same clinical signs of disease, hormonal imbalances and histological modifications as patients with Hashimoto's thyroiditis (Quaratino et al. 2004).

I therefore investigated the role and functions of MDSC in the TAZ10 mouse model of autoimmune thyroiditis and assessed their ability to control the activation and function of self-reactive T cells.

3.2 – Results Part 1: MDSC accumulate in TAZ10 mice and display inhibitory functions on T cells

AID arise from the breakdown of immunological tolerance to self-antigens. If mechanisms of peripheral tolerance fail to suppress the activation and expansion of self-reactive T cells, the destruction of a specific target tissue occurs. While $Foxp3^+$ Tregs are critical to keep these pathogenic self-reactive T cells at bay, MDSC have also been described to be part of this regulatory network. Their role in promoting tumour expansion has been extensively studied and MDSC have been shown to accumulate in tumours and lymphoid organs of tumour models and cancer patients where they inhibit T cell proliferation and function (Song et al. 2005, Bunt at al. 2006). In this respect, in C57BL/6 mice challenged with the B16 melanoma tumour cell line, $Gr1^+$ MDSC exert a strong inhibition on T cells in response to the agonistic αCD3 antibody. The addition of αCD28 antibody could not abrogate the strong inhibition displayed by MDSC on T cells (Figure 3.1).

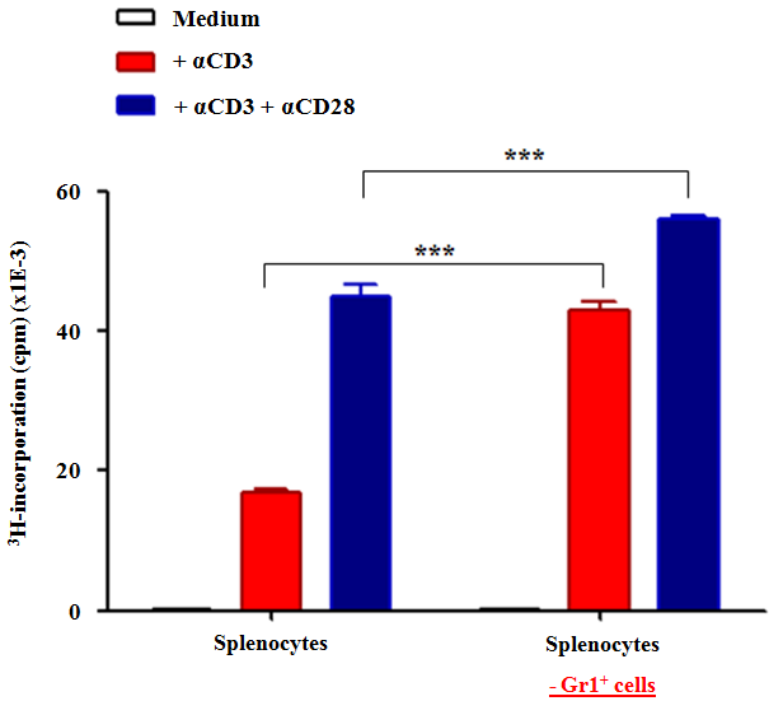

Figure 3.1: MDSC inhibit T cell proliferation in mice challenged with the B16 melanoma cell line
Untreated and Gr1 depleted splenocytes from C57BL/6 mice injected with B16 tumour cells were stimulated with either αCD3 or αCD3-αCD28 agonistic antibodies. Their proliferative activity was assessed by (^{3}H) thymidine incorporation assay. Data are representative of more than 3 experiments and statistics were performed using the unpaired Student's t-test.

In these mice, an accumulation of MDSC was also observed in the bone marrow and various secondary lymphoid tissues 7 and 15 days after tumour challenge (Figure 3.2). Interestingly, MDSC were recruited in the lymph nodes draining and not draining the B16 tumour while being absent in the LN of unchallenged mice. Their presence in lymph nodes not draining the tumour can be explained by the ability of the tumour to quickly metastasize into the lungs (Alterman et al. 1985).

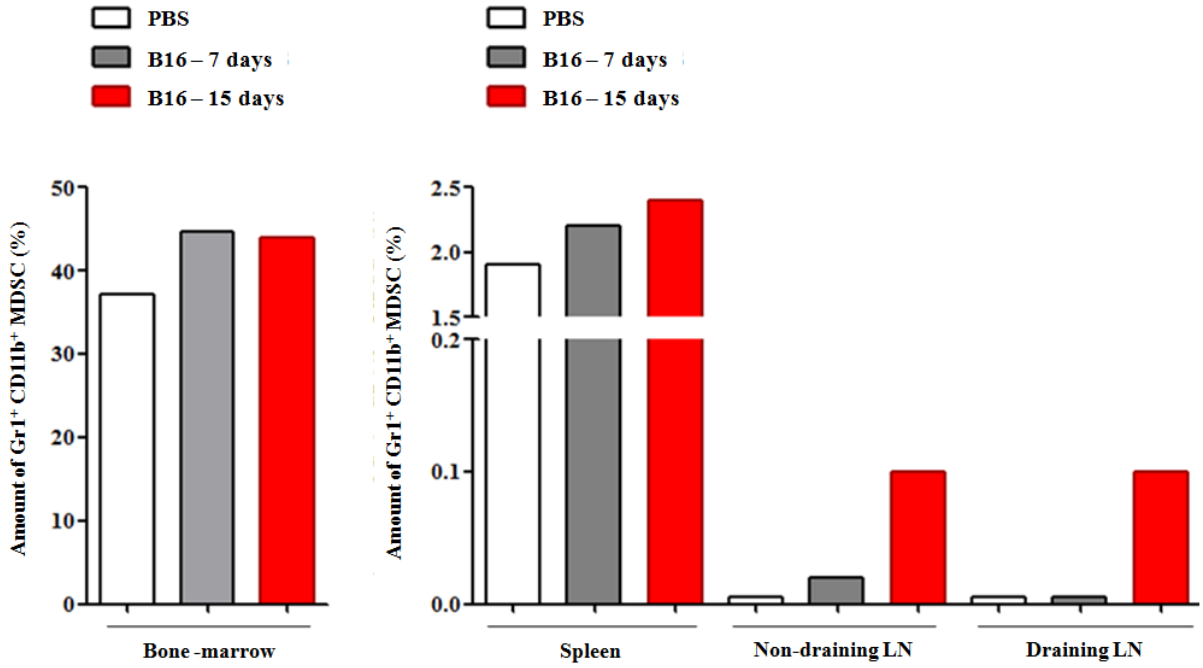

Figure 3.2: MDSC accumulate in lymphoid and non-lymphoid tissues of B16 treated mice
Accumulation of $Gr1^+$ $CD11b^+$ MDSC in the bone marrow, the spleen and lymph nodes (LN) draining and not-draining the tumour in mice challenged with the melanoma B16 tumour cell line. Data shown are representative of one experiment involving 4 mice (1 control mouse injected with PBS and 3 injected with B16) out of two different experiments.

Considering the crucial role of MDSC in cancer, I wanted to explore their function in a model of chronic inflammatory disease such as autoimmune disease. While the importance of regulatory T cells has already been studied in the TAZ10 transgenic mouse model of autoimmune thyroiditis (Ester Badami's PhD Thesis – July 2007), I wanted to address whether MDSC were present and played any role in this model.

3.2.1 – Gr1$^+$ CD11b$^+$ MDSC are present in TAZ10 transgenic mice

Because TAZ10 mice develop autoimmune thyroiditis, MDSC are unable to prevent the activation of self-reactive T cells. I therefore suggested that their number was drastically reduced and/or that their inhibitory function was altered.

By two-colour FACS staining, I investigated the presence of Gr1$^+$ CD11b$^+$ MDSC in the spleen of TAZ10 transgenic mice of 1 month of age (Figure 3.3).

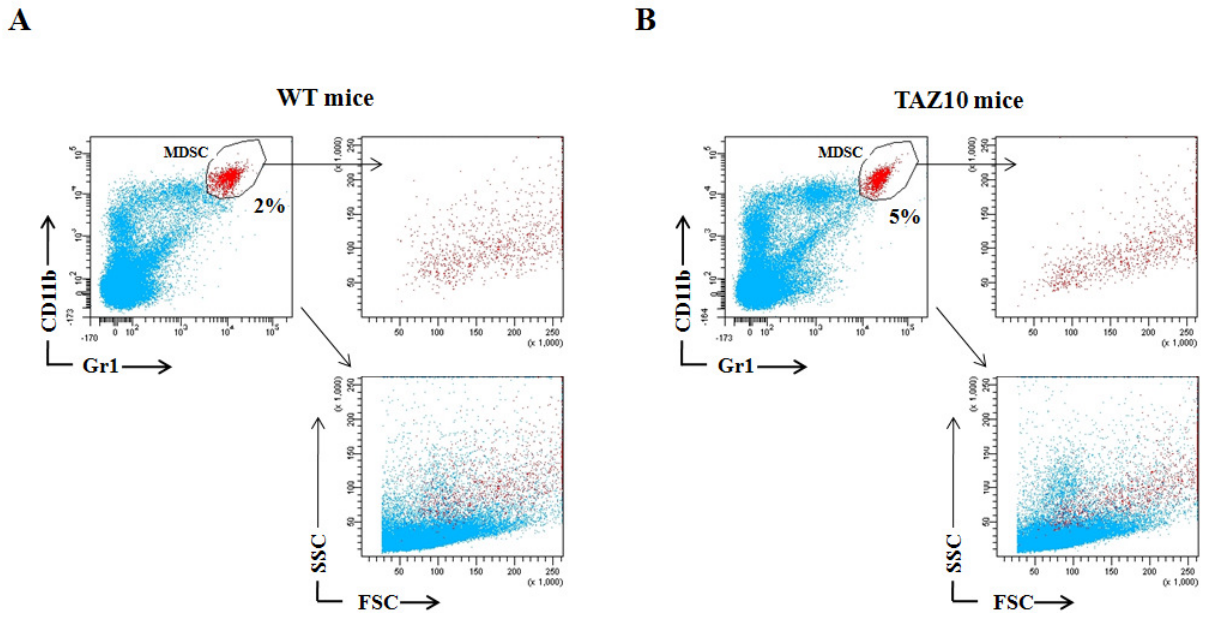

Figure 3.3: Myeloid-derived suppressor cells (MDSC) are present in TAZ10 transgenic mice and express high levels of Gr1 and CD11b markers
Splenocytes from WT **(A)** and TAZ10 mice **(B)** were analysed by 2 colour FACS analysis for the expression of Gr1 and CD11b markers. The morphology of both MDSC and non-MDSC population was investigated by analysing their size (Forward Scatter or FSC) and granularity (Side Scatter or SSC). Data are representative of more than 5 mice of 1 month of age.

A cell population characterised by the high expression of both Gr1 and CD11b markers was present in the spleen of WT and TAZ10 mice (Figure 3.3). This description is in line with previous studies (Chapter 1) and showed that MDSC are present in healthy individuals at a lower frequency compared to TAZ10 mice (2% of the total splenocytes population in WT mice against 5% in TAZ10 mice). Moreover, MDSC population was characterized by a heterogenous morphology as illustrated by their FSC/SSC profile. I was therefore confident that I could use Gr1 and CD11b to identify MDSC both in WT and TAZ10 transgenic mice.

3.2.2 – Recruitment of MDSC at the onset of autoimmune disease

Having shown the presence of MDSC in the spleen of TAZ10 mice, I wanted to investigate their recruitment directly at the onset of the disease. Because of Home Office Regulations, it was impossible to work on mice less than one month old. I therefore needed to recreate the onset of thyroiditis by the adoptive transfer (AT) of naive T cells from TAZ10 mice (TAZ10-T_N) into WT mice.

To this aim, I investigated the impact of the activation of T cells from TAZ10 mice (TAZ10-T) on the recruitment of MDSC.

3.2.2.1 – Initiation of the T cell response in TAZ10 mice

The anatomical locations of the cryptic epitope (P3) in WT mice were first ascertained to determine where the activation of TAZ10-T_N would occur. Thyroids, cervical LN and spleens of up to 80 WT mice were harvested and peptides extracted from these tissues according to the protocol described paragraph 2.11. The ability of the different peptide extracts to induce the proliferation of TAZ10-T mice was then assessed by (^{3}H) thymidine incorporation assay (Figure 3.4).

Because peptide extraction required both the lysis of the cells in formic acid and the use of a 30kDA cutoff filter, we assessed the loss of cryptic epitope through this process using the Caco-2 human colon-carcinoma cell line as a control cell line. Peptides were extracted from the cells with or without prior addition of the cryptic epitope at 1µg/ml. While mature DC pulsed with the P3 peptide induced the proliferation of TAZ10-T cells (black bar, figure 3.4), a decrease in proliferation when mature DC were pulsed with peptide extracts from Caco-2 cells and P3 peptide (blue bar, figure 3.4) highlighted a loss of peptides during the extraction process.

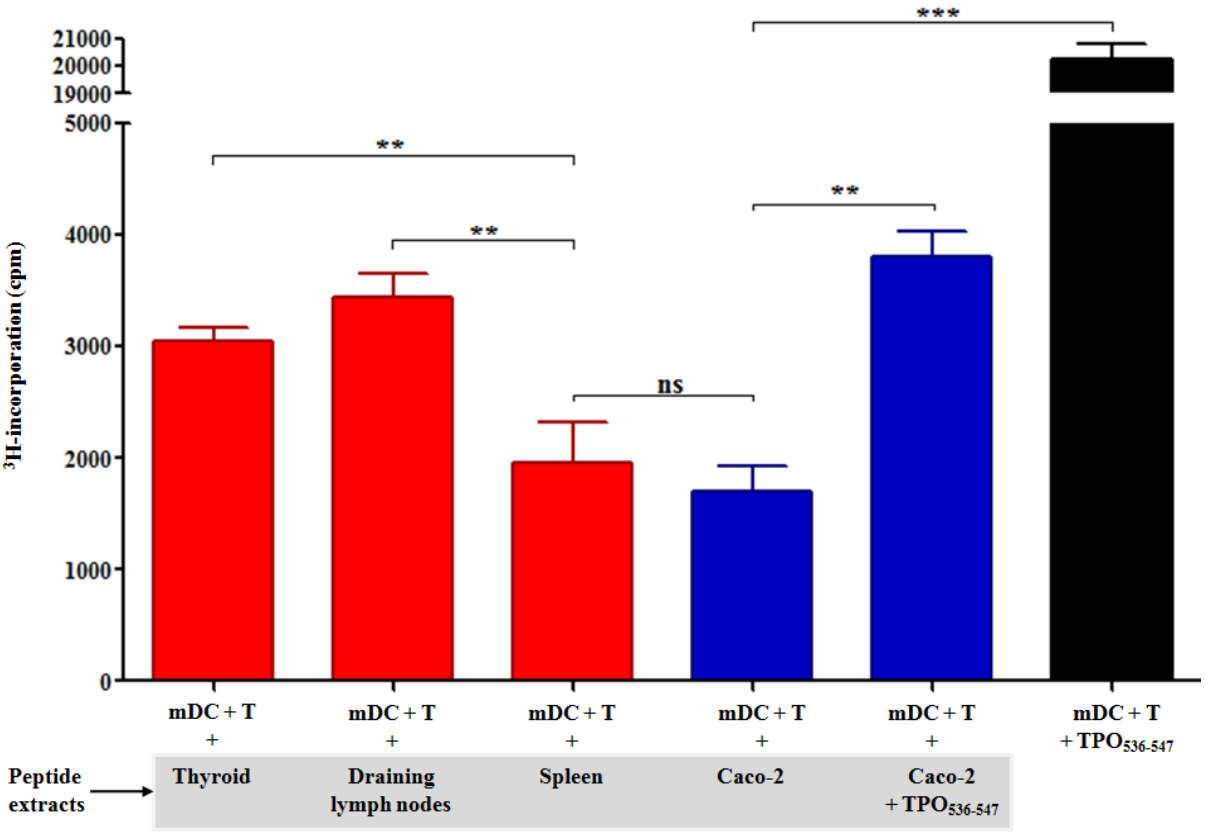

Figure 3.4: The cryptic epitope $TPO_{524-535}$ is present in the thyroid and lymph-nodes draining the thyroid of WT mice

Peptides extractions were performed from various tissues (thyroids, cervical lymph-nodes draining the thyroid and spleens) isolated from up to 80 WT mice. The proliferative activity of $CD4^+$ T cells from TAZ10 mice in response to the peptide extract was assessed by (^{3}H) thymidine incorporation. Mature BM-DC from WT mice (mDC) were used as APC. Peptide extracts from irrelevant Caco-2 cells previously supplemented or not with the cryptic epitope ($TPO_{536-547;}$ P3) at 1µg/mL were used as controls. Statistics were performed using the unpaired Student's t-test. Data shown are representative of two different experiments. (Experiments performed in collaboration with Olivier Cexus, 2009, University of Southampton - PhD thesis).

The proliferation of TAZ10-T cells in response to mature DC pulsed with peptide extracts from thyroids and LN draining the thyroid confirmed that the cryptic epitope was present in both tissues (red bars, figure 3.4). This proliferation was not the result of non-specific activation as TAZ10-T cells did not proliferate in response to mature DC pulsed with peptide extracts from other irrelevant tissues such as the gut and the trachea of WT mice (Olivier Cexus, 2009, University of Southampton - PhD thesis). These results confirmed that the cryptic epitope is naturally generated in the thyroid and that mature DC uptaking dying thyroid epithelial cells (TEC) and migrating to cervical lymph nodes draining the thyroid presented this epitope, thus allowing its "anatomical spreading".

TAZ10-T cells respond to the cryptic epitope present in the thyroid and cervival LN draining the thyroid of WT mice. In order to investigate the ability of TAZ10-T cells to become spontaneously activated *in-vivo*, we performed an AT of CFSE labelled naive $CD4^+$ T cells ($CD4^+$ $CD62L^{high}$) from WT and TAZ10 mice into WT mice. 7 days after AT, blood, spleen, thyroids, DLN and NDLN were analysed for the presence of donor T cells and the CFSE dilution assessed as readout of T cell proliferation *in-vivo* (Figure 3.5).

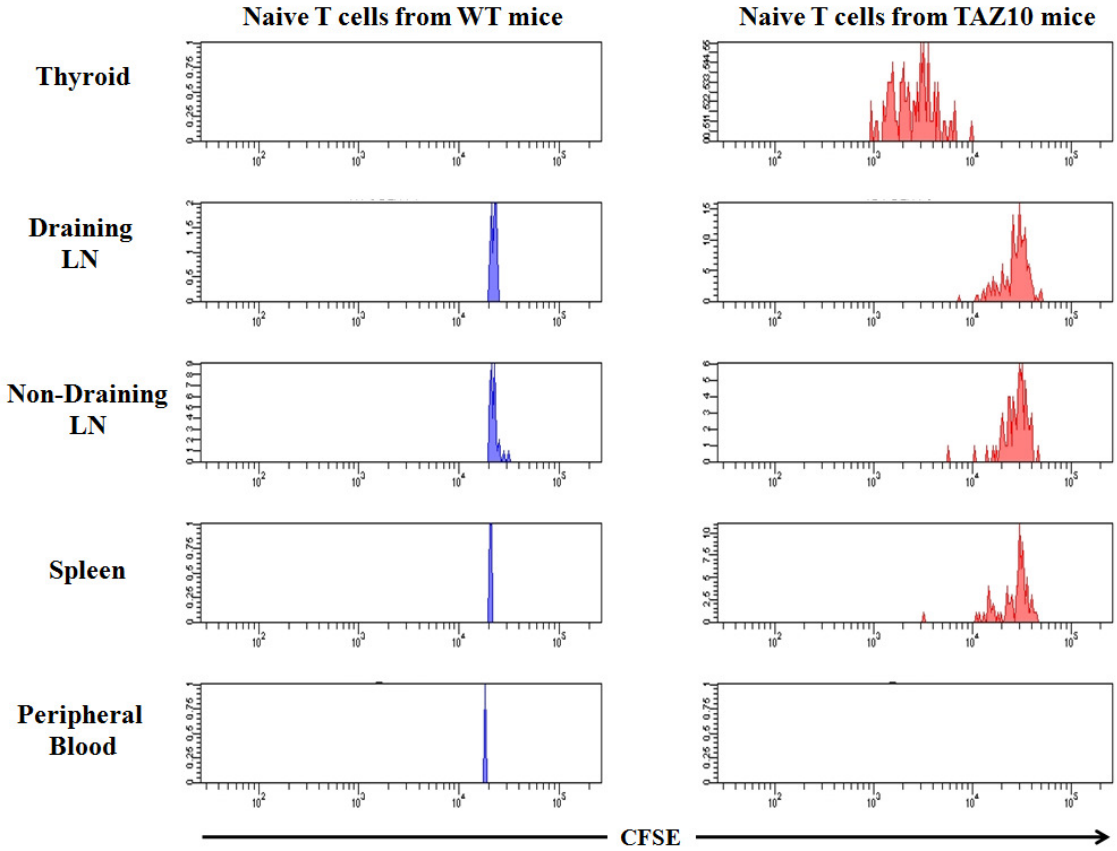

Figure 3.5: Naïve CFSE-labelled TAZ10 T cells proliferate in lymphoid organs of WT mice
WT mice were immunized with $2x10^6$ naïve T cells from WT and TAZ10 $Rag^{-/-}$ mice. 7 days after adoptive transfer, cells from the thyroids, spleens, peripheral blood and lymph nodes draining and not draining the thyroid were stained for CD4 and TCR-Vβ1 and analysed for the presence of T cells expressing CFSE by flow cytometry. Data shown are representative of 7 and 4 different mice for the adoptive transfer of naïve T cells from TAZ10 $Rag^{-/-}$ and WT mice respectively. (Experiments performed in collaboration with Olivier Cexus, 2009, University of Southampton - PhD thesis).

Although T cells from WT mice were still present in the blood of WT recipient mice, I could not detect any T cells from TAZ10 mice as they had all migrated to peripheral lymphoid organs. While T cells from WT mice could be detected in the spleens, DLN and NDLN of WT recipient mice, only transgenic T cells proliferated as suggested by the

important CFSE dilution. Interestingly, this proliferation was stronger in the DLN compared to NDLN and spleens. Most importantly, TAZ10-T cells were present in the thyroids of WT mice after AT while no T cells from WT mice could be detected (Figure 3.5).

We then explored the activation status of T cells from WT and TAZ10 Rag$^{-/-}$ mice after AT (Figure 3.6).

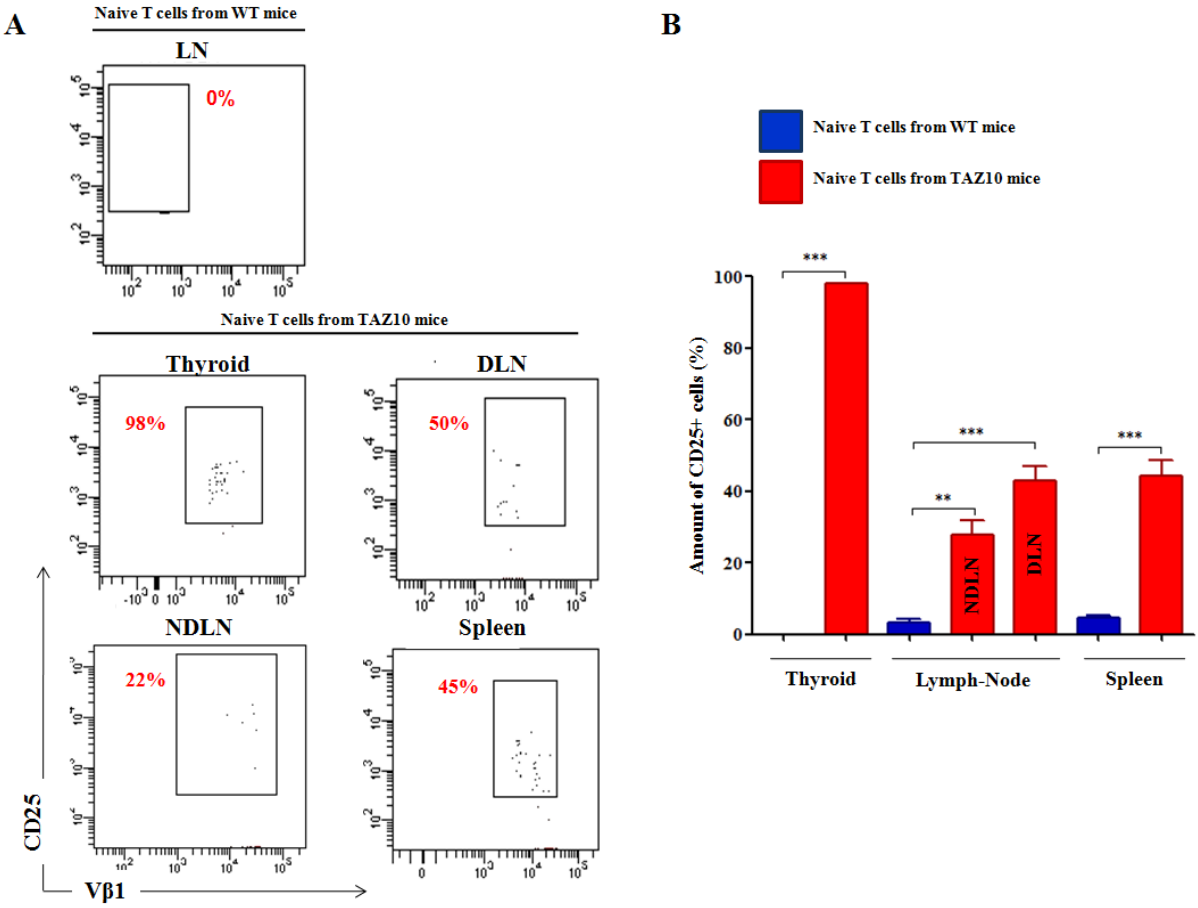

Figure 3.6: TAZ10 transgenic T cells have an activated phenotype in the thyroid and lymphoid organs of WT mice after adoptive transfer

WT mice were injected with 2x10^6 naïve T cells from WT and TAZ10 Rag$^{-/-}$ mice. **(A)** 7 days after adoptive transfer, cells from the thyroids, the spleens, the lymph-nodes draining (DLN) and not draining (NDLN) the thyroid were isolated and stained for CD4 and TCR-Vβ1. T cells expressing CFSE were analyzed for their level of expression of CD25 by flow cytometry. Data shown are representative of 7 and 4 different mice for the adoptive transfer of naïve T cells from TAZ10 Rag$^{-/-}$ and WT mice respectively. **(B)** Cumulative results showing the percentage of T cells expressing CD25 in the various tissues 7 days after adoptive transfer. Statistics were performed using the unpaired Student's t-test. (Experiments performed in collaboration with Olivier Cexus, 2009, University of Southampton - PhD thesis).

Looking at the phenotype of T cells from WT and TAZ10 mice after AT, we noticed that T cells from WT mice did not proliferate and lacked the expression of the CD25 activation marker thus confirming that they had retained their naive phenotype. In comparison, an upregulation of this marker by TAZ10-T cells present in the DLN, NDLN and spleen of recipient mice indicated that they had been activated (Figure 3.6/A). The level of expression of CD25 on transgenic T cells was higher in DLN than in NDLN of $Rag^{-/-}$ mice (22% in NDLN vs 50% in DLN, figure 3.6/B).

While WT-T_N cells did not migrate to the thyroid, TAZ10-T_N had strongly proliferated 7 days after AT. We could suggest that TAZ10-T_N cells are activated in the cervical LN draining the thyroid where the cryptic epitope P3 is presented by APC. These activated TAZ10-T then migrate to the thyroid where they undergo further proliferation. However, we cannot rule out that this activation could also take place primarily in the thyroid due to the limit of detection in our experiments. More work is therefore required to assess whether first priming occurs in the thyroid or in the lymph nodes draining the thyroid. To this aim, different strategies could be considered such as the use of alymphoplasia mice (Aly mice) that are devoid of lymph nodes and Peyer's patches (Miyawaki et al. 1994; Greter et al. 2009), the drug FTY720 that prevents the egress of lymphocytes from LN through the inactivation of sphingosine-1-phosphate receptor ($S1P_1$) (Liao et al. 2007; Matloubian et al. 2004) or the combination of anti-LFA.1 and anti-VLA.4 antibodies to prevent T cells entering the thyroid (Bartholomaus et al. 2009).

Overall these results have shown that naive transgenic $CD4^+$ T cells proliferated and infiltrated the thyroid of WT mice within 7 days after AT while naive $CD4^+$ T cells from WT mice did not. Interestingly, about 50% of transgenic $CD4^+$ T cells in the DLN expressed the activation marker CD25 while it raised to more than 98% in the thyroid. This demonstrated that thyroiditis disease occurs in the very first few days of life in TAZ10 mice. Importantly, I could also conclude that an AT of TAZ10-T_N into WT mice was the adequate tool to recreate the onset of thyroiditis and could therefore be used to investigate the impact of the activation of TAZ10 T cells on the recruitment of MDSC. The generation of bone marrow chimeric mice reconstituted with a mix of bone marrow cells from WT and TAZ10 mice could also be used for this investigation.

3.2.2.2 – The activation of T cells from TAZ10 mice promotes the recruitment of MDSC

Having shown that TAZ10-T_N were activated within days after AT into WT mice, I investigated whether MDSC were recruited at the onset of thyroiditis using this experimental setting. WT mice were adoptively transferred with WT-T_N and TAZ10-T_N. 7, 14 and 21 days after AT, mice were culled and the proportion of $Gr1^+$ $CD11b^+$ MDSC in the lymph nodes draining (DLN) and not-draining (NDLN) the thyroid was investigated by flow cytometry (Figure 3.7).

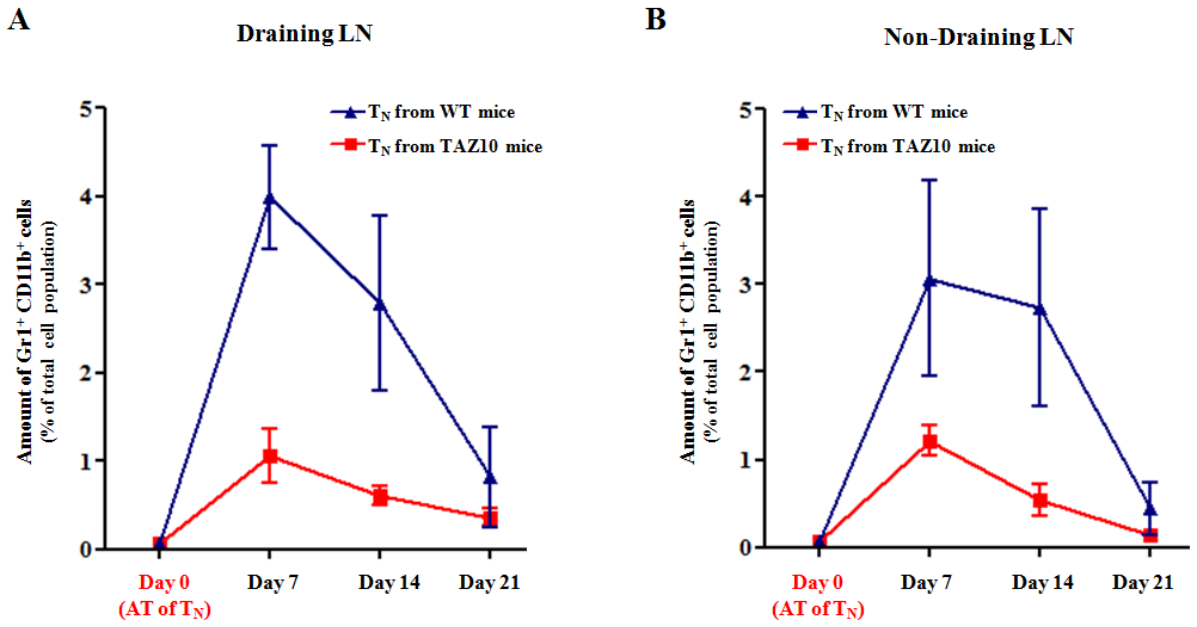

Figure 3.7: The activation of TAZ10 transgenic T cells promotes the recruitment of MDSC
WT mice were immunized with $2x10^6$ naïve T cells from WT or TAZ10 $Rag^{-/-}$ mice. Mice were culled 7, 14 and 21 days after adoptive transfer (AT). Cells from the lymph nodes draining (DLN) **(A)** and not draining (NDLN) **(B)** the thyroid were isolated and stained for Gr1 and CD11b to assess the proportion of MDSC. 9 mice were used per condition (Experiments performed in collaboration with Olivier Cexus).

7 days after AT of WT-T_N and TAZ10-T_N into WT mice, a strong increase in the proportion of MDSC could be observed in the DLN and NDLN to reach background level 21 days after AT. This increase was not as significant in WT mice that had been adoptively transferred with TAZ10-T_N compared to WT-T_N. We could suggest that the soluble factors produced upon the proliferation and activation of TAZ10-T_N was promoting the early accumulation and differentiation of MDSC into APC. This issue will be addressed in Chapter 4.

3.2.3 – Distribution of Gr1$^+$ CD11b$^+$ MDSC during the course of autoimmunity

As TAZ10 mice develop autoimmune thyroiditis, I first assessed whether a deficiency of MDSC in TAZ10 transgenic mice compared to WT mice could provide an explanation for the development of AID. Using the level of expression of Gr1 and CD11b, I investigated the distribution of MDSC in various tissues in WT and TAZ10 transgenic mice over time.

3.2.3.1 – Organ distribution of MDSC in WT and TAZ10 mice

From 1 to 4 months of age, the activation of self-reactive T cells leads to the destruction of the thyroid in almost 100% of TAZ10 mice (Quaratino et al. 2004) thus creating an inflammatory environment that would favour the accumulation of MDSC. By flow cytometry analysis, I first assessed the proportion of MDSC present in different tissues of 1 month old WT and TAZ10 transgenic mice (Figure 3.8).

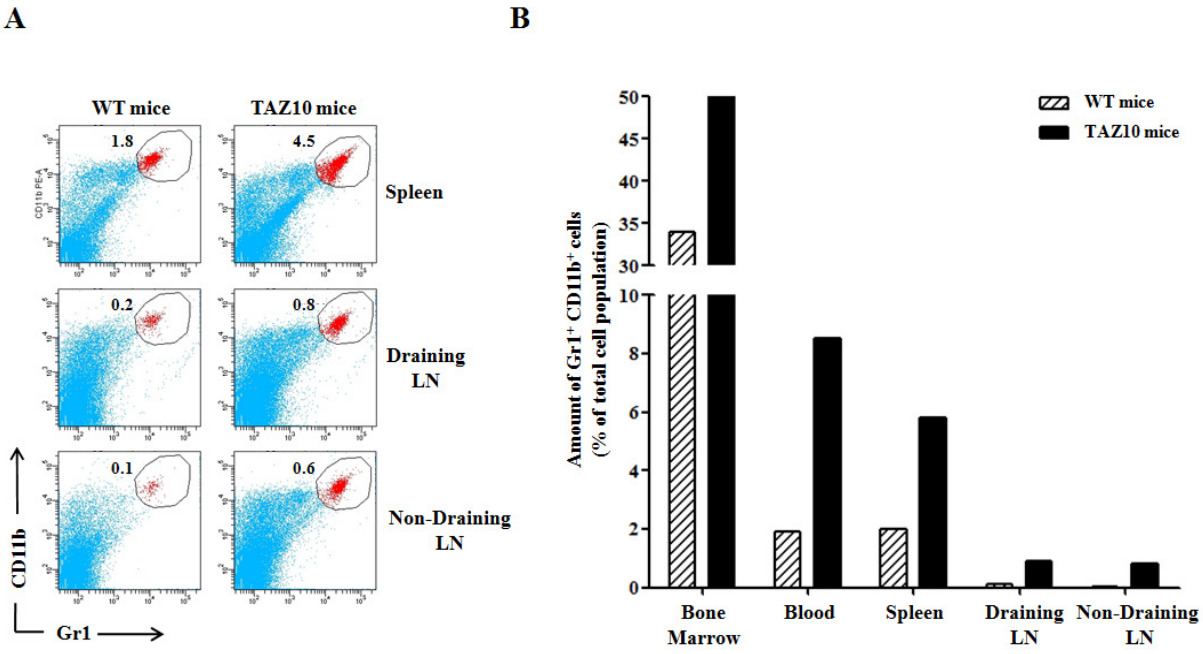

Figure 3.8: MDSC accumulate in both lymphoid and non-lymphoid organs in TAZ10 transgenic mice
(A) The expression of Gr1 and CD11b markers was investigated by flow cytometry in the spleen, lymph nodes (LN) draining and not draining the thyroid of wild-type (WT) and TAZ10 transgenic mice. **(B)** Distribution of Gr1$^+$ CD11b$^+$ cells in various organs of WT and diseased TAZ10 mice as a percentage of total cell population. Data are representative of more than 20 mice of 1 month of age.

MDSC accumulated in the spleen and lymph nodes (LN) draining and not-draining the thyroid of diseased mice. While a 3-fold increase in the number of MDSC in the spleen of TAZ10 mice was observed, their number in the LN was also dramatically enhanced compared to WT mice (Figure 3.8/A). Further analysis looking at other tissues confirmed this trend as MDSC accumulated in all the studied tissues in transgenic mice (Figure 3.8/B). Interestingly, the bone marrow from TAZ10 mice contains 50% of MDSC as opposed to 30% in WT mice. MDSC are generated from common myeloid progenitor cells whose natural niche resides in the bone marrow. The strong accumulation of MDSC in the BM of TAZ10 diseased mice highlighted important alteration in haematopoiesis occurring in these mice.

One major characteristic of TAZ10 mice associated with the disease is the destruction of the thyroid by pathogenic self-reactive T cells. Indeed, thyroids of TAZ10 mice are infiltrated by $CD4^+$ and $CD8^+$ T cells and lose their follicular structure as a result of the death of thyroid epithelial cells (TEC) by apoptosis (Quaratino et al. 2004). Because MDSC accumulated in the cervical lymph nodes draining the thyroid in TAZ10 mice, I wondered whether they were also present in the thyroid to potentially inhibit self-reactive T cells thus controlling their proliferation and function. Sections of OCT-embedded thyroids from both WT and TAZ10 mice of different age were stained for Gr1 and CD11b markers and analysed by confocal microscopy (Figure 3.9).

The expression of Gr1 and CD11b markers could be observed in the thyroid of WT mice confirming the presence of myeloid cells within this tissue. While the level of expression of these markers was similar in the thyroid of 1 month old TAZ10 mice, it was upregulated in 6 and 12 months old mice suggesting a recruitment of myeloid cells over time. Although some staining was present on interfollicular cells, the majority was visible within follicular spaces thus highlighting a disruption of the integrity of TEC epithelium associated with an infiltration of myeloid cells (Figure 3.9/A and 3.9/B). Interestingly, the presence of cells expressing both Gr1 and CD11b markers could be observed in the thyroid of TAZ10 mice but not in WT mice. The expression of these markers was confirmed by the yellow staining resulting from the colocalization of Gr1 (green) and CD11b (red) (Figure 3.9/C). Interestingly, there was a noticeable difference in the level of expression of Gr1 marker.

Because MDSC lose the expression of Gr1 marker when they start to differentiate, these results highlighted that within the MDSC population there was various degree of differentiation.

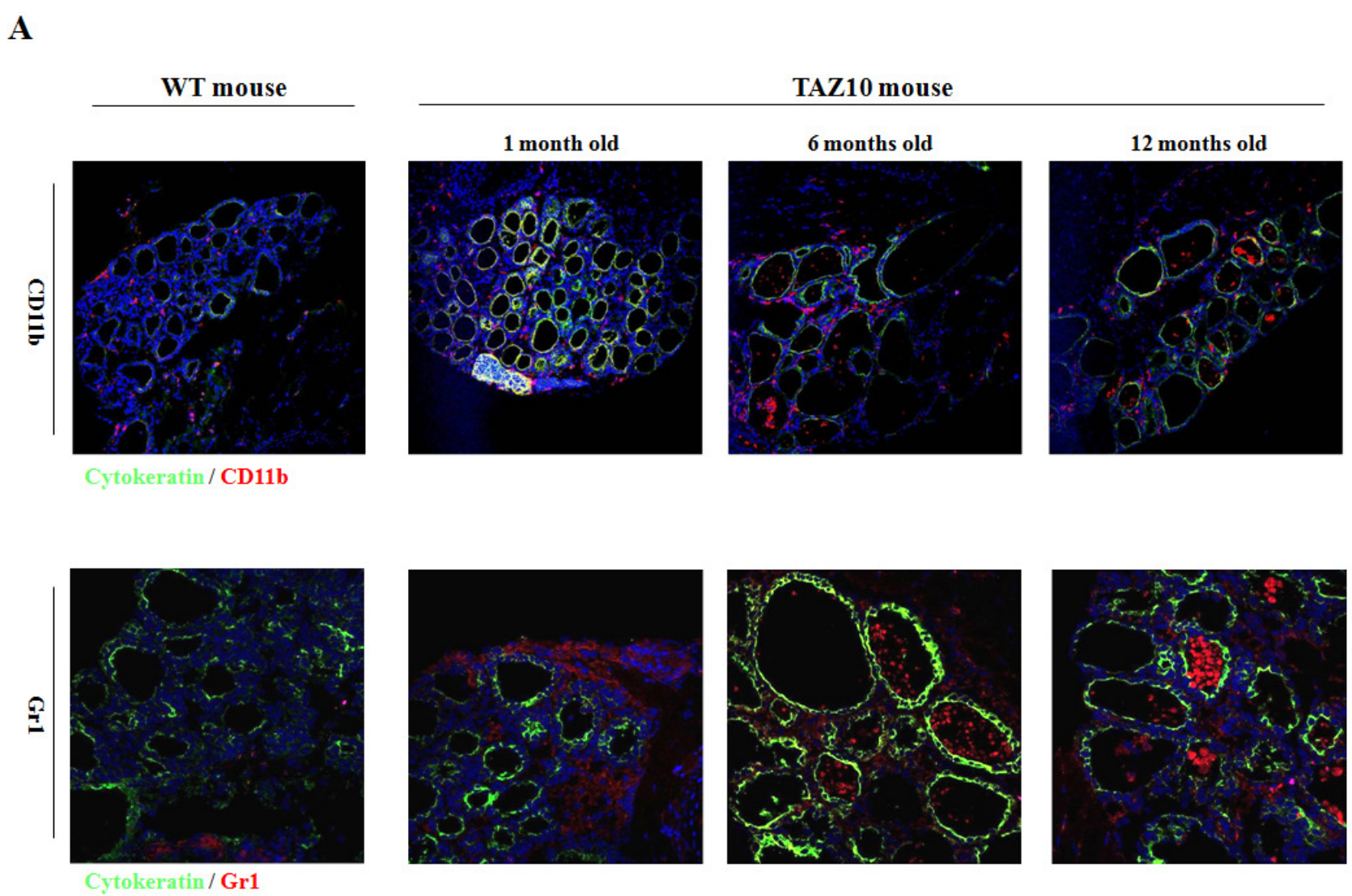
A
WT mouse
TAZ10 mouse
1 month old
6 months old
12 months old
CD11b
Cytokeratin / CD11b
Gr1
Cytokeratin / Gr1

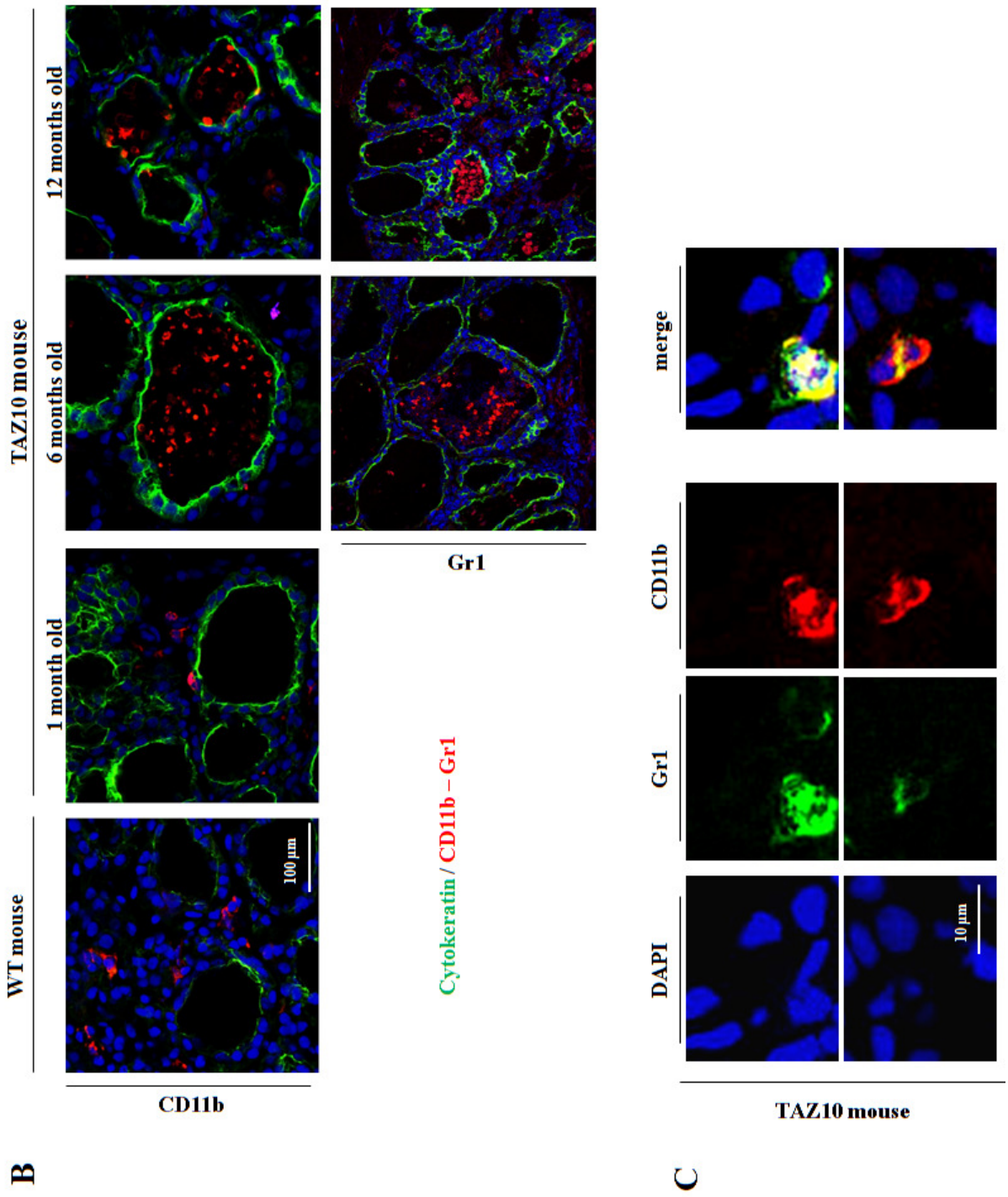

Figure 3.9: Although present in small number, MDSC infiltrate the thyroid of transgenic TAZ10 mice
(A) Confocal microscopy of sections of OCT frozen thyroids from 2 months old WT and TAZ10 mice of different age after dual immunofluorescence staining with αGr1 or αCD11b (red) and αCytokeratin (green) antibodies. Nuclei were counterstained with DAPI. Magnification: x10. **(B)** As previously described in (A) but using a higher magnification (x20) ; Scale bar: 100µm. **(C)** Co-localization of Gr1 (green) and CD11b (red) in the thyroid of TAZ10 mice. DAPI was used to counterstain nuclei. Magnification: x40; Scale bar: 10µm. Data are representative of 10 mice.

These results therefore indicated that while being absent from the thyroids of WT mice, a limited number of $Gr1^+$ $CD11b^+$ MDSC was recruited to the thyroids of TAZ10 mice as a result of the on-going inflammation. Their presence in such a small number raised the question on whether they would be able to exert any suppressive role on self-reactive T cells in the thyroid. This will be further discussed in chapter 4.

In light of the apparent accumulation of MDSC observed in various tissues of TAZ10 mice during the early phase of the disease, I decided to evaluate if there was a link between the proportion of MDSC and the evolution of the disease.

3.2.3.2 – The proportion of MDSC decreases in TAZ10 mice during the course of autoimmunity

In order to gain further insight into the potential role of MDSC in the pathogenesis of the disease, I assessed the percentage of MDSC in the spleen of WT and TAZ10 transgenic mice over time (Figure 3.10).

While no significant variation in the number of MDSC could be observed in the spleen of WT mice over time, this proportion greatly varied in the spleen of TAZ10 mice. Indeed, the distribution of MDSC in these mice showed that they accumulated in the spleen during the acute phase of the disease (about 5% at 1 month of age against 2% in WT mice) (Figure 3.10/A). As the inflammation fades from 4 months of age when the thyroid is destroyed (Quaratino et al. 2004), the proportion of MDSC in the spleen of TAZ10 mice dramatically decreased down to WT level (Figure 3.10/B).

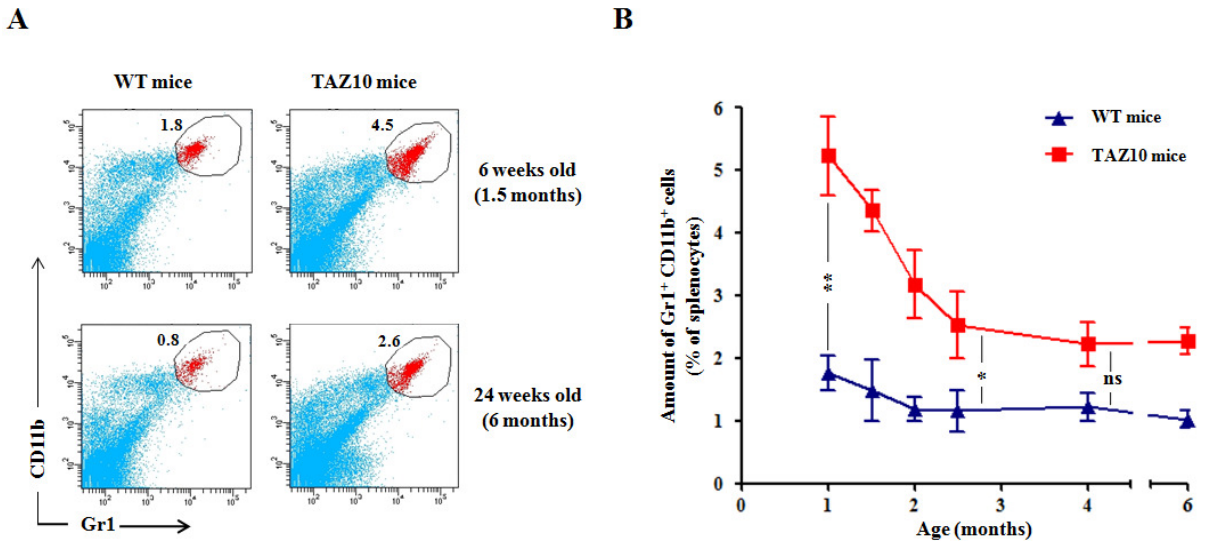

Figure 3.10: Evolution of the proportion of MDSC in the spleen of WT and TAZ10 transgenic mice over time

(A) The expression of Gr1 and CD11b markers was investigated by flow cytometry in splenocytes from WT and TAZ10 mice at 6 and 24 weeks of age. **(B)** Data representative of flow cytometry analysis from more than 20 mice showed an increased number of splenic $Gr1^+$ $CD11b^+$ cells in transgenic mice at 1 month of age. Statistics were done using the unpaired Student's t-test.

A similar evolution of the number of MDSC was observed in another model of autoimmune disease. In the collagen-induced arthritis model (CCIA), transgenic mice expressing the TCR-Vβ12 transgene develop chronic arthritis upon immunization with collagen type II in Complete Freund's Adjuvant (CFA). 16 to 20 days after immunization, CCIA mice develop arthritis showing similar clinical signs of disease as patients with rheumatoid arthritis (Mauri et al. 1997). 40 days after immunization with collagen type II, CCIA mice were culled and the number of MDSC in the spleen investigated. The proportion of MDSC peaked during the acute phase of inflammation while it decreased down to WT level as the disease became chronic (Tan LA, Cexus O et al. Manuscript in preparation). In keeping with the present results (Figure 3.10), these observations suggest a correlation between the number of MDSC and the stage of the disease.

I then decided to investigate whether the same accumulation was visible in the lymph nodes (LN) draining and not draining the thyroids of TAZ10 mice. To this aim, the proportion of MDSC in the cervical and inguinal LN of WT and TAZ10 mice was assessed over time (Figure 3.11).

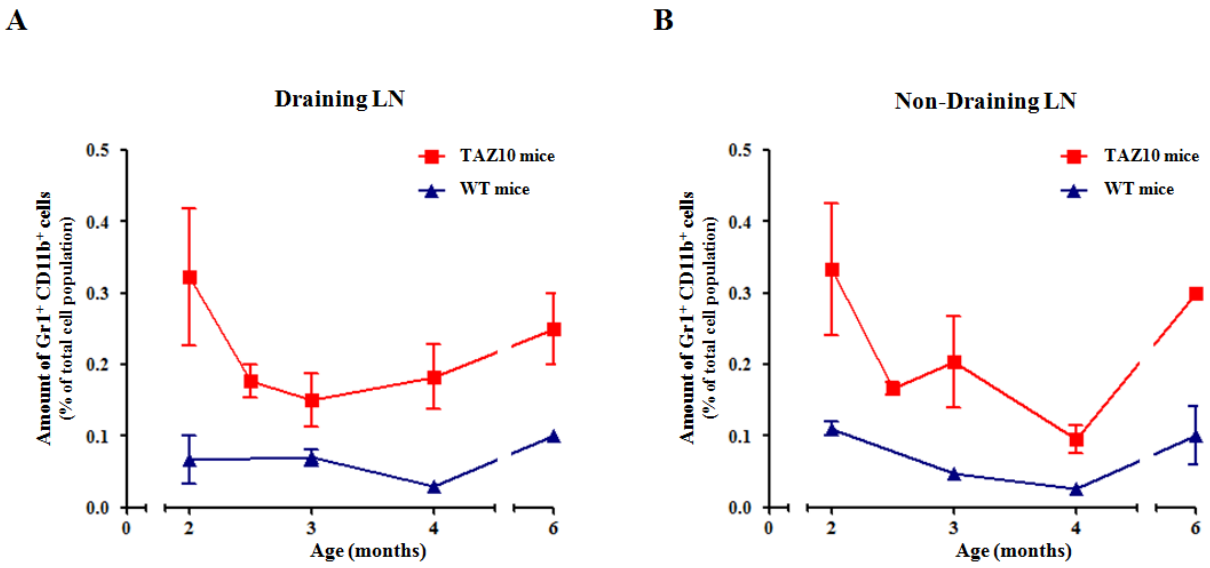

Figure 3.11: The proportion of MDSC in lymph nodes draining and not draining the thyroid of TAZ10 transgenic mice varied over time

Data representative of the flow cytometry analysis from more than 20 mice (8 to 24 weeks of age) investigating the number of $Gr1^+$ $CD11b^+$ cells in lymph nodes (LN) draining **(A)** and not draining **(B)** the thyroid of wild-type (WT) and TAZ10 transgenic mice.

Similarly to what was previously observed in the spleen, there was no significant variation over time in the proportion of MDSC in the LN (cervical and inguinal) of WT mice. In contrast, MDSC accumulated in the draining and non-draining LN of TAZ10 mice during the acute phase of the disease (about 0.35% at 1 month of age in both LN against 0.1% in WT mice) while their number decreased down to WT level as the inflammatory process faded in 3-4 months old TAZ10 mice (Figure 3.11/A and 3.11/B).

Altogether, these results confirmed the presence of MDSC in a mouse model that spontaneously develops autoimmune disease. In TAZ10 mice, the inflammation leads to the progressive destruction of the thyroid and is responsible for the accumulation of MDSC in various lymphoid and non-lymphoid organs. Despite their presence, MDSC cannot prevent the initiation and the development of the disease. I therefore wondered why an increased number of MDSC was not sufficient to control the activation of self-reactive T cells and I hypothesized that MDSC from TAZ10 mice do not display the same inhibitory functions on T cells as it has already been described in cancer.

3.2.4 – MDSC from TAZ10 mice display a strong inhibitory function on T cells *in-vitro*

The suppressive function of MDSC was investigated by measuring their effect on the proliferative activity of T cells from TAZ10 mice. $Gr1^+$ MDSC were either depleted or isolated from splenocytes with magnetic beads coated with a monoclonal antibody to mouse Gr1 (BD Biosciences, USA).

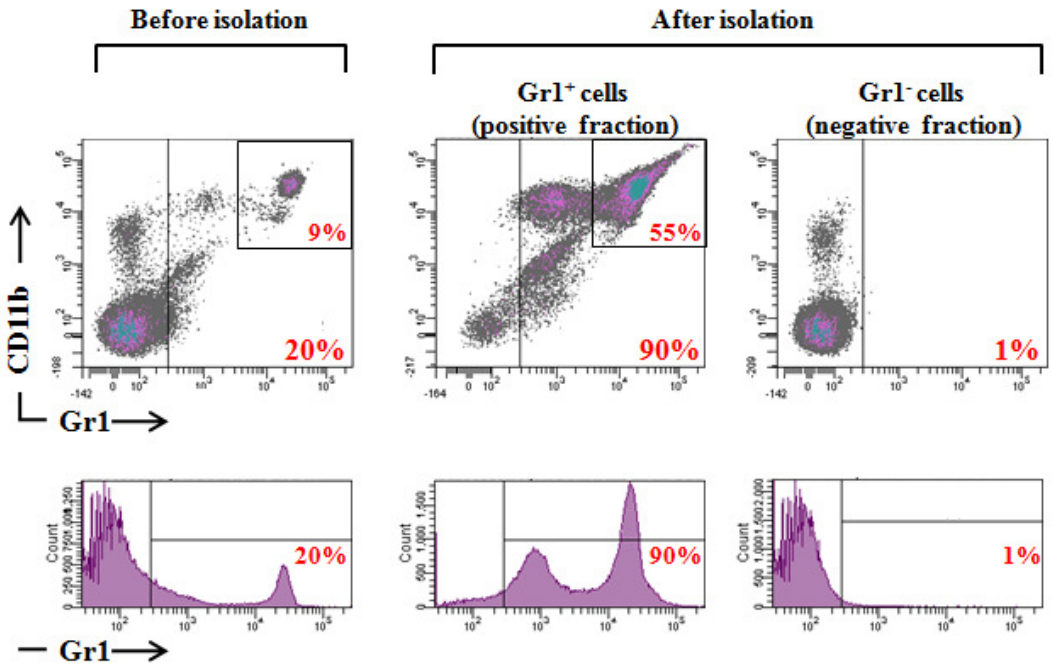

Figure 3.12: Depletion of Gr1 positive cells removes the population of myeloid derived suppressor cells
Splenocytes were labelled with magnetic nanoparticles coated with αGr1mAb and then isolated using columns on a magnetic field. Negative and positive fractions were collected and the efficiency of isolation estimated by flow cytometry. Data are representative of more than 20 experiments.

The efficiency of the purification or depletion of MDSC performed *in-vitro* was determined by flow cytometry using an antibody targeting the Gr1 marker (clone RB6-8C5). As shown figure 3.12, the positive fraction collected after separation contained 90% of $Gr1^+$ cells while only 1% of $Gr1^+$ cells were present in the negative fraction. Although the positive fraction was not 100% pure, the procedure was considered successful in providing the necessary level of purity to confidently investigate the effect of MDSC on the proliferative activity of T cell. This result is in line with numerous studies using the same technique to purify MDSC.

3.2.4.1 – MDSC inhibit T cell proliferation in response to αCD3-αCD28

MDSC have previously been shown to inhibit T cell proliferation in response to αCD3 and αCD3-αCD28 in tumour models (Kusmartsev et al. 2000). The effect of the addition or depletion of MDSC on the proliferative activity of T cells from TAZ10 mice to either αCD3 or αCD3-αCD28 antibodies was assessed by (^{3}H) thymidine incorporation assay.

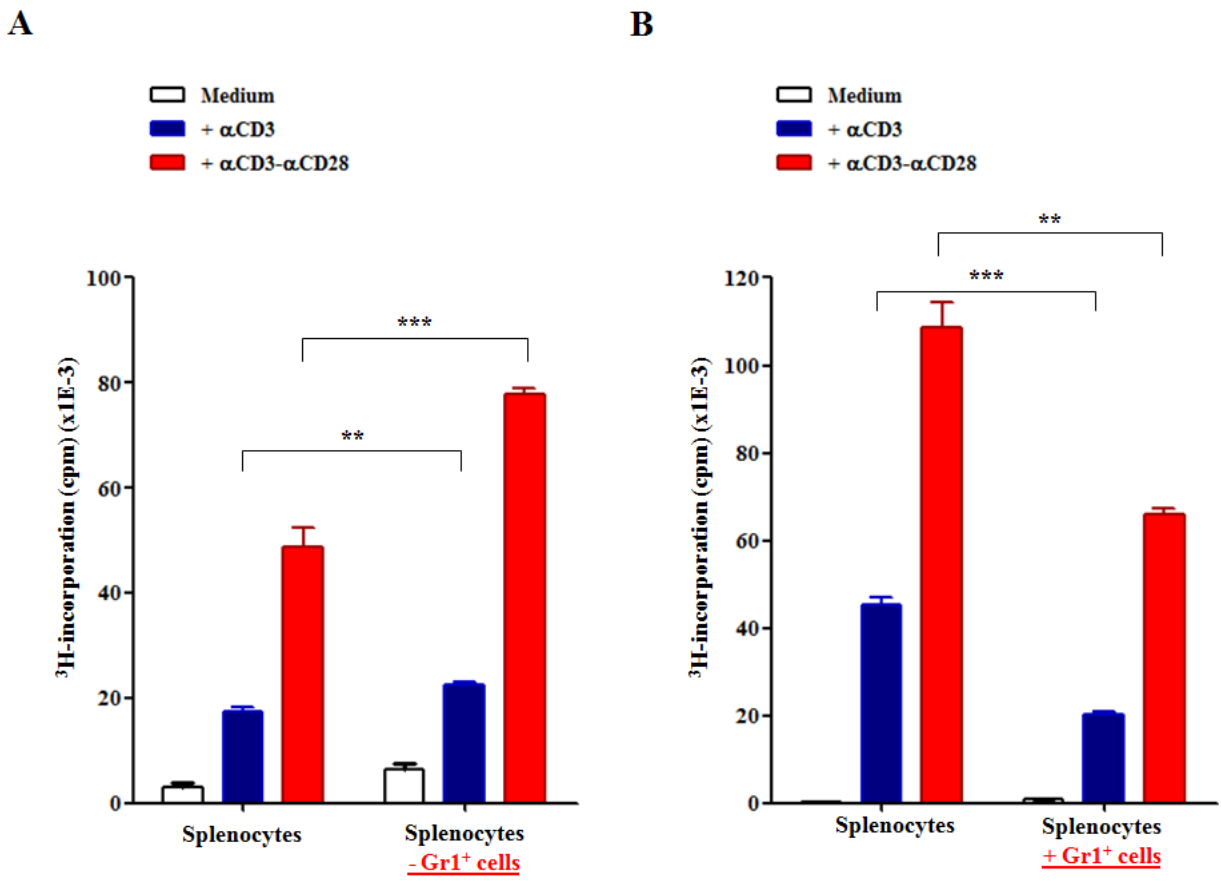

Figure 3.13: Gr1$^+$ MDSC from TAZ10 transgenic mice inhibit T cell proliferation upon stimulation with αCD3 and αCD3-αCD28 antibodies

(A) Untreated and Gr1 depleted splenocytes from TAZ10 mice were stimulated with either αCD3 or αCD3-αCD28 agonistic antibodies and their proliferative activity assessed by (^{3}H) thymidine incorporation assay. **(B)** Gr1$^+$ cells isolated from transgenic mice were added to splenocytes activated with either αCD3 or αCD3-αCD28. MDSC were added at a splenocyte:MDSC ratio of 1:1. Data are representative of 3 different experiments. Statistics were performed using the unpaired Student's t-test.

The removal of MDSC resulted in an increased T cell proliferation to both αCD3 and αCD3-αCD28 antibodies (Figure 3.13/A). This showed that the depletion of MDSC lifted the inhibition normally displayed by these cells on splenocytes (SN). This was further

demonstrated when the addition of MDSC to SN from TAZ10 mice stimulated with αCD3 antibody resulted in a two-fold decrease in proliferation. The addition of αCD28 antibody was unable to reverse this strong inhibitory effect displayed by MDSC on T cells (Figure 3.13/B).

To further characterise the inhibitory functions of MDSC in autoimmunity, I investigated whether their action was dose-dependent. MDSC from TAZ10 transgenic mice were added to splenocytes stimulated with αCD3 or αCD3-αCD28 antibodies either at a SN:MDSC ratio of 5:1 or 1:1 and the proliferative activity of T cells measured by (^{3}H) thymidine incorporation assay (Figure 3.14).

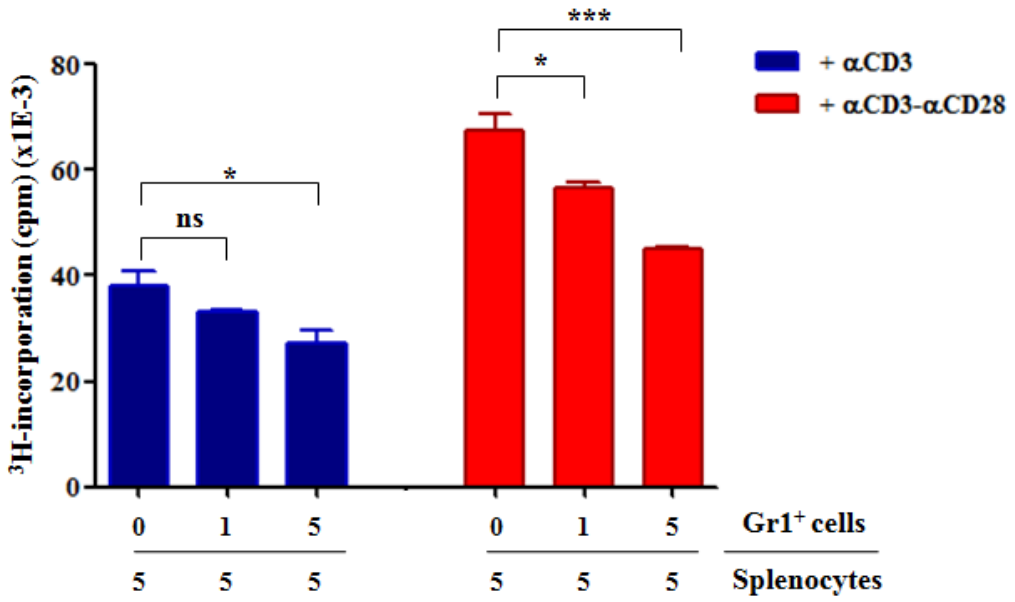

Figure 3.14: The addition of MDSC inhibits T cell proliferation in a dose-dependent manner
Gr1$^+$ cells were isolated and added to splenocytes (either at a splenocyte:MDSC ratio of 1:1 or 5:1) stimulated with either αCD3 or αCD3-αCD28 antibodies. Data are representative of 3 independent experiments. Statistics were done using the unpaired Student's t-test.

While the addition of MDSC resulted in an inhibition of T cell proliferation in response to αCD3-αCD28 regardless of the SN:MDSC ratio, only a SN:MDSC ratio of 1:1 was able to significantly decrease the proliferation of splenocytes to αCD3 (Figure 3.14). These observations suggested that the level of activation of T cells has a strong impact on the inhibitory activity of MDSC which was dose-dependent. Indeed, the suppressive function of

MDSC mediated in part through the modulation of the metabolism of L-arginine using iNOS and Arg-1, is under the direct influence of Th1 and Th2 cytokines (Bronte et al. 2005).

I have previously highlighted the important role of $CD4^+$ $CD25^+$ Tregs in the prevention of AID by suppressing the activation and expansion of self-reactive T cells (Chapter 1). While the depletion of $CD4^+$ $CD25^+$ T cells leads to the development of AID, the restoration of Tregs can provide protection (Sakaguchi et al. 1995). Because MDSC and regulatory T cells are both involved in the maintenance of peripheral tolerance, I wanted to compare their ability to inhibit the proliferation of pathogenic self-reactive T cells (Figure 3.15).

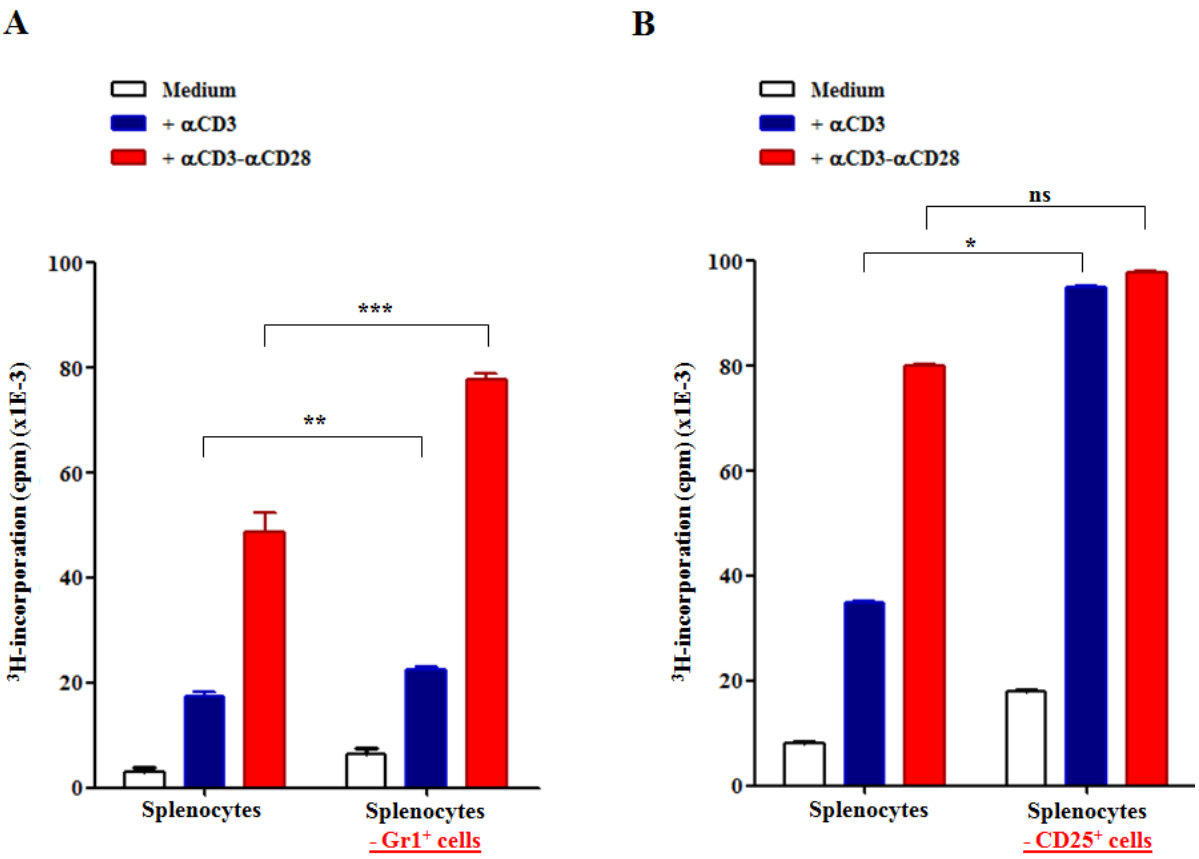

Figure 3.15: MDSC display a stronger inhibitory activity on T cell proliferation to αCD3-αCD28 antibodies than regulatory T cells

Untreated splenocytes and splenocytes depleted of $Gr1^+$ cells **(A)** or $CD25^+$ cells **(B)** were stimulated with αCD3 and αCD3-αCD28 antibodies and their proliferative activity assessed by (^{3}H) thymidine incorporation assay. Data are representative of 5 independent experiments. Data on the effect of the depletion of $CD25^+$ cells were performed by Ester Badami. Statistics were performed using the unpaired Student's t-test.

Proliferation of T cells in response to αCD3 stimulation was increased by 3-fold when $CD25^+$ cells were depleted while this removal did not have any significant impact on the proliferation of T cells to αCD3-αCD28 antibodies (Figure 3.15/B). This confirmed previous reports showing that αCD28 can break Tregs mediated suppression (Thornton et al. 1998). In contrast, the addition of αCD28 was not able to abrogate the strong inhibitory activity displayed by MDSC (Figure 3.15/A).

Together, these results show that a strong stimulation mimicked by αCD3-αCD28 antibodies abrogated Treg-mediated but not MDSC-mediated T cell inhibition thus highlighting that MDSC have a strong suppressive function on T cells.

3.2.4.2 – MDSC from TAZ10 mice inhibit T cell proliferation when full costimulation is provided by mature dendritic cells

Having demonstrated the ability of MDSC to inhibit T cell proliferation in response to αCD3 and αCD3-αCD28 stimulation, I wanted to further investigate the efficiency of this suppressive function when full costimulation was provided by mature DC. In all the previous experiments, T cell activation was achieved by stimulating the T cell receptor (TCR) using an αCD3 agonistic antibody and engagement of the costimulatory molecule CD28 using αCD28 agonistic antibodies. However, it is well documented that T cells require three combined signals provided by antigen presenting cells to be fully activated. The first signal is mediated through the TCR following its interaction with antigenic peptide-MHC complexes while the second is delivered after engagement of costimulatory molecules like CD28 on T cells and CD80 on APC (Allison et al. 1994; Robey et al. 1995). The third signal is mediated through the secretion of various cytokines as a result of the communication between T cells and DC (Kapsenberg et al. 2003). Although monoclonal antibodies specific for the TCR complex and CD28 are useful to mimic T cell activation *in-vitro*, they are not able to mimic the full costimulation provided to T cells by mature DC. I therefore decided to use bone marrow-derived dendritic cells in my assays rather than αCD28 antibody. They represent a better source of costimulation as they can engage CD28 and other costimulatory molecules in a more physiological way while providing the various cytokines necessary for a full T cell activation.

A costimulation assay to assess the level of costimulation provided by mature DC to T cells using an agonistic αCD3 antibody to mimic TCR engagement (Olivier Cexus, 2009, University of Southampton - PhD thesis) was performed (Figure 3.16).

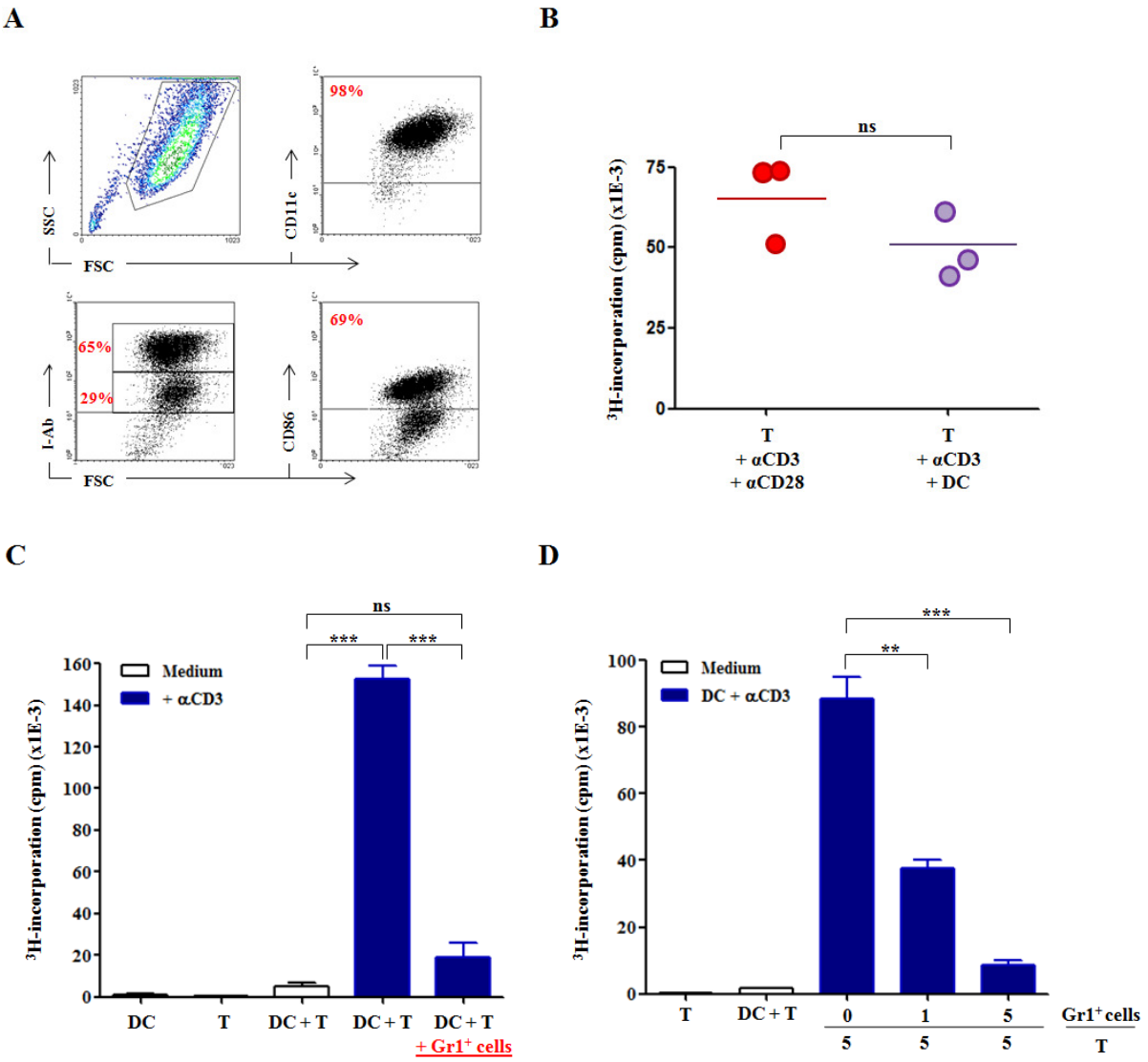

Figure 3.16: MDSC have the ability to inhibit the strong costimulatory activity provided by mature DC to T cells

(A) The level of expression of CD11c, CD86 and I-Ab molecules on mature dendritic cells (DC) was evaluated by flow cytometry. **(B)** The costimulatory activity of mature DC was assessed by cocultivating T cells with DC and αCD3. Their proliferative activity was assessed using the (^{3}H) thymidine incorporation assay. **(C)** T cells were activated by αCD3 antibody and costimulatory signals provided by mature DC. Gr1$^+$ MDSC were isolated and added to T cells at a T:MDSC ratio of 1:1. **(D)** The dose dependent inhibition of T cell proliferation by MDSC was investigated by the addition of Gr1$^+$ MDSC to T cells either at a T:MDSC ratio of 1:0, 1:1 or 5:1. Data are representative of 3 independent experiments. T cell proliferative activity was assessed by (^{3}H) thymidine incorporation and statistics were performed using the unpaired Student's t-test. Experiments investigating the phenotype of DC and their costimulatory activity were performed and kindly donated by Olivier Cexus, 2009, University of Southampton - PhD thesis.

Following their maturation with LPS, 98% of mature DC expressed the CD11c myeloid marker while 69% and 65% expressed the costimulatory marker CD86 and high levels of I-A^b MHC-II molecules respectively (Figure 3.16/A). To address whether mature DC generated could provide a powerful costimulation and be substituted to αCD28 antibody, the proliferative activity of T cells in response to αCD3-αCD28 antibodies or αCD3 and mature DC was compared (Figure 3.16/B). Although the level of proliferation of T cells measured by (^{3}H) thymidine incorporation was higher when stimulated with both αCD3-αCD28 antibodies, mature DC were potent at providing the strong costimulatory signals required to induce T cell activation. These results therefore confirmed the mature phenotype of the DC population generated.

While mature DC alone did not induce any T cell proliferation, the addition of αCD3 antibody resulted in a significant increase in T cell proliferation (Figure 3.16/C). This T cell proliferation was however strongly inhibited by the addition of MDSC at a T:MDSC ratio of 1:1 further highlighting their powerful suppressive activity on T cells (Figure 3.16/C). The action of MDSC was also dose-dependent as their addition at a T:MDSC ratio of 1:1 resulted in a stronger inhibition than at a T:MDSC ratio of 5:1 (Figure 3.16/D).

MDSC strongly inhibited T cell proliferation in response to αCD3-αCD28 and αCD3-mature DC in a dose-dependent manner. Pro-inflammatory cytokines have been shown to promote the suppressive function of MDSC by increasing their expression of Arg-1 and/or iNOS and the release of TGF_β (Gabrilovich et al. 2009). I therefore wondered whether the inhibitory activity of MDSC could be influenced by the on-going inflammation that occurs in TAZ10 mice.

3.2.4.3 – Differential suppressive activity of MDSC on T cell proliferation

To address this question, I assessed and compared the suppressive activities of MDSC from both WT and TAZ10 mice on T cells stimulated by mature DC in the presence of agonistic αCD3 antibody (Figure 3.17).

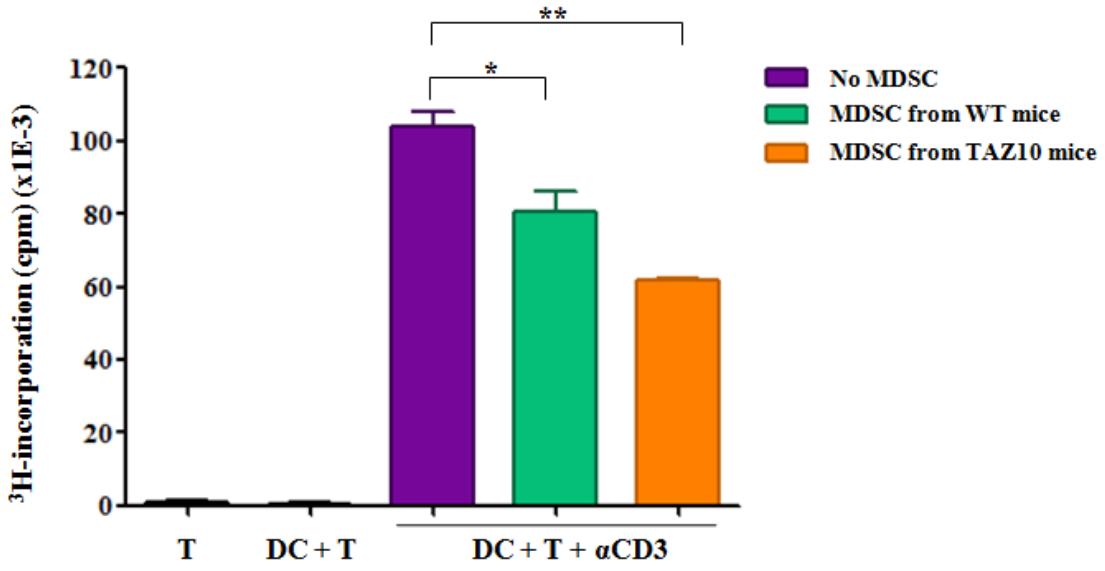

Figure 3.17: MDSC from TAZ10 transgenic mice are more potent than from wild-type mice
The T cell proliferative activity in the presence of MDSC from WT and TAZ10 transgenic mice was assessed using the (^{3}H) thymidine incorporation assay. T cell activation was induced by αCD3 and costimulatory molecules provided by mature dendritic cells (DC). Gr1$^+$ MDSC from WT and TAZ10 mice were added to T cells at a T:MDSC ratio of 5:1. Data are representative of 2 separate experiments. Statistics were done using the unpaired Student's t-test.

T cell proliferation was decreased when MDSC from both WT and TAZ10 mice were added to the culture. Interestingly, although equal numbers of MDSC were used, the addition of MDSC from TAZ10 mice resulted in a stronger inhibition compared to MDSC from WT mice, thus suggesting that they were more potent at inhibiting T cell proliferation (Figure 3.17).

I however wondered whether these observations were not exclusive to the TAZ10 transgenic mouse model and therefore decided to investigate the differential suppressive activity of MDSC from the CCIA mouse model of rheumatoid arthritis. In contrast to TAZ10 transgenic mice that spontaneously develop autoimmune thyroiditis, CCIA mice (DBA/1 TCR-Vβ12) develop chronic arthritis upon immunization with collagen type II in Complete Freund's Adjuvant (CFA). MDSC were isolated from the spleen of DBA/1 mice injected with PBS (WT) or immunized with collagen II (21 days after immunization) and added to T cells stimulated by mature DC and αCD3 antibody (Figure 3.18).

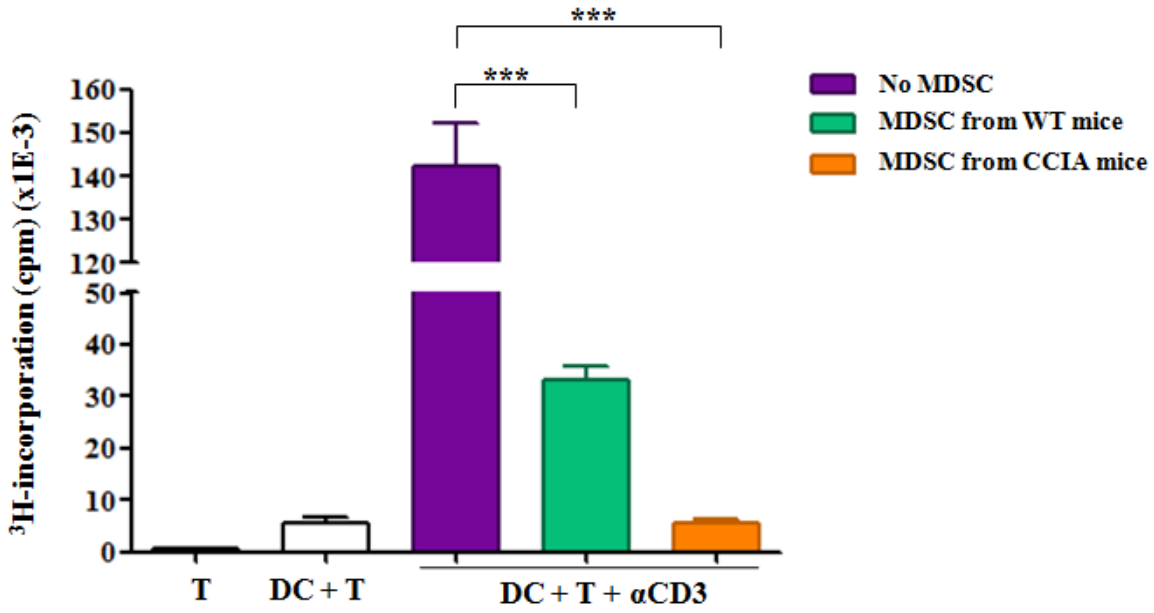

Figure 3.18: MDSC from CCIA mice display stronger inhibitory activity on T cell proliferation than MDSC from WT mice

$Gr1^+$ cells were isolated from WT and CCIA mice and added to T cells stimulated with αCD3 and costimulatory signals provided by mature dendritic cells (DC). $Gr1^+$ MDSC were added to T cells at a T:MDSC ratio of 1:1. Data are representative of 2 experiments. The T cell proliferative activity was assessed by (^{3}H) thymidine incorporation and statistics were done using the unpaired Student's t-test.

Similarly to figure 3.17, the addition of MDSC from WT and CCIA mice resulted in a decrease in T cell proliferation (Figure 3.18). Although MDSC from non-immunised mice reduced T cell proliferation by about three-fold, MDSC from Collagen II-immunized mice had a much stronger inhibitory effect as the proliferation was decreased down to background level. These results showed that the previous observations were not exclusive to the TAZ10 model and confirmed that MDSC from mice with AID are more potent at inhibiting T cell proliferation than MDSC from WT mice.

Taking into consideration previous results (Figure 3.17), it appears that the ongoing inflammation in TAZ10 mice has an effect on the accumulation of MDSC and is also associated with a gain of suppressive function. To further explore the impact of this inflammatory environment on the suppressive activity of MDSC, I investigated the effect of the depletion of MDSC on the proliferative activity of T cells in TAZ10 mice at different age. Indeed, the level of inflammation in TAZ10 would vary over time: while in mice of less than 3 months of age the inflammation would be at its maximum as the thyroid gets progressively destroyed, it would fade in older mice as the disease becomes more chronic.

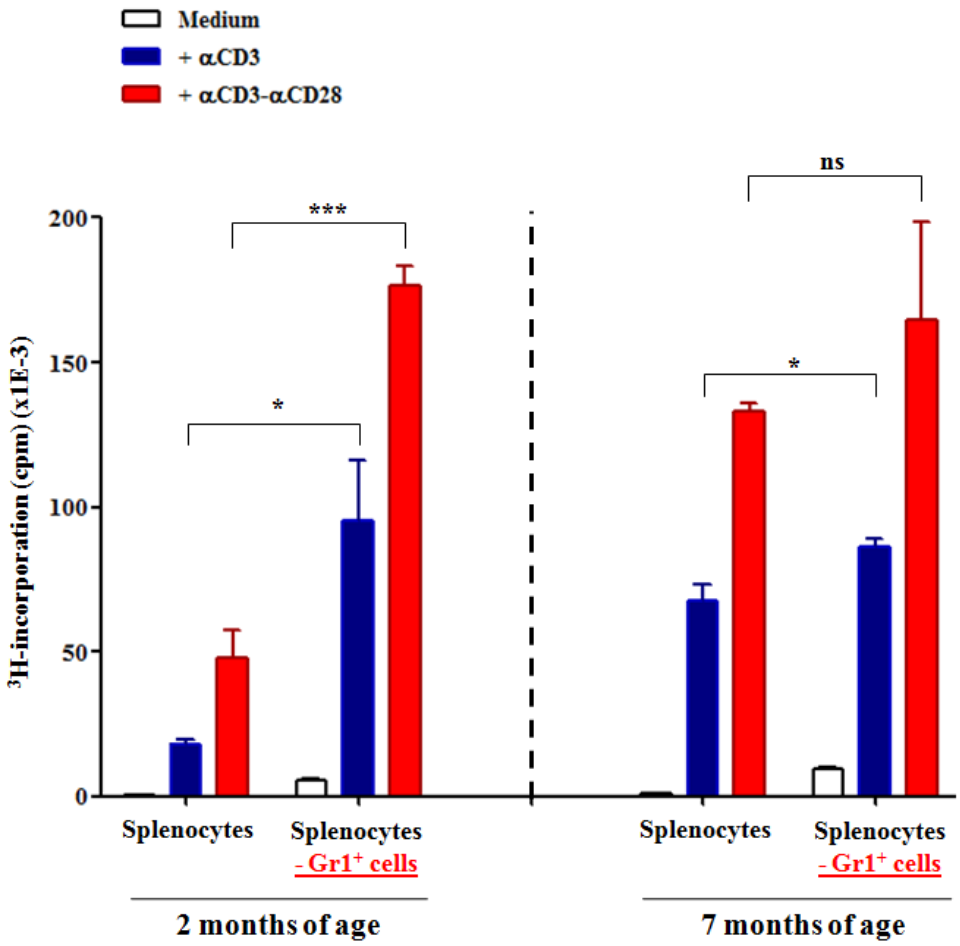

Figure 3.19: The suppressive function of MDSC depends on the level of inflammation
Untreated and Gr1 depleted splenocytes (SN) from TAZ10 mice of 2 and 7 months of age were stimulated with either αCD3 or αCD3-αCD28 antibodies and their proliferative activity assessed by (^{3}H) thymidine incorporation assay. Gr1$^+$ MDSC were added to splenocytes at a SN:MDSC ratio of 1:1. Data are representative of 3 different experiments. Statistics were performed using the unpaired Student's t-test.

While the depletion of MDSC from 2 and 7 months old TAZ10 mice resulted in an increased T cell proliferation in response to αCD3, only MDSC from 2 months old TAZ10 mice were able to significantly inhibit the proliferative activity of T cells in response to αCD3-αCD28. These results suggested that MDSC had a stronger suppressive activity in young mice during the acute phase of the disease. However, as shown figure 3.10, the number of MDSC varies in the spleen of TAZ10 mice over time. About 3.5% of MDSC are present in the spleen of 2 months old TAZ10 mice against 2% in 7 months old mice. The effect of the addition of an equal number of MDSC isolated from WT and TAZ10 mice at different age on the proliferative activity of T cells was assessed (Figure 3.20).

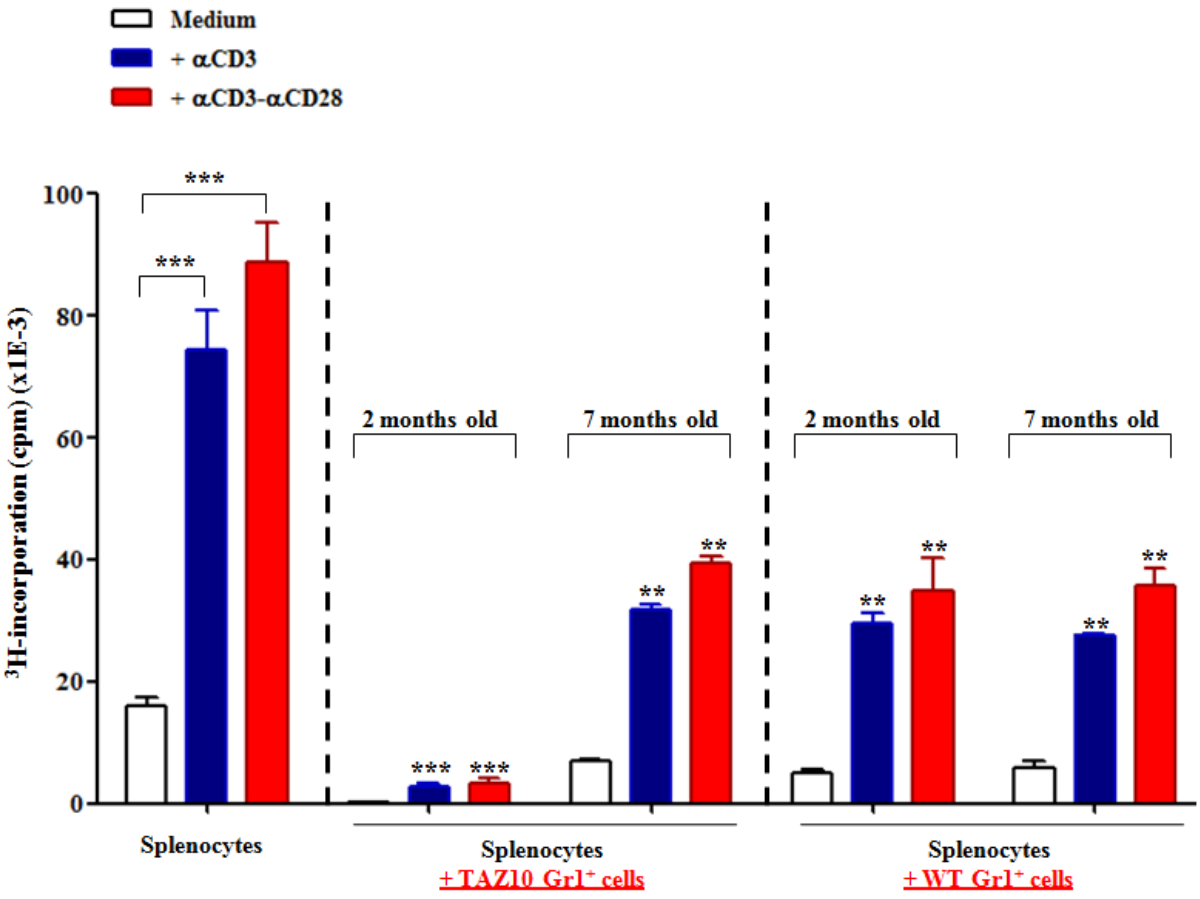

Figure 3.20: MDSC from 2 months old TAZ10 mice display a more suppressive activity on T cells than MDSC from older mice

Gr1$^+$ cells isolated from the spleen of 2 and 7 months old WT and TAZ10 mice were added to transgenic splenocytes activated with either αCD3 or αCD3-αCD28 antibodies. The proliferative activity of T cells was assessed by (^{3}H) thymidine incorporation. Gr1$^+$ MDSC were added to splenocytes at a splenocyte:MDSC ratio of 1:1. Data are representative of 3 different experiments. Statistics were performed using the unpaired Student's t-test and done using splenocytes stimulated with αCD3 for blues bars and splenocytes stimulated with αCD3-αCD28 for red bars as references.

The addition of MDSC isolated from 2 months old TAZ10 mice to splenocytes stimulated with αCD3 or αCD3-αCD28 antibodies resulted in an important decrease in proliferation. While the addition of MDSC from 2 months old WT mice also resulted in a decreased proliferation, this inhibition was not as significant when compared to the effect of the addition of MDSC from 2 months old TAZ10 mice. This highlighted that MDSC from transgenic mice were more potent at suppressing T cell function than MDSC from WT mice. Interestingly, if MDSC from WT mice displayed the same inhibitory function on T cells over time, the ability of MDSC from TAZ10 mice to suppress T cell proliferation was age-dependent. Indeed, the addition of MDSC from 2 months old TAZ10 mice nearly abrogated T

cell proliferation while a two-fold decrease in T cell proliferation was observed when MDSC from WT or MDSC from 7 months old TAZ10 mice were used.

These results showed that the inflammation present in TAZ10 mice had a major impact on the accumulation and suppressive function of MDSC. While MDSC accumulate and display strong inhibitory function on T cells during the acute phase of the disease as the thyroid gets progressively destroyed, their number decreases as the inflammatory process fades, phenomenon associated with a reduced suppressive activity over time. I next wanted to understand how MDSC exert their inhibitory activity on T cells and how the inflammation in transgenic mice modulates this suppressive function.

3.3 – Results Part 2: Investigation of mechanisms displayed by MDSC to suppress T cell responses

I have previously shown that MDSC accumulated in lymphoid and non-lymphoid organs from the onset of the disease in TAZ10 mice and displayed strong inhibitory functions on T cells *in-vitro*. I then wanted to investigate some of the mechanisms by which MDSC mediate this suppressive function.

3.3.1 – MDSC cannot induce T cell proliferation in response to a MHC class II restricted peptide

MDSC originate from common myeloid precursor cells and have the ability to differentiate into mature myeloid cells such as macrophages and dendritic cells depending on the nature of the microenvironment (Gabrilovich et al. 2009). I therefore wanted to explore whether the inflammatory environment present in TAZ10 mice had any impact on the level of expression of APC-specific markers by MDSC. To this aim, the expression of various markers of APC such as CD11c, F4/80, CD86 and I-A^b by MDSC from the spleen of both WT and TAZ10 transgenic mice was assessed by flow cytometry.

MDSC from WT and TAZ10 mice expressed CD11c and F4/80 (Figure 3.21/A). Interestingly, this expression was increased by more than two-fold in MDSC from TAZ10 mice compared to MDSC from WT mice. This was further associated with an upregulation of the expression of maturation markers: 23% of MDSC from TAZ10 mice expressed CD86 and 65% of them expressed I-A^b MHC-II molecules against 7% and 48% respectively for MDSC from WT mice (Figure 3.21/B). These results showed a significant difference in the phenotype of MDSC from WT and TAZ10 mice. In addition to its role on the accumulation and function of MDSC previously highlighted chapter 3/part 1, it appeared that the inflammatory status of TAZ10 mice modulates the phenotype of MDSC.

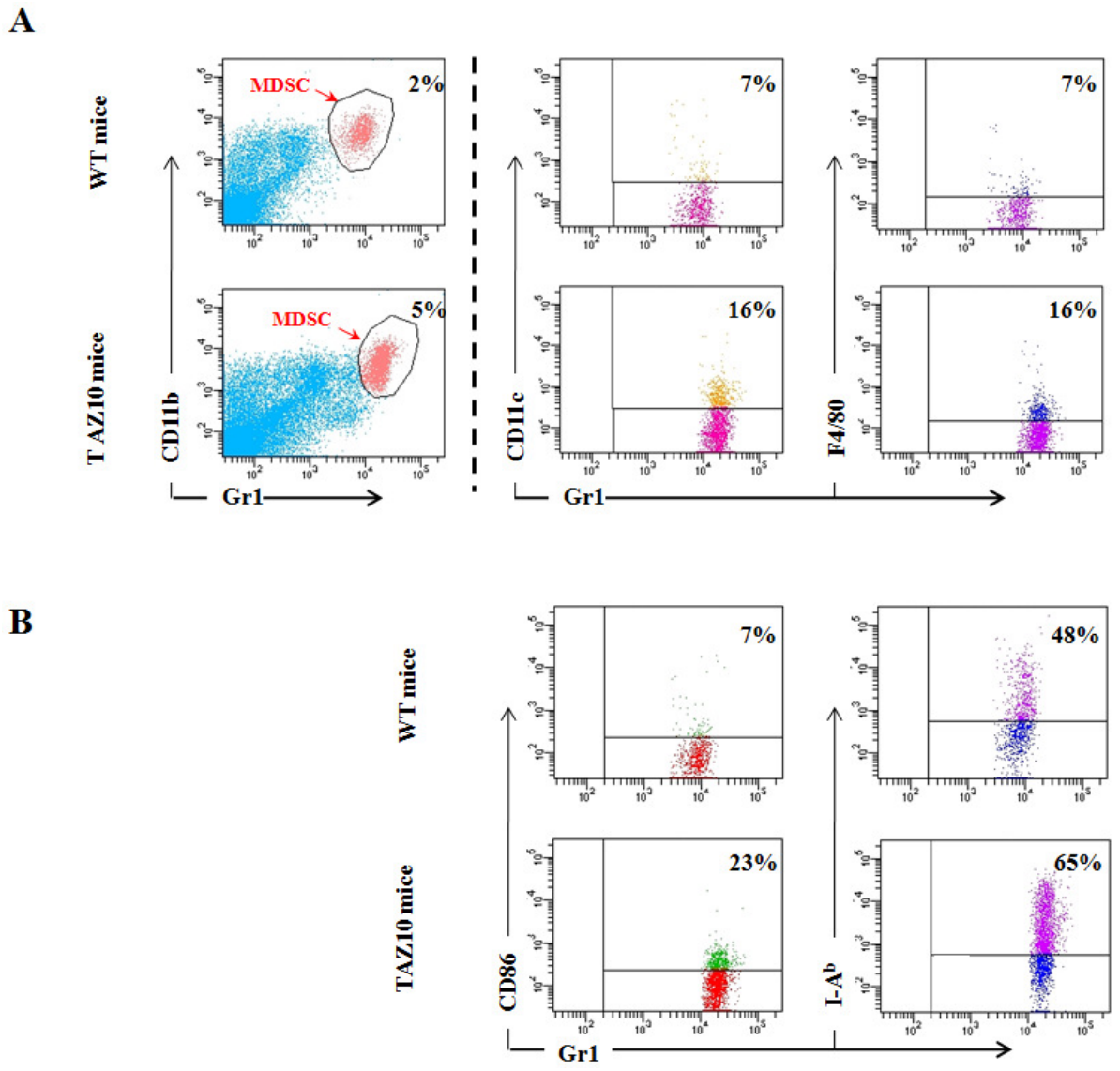

Figure 3.21: MDSC from the spleen of TAZ10 transgenic mice express markers specific of antigen presenting cells (APC)
MDSC from the spleen of WT and TAZ10 mice were analysed by flow cytometry for their expression of APC specific markers such as CD11c and F4/80 **(A)** and maturation markers, such as CD86 and I-A^b **(B)**. Data are representative of more than 10 mice in each group.

MDSC originating from the bone marrow, I wondered whether the inflammatory status in TAZ10 mice would also alter their phenotype. MDSC from the bone marrow of WT and TAZ10 mice were therefore analysed for their expression of CD11c, CD86, F4/80 and I-A^b molecules (Figure 3.22).

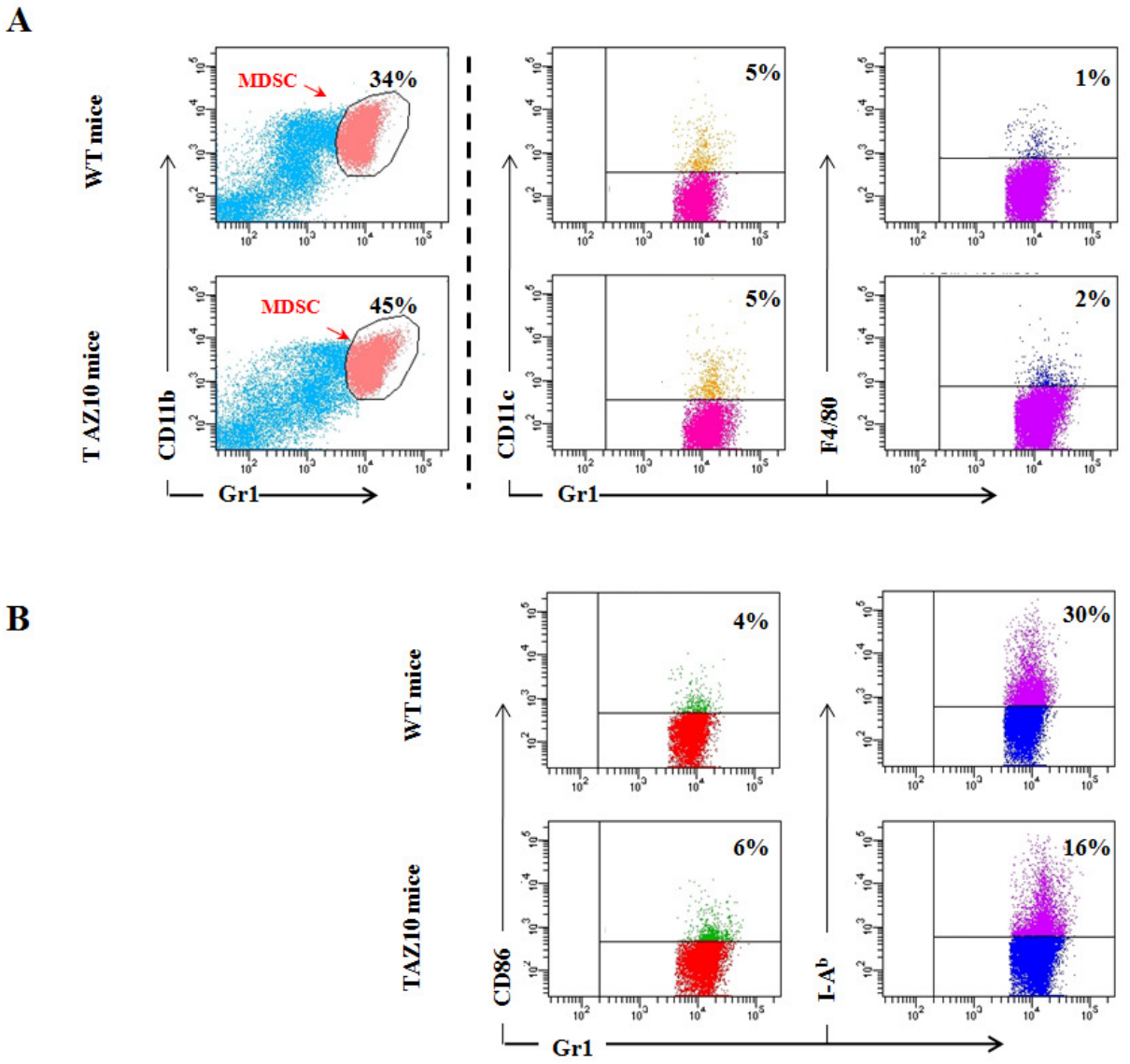

Figure 3.22: The phenotype of MDSC from the bone marrow of TAZ10 transgenic mice does not considerably differ from WT mice

The expression of APC specific markers such as CD11c and F4/80 **(A)** and maturation markers, such as CD86 and I-A^b **(B)** was analysed by flow cytometry on MDSC from the bone marrow of WT and TAZ10 mice. Data are representative of more than 10 mice in each group.

Contrary to the phenotype of MDSC observed in the spleen, there was no difference in the expression of CD11c, CD86 and F4/80 markers in MDSC from the bone marrow between WT and TAZ10 mice (Figure 3.22). The level of expression of these markers remained low as only 5% of MDSC expressed CD11c and only 2% and 5% expressed F4/80 and CD86 respectively. In contrast, 30% of MDSC from the bone marrow of WT mice expressed MHC-II molecules compared to only 16% in TAZ10 mice. Overall, MDSC from WT mice displayed a more differentiated phenotype once they leave the bone marrow especially in

term of MHC-II expression. While promoting the accumulation of MDSC in secondary lymphoid tissues, the inflammatory status present in TAZ10 mice also enhanced this differentiation as suggested by the increased expression of CD11c, CD86 and F4/80. Interestingly, the lower expression of MHC-II molecules by MDSC from the bone marrow in TAZ10 mice compared to WT mice did not reflect this and could simply highlight their direct migration from the bone marrow to the secondary lymphoid organs.

Because MDSC expressed various markers of APC, I next wanted to determine whether they shared any function known to APC and suggested a potential role of MDSC in the processing and presentation of endogenous and exogenous antigens. I first investigated the endocytic capacity of MDSC by assessing their ability to uptake latex beads.

BM-DC and MDSC purified from the spleen of TAZ10 mice were incubated with 3µm IgG opsonised latex beads at 37ºC for various times. The internalization of the beads was initially assessed by flow cytometry analysis (data not shown) but this method was excluded as I could not discriminate between cell-association and actual internalization of the beads. The examination of the cells by confocal microscopy provided clear evidence of uptake (Figure 3.23). Because the protocol for the isolation of MDSC by magnetic cell separation did not provide a level of purity of 100% (Figure 3.12), I confirmed that the cells uptaking latex beads were MDSC by staining for both Gr1 and CD11b markers.

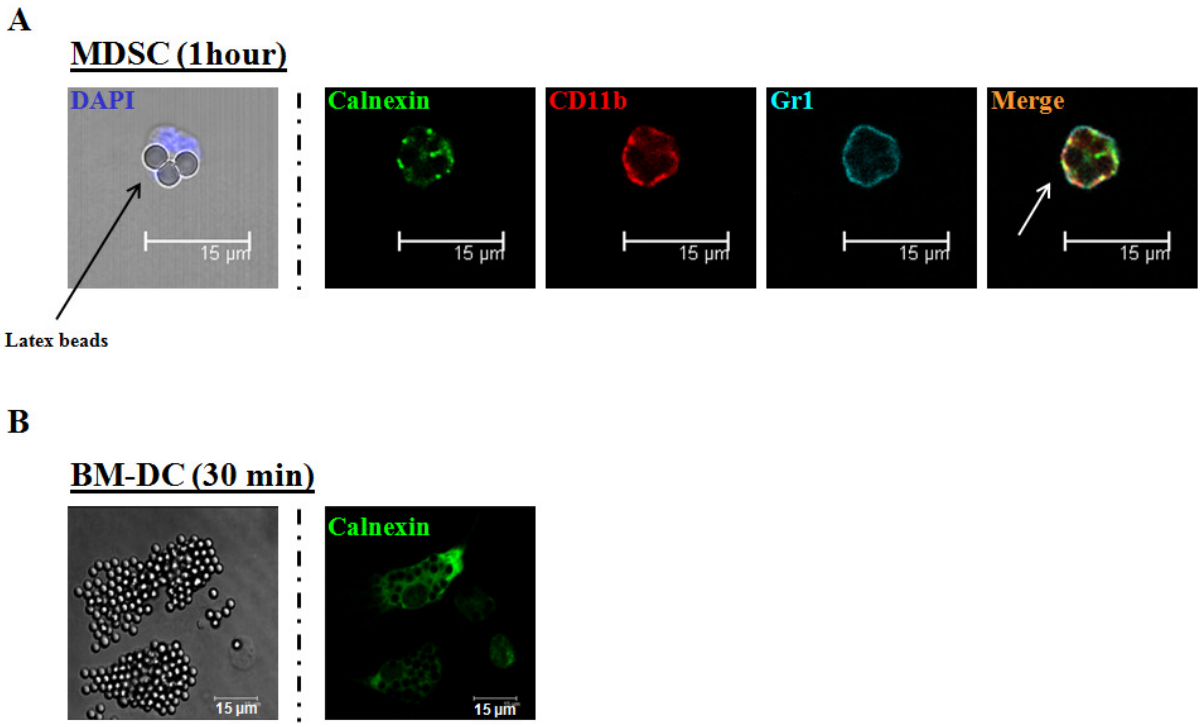

Figure 3.23: MDSC can uptake latex beads by phagocytosis
(A) $Gr1^+$ MDSC purified from spleen of TAZ10 transgenic mice were incubated for 1 hour with IgG-coated latex beads. Cells were then stained for calnexin (green), CD11b (red), Gr1 (turquoise) and DAPI (blue-nucleus). Analysis was performed at a magnification of x63 on a confocal microscope. **(B)** Uptake of latex beads by bone-marrow derived DC (BM-DC) was assessed by incubating the cells with latex beads for 30 min. Cells were stained for calnexin (green) and analysed by confocal microscopy. Pictures on the uptake of latex beads by BM-DC have been kindly donated by Dr Alexandra Mant. Data shown are representative of 5 distinct experiments.

MDSC expressed Gr1 and CD11b markers as shown by the red and turquoise staining present primarily on their cell surface (Figure 3.23/A). These cells along with BM-DC (Figure 3.23/B) were able to take up the latex beads as revealed by the colocalization of beads with the ER-specific marker calnexin. Furthermore, the presence of some staining for Gr1 and CD11b inside MDSC ascertained that some parts of the plasma membrane had been taken up with the latex beads during internalization.

While BM-DC managed to take up a large number of beads in only 30 minutes (Figure 3.23/B), MDSC only managed to take up 3 beads within 45 minutes thus highlighting a difference in the kinetics of internalization and therefore a reduced phagocytic activity for MDSC compared to BM-DC.

I then wondered whether MDSC could present a specific peptide and induce the proliferation of antigen-specific T cells. I therefore assessed the ability of MDSC to induce the proliferation of TAZ10-T in response to the class II restricted cognate P3 antigen in a (^{3}H) thymidine proliferation assay using MDSC as APC (Figure 3.24)

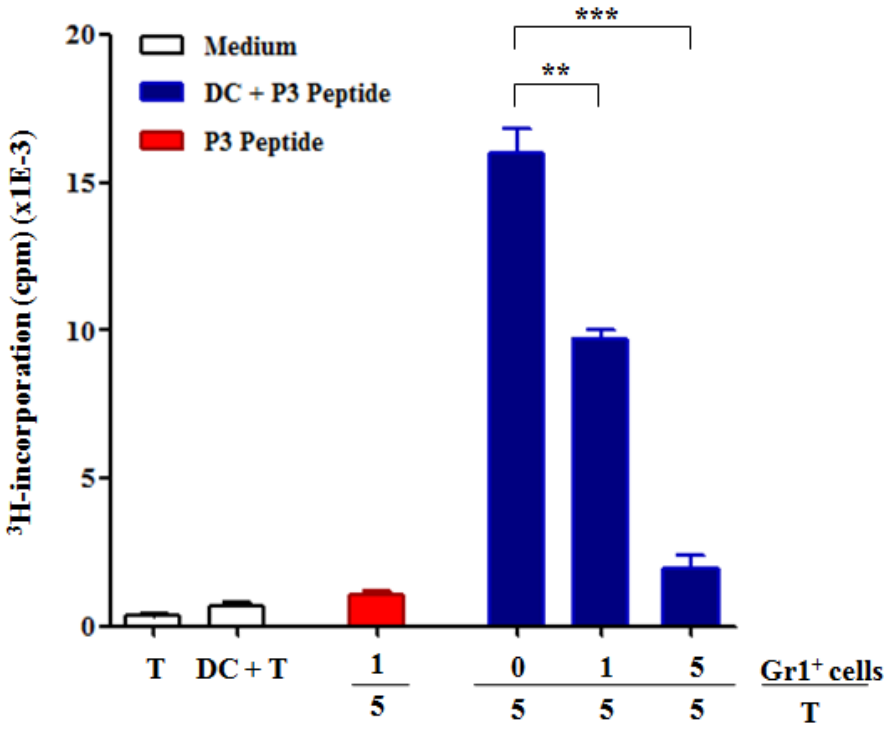

Figure 3.24: MDSC are unable to prime an immune response but can inhibit antigen-specific T cell proliferation

MDSC from the spleen of TAZ10 mice were added to the culture of mature DC (DC) and T cells at different T:MDSC ratio (5:1 or 1:1) to assess their inhibitory activity on T cells (Blue bars). The ability of MDSC to induce T cell proliferation in response to the cognate peptide P3 was investigated using MDSC as APC (Red bars). T cell proliferation was measured by (^{3}H) thymidine incorporation assay. Data are representative of 5 independent experiments. Statistics were performed using the unpaired Student's t-test.

Although TAZ10-T cells did proliferate when P3 was presented by mature DC, the addition of MDSC resulted in an inhibition of T cell proliferation. This inhibition was dose-dependent as MDSC added at a T:MDSC ratio of 1:1 inhibited T cell proliferation more strongly than at a ratio of 5:1 (Blue bars; figure 3.24). Despite the expression of high levels of MHC-II molecules, MDSC were unable to induce the proliferation of antigen-specific T cells (Red bars; figure 3.24).

3.3.2 – The suppressive activity of MDSC is associated with the metabolism of L-arginine

One mechanism by which MDSC mediate their immunosuppressive function involves the metabolism of L-arginine. In a Th1-like cytokine environment, MDSC upregulate the expression of iNOS. This enzyme oxidizes L-arginine to generate L-citrulline and NO that impairs the IL-2R signalling pathway and promotes T cell apoptosis (Mazzoni et al. 2002). In a Th2-like cytokine environment, the upregulation of Arg-1 expression results in the depletion of L-arginine from the microenvironment and the production of urea and L-ornithine from the degradation of L-arginine. The shortage of L-arginine alters the synthesis of CD3ζ preventing T cells from proliferating in response to a cognate peptide (Rodriguez et al. 2003).

Similarly to Th17 cells, Th1 cells have been shown to be capable of inducing the disease in two different models of autoimmunity (Steinman. 2008). Both Th1 and Th17 cells could induce disease in an Experimental model of Autoimmune Uveitis (EAU) although the pathology differed depending on the effector population mediating the disease (Luger et al. 2008). At the same time, disease in an Experimental model of Autoimmune Encephalitis (EAE) could be driven either by Th17 or Th1 with the main effector phenotype being defined by the conditions present during the first encounter with the autoantigen (Kroenke et al. 2008). This information is of great interest when considering the function of MDSC that is directly dependent on the inflammatory status characterised by a balance between pro versus anti-inflammatory cytokines. Considering the important role of Th1 in the pathogenesis of AID, I first wanted to explore the role played by iNOS and the subsequent release of nitric oxide (NO) in the inhibition of T cells mediated by MDSC.

3.3.2.1 – Investigation of the role of iNOS and the release of NO on the ability of MDSC to inhibit T cell functions

To assess whether MDSC could secrete NO, I first measured the amount of NO produced by splenocytes from both WT and TAZ10 transgenic mice. The analysis was performed *ex-vivo* on unstimulated cells using the DAF-FM probe (Chapter 2.8), a reagent

developed for the detection of low concentrations of NO by flow cytometry analysis (Figure 3.25)

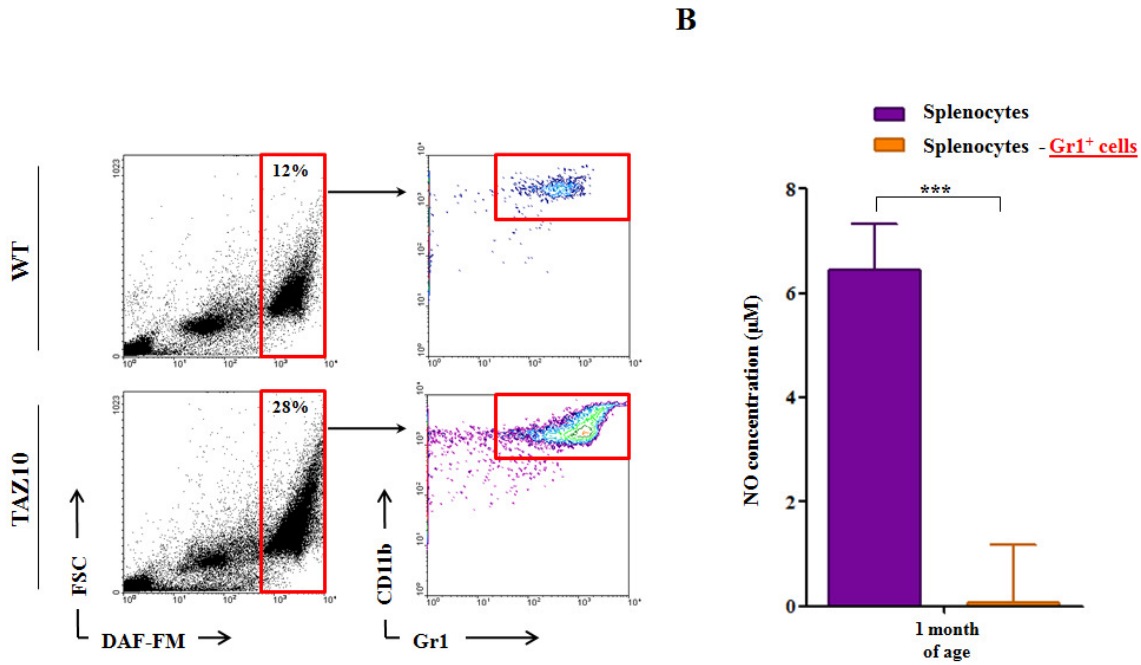

Figure 3.25: MDSC from TAZ10 transgenic mice produce high levels of nitric oxide (NO)
(A) Three colour FACS staining using DAF-FM probe was performed to quantify intracellular NO in splenocytes from WT and TAZ10 mice. Gated populations were analysed for their expression of CD11b and Gr1 markers. **(B)** The amount of NO released in the medium by splenocytes from TAZ10 transgenic mice activated with αCD3-αCD28 antibodies was measured using the Griess Reagent method. The role played by MDSC on the amount of NO secreted was investigated by depleting $Gr1^+$ cells. Data are representative of 5 separate experiments and statistics were performed using the unpaired Student's t-test.

$Gr1^+$ $CD11b^+$ cells from the spleen of WT and TAZ10 mice were responsible for the majority of the production of NO with MDSC from TAZ10 mice producing more NO (28% versus 12% in WT mice) (Figure 3.25/A). This was confirmed by measuring the amount of NO released in the medium by activated splenocytes in the presence or absence of MDSC. The depletion of MDSC nearly abrogated the release of NO thus highlighting that this cell population was indeed the major producer of NO (Figure 3.25/B). The increased ability of MDSC from TAZ10 mice to produce NO was in line with previous observations (Figure 3.17) where the inflammation present in TAZ10 mice enhanced the suppressive activity of MDSC on T cells.

I have described that MDSC accumulate in lymphoid organs of TAZ10 transgenic mice and display a stronger inhibitory activity on T cells during the acute phase of the disease. I therefore assessed the ability of MDSC from 1 and 5 months old WT and TAZ10 mice to

secrete NO over time. The amount of NO released from WT and TAZ10 splenocytes stimulated with αCD3-αCD28 antibodies was measured using the Griess method (Figure 3.26).

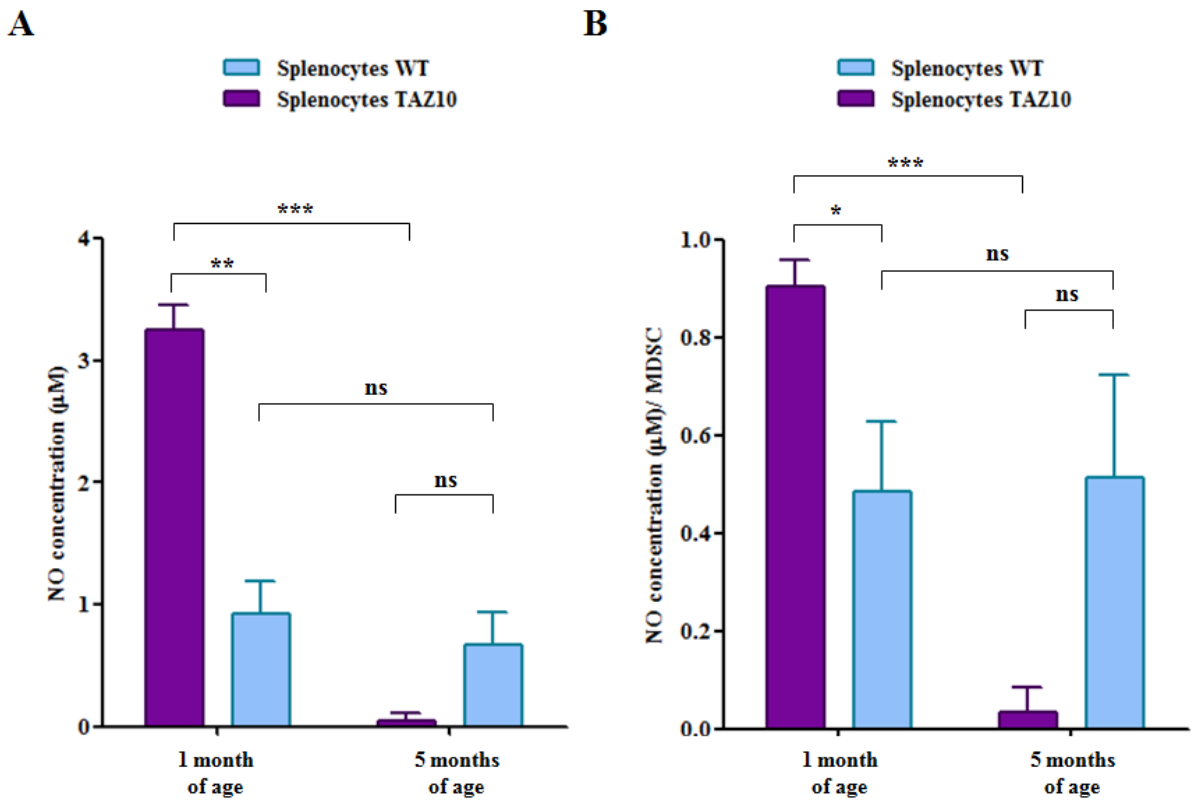

Figure 3.26: MDSC from TAZ10 mice display a reduced production of nitric oxide (NO) during the course of autoimmunity
(A) Splenocytes from TAZ10 transgenic mice and WT mice (1 and 5 months old) were stimulated using αCD3 and αCD28 antibodies and the amount of NO released in the medium was measured using the Griess method. **(B)** The secretion of NO on a cell basis was assessed in transgenic and WT mice. Data are representative of 3 different experiments. Statistics were performed using the unpaired Student's t-test.

While NO concentration remained unchanged in WT mice over time, it dramatically decreased in 5 month old TAZ10 mice. Interestingly, the amount of NO produced by splenocytes from 1 month old TAZ10 mice was much higher than in WT mice (Figure 3.26/A). I have shown that after 5 months, the number of MDSC in the spleen of TAZ10 mice was much lower compared to 1 month old mice. To ascertain that MDSC from TAZ10 mice were producing less NO over time, the secretion of NO was considered on a per cell basis (Figure 3.26/B). MDSC from WT mice produced the same quantity of NO over time. In comparison, NO secretion by splenocytes from one month old TAZ10 mice was increased by

two-fold compared to splenocytes from 5 month old mice. This further highlighted that MDSC secreted more NO during the acute phase of the disease when the inflammation is at its maximum as the thyroid gets progressively destroyed. These results therefore showed that the ability of MDSC to produce NO along with their suppressive activity on T cells depended on the inflammatory context in TAZ10 mice.

Because the secretion of NO was enhanced in TAZ10 mice compared to WT mice, I decided to investigate the impact of NO in the suppressive activity of MDSC on T cell responses. To determine the role of iNOS in the ability of MDSC to inhibit T cell proliferation, the L-NMMA specific irreversible inhibitor of iNOS was used.

Splenocytes were activated with αCD3-αCD28 antibodies in presence or absence of MDSC and the amount of NO released in the medium was measured using the Griess method (Figure 3.27/B).

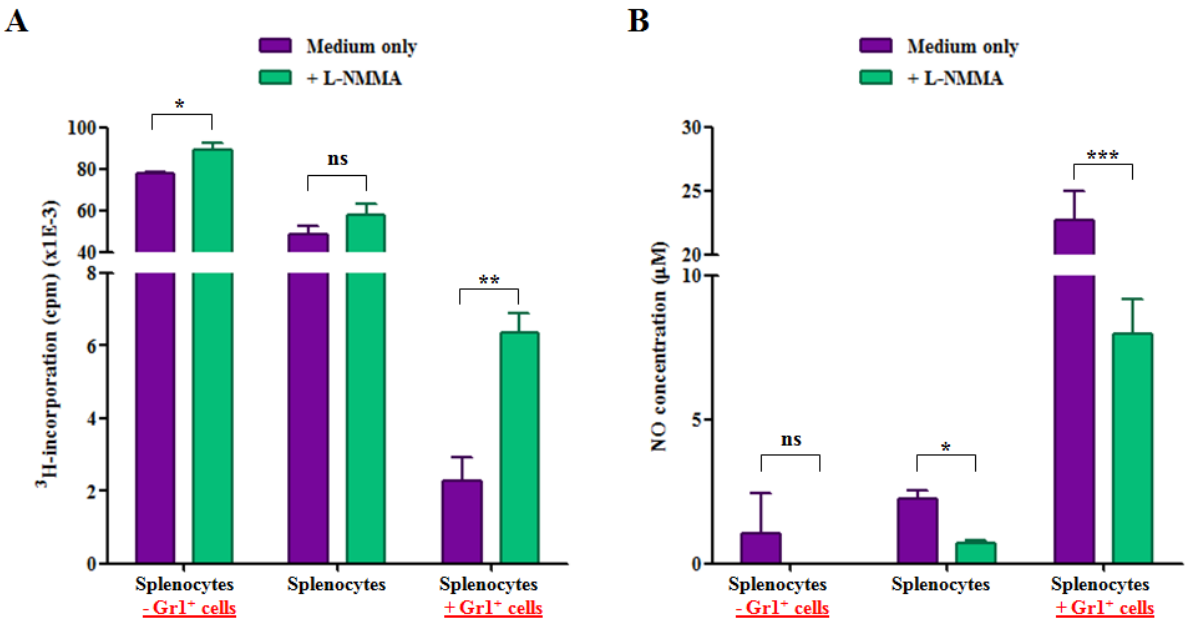

Figure 3.27: The release of NO by MDSC from TAZ10 mice is not the key mechanism involved in the inhibition of T cell proliferation

Untreated, Gr1 depleted and Gr1 enriched (Splenocytes:MDSC ratio of 1:1) splenocytes were activated by αCD3-αCD28 antibodies. The proliferative activity of T cells was assessed by ^{3}H thymidine incorporation assay **(A)** and the amount of NO released in the medium was measured using the Griess method **(B)**. The role of inducible nitric oxide synthase (iNOS) in the secretion of NO and its subsequent effect on T cell proliferation was investigated by using the iNOS inhibitor L-NMMA. Data are representative of 3 different experiments. Statistics were done using the unpaired Student's t-test.

The addition of MDSC to splenocytes at a splenocytes:MDSC ratio of 1:1 resulted in a significant increase in NO production while their depletion reduced the secretion of NO (Figure 3.27/B). When L-NMMA was added to the culture, NO production was dramatically decreased thus highlighting the role played by iNOS in the secretion of NO by MDSC.

I then assessed whether NO secreted by MDSC had any effect on the suppression of T cell proliferation. In the same experimental settings, the proliferative activity of T cells by (^{3}H) thymidine incorporation was measured. Addition of MDSC significantly decreased T cell proliferation while their depletion abrogated this inhibition (Figure 3.27/A).

While the inhibition of iNOS resulted in a reduced NO production, it was also associated with an increased T cell proliferation (Figure 3.27/A). Although the secretion of NO by untreated splenocytes was halved in presence of L-NMMA, it could not completely reverse MDSC-mediated inhibition of T cell proliferation thus suggesting that iNOS upregulation may not be a key mechanism involved in MDSC suppressive activity in TAZ10 mice. This was further illustrated when L-NMMA could not restore the proliferation of T cells when MDSC were added at a Splenocyte:MDSC ratio of 1:1.

3.3.2.2 – MDSC mediate their suppressive function in part through the degradation of L-Arginine by Arg-1

Having shown that the upregulation of iNOS and the subsequent release of NO might not be the key mechanism used by MDSC to inhibit the proliferative activity of T cells in TAZ10 mice, I then investigated whether the suppressive function of MDSC was preferentially mediated by the degradation of L-arginine through the action of Arg-1.

Splenocytes in the presence or absence of MDSC were stimulated with αCD3-αCD28 antibodies and the amount of NO released as well as the proliferative activity of T cells measured. The role of Arg-1 was assessed using the NOHA specific inhibitor (Figure 3.28).

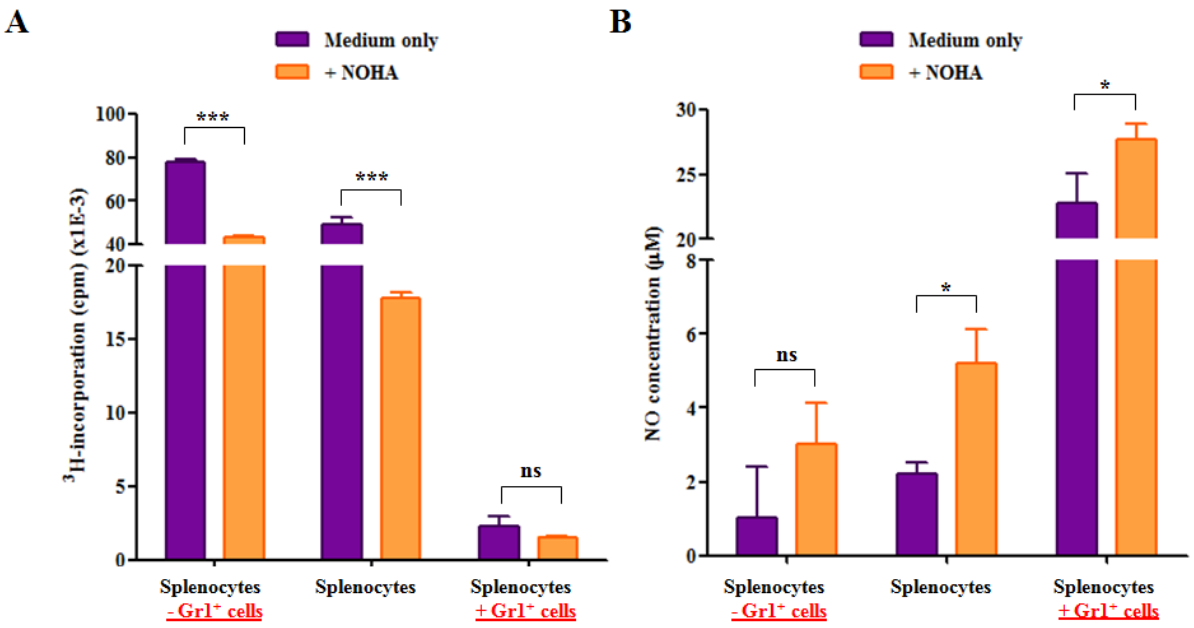

Figure 3.28: Investigation of the role of arginase 1 in the mechanisms of action of MDSC
(A) Untreated, Gr1 depleted and Gr1 enriched (Splenocytes:MDSC ratio of 1:1) splenocytes were activated by αCD3-αCD28 antibodies and the proliferative activity of T cells was assessed by (^{3}H) thymidine incorporation assay. **(B)** The amount of NO released in the medium was measured using the Griess method. The role arginase 1 (Arg-1) in the secretion of NO and its subsequent effect on T cell proliferation was investigated by adding the Arg-1 inhibitor NOHA to the culture. Data are representative of 3 distinct experiments. Statistics were done using the unpaired Student's t-test.

As previously shown figure 3.27, the addition of MDSC resulted in an increase secretion of NO while it decreased as MDSC were depleted (Figure 3.28/B). Interestingly, when NOHA was added to the culture, the secretion of NO was systematically enhanced in all conditions confirming that the inhibition of Arg-1 favoured the production of NO. While iNOS metabolizes L-arginine to generate NO, Arg-1 degrades this essential amino acid into urea and L-ornithine. Therefore, by blocking the activity of Arg-1, the degradation of L-arginine is redirected through iNOS and results in an increased production of NO (Figure 3.28/B).

The direct consequence of this increase in NO production was an inhibition of T cell proliferation (Figure 3.28/A). While the addition of NOHA resulted in a non-significant increase of NO secretion by Gr1 depleted splenocytes, it resulted in a significant inhibition of T cell proliferation in both splenocytes and splenocytes depleted of MDSC.

Overall these results showed that the inhibitory activity of MDSC was in part mediated through the metabolism of L-arginine. However, I should point out that this experiment using

αCD3-αCD28 simulation may not reflect the relevance of this inhibitory mechanism in physiological conditions.

3.3.3 – MDSC promote the induction of Foxp3$^+$ regulatory T cells

Another mechanism displayed by MDSC to inhibit T cell proliferation is the induction of Tregs. While this function has been described in various studies in tumour models (Serafini et al. 2008, Huang et al. 2006), there is currently no report of such mechanism in autoimmunity. I therefore investigated whether MDSC could promote the induction of Foxp3$^+$ Tregs in TAZ10 mice.

3.3.3.1 – MDSC promote the de-novo development of Tregs

The first step was to determine an experimental protocol that would allow this investigation. Previous work performed in TAZ10 mice has highlighted the absence of Foxp3$^+$ Tregs in TAZ10 Rag$^{-/-}$ mice (Ester Badami's PhD thesis – July 2007). A gating strategy was put in place in order to investigate the expression of Foxp3 by CD4$^+$ T cells from TAZ10 mice. TAZ10 Rag$^{-/-}$ mice do not have any T cells other than TPO specific V_β1-V_α15 TAZ10 T cells (Quaratino et al. 2004). CD4$^+$ T cells from these mice are identified by their expression of TCR-Vβ1 marker and successive gating on CD4$^+$ cells and then on TCR-V_β1$^+$ cells would therefore specifically target transgenic CD4$^+$ T cells (Figure 3.29/A).

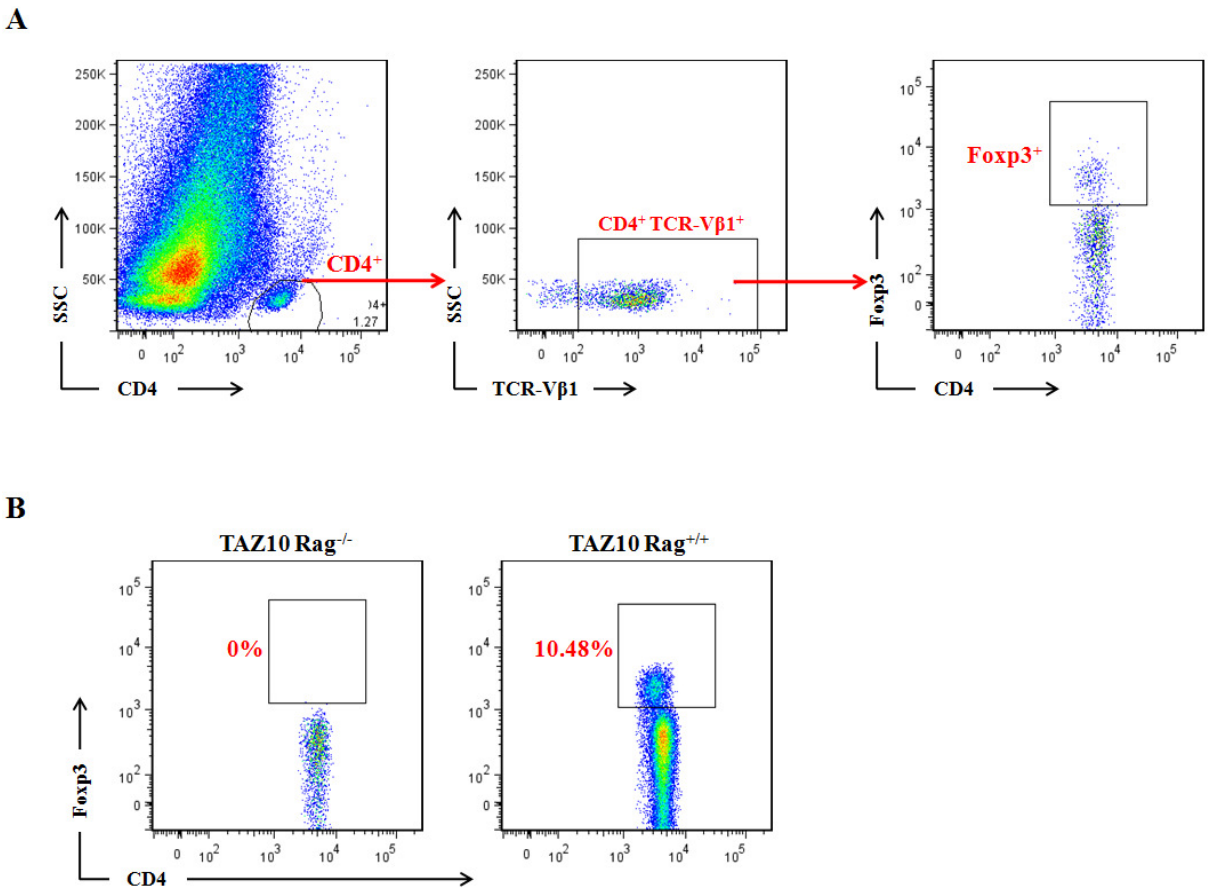

Figure 3.29: Foxp3$^+$ Tregs are absent in TAZ10 Rag$^{-/-}$ mice and present in TAZ10 Rag$^{+/+}$ mice
(A) Gating strategy used to investigate the induction of Tregs by MDSC by flow cytometry. Gated CD4$^+$ cells were analysed for their expression of TCR-V$_\beta$1. The expression of Foxp3 by CD4$^+$ TCR-V$_\beta$1$^+$ cells was then assessed. **(B)** The presence of CD4$^+$ TCR-V$_\beta$1$^+$ Foxp3$^+$ cells in the spleen of TAZ10 Rag$^{-/-}$ and TAZ10 Rag$^{+/+}$ mice was investigated. Data are representative of more than 10 experiments.

I first investigated the presence of Tregs in the spleen of TAZ10 Rag$^{-/-}$ and Rag$^{+/+}$ mice. While about 10.5% of CD4$^+$ T cells expressed Foxp3 in the spleen of TAZ10 Rag$^{+/+}$ mice, this expression was null in the spleen of TAZ10 Rag$^{-/-}$ mice (Figure 3.29/B). The use of splenocytes from TAZ10 Rag$^{-/-}$ mice to determine the ability of MDSC to induce Tregs was therefore ideal as any Foxp3$^+$ cells detected would be the result of a *de-novo* induction of Tregs.

I next determined that the fraction of MDSC used to perform these experiments did not contain any Foxp3$^+$ cells as they were purified from TAZ10 Rag$^{+/+}$ mice. I could however rule out the presence of any Tregs and more generally CD4$^+$ T cells as MDSC were purified from the spleen of TAZ10 Rag$^{+/+}$ mice that had been depleted of CD4$^+$ T cells *in-vivo* (Figure 3.30).

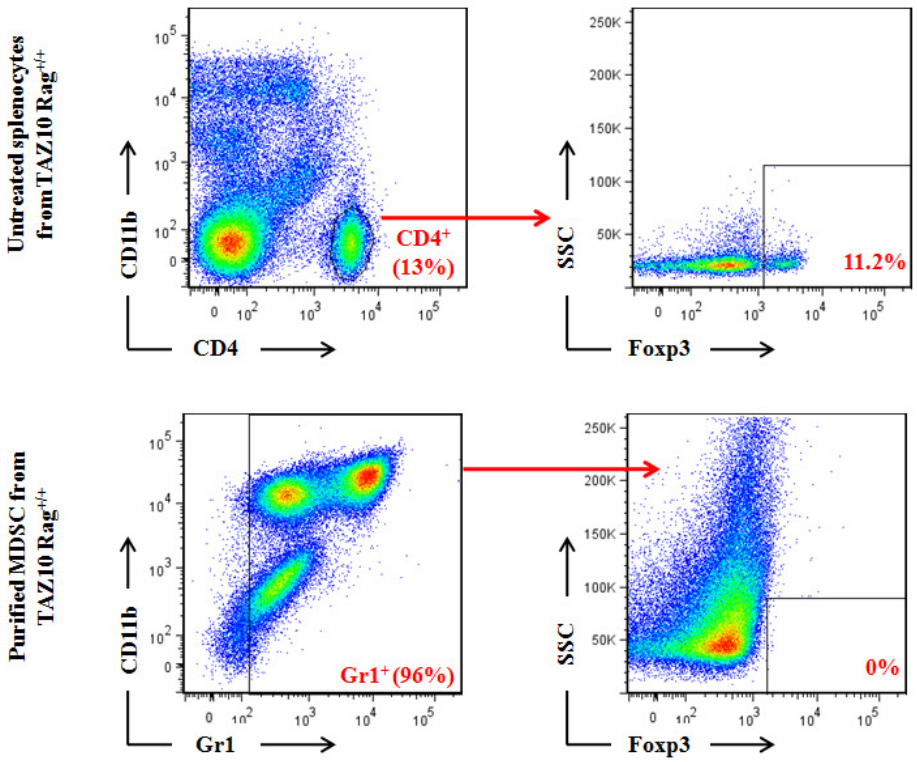

Figure 3.30: Purified MDSC do not contain Foxp3$^+$ Tregs
The expression of Foxp3 was investigated in the fraction of MDSC purified from the spleen of CD4 depleted TAZ10 Rag$^{+/+}$ mice (Top panels). CD4$^+$ cells from the spleen of untreated TAZ10 Rag$^{+/+}$ mice were used as a positive control for the expression of Foxp3 (Lower panels). Data are representative of more than 10 experiments.

Splenocytes from TAZ10 Rag$^{+/+}$ mice were used as positive control as about 11% of CD4$^+$ cells express Foxp3. By contrast, the fraction of MDSC purified from the spleen of CD4 depleted TAZ10 Rag$^{+/+}$ mice contained 96% of Gr1$^+$ cells and no Foxp3$^+$ cells. I was therefore confident I could use MDSC purified from CD4 depleted TAZ10 Rag$^{+/+}$ mice to study their ability to induce Tregs in TAZ10 mice.

Splenocytes (SN) from TAZ10 Rag$^{-/-}$ mice were cultured in the absence or presence of MDSC purified from the spleen of CD4 depleted TAZ10 Rag$^{+/+}$ mice at a SN:MDSC ratio of 1:1 or 5:1. The level of expression of Foxp3 was investigated by flow cytometry after 3, 4 and 5 days of culture (Figure 3.31).

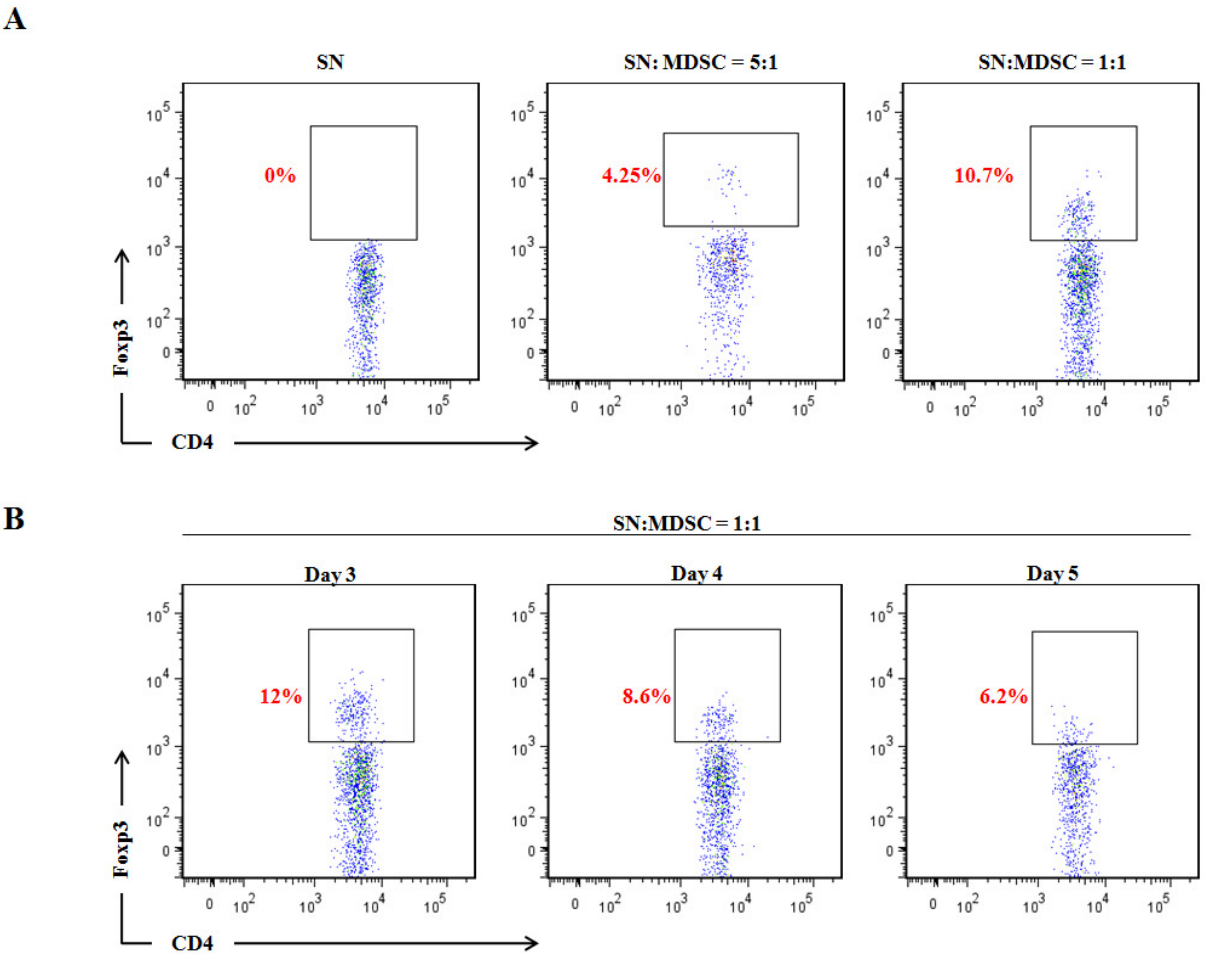

Figure 3.31: MDSC induce the *de-novo* development of Foxp3$^+$ Tregs in a dose-dependent manner
(A) Splenocytes (SN) from TAZ10 Rag$^{-/-}$ were cultured in absence or presence of MDSC purified from the spleen of CD4 depleted TAZ10 Rag$^{+/+}$ mice at a SN:MDSC ratio of 1:1 or 5:1. The expression of Foxp3 was assessed by flow cytometry after 3 days of culture **(B)** Time course of the induction of Foxp3$^+$ Tregs by MDSC. Splenocytes from TAZ10 Rag$^{-/-}$ mice were cocultured with MDSC from CD4 depleted TAZ10 Rag$^{+/+}$ mice at a SN:MDSC ratio of 1:1 and the expression of Foxp3 investigated after 3, 4 or 5 days of culture. Data are representative of more than 10 experiments.

While CD4$^+$ T cells did not express Foxp3 after 3 days of culture in the absence of MDSC, the addition of MDSC to the culture resulted in an increased level of expression of Foxp3 as about 10% of CD4$^+$ TCR-V$_\beta$1$^+$ T cells were Foxp3$^+$. Interestingly, only 4% of CD4$^+$ T cells expressed Foxp3 when MDSC were added at a SN:MDSC ratio of 5:1 (Figure 3.31/A). These results therefore highlighted that MDSC were able to induce the development of Foxp3$^+$ Tregs *in-vitro* and that this mechanism was dose-dependent. The highest number of Foxp3-expressing CD4$^+$ T cells was obtained after 3 days and this proportion decreased over time to be halved after 5 days (Figure 3.31/B).

3.3.3.2 – MDSC-mediated development of Tregs does not require TGFβ but is cell-cell contact dependent

I first investigated whether the addition of the TPO cryptic epitope P3 would have any effect on the induction of Tregs by MDSC. MDSC purified from the spleen of CD4 depleted TAZ10 $Rag^{+/+}$ mice were added to splenocytes at a SN:MDSC ratio of 1:1 in the absence or the presence of P3 peptide. The presence of $Foxp3^+$ $CD4^+$ transgenic cells was assessed by flow cytometry after 72 hours of culture (Figure 3.32). Interestingly, the proportion of $Foxp3^+$ Tregs generated remained identical regardless of the presence of peptide (Figure 3.32/A). This was further demonstrated by semi-quantitative PCR assessing the level of expression of foxp3 mRNA. As previously mentioned, $Foxp3^+$ Tregs are absent in TAZ10 $Rag^{-/-}$ mice but they are present in TAZ10 $Rag^{+/+}$ as highlighted by the high expression of foxp3 mRNA. While the expression of Foxp3 was not detected in splenocytes from TAZ10 $Rag^{-/-}$ mice cultured with P3 for 3 days, it was significantly upregulated when MDSC were added to the culture to reach the level of expression of TAZ10 $Rag^{+/+}$ splenocytes (Figure 3.32/B). The induction of Tregs mediated by MDSC was therefore not antigen-specific.

Numerous studies have reported that immunosuppressive activities of MDSC are mediated through direct cell-cell contact (Bronte et al. 1999; Mazzoni et al. 2002). In addition, the polarization towards specific T cell subsets has been shown to be mediated through the engagement of CD11b (Ehirchiou et al. 2007). To assess whether cell-cell contact was required in the generation of Tregs by MDSC, transwells were used to separate MDSC from the culture so that only soluble factors could have an effect on the induction of Tregs. As shown figure 3.32/A, it appeared that the induction of Tregs required cell-cell contact. Indeed, the absence of contact between MDSC and splenocytes from the use of transwell resulted in the absence of $Foxp3^+$ Tregs being induced.

I could therefore conclude that the *de-novo* development of $Foxp3^+$ Tregs by MDSC was not antigen-specific but required cell-cell contact between MDSC and splenocytes.

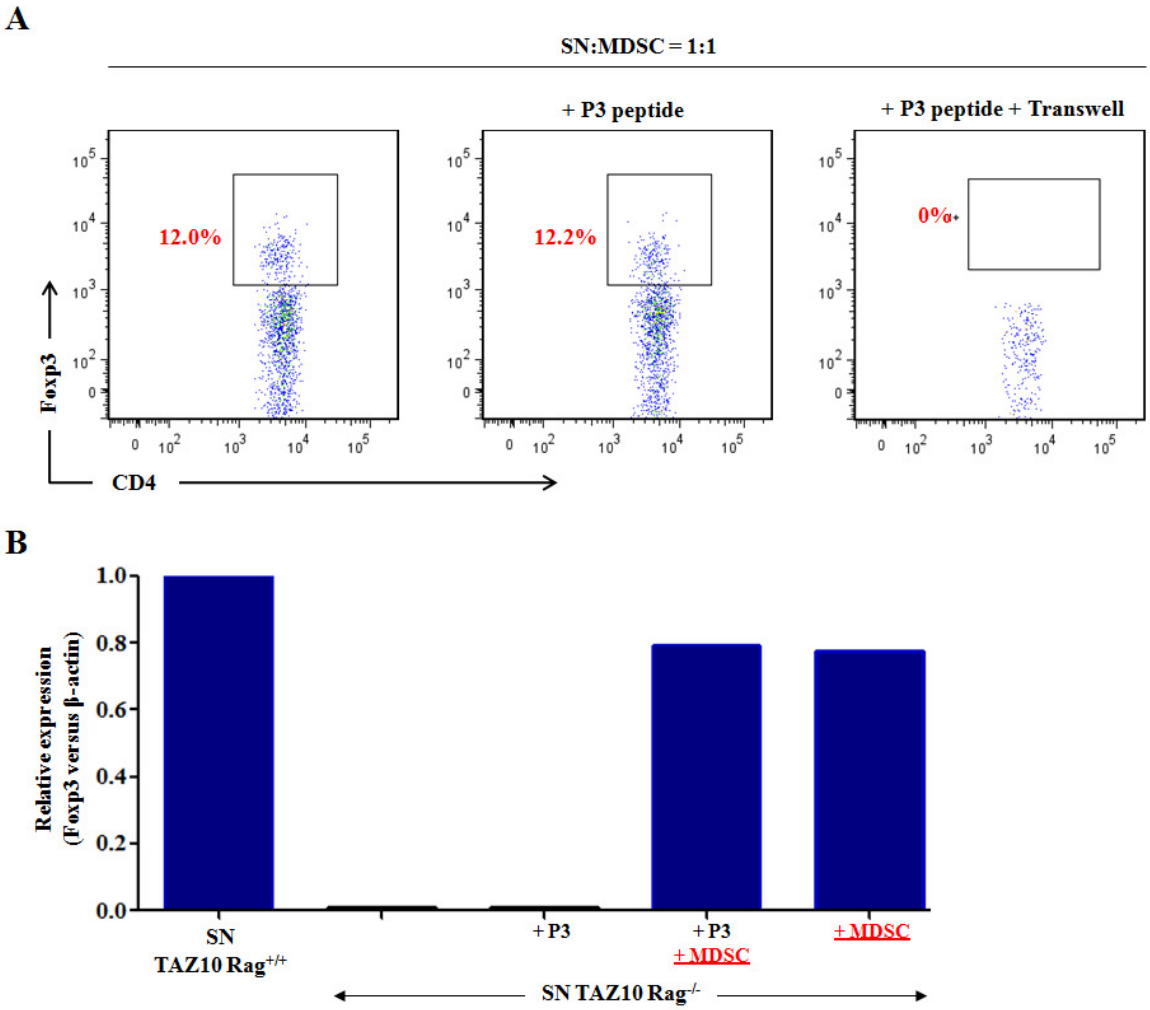

Figure 3.32: The induction of Foxp3$^+$ Tregs by MDSC is not antigen specific
(A) Splenocytes (SN) from TAZ10 Rag$^{-/-}$ mice were cocultured or separated using a transwell with MDSC purified from the spleen of CD4 depleted TAZ10 Rag$^{+/+}$ mice at a SN:MDSC of 1:1. Where mentioned, the TPO cryptic epitope P3 was added at 2µg/ml. The expression of Foxp3 was investigated by flow cytometry after 72 hours. **(B)** The level of expression of Foxp3 was assessed by semi-quantitative RT-PCR using splenocytes from TAZ10 Rag$^{+/+}$ mice as a positive control and splenocytes from TAZ10 Rag$^{-/-}$ mice as a negative control. Results were normalised against the housekeeping gene βactin. Data are representative of more than 10 experiments.

Because of the importance of TGF$_\beta$ in the development of Tregs (Zhu et al. 2008; Luo et al. 2007; Ghinringhelli et al. 2005), I next investigated whether TGF$_\beta$ was required in the generation of Foxp3$^+$ Tregs by MDSC. To this aim, a neutralizing antibody to TGF$_\beta$ (αTGF$_\beta$) was added to the co-culture of splenocytes from TAZ10 Rag$^{-/-}$ mice and MDSC from CD4 depleted TAZ10 Rag$^{+/+}$ mice and the induction of Foxp3$^+$ cells assessed by flow cytometry (Figure 3.33).

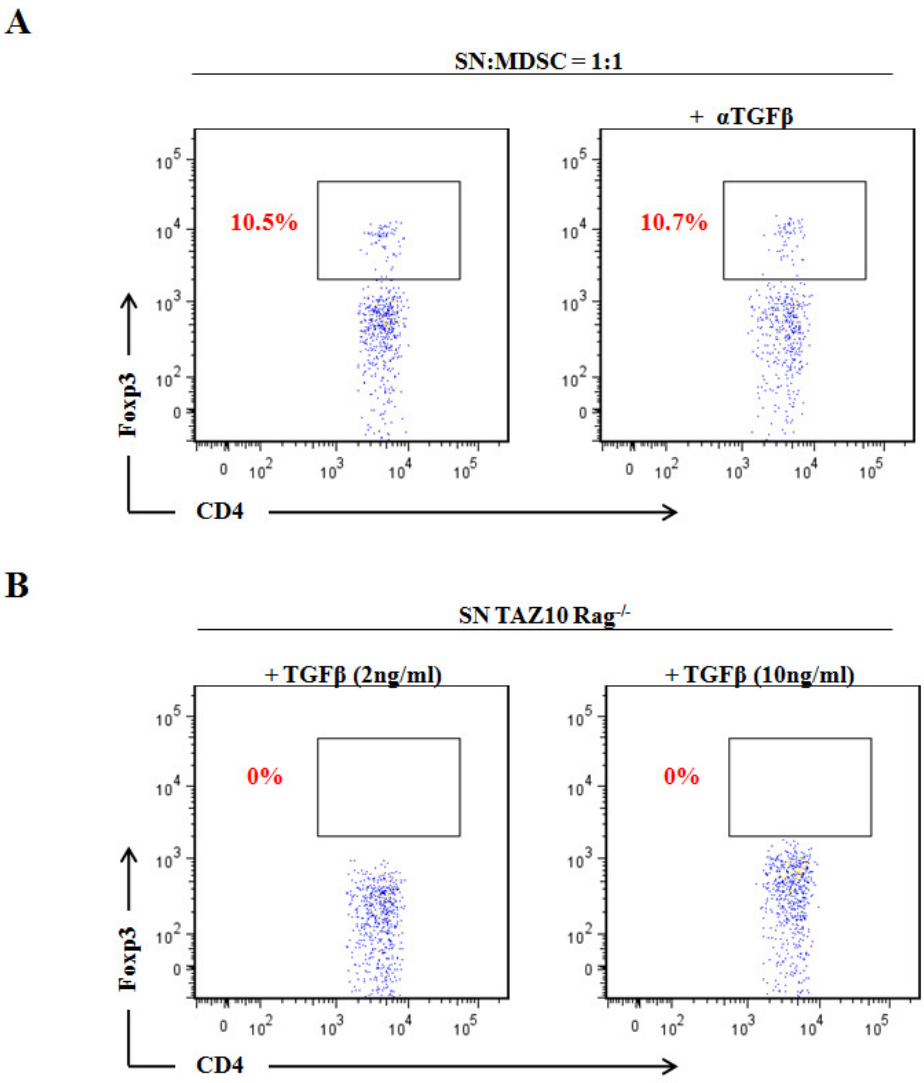

Figure 3.33: The induction of Foxp3$^+$ transgenic T cells by MDSC is not TGF$_\beta$-dependent
(A) The involvement of TGF$_\beta$ was investigated by adding a neutralizing anti-TGF$_\beta$ (αTGF$_\beta$) used at 1µg/ml to the coculture of splenocytes from TAZ10 Rag$^{-/-}$ mice and MDSC purified from the spleen of CD4 depleted TAZ10 Rag$^{+/+}$ mice (SN:MDSC of 1:1). **(B)** Splenocytes from TAZ10 Rag$^{-/-}$ mice were cultured in presence of TGF$_\beta$ at 2ng/ml and 10ng/ml. In all conditions, the expression of Foxp3 was investigated by flow cytometry after 72 hours of culture. Data are representative of 2 distinct experiments.

The addition of αTGF$_\beta$ to the culture did not have any impact on the generation of Tregs as the proportion of CD4$^+$ T cells expressing Foxp3 remained identical (Figure 3.33/A). To further address the importance of TGF$_\beta$ in the induction of Tregs, I assessed whether the addition of TGF$_\beta$ to splenocytes from TAZ10 Rag$^{-/-}$ mice would have a positive impact on the generation of transgenic Tregs. This addition of TGF$_\beta$ to splenocytes at various concentrations was not able to promote the induction of Tregs as suggested by the absence of

$CD4^+$ T cells expressing Foxp3 (Figure 3.33/B). These results highlighted that the induction of transgenic TCR-V$\beta1^+$ Tregs by MDSC was not mediated by TGF_β.

Overall these results showed that MDSC inhibit the proliferation of T cells in TAZ10 mice through different mechanisms. Despite their expression of markers of APC and their ability to uptake, MDSC could not induce T cell proliferation. The inhibitory activity of MDSC was in part mediated through the metabolism of L-arginine and the *de-novo* induction of Tregs *in-vitro*. This latest mechanism did not depend on TGF_β nor the presence of the specific cryptic epitope but required cell-cell contact between MDSC and splenocytes.

3.4 – Summary

Although numerous reports have investigated the function of MDSC in cancer patients and tumour models, their role in chronic inflammatory conditions such as AID is still elusive. I therefore decided to explore whether MDSC had any role in autoimmunity. To this aim, I established the presence of MDSC in a mouse model that spontaneously develops autoimmune disease. The TAZ10 model is a humanised TCR transgenic model that develops spontaneous autoimmune hypothyroidism, characterised by thyroid histological changes, hormones imbalances and clinical symptoms comparable to Hashimoto's thyroiditis (Quaratino et al. 2004). The presence of MDSC has been described in other mouse models of AID such as Experimental Autoimmune Encephalomyelitis (EAE) and Experimental Autoimmune Uveoretinitis (EAU) (Kerr et al. 2008, Zhu et al. 2007a). The disease in these models does not however develop spontaneously and has to be induced by immunization with antigens in the presence of adjuvants. While the use of adjuvant has been shown to alter the immune response as reported in the EAE mouse model (Korn et al. 2008), the action of Th1 and Th17 cells have been described in the pathogenesis of AID (Steinman 2008). They can both induce disease in EAU and EAE models although the clinical signs of the pathology differed depending on the population of effector T cells mediating the disease (Luger et al. 2008; Kroenke et al. 2008). This could have a direct impact on MDSC as their accumulation, function and differentiation is dependent on the balance between pro- versus anti-inflammatory factors. TAZ10 transgenic mice represent therefore a unique model spontaneously developing AID without the use of adjuvant (Quaratino et al. 2004).

While MDSC suppress T cell responses in tumour models (Figure 3.1), they are unable to prevent and inhibit the activation of self-reactive T cells as TAZ10 mice develop autoimmune thyroiditis. I therefore hypothesized that this cell population was not present and/or had its function altered in this model. However, $Gr1^+$ $CD11b^+$ MDSC were present in TAZ10 mice from the onset and their proportion was increased in TAZ10 mice compared to WT mice (Figure 3.3). The recruitment of MDSC was associated with the spontaneous activation of self-reactive T cells in TAZ10 mice (Figures 3.6 and 3.7). MDSC then accumulated during the early phase of the disease in the peripheral blood, the spleen and the lymph nodes draining and not draining the thyroid of diseased mice (Figure 3.8). Interestingly, they also accumulated in the bone marrow of TAZ10 mice, which constitutes

their natural niche, thus highlighting the important effect of the disease in hematopoiesis. Absent in the thyroid of WT mice, small number of MDSC were present in the thyroid of TAZ10 mice (Figure 3.9) which is directly targeted by self-reactive T cells promoting its destruction over time.

When investigating a potential link between the number of MDSC and the progression of the disease in TAZ10 mice, MDSC accumulated in peripheral lymphoid organs during the acute phase of the disease while their proportion decreased after the thyroid is destroyed and as the inflammatory process fades (Figures 3.10 and 3.11). Such variation in the proportion of MDSC during the course of autoimmunity has also been shown in the EAE model of multiple sclerosis where MDSC were mobilised in the blood at an increased rate before EAE exacerbation. They accumulated in the central nervous system during the preclinical phase of EAE while their number gradually decreased after the peak of clinical EAE (Zhu et al. 2007a; King et al. 2009). In contrast, the study of Tregs in TAZ10 mice (Badami et al. Paper in preparation) showed the opposite effect as the proportion of $CD4^+$ $CD62L^{high}$ $CD25^{bright}$ Tregs was drastically reduced in the lymphoid organs of TAZ10 mice compared to WT mice. However, the proportion of Tregs followed the same trend as MDSC since their number decreased over time. These observations suggested a correlation between the reduction in the number of Tregs, the accumulation of MDSC and thyroid destruction.

Overall, I showed that the inflammation present in TAZ10 mice drives the recruitment and the accumulation of MDSC. If VEGF and GMCSF have been linked with the accumulation of MDSC (Gabrilovich et al. 1998, Bronte et al. 1999), the potent inflammatory mediator IL-1β has been shown to favour tumour growth by enhancing the accumulation of MDSC at the tumour site (Bunt et al. 2006) while a reduced IL-1β-induced inflammation was associated with a delayed recruitment of MDSC and a reduced tumour growth and metastasis (Bunt et al. 2007). Interestingly, while the inflammatory environment plays a role in the accumulation of MDSC, it also directly modulates their suppressive function. MDSC induced in presence of IL-1β had increased levels of ROS and enhanced suppressive activity against $CD4^+$ and $CD8^+$ T cells (Tu et al. 2008). This was also demonstrated in TAZ10 mice where MDSC were more potent at inhibiting the proliferation of T cells than MDSC from WT mice (Figure 3.17). Moreover, the suppressive activity of MDSC was stronger during the acute phase of thyroiditis where the level of inflammation is at its maximum as the thyroid is progressively destroyed (Figures 3.19 and 3.20). This highlighted the gain of suppressive

function of MDSC associated with the important inflammatory status in TAZ10 mice. MDSC from TAZ10 mice secreted high levels of NO compared to MDSC from WT mice and this secretion was increased during the acute phase of the disease. Although the metabolism of L-arginine is widely used by MDSC to inhibit T cell responses in tumour models (Rodriguez et al. 2008, Bronte et al. 2005), it does not seem to be the key mechanism displayed by MDSC to inhibit T cells in TAZ10 mice. Indeed MDSC were also able to induce the *de-novo* development of $Foxp3^+$ Tregs *in-vitro* thus promoting T cell tolerance. Such mechanism has been described in tumour models where MDSC either promoted the generation of Tregs from naive T cells or mediated the expansion of pre-existing Tregs (Yang et al. 2006, Serafini et al. 2008). Interestingly, the induction of Tregs mediated by MDSC has been shown to require IFNγ and IL-10 while being independent on the production of NO in a mouse model of colon carcinoma (Huang et al. 2006). By contrast, this process was mediated through Arg-1 activity and required the capture, processing and presentation of TAA by MDSC while being independent of TGF_β in a B cell lymphoma mouse model (Serafini et al. 2008). While TGF_β was required for the generation of antigen-specific Tregs from naive T cells by DC in the NOD mouse model of type 1 diabetes (Luo et al. 2007), I could rule out that TGF_β and the TPO cryptic epitope P3 was involved in the generation of TPO specific Tregs in TAZ10 mice. However, the induction of Tregs was cell-cell contact and dose-dependent. Further work would be needed to determine precisely the soluble factors involved such as IFNγ, IL-10 or IL-2 that have been shown to be essential in the conversion of naive $CD4^+$ $CD25^-$ T cells to $Foxp3^+$ Tregs (Zheng et al. 2007). The suppressive function of the newly-induced $Foxp3^+$ cells on $CD4^+$ and $CD8^+$ T cells would also need to be investigated.

Finally, although MDSC share many features with APC, such as the expression of CD11c, costimulatory molecules and the ability to uptake, they were unable to induce the antigen specific proliferation of T cells from TAZ10 mice. An important mechanism used by MDSC has been recently described where MDSC induce nitration of TCR and CD8 molecules of $CD8^+$ T cells through hyperproduction of ROS and peroxynitrite during cell-cell contact. This results in a substantial decrease in the ability of $CD8^+$ T cells to bind peptide/MHC complexes making them unresponsive to antigen-specific stimulation (Nagaraj et al. 2007).

Altogether, these results showed that the inflammatory context present in TAZ10 mice was responsible for the accumulation of MDSC and the gain of suppressive activity. It also

has an important impact on their phenotype as MDSC from TAZ10 mice displayed higher levels of expression of markers of myeloid APC (such as CD11c and F4/80) and costimulation when compared to MDSC from WT mice highlighting a more "differentiated" phenotype.

Despite their strong suppressive function displayed on T cells *in-vitro*, MDSC could not prevent the development of the disease in TAZ10 mice. I therefore investigated the use of inhibitory MDSC *in-vivo* as a therapeutic tool in TAZ10 mice to control the activation of self-reactive T cells and dampen the severity of the disease. I will also assess whether MDSC could be used to prevent the activation of self-reactive and the onset of autoimmune thyroiditis when adoptively transferred in WT mice prior to the AT of self-reactive TAZ10-T_N.

4 – Evaluation of the use of MDSC as a therapeutic strategy to prevent the development of autoimmune diseases

4.1 – Introduction

I have previously highlighted the presence of inhibitory MDSC in the TAZ10 mouse model of spontaneous thyroiditis (Chapter 3). This accumulation in various lymphoid and non-lymphoid tissues was highly dependent on the status of inflammation. Greater amounts of MDSC were observed during the acute phase of the disease while their number decreased as the inflammatory process fades and the disease becomes more chronic. In addition to the impact on the recruitment of MDSC, the inflammatory environment led to a gain of suppressive function on T cells.

Alongside $CD4^+$ $CD25^+$ $Foxp3^+$ Tregs, MDSC are considered to be a key player in regulatory networks of peripheral tolerance by controlling the activation and function of self-reactive T cells. Failure of these mechanisms of peripheral tolerance is linked with the activation of self-reactive T cells that have escaped negative thymic selection, thus promoting the occurrence of AID. Because of their strong suppressive function on T cells displayed *in-vitro*, I suggested that the adoptive transfer of MDSC in TAZ10 mice would dampen the severity of autoimmune thyroiditis. Indeed, MDSC could inhibit the activation and functions of self-reactive T cells *in-vivo* and therefore delay the progression of the disease. As a result, the use of inhibitory MDSC *in-vivo* as a therapeutic tool was assessed in TAZ10 mice.

4.2 – The adoptive transfer of inhibitory MDSC *in-vivo* fails to dampen the severity of autoimmune disease

While the detrimental role of MDSC in cancer has led to the development of therapeutic strategies targeting their accumulation, suppressive function and maturation, their importance in chronic inflammatory conditions such as AID is still elusive. I have shown that MDSC accumulating in the lymphoid organs of TAZ10 mice suppress the proliferation of T cells *in-vitro.* If the suppressive function displayed by MDSC *in-vitro* is retained *in-vivo*, MDSC could be used *in-vivo* as a new strategy to prevent and dampen the progression of the disease by inhibiting the activation of self-reactive T cells. I therefore tested this hypothesis by performing adoptive transfers of purified MDSC into TAZ10 mice.

4.2.1 – Adoptive transfer of MDSC from TAZ10 $Rag^{+/+}$ mice into TAZ10 $Rag^{-/-}$ mice strongly exacerbates the disease

To assess whether MDSC could block the progression of the disease, $Gr1^{+}$ MDSC isolated from the spleen of TAZ10 $Rag^{+/+}$ mice were adoptively transferred into 6 weeks old TAZ10 $Rag^{-/-}$ mice (Figure 4.1/A). The survival and weight were recorded on a weekly basis as a readout of hypothyroidism. TAZ10 $Rag^{-/-}$ mice were chosen as recipient mice as they display signs of autoimmune thyroiditis that are more detectable than in TAZ10 $Rag^{+/+}$ mice.

While non-treated control mice gained weight over time as previously reported (Quaratino et al. 2004), adoptively transferred mice started to lose weight after 21 days (Figure 4.1/B). This loss of weight was surprisingly associated with the premature death of treated mice as all died between 40 and 50 days after AT while the survival of control mice was not affected (Figure 4.1/C). Contrary to my initial hypothesis, an AT of MDSC purified from the spleen of TAZ10 mice was therefore detrimental as it dramatically worsened the disease.

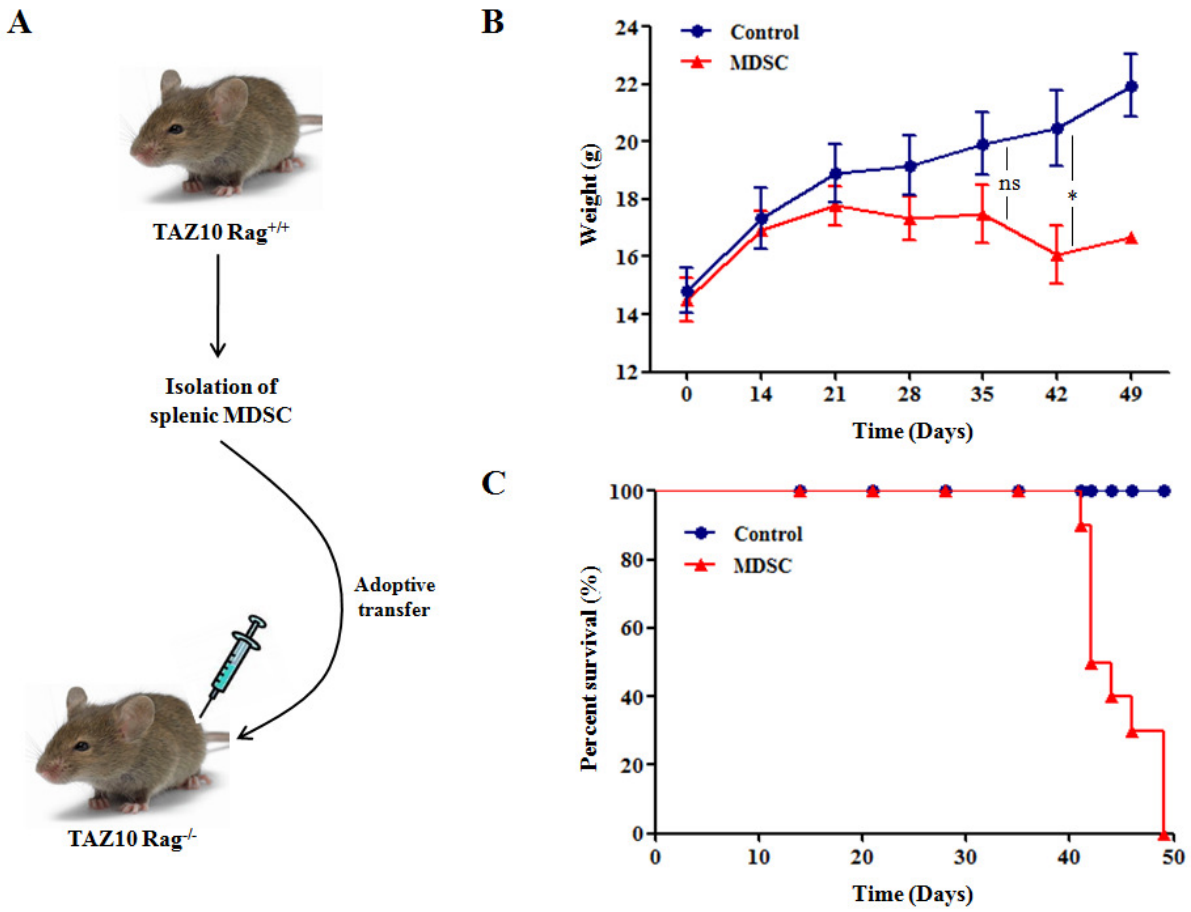

Figure 4.1: Adoptive transfer of Gr1$^+$ MDSC fails to prevent the progression of the disease in TAZ10 Rag$^{-/-}$ mice

(A) Gr1$^+$ cells isolated from the spleens of 3 months old TAZ10 Rag$^{+/+}$ mice were adoptively transferred into 6 weeks old TAZ10 Rag$^{-/-}$ mice. Their weight **(B)** was recorded on a weekly basis and their survival **(C)** assessed over a period of 50 days. Data shown are representative of two independent experiments, each involving 5 mice per group. Statistical analysis was performed using the unpaired Student's t-test.

MDSC originate in the bone marrow from common myeloid precursors and are recruited to secondary lymphoid organs (e.g. spleen) in healthy individuals. This recruitement is exacerbated in autoimmune conditions as a result of the on-going inflammation and the associated release of various pro-inflammatory cytokines and soluble factors (Gabrilovich et al. 2009). I have shown that the inflammatory environment present in TAZ10 mice has an impact on the phenotype and functions of MDSC. MDSC purified from the bone marrow are indeed phenotypically distinct to MDSC from the spleen of TAZ10 mice (Figures 3.21 and 3.22). Moreover, the chemokine expression profile of MDSC is associated with the tissue of origin. While the expression of the BV8 receptor by MDSC from the bone marrow in tumour-bearing mice allowed their mobilization to the peripheral blood (Shojaei et al. 2007), splenic

MDSC expressing CCL1 were recruited to the dermis through the chemotactic factor CCR8 in a model of autoimmune alopecia areata affecting hair follicles (Marhaba et al. 2007). Because of their differential phenotype, I wondered whether an AT of MDSC from the bone marrow would have the same adverse effect on TAZ10 mice than the AT of MDSC from the spleen.

To this aim, purified MDSC from the bone marrow of TAZ10 $Rag^{+/+}$ mice were adoptively transferred into 6 weeks old TAZ10 $Rag^{-/-}$ mice (Figure 4.2/A). The weight was recorded on a weekly basis as a readout of hypothyroidism and the survival monitored over time.

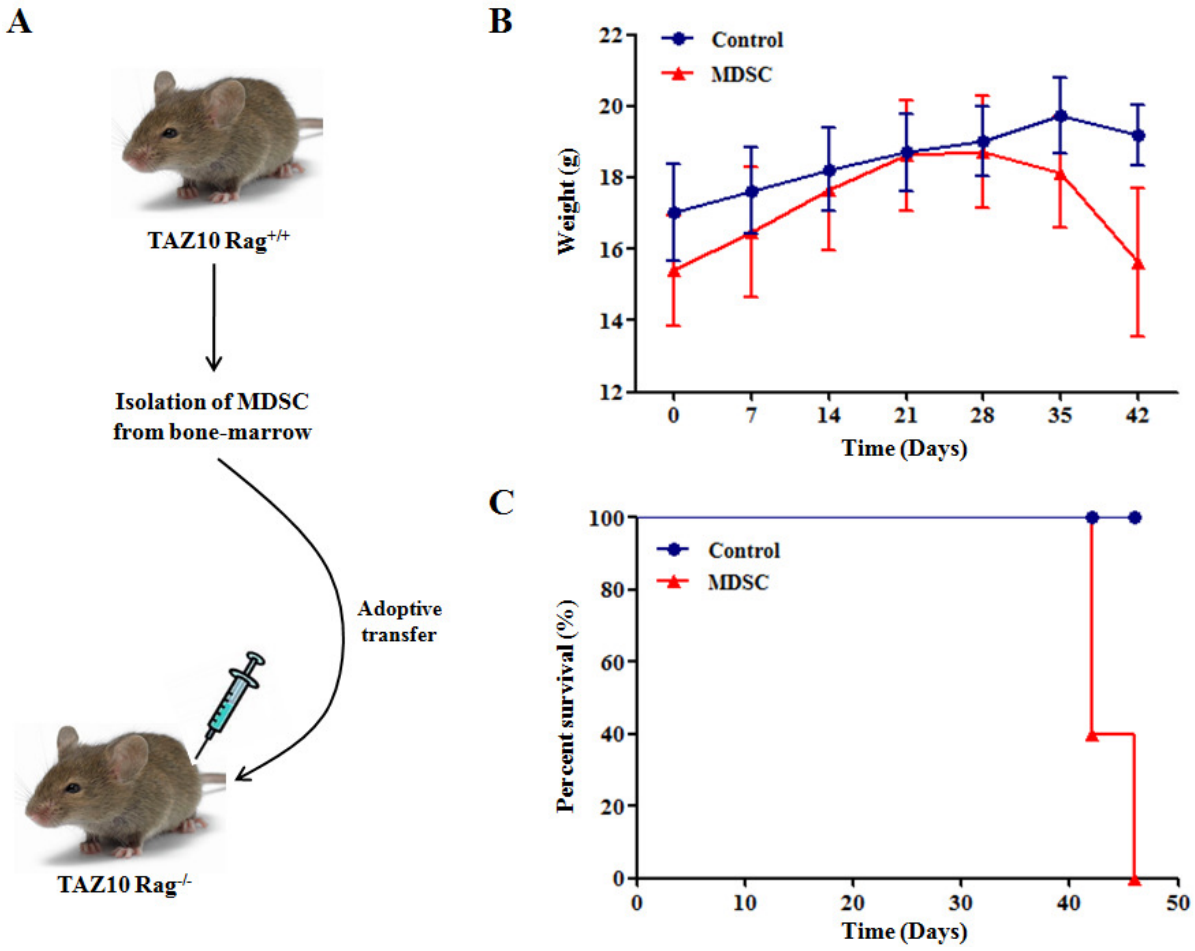

Figure 4.2: Adoptive transfer of $Gr1^+$ MDSC isolated from the bone marrow of TAZ10 $Rag^{+/+}$ mice has an adverse impact on the disease in TAZ10 $Rag^{-/-}$ transgenic mice

(A) $Gr1^+$ cells purified from the bone marrow of 3 months old TAZ10 $Rag^{+/+}$ were adoptively transferred into 6 weeks old TAZ10 $Rag^{-/-}$ mice. Their weight **(B)** and survival **(C)** were recorded on a weekly basis over a period of 46 days. Data shown are representative of two independent experiments, involving 5 mice per group.

As shown figure 4.2, the loss of weight affecting TAZ10 mice treated with $Gr1^+$ MDSC correlated with their premature death as they all died between 42 and 46 days after AT. In comparison, control TAZ10 mice gained weight over time while their survival was not affected (Figure 4.2/B and 4.2/C). Similarly to the outcome of the AT of MDSC purified from the spleen of TAZ10 mice (Figure 4.1), the use of MDSC purified from the bone marrow of TAZ10 mice was detrimental as shown by the unexpected death of the treated mice. These results suggested that the outcome of the AT was not influenced by the origin of MDSC.

The previous observations highlighting the failure of MDSC to dampen signs of AID in TAZ10 $Rag^{-/-}$ mice prompted us to examine whether they had lost their suppressive function and/or differentiated into immunostimulatory APC. $Gr1^+$ $eYFP^+$ MDSC purified from the spleen and bone marrow of B6.eYFP mice ubiquitously expressing eYFP were adoptively transferred into $Rag^{-/-}$ and TAZ10 $Rag^{-/-}$ mice. 7 days after adoptive transfer, mice were culled and the fate of the $Gr1^+$ $eYFP^+$ MDSC adoptively transferred at day 0 investigated by assessing their proportion and phenotype in various tissues (Figure 4.3/A).

While MDSC originating from the spleen of B6.eYFP mice did not preferentially migrate to the bone marrow of $Rag^{-/-}$ mice, they were mainly recruited to the spleen and most importantly the lymph nodes where they differentiated as suggested by the virtual absence of $eYFP^+$ $Gr1^+$ $CD11b^+$ cells. By contrast, the process was exacerbated in TAZ10 $Rag^{-/-}$ mice as $eYFP^+$ cells strongly accumulated in the spleen but also in lymph nodes with a prevalence in the lymph nodes draining the thyroid. Similarly to what was observed after AT of MDSC from B6.eYFP into $Rag^{-/-}$ mice, MDSC had all differentiated in TAZ10 $Rag^{-/-}$ mice as few cells still expressed both Gr1 and CD11b (Red squares, figure 4.3/B and 4.3/C).

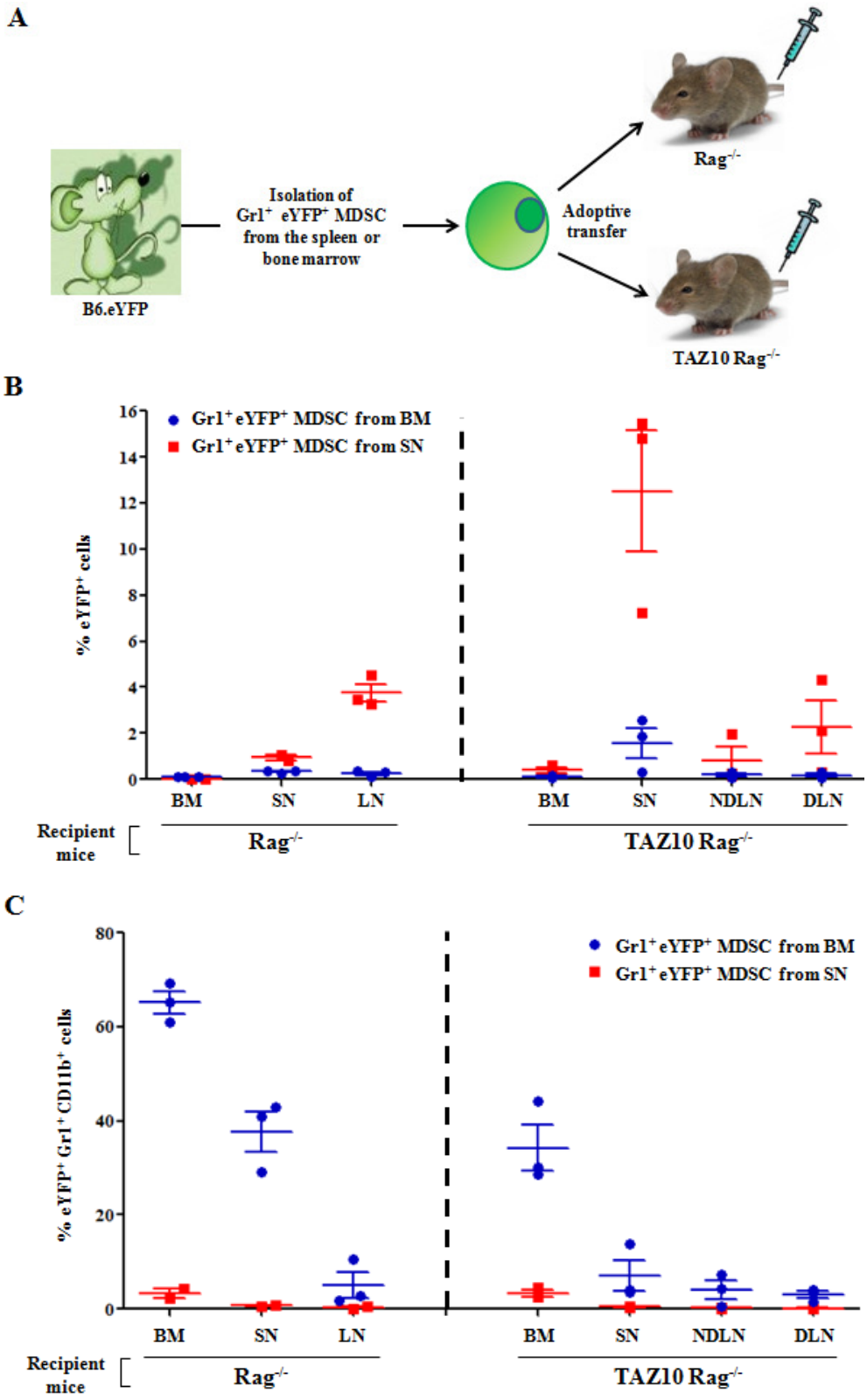

Figure 4.3: Migration dynamics and differentiation of MDSC depend on the tissue they originate from
(A) Gr1$^+$ eYFP$^+$ MDSC purified from the spleen (SN, red squares) or the bone marrow (BM, blue dots) of B6.eYFP mice were adoptively transferred into Rag$^{-/-}$ and TAZ10 Rag$^{-/-}$ mice. 7 days after adoptive transfer, mice were culled. The percentage of eYFP$^+$ cells **(B)** and eYFP$^+$ Gr1$^+$ CD11b$^+$ cells **(C)** was investigated in the bone marrow, spleen and lymph nodes (draining and not the thyroid of TAZ10 mice; DLN and NDLN respectively). Data shown are representative of three independent experiments involving 3 mice per group.

This trend differed when analysing the outcome of the AT of MDSC originating from the bone marrow. There was no accumulation in all tissues of $Rag^{-/-}$ mice and while more than 60% of $eYFP^{+}$ cells retained their phenotype of MDSC in the BM, they preferentially differentiated in secondary lymphoid organs with a preponderance in LN where only about 5% of them still expressed both Gr1 and CD11b markers. In contrast, similar trend of accumulation to MDSC originating from the spleen was observed when MDSC from the BM of B6.eYFP mice were adoptively transferred into TAZ10 $Rag^{-/-}$ mice, although they tended to accumulate preferentially in the spleen. Compared to $Rag^{-/-}$ mice, more cells lost their MDSC phenotype in TAZ10 $Rag^{-/-}$ mice as the majority had differentiated in the spleen while this proportion was strongly reduced when considering the BM (65% in $Rag^{-/-}$ versus 40% in TAZ10 $Rag^{-/-}$ mice) (Blue dots, figure 4.3/B and 4.3/C).

MDSC naturally differentiate into APC in non-diseased mice as shown by the AT of MDSC in $Rag^{-/-}$ mice. These observations are in line with previous studies showing that myeloid progenitors differentiate into APC and are recruited in peripheral tissues where they contribute to the replenishment of the pool of APC (Fogg et al. 2006). The inflammatory environment in TAZ10 mice exacerbated the recruitment and differentiation of MDSC. In addition, the tissue MDSC originated from also governed their migration and was therefore a key factor in determining their fate.

4.2.2 – Differential impact of the adoptive transfer of MDSC from TAZ10 $Rag^{+/+}$ or WT mice in TAZ10 $Rag^{-/-}$ mice

I have previously shown that the inflammatory environment present in TAZ10 mice has an impact on the accumulation and phenotype of MDSC while it is also associated with a gain of suppressive function (Chapter 3). I therefore compared the impact an AT of MDSC from WT or TAZ10 $Rag^{+/+}$ mice would have on the progression of the disease and the survival of TAZ10 $Rag^{-/-}$ mice.

$Gr1^{+}$ MDSC were isolated from WT and TAZ10 $Rag^{+/+}$ mice and adoptively transferred into TAZ10 $Rag^{-/-}$ mice (Figure 4.4/A). The weight was recorded on a weekly basis as a readout of hypothyroidism and the survival was followed over time.

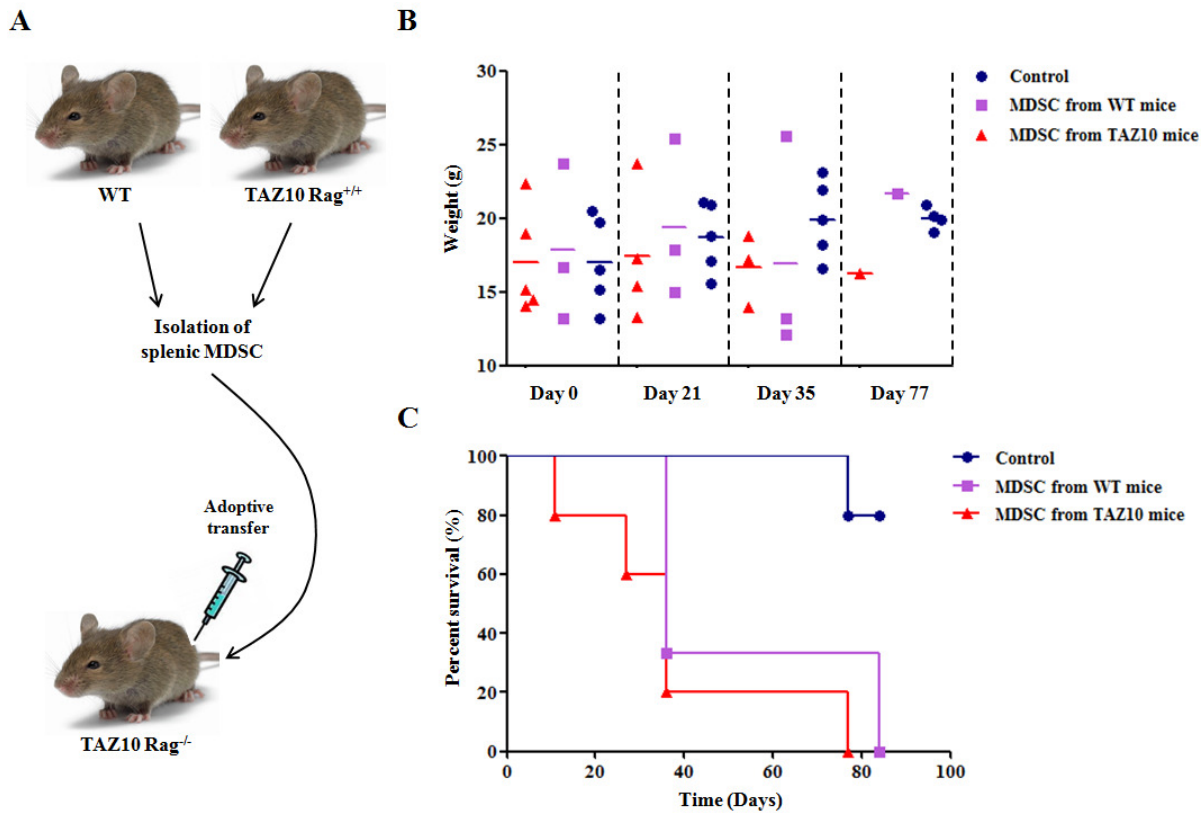

Figure 4.4: Adoptive transfer of MDSC from WT or TAZ10 Rag$^{+/+}$ mice have a different impact on the disease

(A) Gr1^{+} cells were isolated from the spleens of 3 months old WT and TAZ10 Rag$^{+/+}$ mice and adoptively transferred into 6 weeks old TAZ10 Rag$^{-/-}$ mice. Their weight **(B)** was recorded on a weekly basis and their survival **(C)** assessed over a period of 84 days. Data shown are representative of two independent experiments, each involving 5 control mice, 5 mice injected with purified Gr1^{+} cells from TAZ10 mice and 3 mice injected with purified Gr1^{+} cells from WT mice.

As expected from the results obtained figures 4.1 and 4.2, mice injected with purified MDSC from WT and TAZ10 mice started to lose weight 35 days after AT while non-injected control mice gained weight over time (Figure 4.4/B). This was associated with the premature death of adoptively transferred mice as more than half of them died within 40 days after AT (Figure 4.4/C). Overall, all mice treated with Gr1^{+} MDSC died within 84 days further demonstrating that an AT of MDSC is detrimental and worsens the disease in TAZ10 mice.

Interestingly, the kinetics of survival were different whether TAZ10 mice were injected with MDSC purified from WT (purple line, Figure 4.4C) or TAZ10 Rag$^{+/+}$ mice (red line, figure 4.4/C). The AT of MDSC from TAZ10 Rag$^{+/+}$ mice had a more severe impact on the disease as mice started to die only 10 days after treatment compared to 38 days when MDSC originated from WT mice. I previously showed that MDSC from the spleen of TAZ10 mice expressed higher levels of markers of APC (e.g. CD11c) and markers of maturation (e.g.

CD86) than MDSC from the spleen of WT mice, thus suggesting a more "differentiated" phenotype (Figure 3.21). While tracking down MDSC *in-vivo*, I showed that MDSC originating from the spleen accumulated in the spleen and LN of $Rag^{-/-}$ mice. This phenomenon was exacerbated in TAZ10 $Rag^{-/-}$ mice as shown by the strong accumulation in the spleen and LN draining the thyroid which was associated with a complete differentiation within 7 days after AT.

MDSC are naturally recruited in tissues of non-diseased mice where they differentiate into cells of the myeloid lineage (Figure 4.3; Gabrilovich et al. 2009). This phenomenon being amplified in TAZ10 mice as a result of the on-going inflammation, it could lead to an increased number of differentiated MDSC that would promote the development of the disease. This could explain the more severe impact observed when considering the AT of MDSC from TAZ10 versus WT mice.

4.2.3 – Upon adoptive transfer into TAZ10 $Rag^{-/-}$ mice, MDSC do not retain their suppressive phenotype

I previously described that an AT transfer of MDSC in TAZ10 $Rag^{-/-}$ mice was detrimental as all mice died prematurely within 6 weeks due to an aggressive autoimmune condition (Figure 4.1). I also showed that they accumulated and suggested that they differentiated in various lymphoid and non-lymphoid tissues within 7 days after AT. Taken together, these results strongly suggested that MDSC had differentiated into cells capable of promoting inflammation. I therefore decided to ascertain this hypothesis by tracking down MDSC from B6.eYFP mice *in-vivo* following their AT into control and TAZ10 mice.

4.2.3.1 – Following adoptive transfer, MDSC give rise to cells displaying higher expression of specific markers of APC

I first assessed the fate and phenotype of MDSC following the AT. $Gr1^{+}$ $eYFP^{+}$ MDSC were purified from the spleen of B6.eYFP mice and adoptively transferred into $Rag^{-/-}$ or TAZ10 $Rag^{-/-}$ mice (Figure 4.5/A). Mice were culled 7 days after AT and the percentage of

eYFP^{+} cells present in the spleen investigated. eYFP^{+} cells were further analysed for their expression of Gr1, CD11b, CD11c and I-A^{b} markers (Figure 4.5/B).

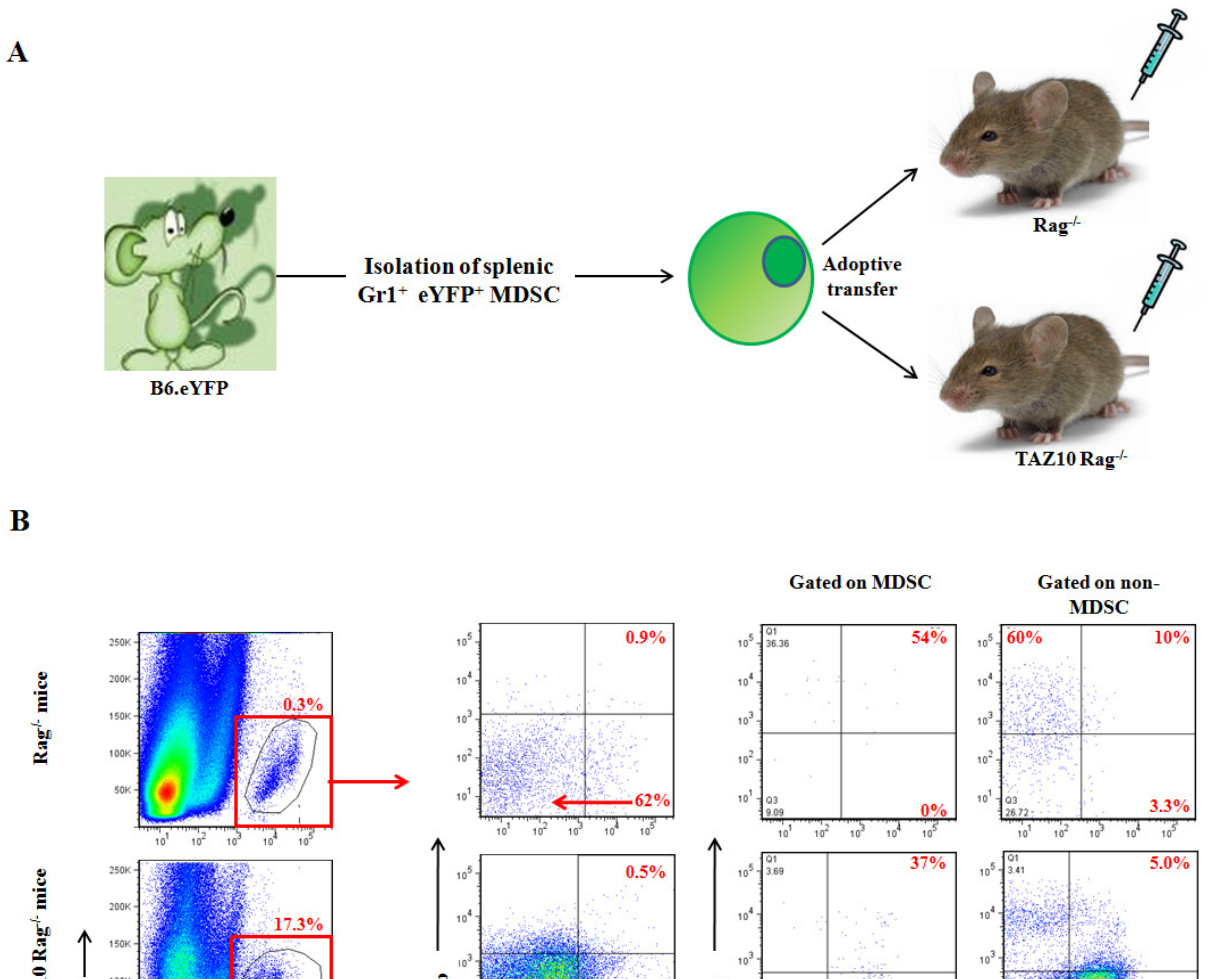

Figure 4.5: MDSC differentiate into cells expressing CD11c and I-A^{b} markers following AT in TAZ10 Rag$^{-/-}$ mice

(A) Gr1^{+} eYFP^{+} cells were isolated from the spleens of B6.eYFP mice and adoptively transferred into 2 months old Rag$^{-/-}$ or TAZ10 Rag$^{-/-}$ mice. **(B)** 7 days after adoptive transfer, Rag$^{-/-}$ and TAZ10 Rag$^{-/-}$ mice were culled and the expression of eYFP in the spleen measured by flow cytometry. eYFP^{+} cells were analysed for the expression of Gr1 and CD11b. Gated MDSC and non-MDSC populations were further analysed for their expression of CD11c and I-A^{b}. Data shown are representative of 5 experiments.

While only 0.3% of the cells express eYFP in the spleen of Rag$^{-/-}$ mice after AT, this percentage significantly increased to 17% in the spleen of TAZ10 Rag$^{-/-}$ mice, demonstrating an important accumulation of eYFP^{+} cells (Figure 4.5/B). In both cases, only a small

percentage of these eYFP^{+} still expressed the Gr1 and CD11b markers (0.9% in Rag$^{-/-}$ mice for 0.5% in TAZ10 Rag$^{-/-}$ mice) confirming previous observations that MDSC did not retain their phenotype and naturally differentiated upon AT in Rag$^{-/-}$ or TAZ10 Rag$^{-/-}$ mice (Figures 4.3 and 4.4). Nearly all the MDSC still present after AT in TAZ10 Rag$^{-/-}$ mice expressed CD11c with 37% of them co-expressing MHC-II molecules. In the spleen of Rag$^{-/-}$ mice, MDSC mainly gave rise to cells expressing MHC-II molecules but not CD11c molecules (60% and 3.3% respectively). By contrast, 76% of eYFP^{+} Gr1^{-} CD11b^{-} cells present in the spleen of TAZ10 Rag$^{-/-}$ mice 7 days after AT were expressing the CD11c marker with the appearance of a discrete cell population expressing both CD11c and MHC-II molecules.

While MDSC preferentially differentiated into CD11c^{-} I-A^{b+} cells into the spleen of Rag$^{-/-}$ mice, they accumulated and differentiated into mature myeloid cells expressing high levels of CD11c molecules in the spleen of TAZ10 Rag$^{-/-}$ mice. This trend was confirmed when cumulative results on all the experiments performed were considered (Figures 4.6 and 4.7)

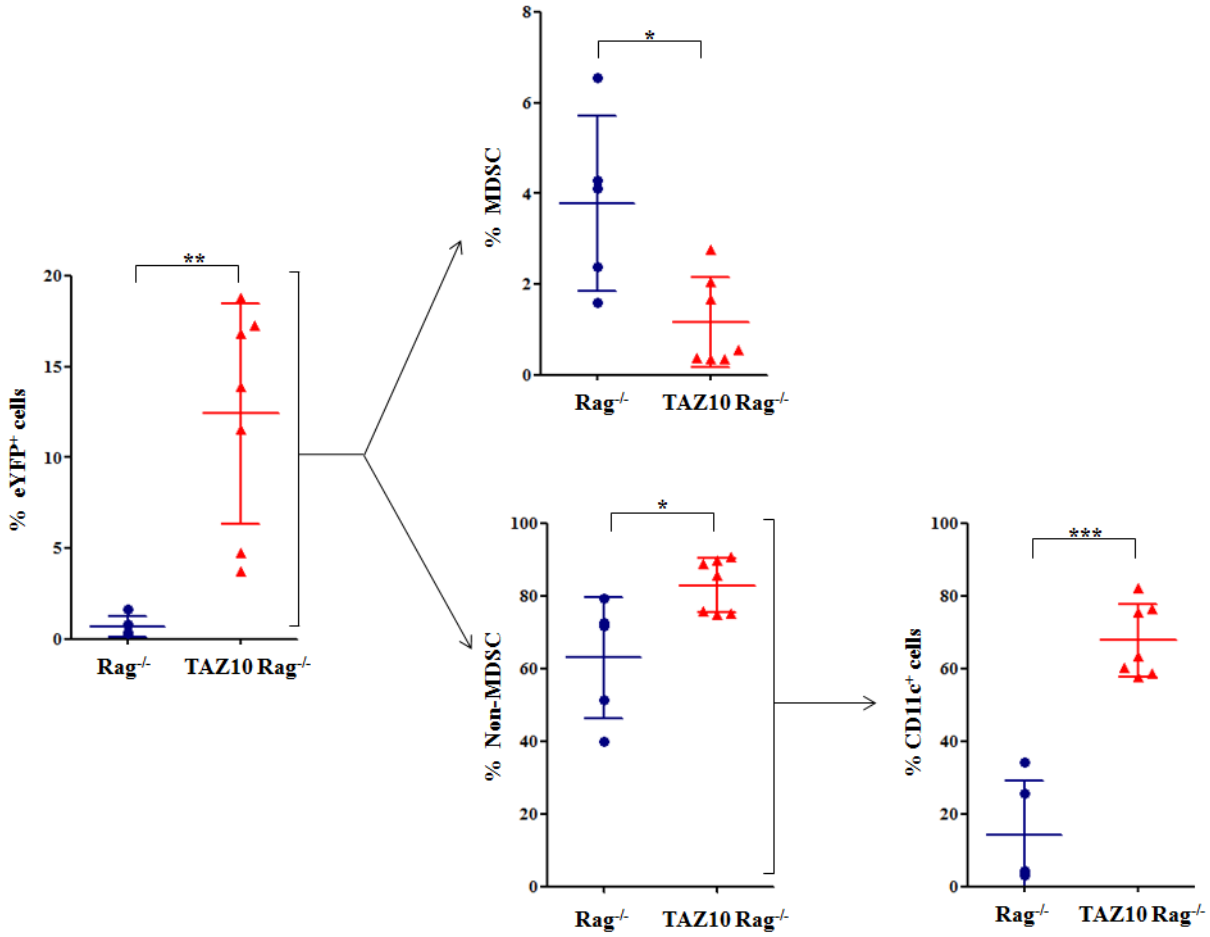

Figure 4.6: Following adoptive transfer in TAZ10 Rag$^{-/-}$ mice, MDSC give rise to cells expressing high levels of CD11c in the spleen

Cumulative results showing the percentage of cells expressing eYFP in the spleen of Rag$^{-/-}$ and TAZ10 Rag$^{-/-}$ mice 7 days after adoptive transfer. The percentage of eYFP^{+} cells that express both Gr1 and CD11b (MDSC) or none of these markers (non-MDSC) was assessed while further analysis on the expression of CD11c by non-MDSC cells was performed. Data shown are representative of 3 experiments, each including 5 Rag$^{-/-}$ and 7 TAZ10 Rag$^{-/-}$ mice. Statistics were performed using the unpaired Student's t-test.

As shown in figure 4.6, eYFP^{+} cells accumulated in the spleen of TAZ10 Rag$^{-/-}$ compared to Rag$^{-/-}$ mice (12% versus 1% respectively). The majority of eYFP^{+} cells did not retain the expression of the Gr1 and CD11b markers (63% and 72% in Rag$^{-/-}$ and TAZ10 Rag$^{-/-}$ mice respectively) and 70% of non-MDSC present in TAZ10 Rag$^{-/-}$ mice had differentiated into CD11c^{+} myeloid cells following AT.

The importance of the lymph nodes draining the thyroid at the onset of the disease has been highlighted in chapter 3. I have shown that the AT of MDSC from the spleen resulted in their accumulation in the spleen and the DLN of recipient TAZ10 Rag$^{-/-}$ mice. I therefore wanted to assess the ability of MDSC to differentiate into APC in DLN and NDLN. MDSC

purified from the spleen of B6.eYFP mice were adoptively transferred into $Rag^{-/-}$ and TAZ10 $Rag^{-/-}$ mice. Mice were culled 7 days after AT and the proportion of $eYFP^{+}$ cells in the LN of these mice assessed. Further analysis was performed to investigate their respective expression of Gr1, CD11b and CD11c (Figure 4.7).

Although more than 85% of $eYFP^{+}$ cells present in the LN of $Rag^{-/-}$ mice did not express the Gr1 and CD11b markers, only 5% of these cells expressed the CD11c myeloid marker suggesting that MDSC had migrated to the LN of $Rag^{-/-}$ mice where they differentiated. Further analysis on the expression of other cell surface markers would be required to determine precisely their phenotype. I therefore showed that in healthy individuals, MDSC naturally enter lymphoid tissues where they lose their expression of both Gr1 and CD11b and differentiate into cells that do not express the myeloid CD11c marker (Figure 4.7).

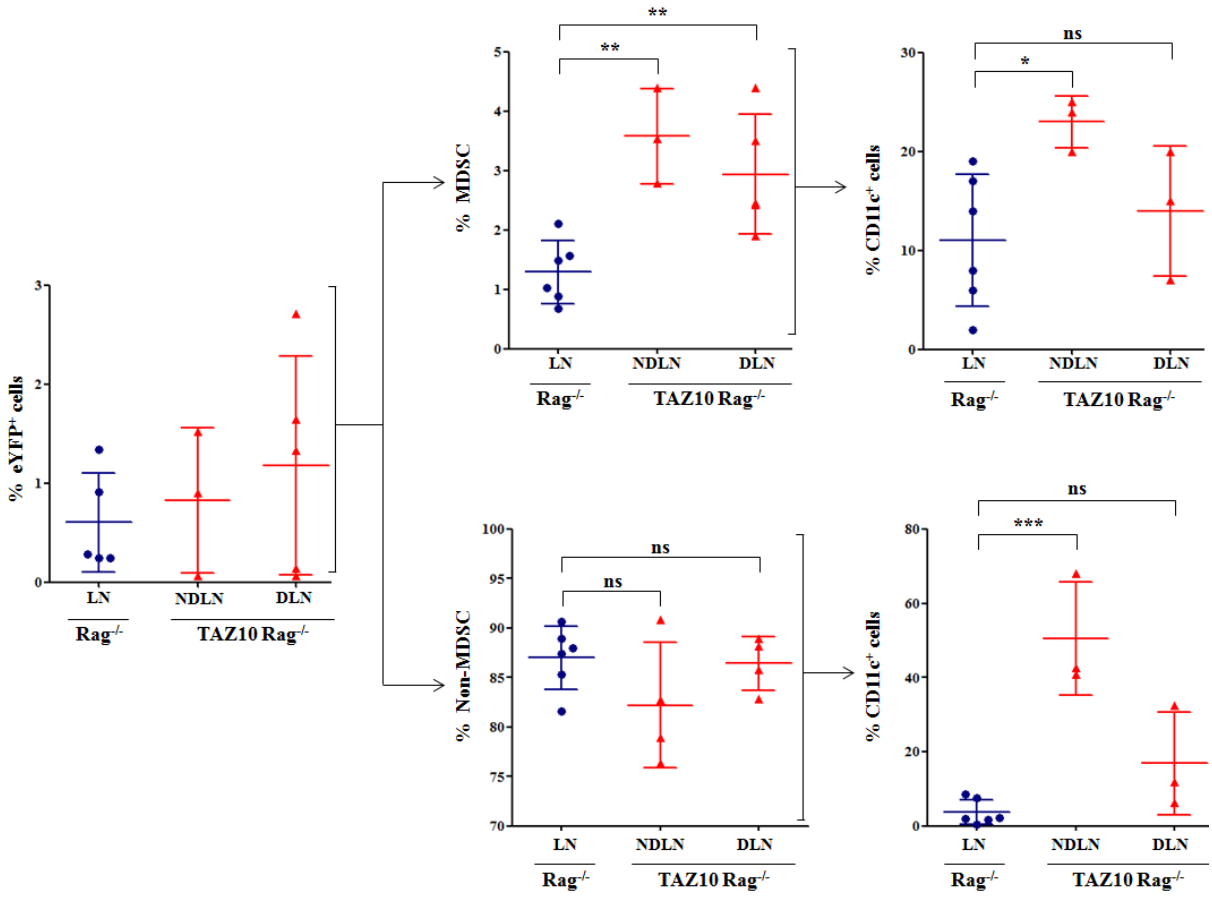

Figure 4.7: Following adoptive transfer, MDSC differentiate into cells expressing the CD11c myeloid marker in the lymph nodes draining and not draining the thyroid in TAZ10 mice
Rag$^{-/-}$ and TAZ10 Rag$^{-/-}$ mice were adoptively transferred with MDSC from the spleen of B6.eYFP mice. 7 days after AT, the presence and phenotype of eYFP^{+} cells were assessed in the LN of Rag$^{-/-}$ mice and LN draining (DLN) and not draining (NDLN) the thyroid in TAZ10 Rag$^{-/-}$ mice. Data shown are representative of 2 distinct experiments. Statistics were performed using the unpaired Student's t-test.

In contrast, a slight increase in the percentage of eYFP^{+} cells observed in the DLN and NDLN of TAZ10 Rag$^{-/-}$ mice suggested that MDSC were preferentially recruited to these tissues in diseased mice. 15% of the remaining MDSC expressed CD11c in the DLN of TAZ10 Rag$^{-/-}$ mice compared to 25% in the NDLN. In addition, although non-MDSC were present in similar number in LN of both Rag$^{-/-}$ and TAZ10 Rag$^{-/-}$ recipients, the proportion of cells expressing CD11c was increased in the NDLN compared to the DLN of TAZ10 Rag$^{-/-}$ recipients (20% versus 50% respectively). Because of their ability to differentiate, the study of MDSC must not focus on the sole Gr1^{+} CD11b^{+} MDSC population but must also take into consideration their ability to progressively acquire other markers while losing their expression of Gr1 as they differentiate into mature myeloid cells. The potential migration of differentiated MDSC from lymphoid organs into target tissues must also be considered.

Indeed looking at figure 4.7, I could hypothesize that the differentiation of MDSC into $CD11c^+$ cells did not prevail in DLN. The strong accumulation of $Gr1^+$ and $CD11b^+$ cells into the thyroid of TAZ10 mice (Chapter 3) could potentially highlight the mobilization of differentiated MDSC from the DLN to the thyroid of TAZ10 $Rag^{-/-}$ mice. Complementary experiments previously highlighted could be performed to address these questions (Chapter 3, Paragraph 3.2.2.1).

Overall, I showed that the accumulation and differentiation of MDSC into myeloid cells naturally occurring in non-diseased mice was exacerbated in TAZ10 mice. Indeed, the inflammatory microenvironment present in TAZ10 mice had a dramatic impact on MDSC as they differentiated into cells expressing high levels of CD11c with the apparition of a discrete population of $CD11c^+$ $I\text{-}A^{b+}$ cells.

4.2.3.2 – MDSC differentiate into cells that have an activatory function in TAZ10 mice

I next wondered whether the gradual expression of myeloid markers by MDSC and their differentiation into $CD11c^+$ cells was associated with the acquisition of an immunostimulatory function on T cells. This would explain why an AT of MDSC in TAZ10 $Rag^{-/-}$ mice failed to delay the progression of the disease. I therefore assessed their ability to promote or inhibit T cell responses in a (^{3}H) thymidine proliferation assay. 7 days after AT, mice were culled and the function of purified $eYFP^+$ cells from the spleen of TAZ10 $Rag^{-/-}$ mice on T cells was assessed (Figure 4.8). Because there was only 1% of $eYFP^+$ cells in the spleen of $Rag^{-/-}$ recipient mice, technical difficulties made the purification of these cells by FACS sorting and the study of their impact on T cells impossible. The purification of $eYFP^+$ cells from TAZ10 $Rag^{-/-}$ treated mice by FACS sorting was however successful as 95% of purified cells were expressing eYFP. This level of purity was sufficient to confidently assess their effect on the proliferative activity of T cells (Figure 4.8/A).

As previously observed chapter 3, the addition of $Gr1^+$ $eYFP^+$ MDSC (prior to AT) to splenocytes from WT mice resulted in a three-fold decrease in T cell proliferation to the agonistic αCD3 antibody. In comparison, the addition of $eYFP^+$ cells isolated from TAZ10 $Rag^{-/-}$ 7 days after AT of $Gr1^+$ $eYFP^+$ MDSC significantly increased T cell proliferation to

αCD3 (Figure 4.8/B). Therefore, while MDSC displayed inhibitory function on T cells before AT, they differentiated into myeloid cells capable of promoting T cell proliferation following the AT that could account for the premature death of treated Rag$^{-/-}$ mice.

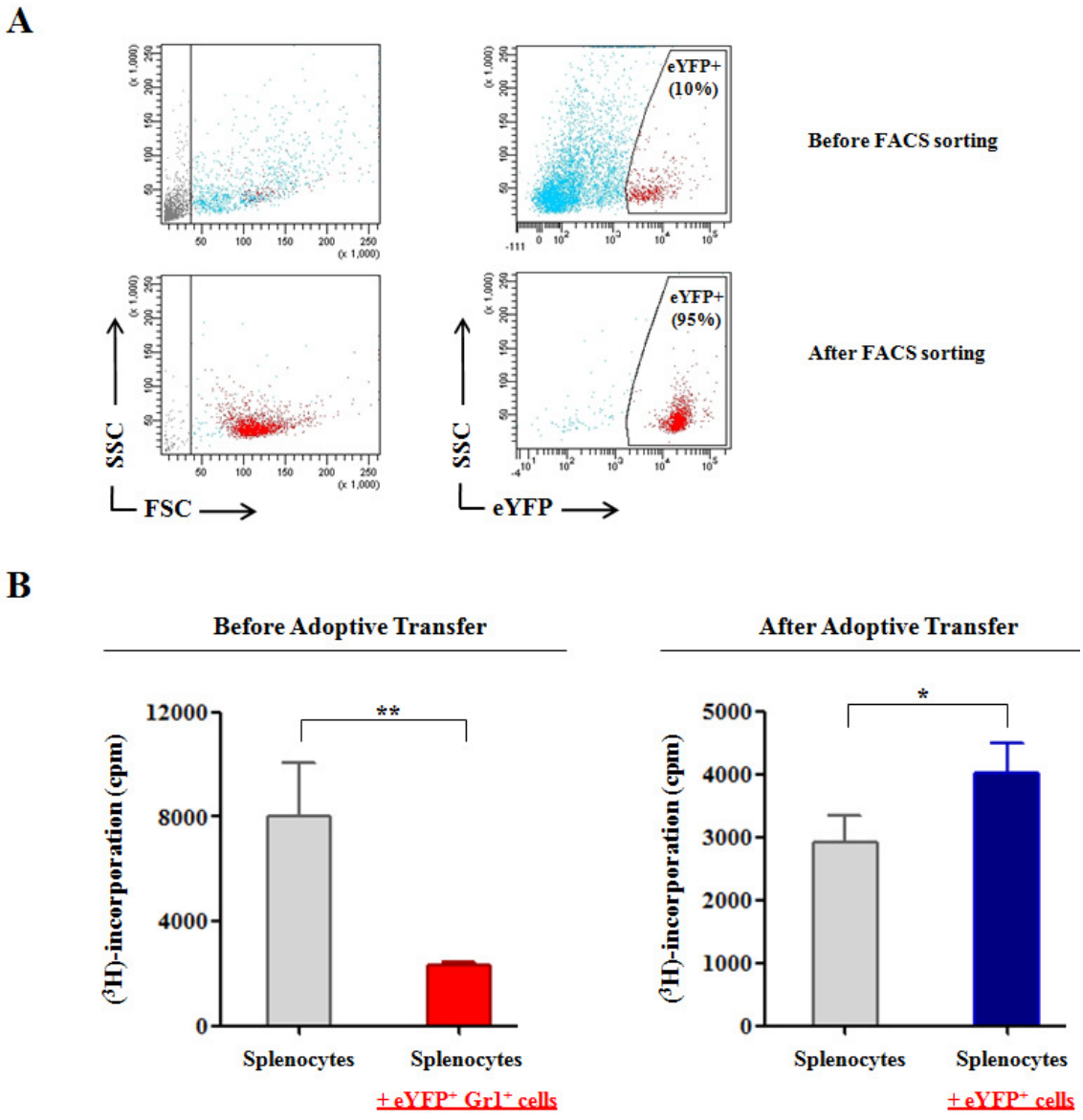

Figure 4.8: Following adoptive transfer in TAZ10 Rag$^{-/-}$ mice, MDSC differentiate into activatory cells
(A) 7 days after adoptive transfer of purified eYFP^{+} Gr1^{+} MDSC from B6.eYFP mice in TAZ10 Rag$^{-/-}$ mice, eYFP^{+} cells were sorted on FACSAria. **(B)** Purified eYFP^{+} cells were added to WT splenocytes activated with αCD3 at a splenocyte:eYFP^{+} cells ratio of 1:1. The proliferative activity of T cells was assessed by (^{3}H) thymidine incorporation assay. Data are representative of 2 different experiments. Statistics were performed using the unpaired Student's t-test.

This surprising outcome was in great contrast with previous observations on Tregs in TAZ10 mice. While their depletion (using PC61 mAb) or blocking (using DTA.1 mAb) was shown to exacerbate thyroiditis in TAZ10 mice, a transfer of non-antigen specific Tregs managed to slow down and alleviate thyroiditis in TAZ10 mice (Ester Badami's PhD Thesis – July 2007). Although it has been shown that Tregs can differentiate under certain conditions into Th17 cells that have a pathogenic role in AID (Elias et al. 2008; Mucida et al. 2007), MDSC being precursor cells are meant to differentiate into mature myeloid cells in a strong pro-inflammatory environment. Therefore, despite a gain in suppressive function, MDSC are unable to control the activation of self-reactive T cells as they differentiate into immunostimulatory APC.

4.2.4 – The depletion of MDSC *in-vivo* does not dampen the severity of the disease in TAZ10 Rag$^{-/-}$ mice

Because the addition of Gr1^{+} MDSC was detrimental and exacerbated the disease in TAZ10 Rag$^{-/-}$ mice (Figures 4.1 and 4.2), I wondered whether their removal would dampen the severity of the disease and improve their survival. To this aim, Gr1^{+} cells were depleted in 2 months old TAZ10 Rag$^{-/-}$ mice that had already started to develop thyroiditis by performing weekly intraperitoneal injections of αGr1 mAb (clone RB6-8C5) (Figure 4.9/A). Weight was recorded every two weeks as a readout of hypothyroidism and their survival monitored over time.

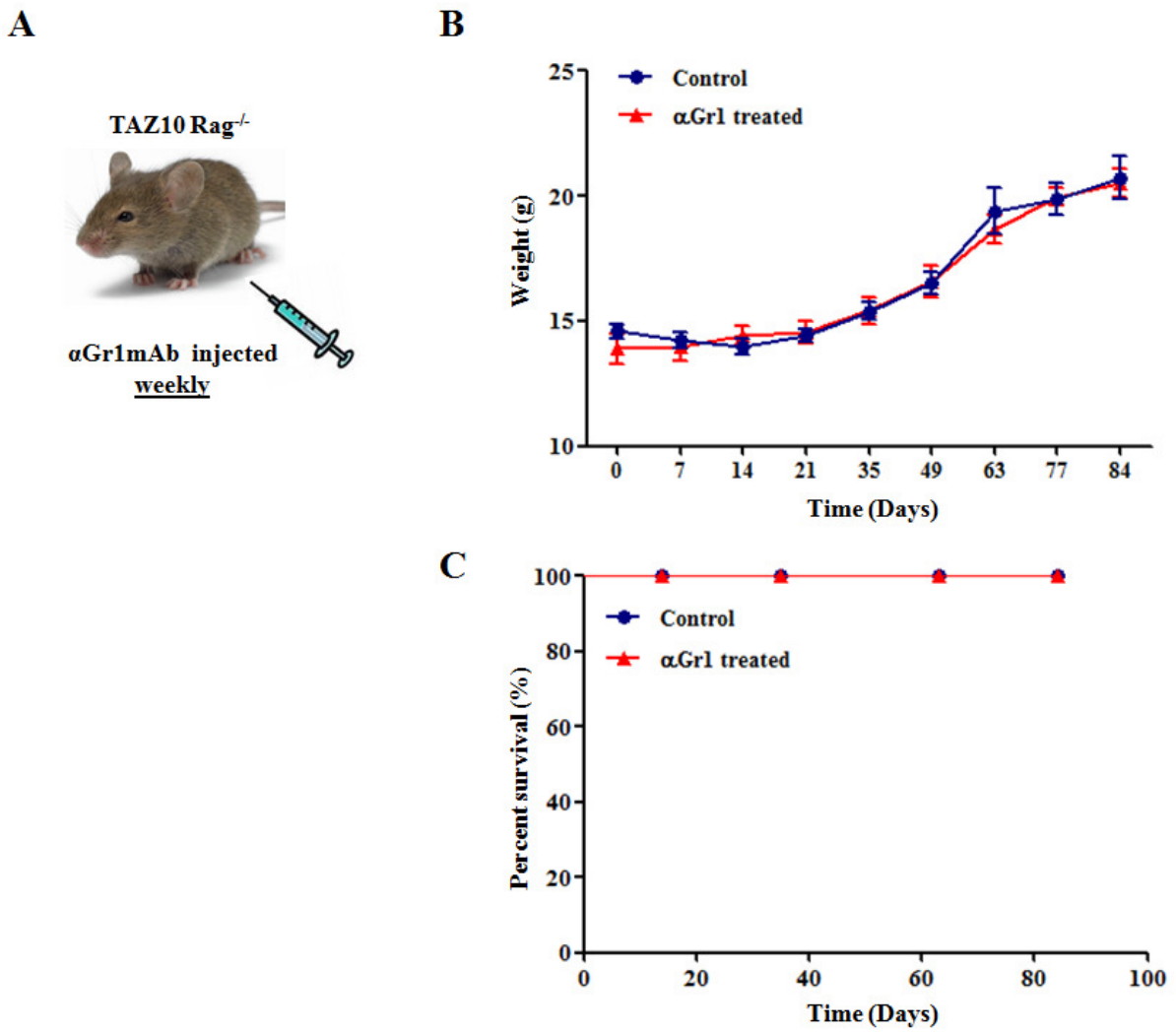

Figure 4.9: *In-vivo* depletion of Gr1$^+$ MDSC from TAZ10 Rag$^{-/-}$ mice does not have an impact on the progression of autoimmune disease

(A) The depletion of Gr1$^+$ cells was achieved by injecting 2 months old TAZ10 Rag$^{-/-}$ mice weekly with 300µg of αGr1 mAb (clone RB6-8C5). Their weight **(B)** was recorded on a weekly basis and their survival **(C)** assessed over a period of 84 days. Data shown are representative of two independent experiments, each involving 5 mice per group.

Similarly to non-depleted control mice, mice that had been depleted in Gr1$^+$ cells gained weight (Figure 4.9/B) and survived over 84 days (Figure 4.9/C). As the *in-vivo* depletion of Gr1$^+$ cells had no beneficial nor detrimental impact on the progression of the on-going AID, it cannot be considered as a therapeutic tool in TAZ10 mice. By contrast, the beneficial effects of the depletion of MDSC in cancer once the tumour is established have been largely described. Indeed the depletion of Gr1$^+$ MDSC *in-vivo* in combination with the AT of TAA-specific T cells resulted in a robust tumour regression in a transgenic mouse model of breast carcinoma (Morales et al. 2009). The depletion of Gr1$^+$ MDSC was however

detrimental in mice in the first few days after infection with *Toxoplasma gondii*. Indeed, mice that had been depleted of $Gr1^+$ MDSC at the time of infection showed an increased susceptibility to infection while mice depleted during the acute phase of infection became resistant to *Toxoplasma gondii* (Bliss et al. 2001). This strongly suggested that the presence of $Gr1^+$ MDSC was crucial during the first days of infection. This concept of the importance of $Gr1^+$ MDSC at the initiation of immune responses will be further explored when investigating the onset of anti-tumour responses in the CT26 mouse model of colon carcinoma (Chapter 5). The impact of MDSC at the onset of autoimmune thyroiditis could however be measured by depleting $Gr1^+$ cells prior and after induction of the disease in WT mice by AT of TAZ10-T_N.

4.3 – MDSC fail to prevent the onset of autoimmune diseases

Despite their accumulation at the onset of the disease and their inhibitory function displayed *in-vitro* (Chapter 3), MDSC failed to prevent the development of thyroiditis in TAZ10 mice. Whilst the destruction of the thyroid occurs, I showed that an AT of MDSC could not control the progression of the disease. MDSC differentiated into immunostimulatory APC thus promoting inflammation and causing the exacerbation of the disease. While the outcome of the AT of MDSC was observed in mice with on-going autoimmune thyroiditis, I wondered whether the same differentiation would occur at the onset of the disease and account for the failure of this regulatory network of peripheral tolerance to control the activation and function of self-reactive T cells. Indeed, at the onset of the disease, the activation of self-reactive T cells would not be yet associated with an inflammation resulting from the destruction of the thyroid and the consequence on the differentiation of MDSC could be different.

I have previously described that an AT of naive T cells purified from TAZ10 mice into WT mice was the adequate tool to recreate the onset of thyroiditis (Chapter 3). Naive T cells from TAZ10 mice were activated within 7 days after AT as 50% and 98% of $CD4^+$ transgenic T cells expressed the CD25 activation marker in the DLN and thyroid respectively. Autoimmune thyroiditis would therefore start in the very first few days of life of TAZ10 mice. In order to establish the role of MDSC at the onset of thyroiditis, $eYFP^+$ $Gr1^+$ MDSC were purified from the bone marrow of B6.eYFP mice and adoptively transferred into WT mice. An AT of naive T cells from WT and TAZ10 $Rag^{-/-}$ mice (WT-T_N and TAZ10-T_N respectively) was performed 2 days later to mimic the onset of thyroiditis (Figure 4.10/A). 21 days after AT, mice were culled and the proportion and phenotype of $eYFP^+$ cells in the spleen investigated (Figure 4.10/B).

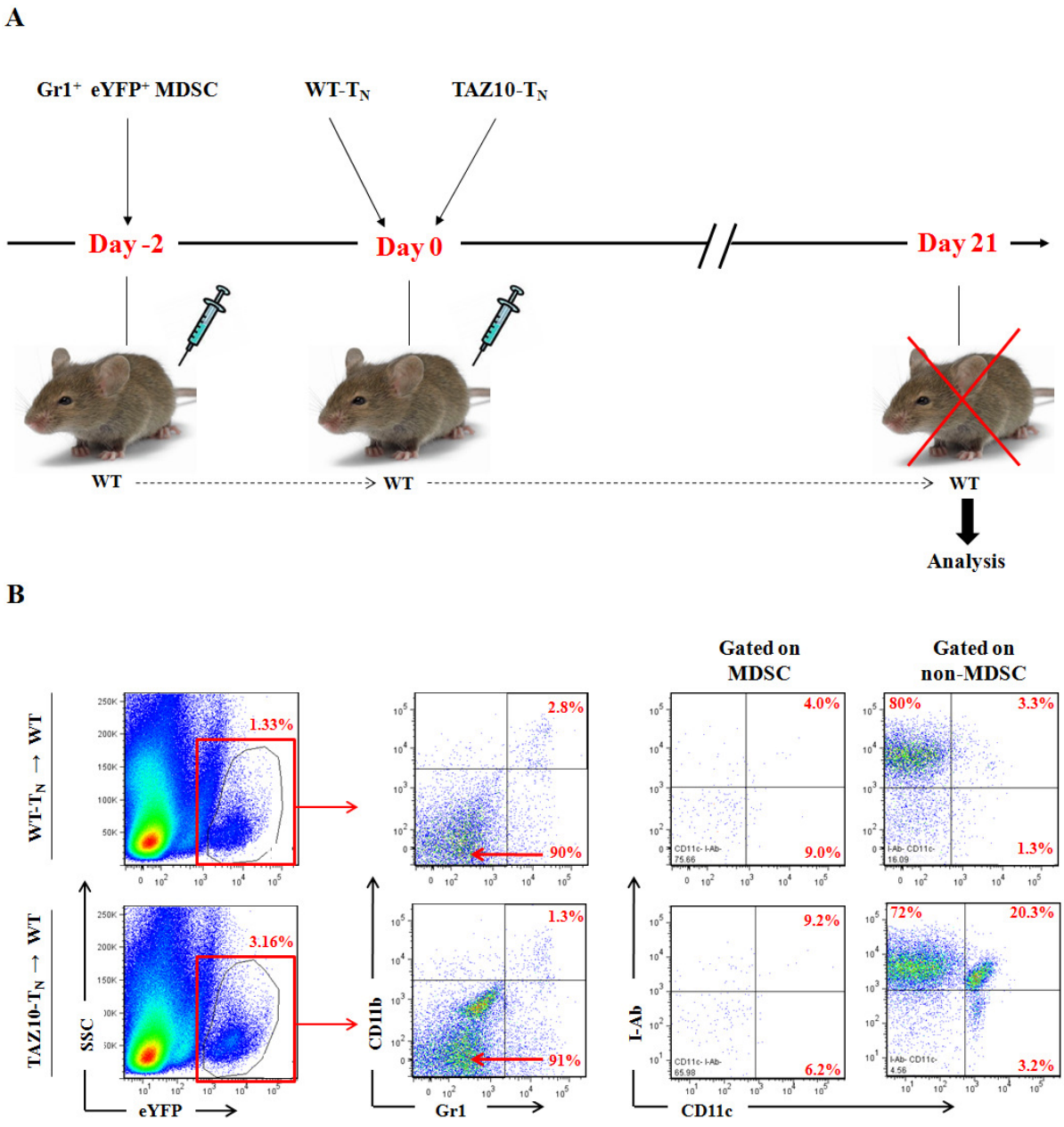

Figure 4.10: MDSC differentiate into mature myeloid cells at the onset of thyroiditis
(A) Gr1$^+$ eYFP$^+$ cells were isolated from the bone marrow of B6.eYFP mice and adoptively transferred into WT mice. 2 days later, mice were adoptively transferred with CD4$^+$ CD62L$^+$ naive T cells purified from the spleen of WT or TAZ10 Rag$^{-/-}$ mice (WT-T_N or TAZ10-T_N). **(B)** 21 days after adoptive transfer, mice were culled and the expression of eYFP in the spleen analysed by flow cytometry. The expression of Gr1 and CD11b was then assessed on gated eYFP$^+$. Gated MDSC and non-MDSC populations were further analysed for their expression of CD11c and I-A^b molecules. Data shown are representative of two experiments with 3 mice per group.

While eYFP$^+$ cells could be observed in the spleen of WT mice that had been adoptively transferred with WT-T_N, this proportion was increased by two-fold when WT

mice were adoptively transferred with TAZ10-T_N. In both cases, only 1 to 3% of the cells still expressed the MDSC markers Gr1 and CD11b. This highlighted that 21 days after AT, MDSC had lost their phenotype and had differentiated. Further analysis revealed that MDSC mainly gave rise to cells expressing MHC-II molecules but not CD11c (80% and 1.3% respectively) following AT of WT-T_N. In comparison, 92% of non-MDSC expressed I-A^b molecules in the spleen of WT mice treated with TAZ10-T_N while 20% expressed both MHC-II molecules and CD11c (Figure 4.10/B). These results therefore suggested that MDSC had differentiated into mature myeloid cells at the onset of thyroiditis.

As TAZ10-T_N were activated within 7 days after AT into WT mice, I investigated whether this had any impact on the ability of MDSC to differentiate into immunostimulatory mature myeloid cells, providing an explanation for their inability to prevent/control the activation of self-reactive T cells. Using the previous experimental schedule described figure 4.11/A, the percentage and phenotype of $eYFP^+$ cells were analysed 3, 5, 7 and 21 days after AT of WT-T_N or TAZ10-T_N in WT mice (Figure 4.11).

An accumulation of MDSC associated with a slow increase in the number of $eYFP^+$ cells could be observed up to 7 days after AT in the spleen of WT recipient mice regardless of the mouse origin of naive T cells adoptively transferred. Interestingly, 5 days after AT of TAZ10-T_N into WT mice, a discrete population of $CD11c^+$ I-A^{b+} cells could be observed in the spleen while this cell population remained low and relatively stable in WT mice adoptively transferred with WT-T_N. This trend could be confirmed 7 days after AT thus suggesting that the activation of TAZ10-T_N cells was sufficient to promote the differentiation of MDSC into immunostimulatory APC that would favour inflammation.

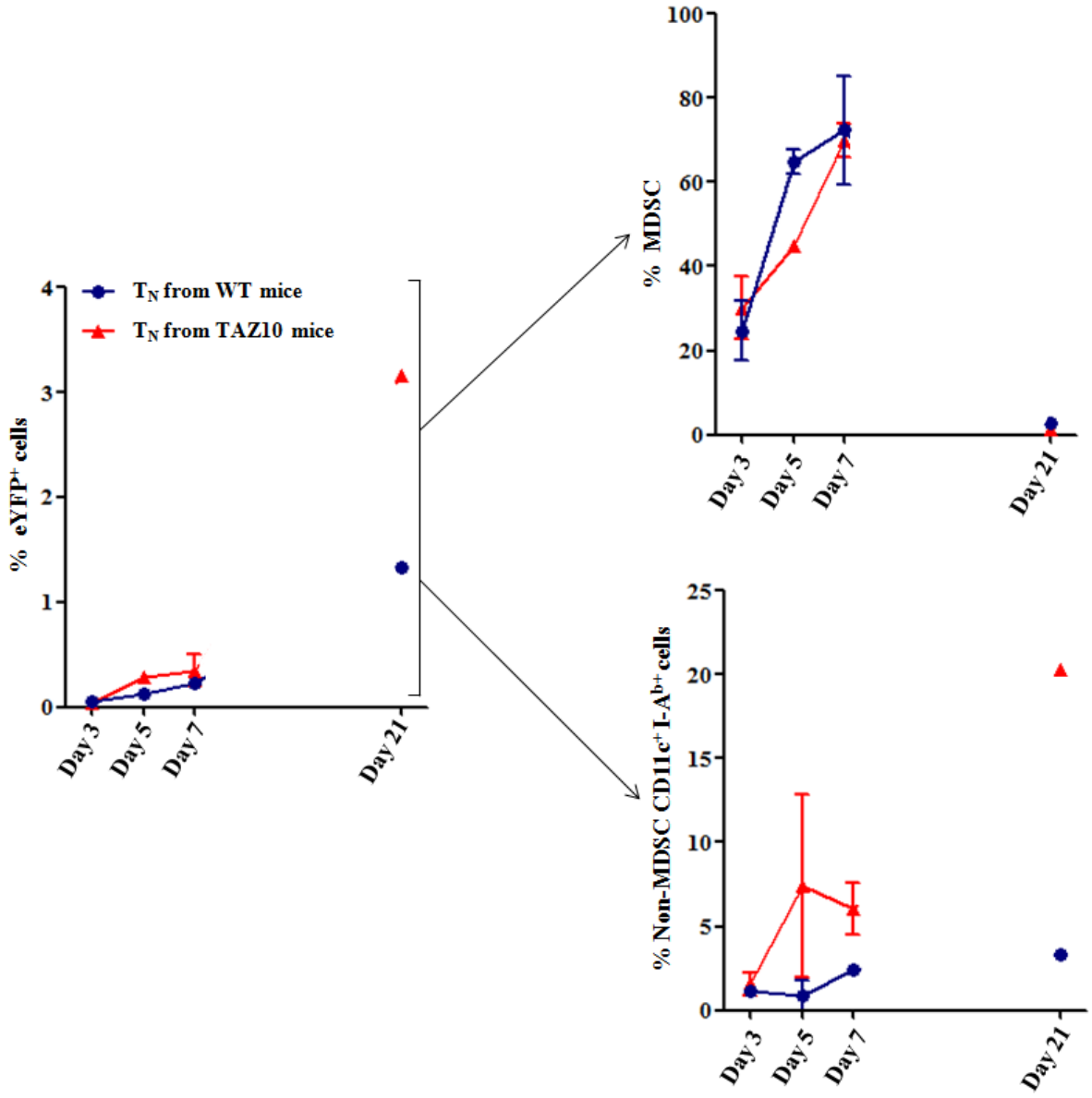

Figure 4.11: The activation of self-reactive T cells promotes the differentiation of MDSC into mature myeloid cells

WT mice were adoptively transferred with eYFP$^+$ Gr1$^+$ MDSC isolated from the bone marrow of B6.eYFP mice followed 2 days later by the AT of naive T cells (T_N) from WT or TAZ10 Rag$^{-/-}$ mice. Mice were culled 3, 5, 7 and 21 days after AT and the percentage of eYFP$^+$ cells in the spleen of these mice assessed. Further analysis investigated the expression of Gr1and CD11b markers by eYFP$^+$ cells as well as the expression of CD11c and I-A^b MHC-II molecules by non-MDSC cells.

21 days after AT, the accumulation of eYFP$^+$ cells previously observed at day 5 and 7 prevailed in mice that had been adoptively transferred with TAZ10-T_N cells as it reached about 3% of the splenic population compared to 1.4% when considering the AT of WT-T_N cells. This accumulation of eYFP$^+$ cells was associated in both conditions with the absence of eYFP$^+$ MDSC that had further differentiated thus highlighting the limited ability of MDSC for self-renewal previously described in other studies (Gabrilovich et al. 2009, Liu et al.

2007a). The generation of WT bone marrow chimeric mice reconstituted with a mix of cells from the bone marrow of B6.eYFP and TAZ10 mice could be used to study more precisely the kinetic of recruitment of MDSC at the onset of the disease in TAZ10 mice.

Interestingly, the absence of MDSC 21 days after AT was associated with a significant increase in the number $CD11c^{+}$ $I\text{-}A^{b+}$ cells in recipient WT mice where the activation of TAZ10-T_N cells had occurred as opposed to recipient WT mice in which WT-T_N were not activated. These results therefore confirmed that MDSC differentiated into immunostimulatory myeloid cells expressing CD11c and MHC-II molecules at the onset of the disease in TAZ10 mice.

Altogether, I showed that the activation and proliferation of naive T cells from TAZ10 mice at the onset of thyroiditis was sufficient to promote the rapid differentiation of MDSC into $CD11c^{+}$ $I\text{-}A^{b+}$ stimulatory APC that would contribute to the pathogenesis of the disease. The sole activation and proliferation of self-reactive T cells could therefore be considered as a “danger signal”. Although not yet associated with thyroid damage, this “danger signal” is sensed by MDSC that would naturally increase their suppressive activity on T cells to control their proliferation, differentiation and functions. As self-reactive T cells become increasingly activated, the balance of pro- versus anti-inflammatory cytokines in the microenvironment would favour a pro-inflammatory environment promoting the differentiation of MDSC into immunostimulatory myeloid cells that contribute to the progression of the disease.

4.4 – Summary

AID are chronic inflammatory diseases resulting from the activation of self-reactive T and B cells after the breakdown of immunological tolerance to self-antigens and the failure of peripheral regulatory mechanisms to suppress their activation and differentiation. I previously showed that the on-going inflammation present in TAZ10 mice that spontaneously develop AID has an important impact on MDSC (Chapter 3). While MDSC are naturally present in WT mice where they display inhibitory functions on T cells, they accumulate and exhibit stronger suppressive activity on T cells in TAZ10 mice. This effect depends on the level of inflammation as the proportion as well as the inhibitory activity of MDSC are increased during the acute phase of thyroiditis when the thyroid is being destroyed (Chapter 3). Such inflammatory environment characterised by the release of soluble factors such as VEGF, IL-6 or IL-1β has been shown to be responsible for the recruitment of MDSC (Bunt et al. 2007, Tu et al. 2008, Ostrand-Rosenberg et al. 2009). Strikingly, despite these observations, inhibitory MDSC accumulating at the onset of the disease in TAZ10 mice are unable to prevent/control the activation of self-reactive T cells resulting in the development of thyroiditis.

MDSC are cells of the myelomonocytic lineage consisting of myeloid progenitors and immature myeloid cells with the ability to differentiate in healthy individuals into mature myeloid cells such as granulocytes, dendritic cells and macrophages (Figure 4.12). I have indeed shown that following AT in WT mice, MDSC naturally accumulate in the spleen and lymph nodes. This is associated with their differentiation providing a constant replenishment of APC that have a short half-life *in-vivo* (Figures 4.3, 4.5 and 4.6). This process has been previously reported when considering the AT of a common clonogenic myeloid progenitor into WT mice. The proportion of these cells gradually increased in the spleen of recipient mice during the first 7 days after AT while it decreased thereafter as they differentiated and gave rise to steady-state splenic DC (Fogg et al. 2006).

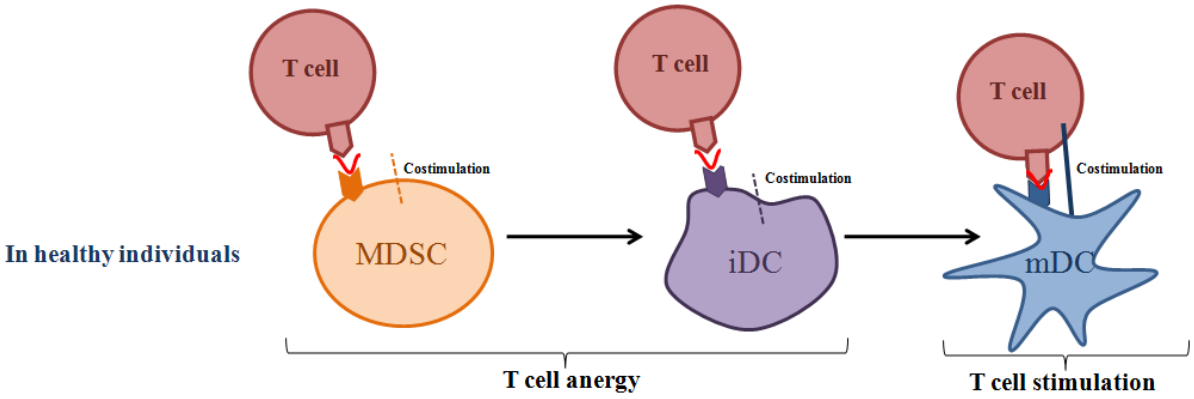

Figure 4.12: In healthy individuals, MDSC naturally differentiate into APC such as dendritic cells or macrophages
MDSC are a heterogenous population of cells of myeloid origin that are generated in the bone marrow from common myeloid progenitor cells. In normal conditions, MDSC migrate to different peripheral organs where their differentiation into granulocytes, macrophages or dendritic cells that contribute to the maintenance of the existing pool of APC. While MDSC and immature DC (iDC) induce T cell anergy, mature DC (mDC) can promote the expansion and differentiation of T cells.

The differentiation of MDSC is driven by various soluble factors that are also involved in their accumulation and increased acquisition of suppressive activity (Chapter 3). While IFNγ and TNFα have been shown to promote the differentiation of MDSC into macrophages (Bronte et al. 2000), MDSC differentiate into immunostimulatory mature APC *in-vitro* upon stimulation with GM-CSF and IL-4 (Bronte et al. 1999). The pro-inflammatory cytokine IL-1β promotes the accumulation of MDSC and their activation through the NF-κB signalling pathway and the subsequent secretion of IL-6 and TNFα (Tu et al. 2008). These two cytokines also influence the differentiation of MDSC to macrophages and DC (Park et al. 2004). MDSC release TGF_{β} upon stimulation with IL-13 secreted by NKT cells and macrophages (Terabe et al. 2003). Increased TGF_{β} concentration suppresses the production of NO by MDSC while promoting their differentiation into $CD206^{+}$ alternatively activated "M2"-type macrophage (Umemura et al. 2008). While MDSC can differentiate into DC and "M1" or "M2" macrophages, they are also able to promote tumour angiogenesis by their secretion of NO and their ability to differentiate into endothelial cells in the tumour microenvironment (Yang et al. 2004).

The pro- versus anti-inflammatory nature of the microenvironment has an important impact on the accumulation, activity and differentiation of MDSC. It was therefore essential

to assess whether the inflammatory status resulting from the proliferation and activation of self-reactive T cells at the onset of the disease in TAZ10 mice was sufficient to drive the accumulation and differentiation of MDSC into immunostimulatory cells that would contribute to the pathogenesis of the disease. The acquisition of the B6.eYFP mouse model that ubiquitously expresses eYFP was decisive to track down MDSC *in-vivo* and investigate their ability to migrate and differentiate in specific tissues.

I previously suggested that the onset of autoimmune thyroiditis in TAZ10 mice occurs within the first few days of life. Indeed, TAZ10-T_N adoptively transferred into WT mice were able to overcome the inhibition displayed by networks of peripheral tolerance (such as Tregs and MDSC) and became activated within days. As not yet associated with the destruction of the thyroid, the sole activation and proliferation of self-reactive T cells was enough to promote the recruitment of MDSC into lymphoid tissues (Figures 3.6 and 3.7). The inflammatory environment resulting from this activation would result in MDSC increasing their inhibitory activity while they would promote the generation of $Foxp3^+$ Tregs. The association of the AT of MDSC from the bone marrow of B6.eYFP mice followed by the AT of TAZ10-T_N and WT-T_N provided an efficient tool to study the impact of the onset of thyroiditis on MDSC. I showed that the activation of self-reactive T cells was not only responsible for the recruitment and accumulation of MDSC in lymphoid organs at the onset of the disease but also for their differentiation into $CD11c^+$ $I\text{-}A^{b+}$ immunostimulatory APC that would promote inflammation (Figures 4.10 and 4.11). This activation of self-reactive T cells exacerbates the differentiation of MDSC into APC that naturally occurs in healthy individuals in the absence of inflammation. The generation of this inflammatory environment in TAZ10 mice increases the differentiation of MDSC into immunostimulatory APC while MDSC still display their inhibitory functions on T cells. The activation of self-reactive T cells gradually becomes prevalent over their inhibition shifting the balance towards an increasing immunostimulatory environment that promotes the development and the progression of the disease (Figure 4.13). Indeed, the inhibitory functions displayed by MDSC on T cells were hindered and overcome by the amplified differentiation of MDSC into immunostimulatory APC.

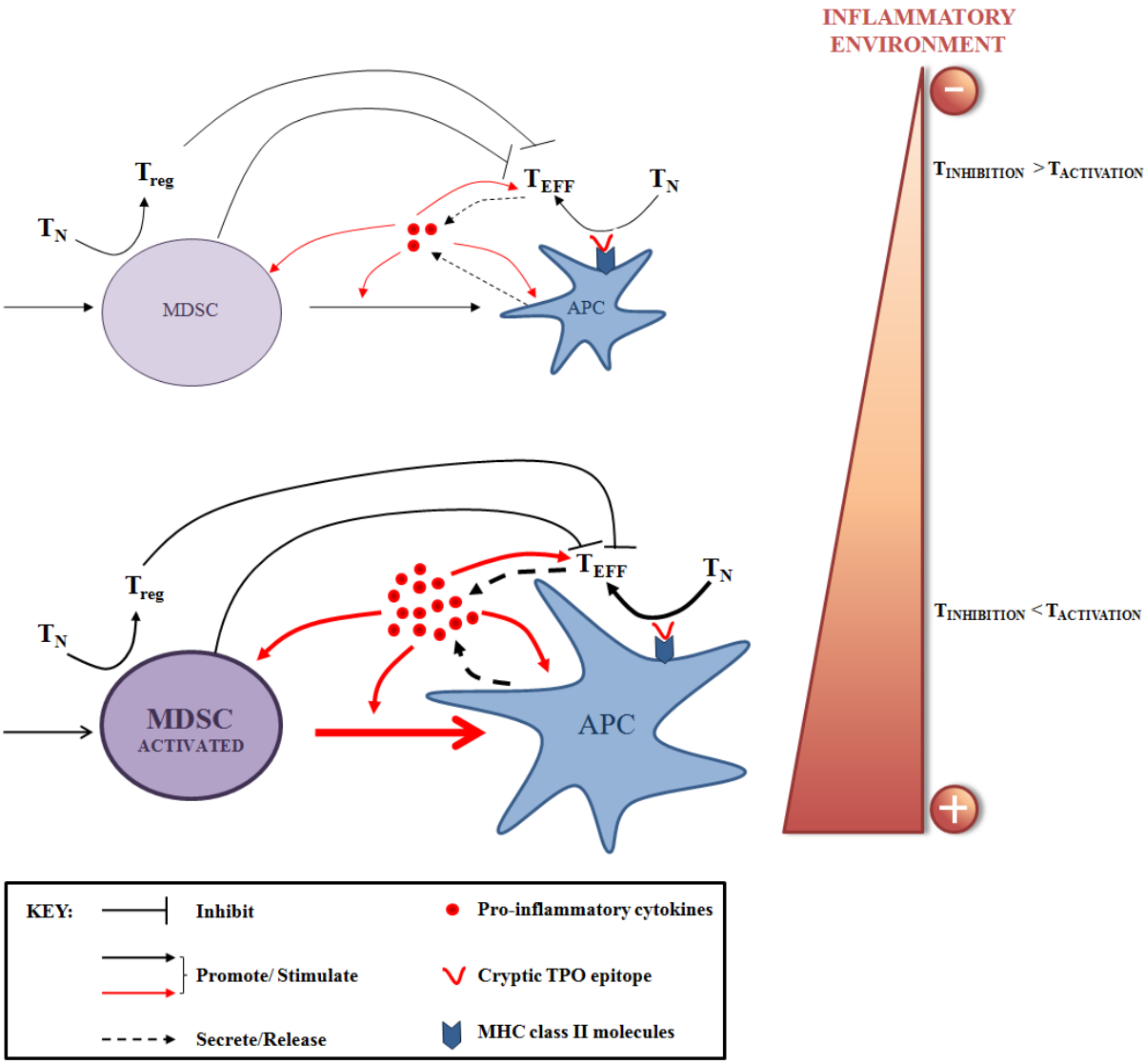

Figure 4.13: The sole activation of self-reactive T cells alters the functions of MDSC
In a non-inflammatory environment, the activation of self-reactive T cells is inhibited by MDSC through their direct action on T cells and the induction of Tregs. Although MDSC naturally differentiate into APC capable of priming immune responses, MDSC can still control the activation of self-reactive T cells. As T cells become more activated resulting in the release of pro-inflammatory cytokines, the differentiation of MDSC into APC is amplified so that the activation of self-reactive T cells is enhanced by the increased presence of immunostimulatory APC. Despite MDSC still displaying inhibitory functions on T cells, immunostimulatory APC overcome the inhibition mediated by MDSC thus leading to an efficient activation, proliferation and differentiation of self-reactive T cells. T_N: Naive T cells; T_{EFF}: Effector T cells; Treg: Regulatory T cells; APC: Antigen presenting cells; MDSC: Myeloid derived suppressor cells.

As the inflammatory process amplifies, self-reactive effector T cells migrate to the thyroid thus promoting its destruction. The inflammatory cascade amplifies and feeds back on itself so that the differentiation of MDSC into APC and the priming of self-reactive T cells are strongly promoted and contribute even more to the intensification of the on-going

inflammation (Figure 4.14). As more self-reactive effector T cells migrate to the thyroid where they induce the death of thyroid epithelial cells (TEC), the pro-inflammatory environment generated favours the recruitment of MDSC in the thyroid and their differentiation into immunostimulatory APC. This allows for the direct priming of more self-reactive T cells thus promoting thyroid damage. This amplification of inflammation within the thyroid directly impacts on the recruitment of MDSC. The increased recruitment of MDSC in response to the inflammatory process would therefore be part of a physiological mechanism aimed at dampening/controlling the adaptive immune response. However, the strong pro-inflammatory nature of the microenvironment prevents this control as MDSC are pushed to differentiate into highly immunostimulatory APC.

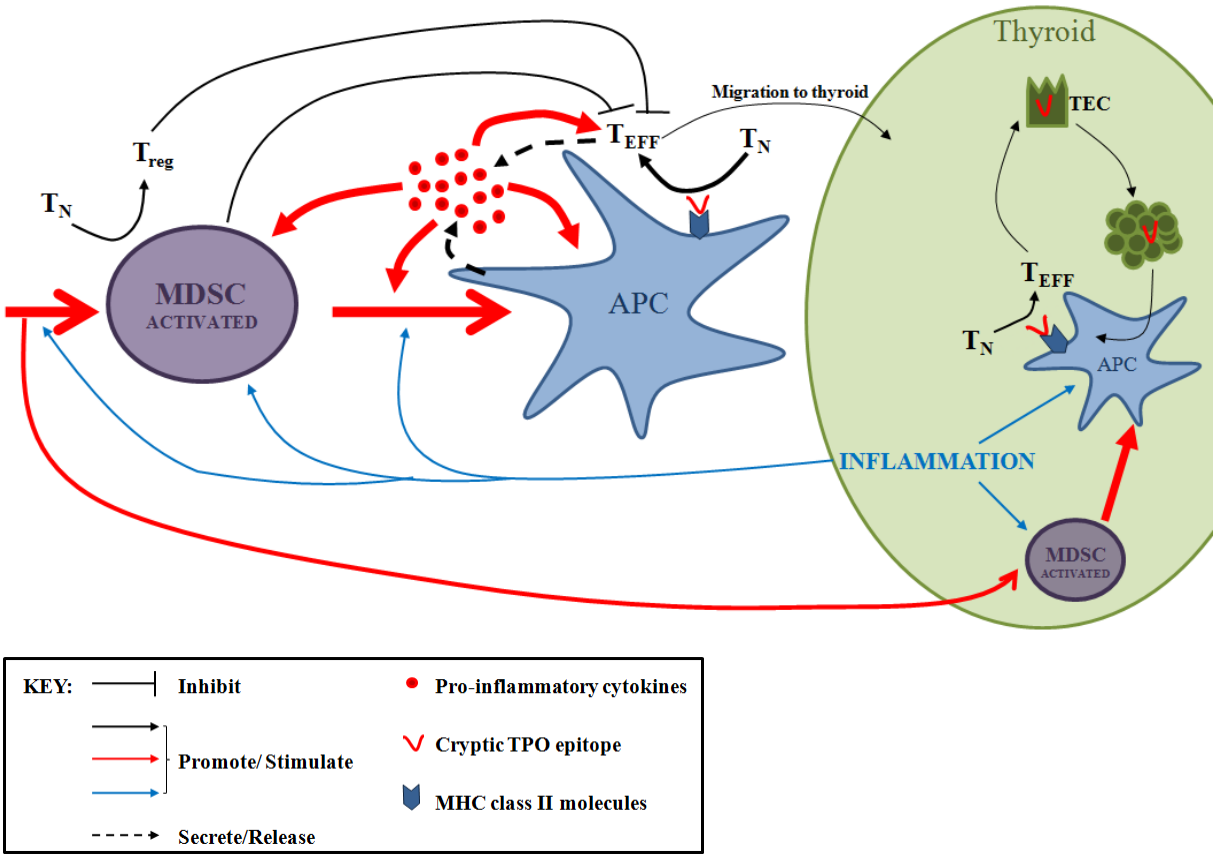

Figure 4.14: The destruction of the thyroid by self-reactive T cells strongly promotes the recruitment and differentiation of MDSC into immunostimulatory APC contributing to the amplification of the inflammatory response

While the destruction of the thyroid occurs through the action of self-reactive T cells, the inflammatory environment created favours the recruitment of MDSC to the thryoid. Their differentiation into APC is also exacerbated so that more self-reactive T cells are activated leading to the destruction of an increased number of thyroid epithelial cells (TEC) and the amplification of the inflammatory response. This in turn promotes the recruitment of MDSC to the thyroid and their differentiation into immunostimulatory APC. T_N: Naive T cells; T_{EFF}: Effector T cells; Treg: Regulatory T cells; APC: Antigen presenting cells; MDSC: Myeloid derived suppressor cells.

These observations therefore provide an explanation for the failure of MDSC to control the activation of self-reactive T cells and dampen the signs of disease. Indeed, in 2 months old TAZ10 $Rag^{-/-}$ mice in which thyroid destruction is ongoing, the AT of MDSC failed to control the progression of the disease as they differentiated into $CD11c^{+}$ and $CD11c^{+}$ $I\text{-}A^{b+}$ immunostimulatory APC promoting T cell proliferation (Figures 4.5, 4.6 and 4.8). Considering the inflammatory context at the time of AT, an addition of MDSC would only result in providing more immunostimulatory APC that would contribute to the exacerbation of the disease, justifying the premature death of the treated mice due to a very aggressive autoimmune condition reflected by the sudden loss of weight.

The AT of myeloid suppressor cells generated from bone-marrow cells cultured in GM-CSF and TGF_{β} was however able to suppress the development of autoimmune diabetes in proinsulin-nonobese diabetic (PI-NOD) transgenic mice. This phenomenon was associated with the differentiation of MDSC *in-vivo* into resting DC that promoted the deletion or anergy of PI-reactive T cells (Steptoe et al. 2005).

While an AT of MDSC could not be used *in-vivo* as a therapeutic strategy to block the progression of thyroiditis in TAZ10 mice, its use as a therapeutic tool in cancer treatment can also not be considered. The transfer of MDSC into tumour-bearing mice increases tumour growth (Kusmartsev et al. 2005) and reduces the number and activity of tumour-specific T cells (Watanabe et al. 2008). In a tumour microenvironment, the inhibitory functions of MDSC on T cells are enhanced while they differentiate into cells promoting tumour growth such as endothelial cells favouring angiogenesis. The ability of MDSC to differentiate into immunostimulatory APC was also strongly impaired in tumour-bearing mice (Kusmartsev et al. 2003a) as they primarily differentiated into immunosuppressive macrophages in the vicinity of the tumour (Kusmartsev et al. 2005).

"Dangers Signals" are mainly associated with the breach of physical barriers, the invasion by pathogens or tissue damage/destruction. The sole activation of self-reactive T cells in the TAZ10 $Rag^{-/-}$ model of spontaneous thyroiditis was enough to represent a "Danger Signal". Indeed, we could exclude the presence of any infections as TAZ10 $Rag^{-/-}$ mice are breed in a confined pathogen-free environment. MDSC are a fine sensor of inflammation and respond to this "Danger Signal" by first enhancing their immunosuppressive functions on T cells. A sustained stimulation by this "Danger Signal"

then promoted the recruitment and differentiation of MDSC into immunostimulatory cells that contribute to the pathogenesis of the disease. The activation of self-reactive T cells in the absence of destruction of the target tissue results in a subtle shift in the balance between pro- versus anti-inflammatory cytokines that is sensed by MDSC.

5 – Impact of MDSC on the initiation of anti-tumour responses

5.1 – Introduction

Autoimmune diseases (AID) are chronic inflammatory diseases, associated with the infiltration of tissues by monocytic cells, the release of soluble factors such as chemokines and cytokines (IFN-γ, TNF-α and IL-1β) and tissue damage (Vanderlugt and Miller, 2002). In recent years, the importance of regulatory networks in the occurrence of AID has been described and the role played by Tregs has been extensively studied (Sakaguchi et al. 2006). While the role and functional importance of MDSC in cancer is well defined, their impact in the course of AID is still elusive. Despite their strong suppressive activity on T cell proliferation displayed *in-vitro,* MDSC could not prevent the development of AID from the onset in TAZ10 mice. Indeed, MDSC quickly accumulate in lymphoid and non-lymphoid organs where they differentiate into immunostimulatory mature myeloid cells (Chapter III and IV).

The importance of the fate of MDSC at the onset of disease in TAZ10 mice prompted us to question their role at the initiation of anti-tumour responses. While previous studies only investigated the role of MDSC once the tumour is established, their importance in the generation of immune responses in the first days after tumour inoculation has never been addressed.

I decided to carry out this investigation in the murine CT26 colon carcinoma mouse model currently under investigation in the laboratory. Preliminary results have shown an accumulation of MDSC in CT26 challenged mice. Indeed, when I examined the percentage of $Gr1^+$ $CD11b^+$ over time after tumour challenge in various tissues (Figure 5.1/A), I identified an increase from 0.01% to 0.04% in the inguinal LN draining (DLN) the CT26 tumour and from 0.03% to 0.08% in the LN not draining the tumour (NDLN). The highest increase was observed in the spleen as the proportion raised 3 fold (2% to 6%) 14 days after tumour challenge (Figure 5.1/B). Interestingly, MDSC accumulated quickly in the LN draining the tumour while this process was delayed by 4 days when considering the spleen and the non-draining LN.

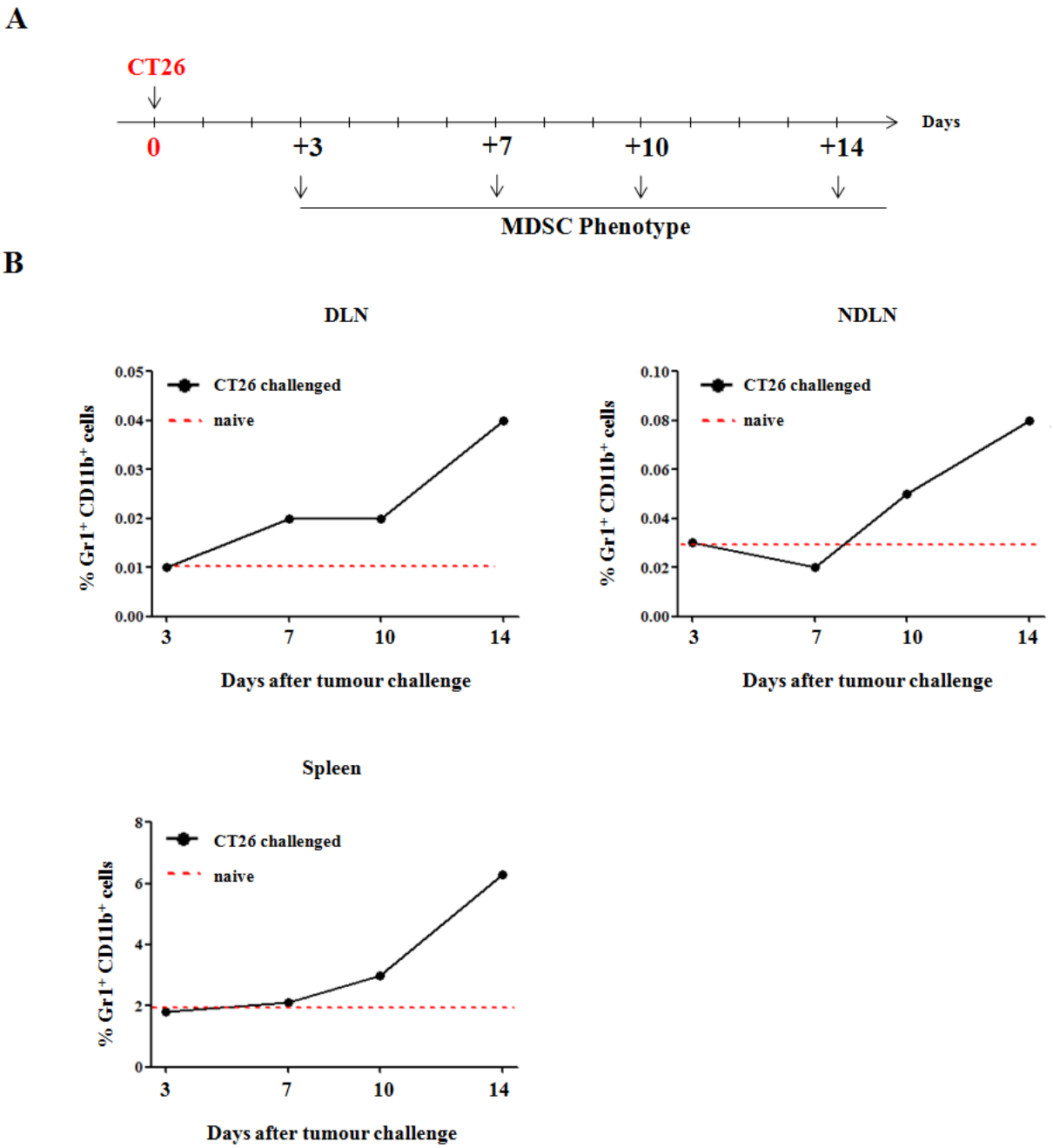

Figure 5.1: Gr1$^+$ MDSC accumulate in lymphoid tissues of CT26 challenged mice
(A) Balb/c mice were subcutaneously injected with CT26 tumour cells. The percentage of Gr1$^+$ CD11b$^+$ cells was then assessed by flow cytometry 3, 7, 10 and 14 days after challenge. **(B)** Percentage of Gr1$^+$ CD11b$^+$ cells in the spleen and the inguinal lymph nodes draining (DLN) and not-draining (NDLN) the tumour of CT26 challenged Balb/c mice. Data shown are representative of three independent experiments.

Previous reports have shown that the challenge of Balb/c mice with CT26 tumour cells engineered to secrete GM-CSF induces long lasting immunity in the presence of CD25$^+$ Tregs (Dranoff et al. 1993). Tumour rejection is mediated by CD8$^+$ CTLs recognizing the tumour antigen AH1 N-SPSYVYHQF-C (aa 423-431 of gp70 protein, the *env* gene product of

endogenous ecotropic murine leukemia provirus (*emv-1*). Adoptive transfer of gp70-specific CTLs isolated from CT26/GM-CSF immunized mice conferred protection to naive CT26 challenged mice which normally succumb within 30 days after challenge (Huang et al. 1996).

Interestingly, Balb/c mice have been shown to reject CT26 tumour cells following *in-vivo* depletion of $CD25^+$ Tregs using PC61 mAb. This initial depletion of $CD25^+$ cells does not only confer immunity to the colon carcinoma CT26 but also induces long-term immunity since the majority of CT26 immune mice are able to reject a second challenge despite the repopulation of $CD25^+$ Tregs. Most importantly, it provides cross-protection to several other tumours of different histological origins such as RENCA (renal cell carcinoma), BCL-1 and A20 (B cell lymphomas) (Golgher et al. 2002). This cross-protective immunity is mediated by both $CD4^+$ and $CD8^+$ T cells. In addition, the CTL response is not AH1-specific but is directed against the GSW11 antigen (also derived from the gp90 gene of *emv-1*) shared among the different tumour cells lines (James et al. 2010).

Considering the importance of the $CD8^+$ T cell response in the CT26 mouse model, we first decided to address whether MDSC can present immunogenic peptide to $CD8^+$ T cells from the processing of endogenous gp90. This will help unravel the role played by MDSC in the generation of anti-tumour responses to CT26 tumour cells.

5.2 – MDSC can process and present peptides in the context of MHC class I molecules

Having previously shown that MDSC were unable to induce the proliferation of $CD4^+$ T cells in the TAZ10 mice (Figure 3.24), I wanted to determine whether they shared any function with professional APC and could present MHC-I restricted peptides to $CD8^+$ T cells. Indeed, I have shown that MDSC from TAZ10 and WT mice expressed some markers of APC, such as CD11c and F4/80 and maturation markers such as CD86 and MHC-II molecules (Figures 3.21). These observations suggested a possible role of MDSC in the processing and presentation of endogenous and exogenous antigens. In the CT26 tumour model, the anti-tumour $CD8^+$ T cell response is restricted to the AH1 or GSW11 MHC-I epitopes derived from the endogenous processing of gp70 and gp90 proteins respectively. By assessing if MDSC can uptake, process and present MHC-I restricted peptides, I wanted to address whether they were playing a role in the initiation of anti-CT26 tumour responses. To this aim, I used a widely known antigen presentation system using ovalbumin (OVA) that is available in the lab. The dominant epitope SIINFEKL (SL8), derived from OVA, can be presented by the mouse MHC-I molecules H-$2K^b$ to B3Z T cells. The H-$2K^b$/SL8 restricted B3Z hybridoma T cell line is lacZ inducible and its stimulation by SL8/H-$2K^b$ complexes can be measured by assessing the lacZ activity and the subsequent hydrolysis of the chromogenic substrate CPRG. Using this system, I would not investigate the classical MHC-I processing pathway but the ability of MDSC to cross-present exogenous OVA and generate the class I restricted SL8 peptide.

5.2.1 – Differential presentation of SL8/H-$2K^b$ to B3Z T cells between BM-DC and MDSC

5.2.1.1 – MDSC can internalize soluble antigens

I previously showed that MDSC were capable of uptaking IgG coated latex beads (Figures 3.23). This endocytic activity was further analysed as I assessed their ability to internalize exogenous soluble OVA. BM-DC and MDSC purified from the spleen of TAZ10 $Rag^{+/+}$ mice were incubated over a period of time with CFSE-conjugated OVA (OVA-CFSE).

Cells were harvested at regular intervals and analysed by flow cytometry to reflect the amount of OVA-CFSE that has been taken up.

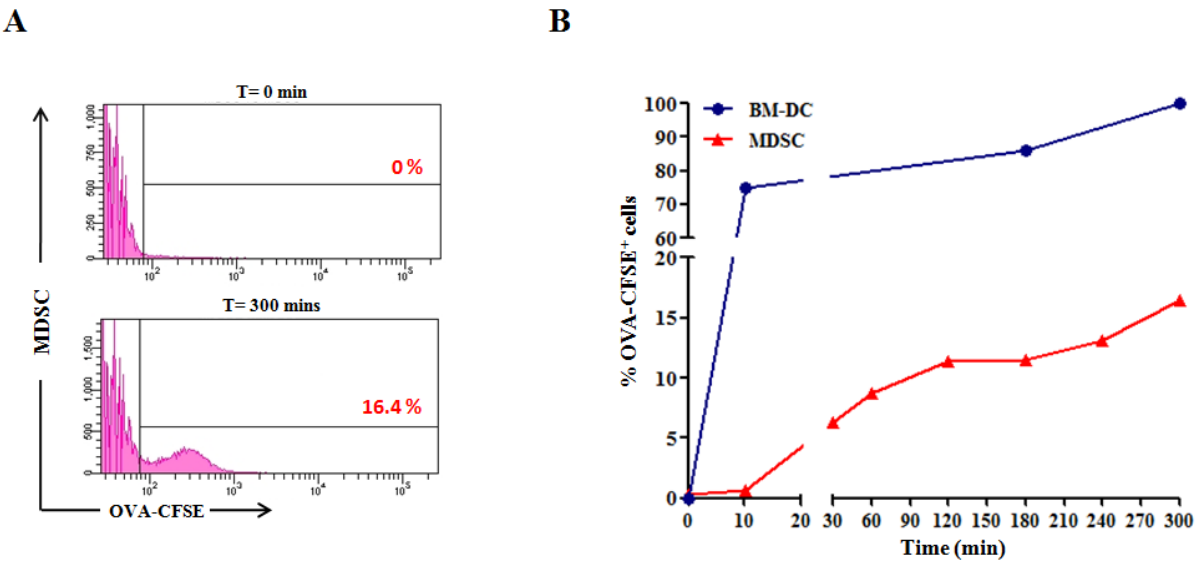

Figure 5.2: MDSC uptake soluble CFSE-labelled OVA
Purified MDSC from the spleen of TAZ10 Rag$^{+/+}$ mice were incubated over 5 hours with CFSE-conjugated ovalbumin (OVA-CFSE). **(A)** MDSC become fluorescently labelled following the uptake of OVA-CFSE and the level of CFSE fluorescence analysed by flow cytometry. Red numbers indicate the percentage of MDSC-CFSE^{+} cells. **(B)** Kinetics of the uptake of OVA-CFSE by MDSC (red line) and BM-DC (blue line) for up to 300 minutes. Data shown are representative of 2 different experiments.

After 300 mins (5 hours) incubation, 16% of MDSC became fluorescent demonstrating that OVA-CFSE had been internalized and that MDSC could take up soluble OVA (Figure 5.2/A). I then investigated whether the uptake of OVA-CFSE over time by MDSC and BM-DC followed the same kinetic. Within the first 30 min, 80% of BM-DC had taken up OVA-CFSE versus only 7% for MDSC (Figure 5.2/B). These results correlate with previous observations (Figure 3.23) where MDSC internalized only 3 beads in 45 min and displayed a lower phagocytic activity than BM-DC. While 100% of BM-DC were OVA-CFSE^{+} after 5 hours incubation, only 16% of MDSC have internalized OVA.

Overall, these results showed that MDSC display an endocytic activity although much slower and less efficient compared to BM-DC.

5.2.1.2 – MDSC efficiently generate the H-2K^b restricted SL8 peptide

Having described that MDSC can uptake soluble antigens, the next step was to determine whether they could process OVA to generate the SL8 immunodominant epitope. BM-DC and MDSC purified from the spleen of TAZ10 Rag$^{+/+}$ mice were incubated for 8 hours with soluble ultra-pure and endotoxin-free OVA that has been extensively dialysed to exclude the presence of free SL8 peptides in the assay. After 8 hours, cells were lysed and peptides extracted. Peptide extracts were then used in a T cell activation assay using K89 expressing H-2K^b as APC (Figure 5.3/A).

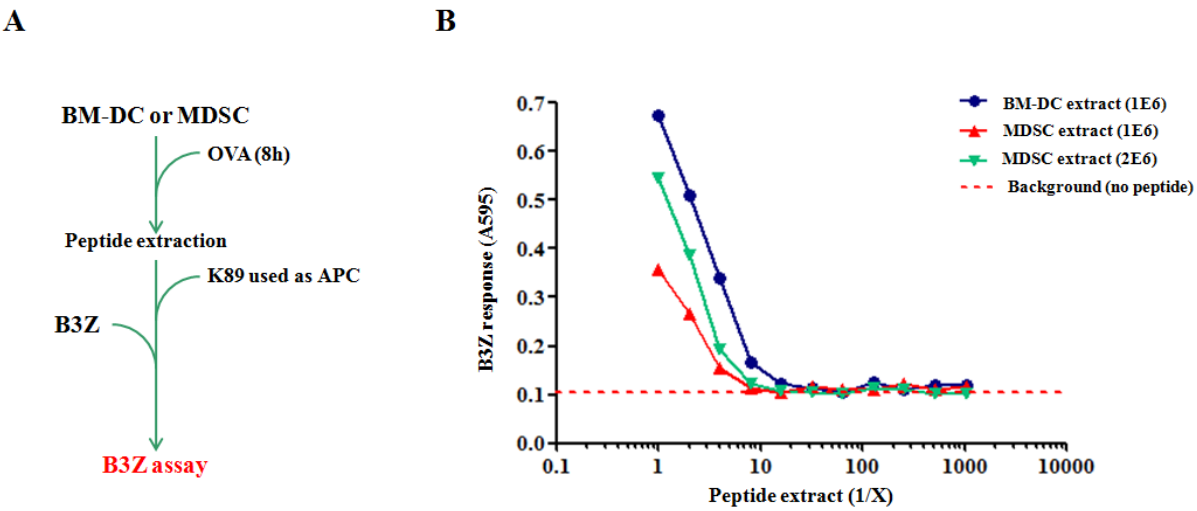

Figure 5.3: Gr1$^+$ MDSC can process exogenous antigens
(A) BM-DC and purified Gr1$^+$ MDSC from the spleen of TAZ10 Rag$^{+/+}$ were incubated for 8 hours with OVA and then lysed to extract peptides. Peptide extracts were assayed for the presence of SL8 peptides using B3Z T cells and K89 as APC. **(B)** The B3Z hybridoma response resulting from the recognition of the SL8/H-2K^b complex by B3Z was measured through CPRG colorimetric substrate reading. MDSC were used in equal or double number to BM-DC (1E6 or 2E6). Data shown are representative of 3 independent experiments.

As observed in figure 5.3/B, both BM-DC and MDSC were able to uptake and process OVA to generate the SL8 peptide. However, the level of stimulation was greater for BM-DC compared to MDSC; at equal number of cells, the B3Z response to MDSC derived SL8/H-2K^b complexes was halved. As K89 were used as APC, the levels of expression of MHC-I molecules were identical in all conditions and therefore I could deduce that less SL8 peptide was produced by MDSC (blue and red line, figure 5.3/B).

Despite their poor endocytic activities, MDSC were efficient at generating SL8 peptides. By doubling the number of MDSC, the B3Z response was largely improved and therefore the quantity of peptide produced increased (green line, figure 5.3/B). This showed

that the response generated by peptides extracted from 16% of 2 x 10^6 MDSC was as good as the response generated by peptides produced by 1 x 10^6 BM-DC.

These results demonstrated that MDSC were efficient in processing antigens despite a poor endocytic activity. However, because of their profound uptake deficiency, their overall efficacy was reduced compared to BM-DC.

5.2.1.3 – MDSC can present SL8 peptide to B3Z T cell in the context of MHC class I molecules

So far, I have shown that MDSC can uptake and process OVA to generate antigenic SL8 peptides. One important feature of APC is their ability to present antigenic peptides to T cells in the context of MHC molecules. The peptide extraction performed in the previous experiment was used as a way of quantitating the amount of peptide presented. Because these peptides were expected to come from MHC/peptide complexes, the amount of peptide extracted should be equivalent to the concentration of these complexes on the cell surface. I therefore examined the ability of MDSC to present SL8 peptides to B3Z T cells. BM-DC and MDSC purified from the spleen of TAZ10 $Rag^{+/+}$ mice were used as APC in a T cell activation assay (Figure 5.4/A). Briefly, MDSC and BM-DC co-cultured with B3Z T cells were incubated with synthetic SL8 peptides and the level of activation of B3Z cells measured 24 hours later.

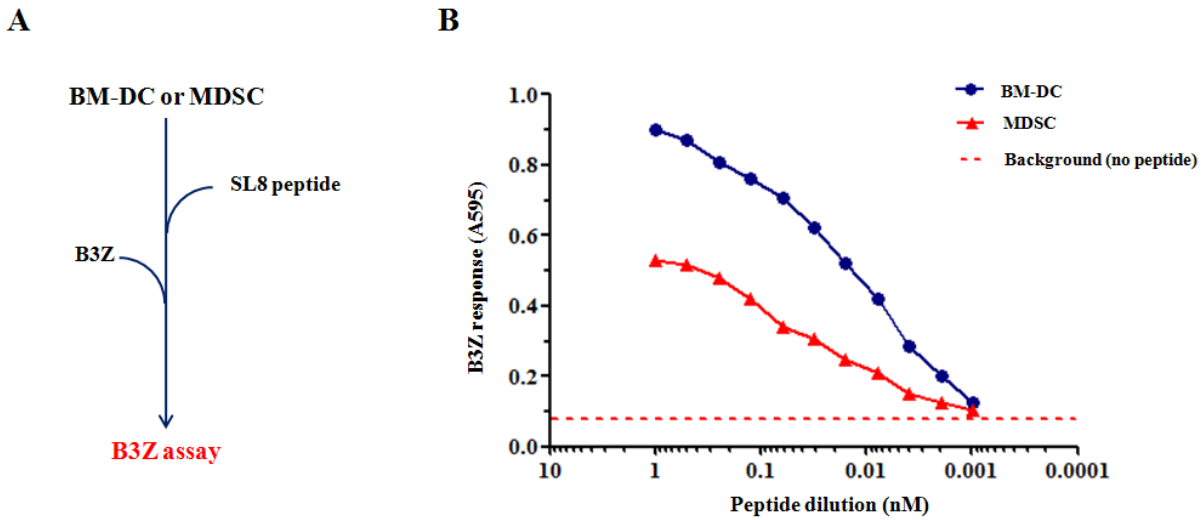

Figure 5.4: Gr1^{+} MDSC are not as efficient as BM-DC in presenting peptides to T cells in the context of MHC class I molecules

(A) BM-DC and purified Gr1^{+} MDSC from the spleen of TAZ10 Rag$^{+/+}$ were used as antigen presenting cells to present the SL8 peptide to B3Z T cells. **(B)** The presentation of the SL8 epitope to B3Z cells was assessed by measuring B3Z response through hydrolysis of the chromogenic substrate CPRG. Starting concentration of SL8 peptide was 1nM and serial dilution of 2 fold were performed. Data shown are representative of 3 different experiments.

A B3Z response was observed when both BM-DC (blue line, figure 5.4/B) and MDSC (red line, figure 5.4/B) were used as APC, suggesting that they were able to present SL8 peptide on their MHC-I molecules. Interestingly, the level of B3Z stimulation was much lower when MDSC were used as APC meaning that there were overall fewer SL8/H-2K^{b} complexes. These observations could be directly confirmed using 25D1 antibody that reacts with SL8 peptide bound to H-2K^{b} molecules as it would indicate whether the difference observed is due to a different concentration of SL8/H-2K^{b} complexes on the cell surface.

However, another potential explanation for this difference in the ability to present SL8 peptides to B3Z T cells could reside in the effect of MDSC on B3Z T cells. Indeed, the stimulation of B3Z could lead to the release of soluble factors which enhance the activity of MDSC subsequently leading to the inhibition of the B3Z response by MDSC. One mechanism by which MDSC inhibit T cell function is the release of NO, which in turn interferes with the IL-2R signalling pathway (Bronte et al. 2005). MDSC have also been shown to degrade L-arginine, effectively depleting this amino acid from the surrounding microenvironment. T cells deprived of L-arginine are arrested in G0-G1 phase of the cell

cycle and also display an impaired expression of CD3ζ chain (Rodriguez et al. 2004, Rodriguez et al. 2007). Both mechanisms could lead to the impairment of B3Z stimulation.

To exclude that the action of MDSC activated by soluble factors released during B3Z stimulation could inhibit B3Z T cells, I decided to use inhibitors of MDSC's activity. L-NMMA is an iNOS inhibitor while NOHA is an arginase inhibitor (Figure 5.5/A).

As described in Figure 5.5/B, the addition of these inhibitors in the culture did not have any effect on the B3Z response. It is therefore unlikely that the reduction in B3Z stimulation is due to the activity of MDSC. However, while the metabolism of L-arginine by iNOS and Arg-1 did not have any impact on the B3Z hybridoma in this assay, I could not rule out its physiological importance on the activation and function of T cells. In addition, I could not exclude the ability of MDSC to inhibit B3Z response resulting from a cell-cell (MDSC-B3Z) contact mechanism. A suitable experiment would be to assess the B3Z response when BM-DC or MDSC are used as APC separated by a transwell (preventing cell-cell contact) compared to normal culture conditions.

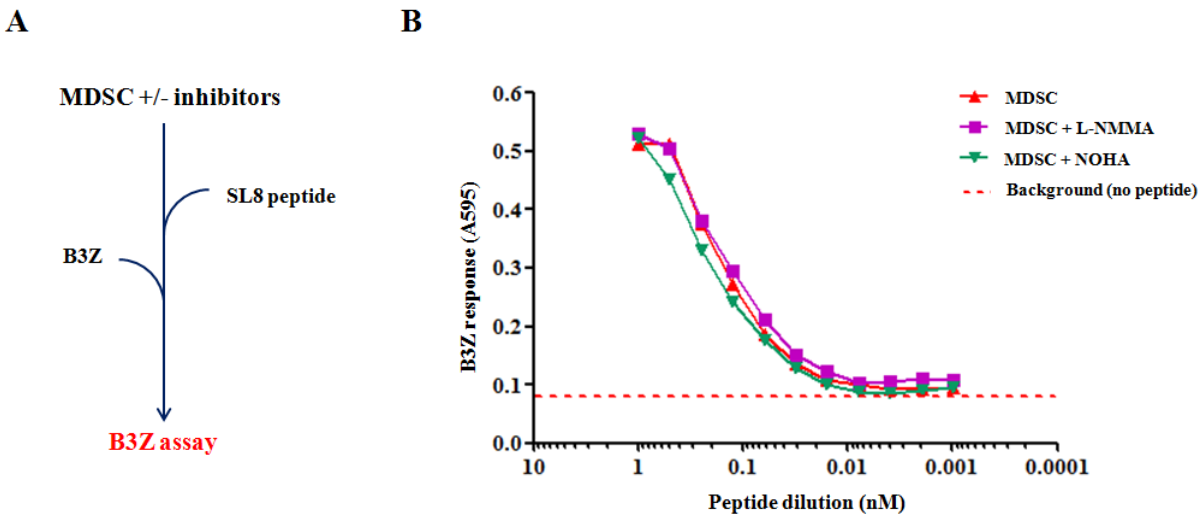

Figure 5.5: The inhibition of MDSC function does not improve B3Z response
(A) Purified $Gr1^{+}$ MDSC from the spleen of TAZ10 $Rag^{+/+}$ were used in T cell activation assay, as previously described in Figure 5.5 but in the presence of the iNOS inhibitor L-NMMA and Arg-1 inhibitor NOHA. **(B)** B3Z hybridoma response to SL8 peptide was assessed through CPRG colorimetric substrate readings. Data shown are representative of 2 different experiments.

Several other possibilities could also be considered to explain the difference observed. MDSC could express less H-2K^b molecules and therefore less SL8/H-2K^b complexes on their cell surface compared to BM-DC, resulting in a reduced B3Z stimulation. Therefore, MDSC would not be as efficient as BM-DC in presenting the immunodominant peptide to T cells. The level of expression of MHC-I molecules on MDSC will be investigated in Paragraph 5.2.2.1.

I have also previously shown that MDSC from TAZ10 Rag$^{+/+}$ mice had a decreased expression of the costimulatory molecules CD80/CD86 compared to BM-DC (Chapter 3 – Part 2). I could however exclude that the level of costimulation provided by MDSC was leading to a reduced ability to promote the stimulation of B3Z T cells as this T cell hybridoma does not require any costimulatory signalling.

5.2.2 – MDSC population is heterogenous for the expression of MHC class I molecules and display distinct presentation abilities

I have previously investigated the capacity of MDSC to uptake, process and present antigens in the context of MHC molecules. MDSC were highly efficient in processing antigens (Figure 5.3) but they had a reduced phagocytic ability compared to BM-DC (Figure 5.2) and were not as efficient in presenting peptides to T cells (Figure 5.4). I next investigated the efficiency of MDSC in presenting SL8 peptides to B3Z T cells as a result of the processing of exogenous OVA.

BM-DC and MDSC purified from the spleen of TAZ10 Rag$^{+/+}$ mice were pulsed for 8 hours with soluble OVA and used as APC in a T cell activation assay (Figure 5.6/A). In this assay, I assessed the ability of MDSC and BM-DC to uptake and process soluble OVA to generate the immunodominant SL8 peptides for its presentation to B3Z T cells.

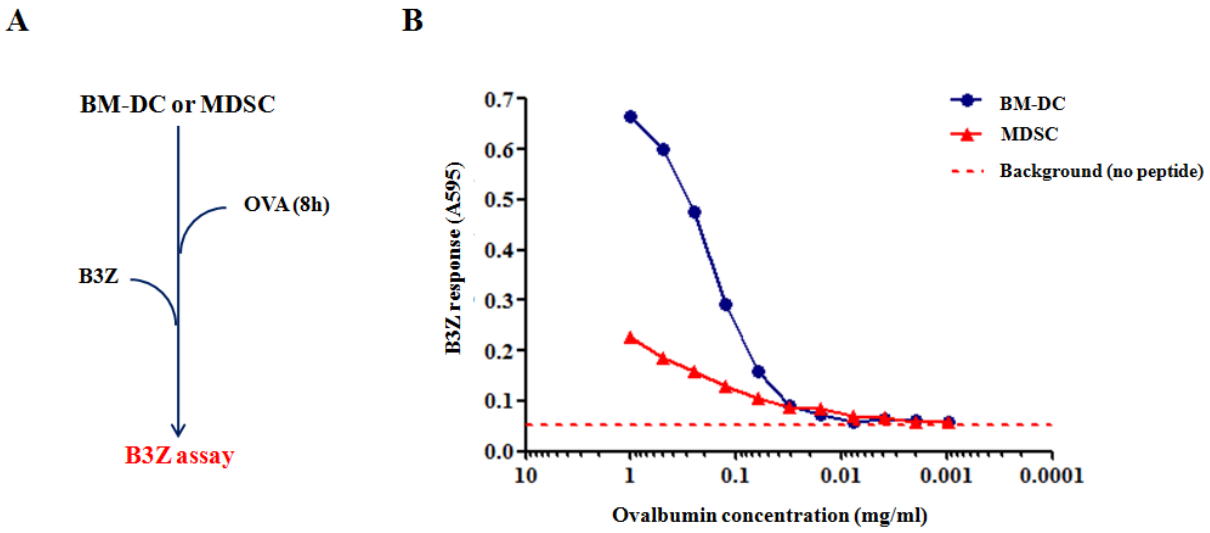

Figure 5.6: Gr1$^+$ MDSC can process and present exogenous antigens to T cells in the context of MHC class I molecules

(A) BM-DC and purified Gr1$^+$ MDSC from the spleen of TAZ10 Rag$^{+/+}$ were incubated for 8 hours with OVA and used directly as antigen presenting cells in T cell activation assay. **(B)** The ability of MDSC and BM-DC to process OVA and present SL8 peptides to B3Z T cell hybridoma was assessed by measuring B3Z activation through IL-2 induced β-gal activity. Data shown are representative of 3 separate experiments.

B3Z T cells were stimulated when both MDSC and BM-DC were used as APC. This meant that MDSC and BM-DC managed to uptake and cross-present OVA to express SL8/H-2K^b complexes at the cell surface (Figure 5.6/B). However, the level of B3Z activation was significantly higher when BM-DC were used (blue line, figure 5.6/B) compared to MDSC (red line, figure 5.6/B). When OVA was used at 1mg/ml, the B3Z response generated by BM-DC showed a three-fold increase.

While it is difficult to explain their uptake deficiency, we hypothesized that the limited ability of MDSC to present peptides compared to professional APC could be due to a lower expression of MHC-I molecules.

5.2.2.1 – Differential expression of MHC class I molecules by MDSC

Although MDSC presented SL8 peptides to B3Z T cells, their efficiency was decreased compared to BM-DC. To investigate whether this could be due to a low level of expression of MHC-I molecules, splenocytes from TAZ10 Rag$^{+/+}$ mice were stained for MDSC marker (Gr1 and CD11b) and the level of expression of H-2K^b molecules analysed (Figure 5.7).

I observed that MDSC did not have a uniform H-2K^{b} expression (Figure 5.7/A). Indeed, within the MDSC population, I could distinguish two distinct cell populations: one was positive for H-2K^{b} expression at an identical level of expression to CD11b^{+} cells (H-2K$^{b\ int}$) while the other displayed a lower expression of H-2K^{b} (H-2K$^{b\ low}$). Interestingly, the population having the lowest expression of H-2K^{b} molecules had the highest expression of Gr1 (Figure 5.7/A) and was associated with a higher granularity (High SSC) in comparison to the H-2K$^{b\ int}$/Gr1^{low} MDSC population (Figure 5.7/B). We know that, as they mature, MDSC downregulate the expression of Gr1 molecules so we hypothesized that this is associated with an increased expression of H-2K^{b} MHC-I molecules.

Overall, these results showed that MDSC have a heterogenous expression of MHC-I molecules. While one population of cells had a normal expression of H-2K^{b} molecules comparable to CD11b^{+} cells, the other displayed a much lower expression. This differential MHC expression level could have a crucial impact on the overall ability of MDSC to present peptides and thus explain the discrepancies observed in the ability of MDSC to present SL8 peptides to T cells.

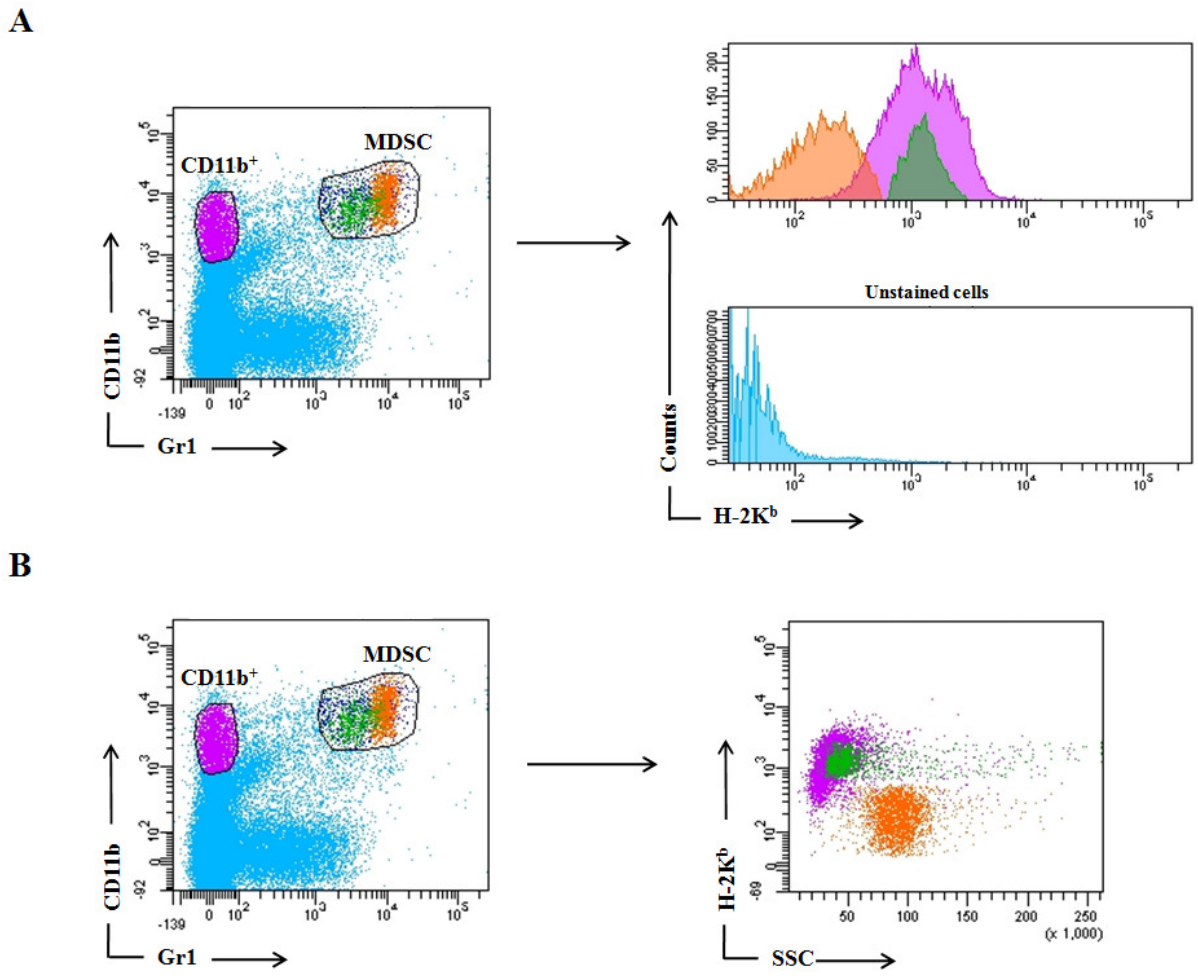

Figure 5.7: MDSC express different levels of MHC class I molecules
(A) Splenocytes from TAZ10 Rag$^{+/+}$ transgenic mice were stained for Gr1 and CD11b molecules. The gated MDSC population was then analysed for its expression of MHC-I molecules (H-2K^{b}). **(B)** SSC profile of the various populations was also analysed. CD11b^{+} cell population was used as a positive control for the expression of H-2K^{b}. Data shown are representative of 3 different experiments.

5.2.2.2 – The level of MHC class I molecules at the cell surface of MDSC dictates their ability to present peptides to T cells

Because MDSC presented a heterogeneous expression of H-2K^{b} molecules, I decided to investigate independently the ability of these two populations to present SL8 peptide to BZ3 T cells. Gr1^{+} cells from TAZ10 Rag$^{+/+}$ mice were sorted according to their level of expression of H-2K^{b} molecules, those expressing low or intermediate level of H-2K^{b} molecules were used as APC in the B3Z T cell activation assay and compared to the whole MDSC population and BM-DC (Figure 5.8/A).

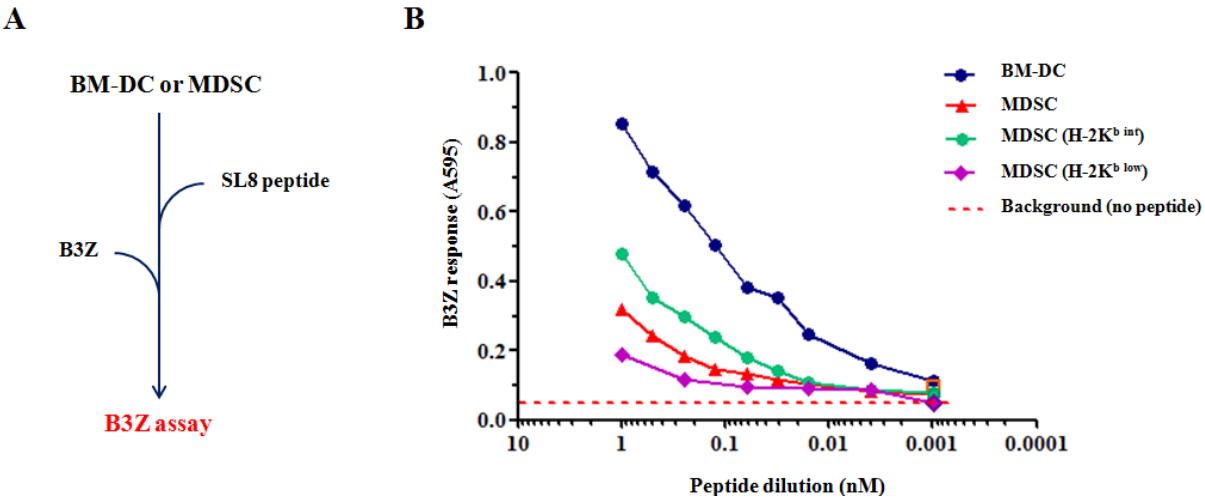

Figure 5.8: The ability of Gr1$^+$ MDSC to present peptides to T cells is highly dependent on their level of expression of MHC class I molecules

(A) Gr1$^+$ MDSC subsets from TAZ10 Rag$^{+/+}$ mice were sorted according to their level of expression of H-2K^b molecules. MDSC expressing either low or intermediate level of H-2K^b molecules (H-2K$^{b\ low}$ and H-2K$^{b\ int}$ respectively), BM-DC and purified Gr1$^+$ cells from TAZ10 Rag$^{+/+}$ mice, were used as antigen presenting cells to present the SL8 peptide to B3Z T cells. **(B)** The presentation of the SL8 peptide was assessed by measuring B3Z activation through hydrolysis of the chrmogenic substrate CPRG. Starting concentration of SL8 peptide was 1nM and two-fold serial dilutions were performed. Data shown are representative of two different experiments.

As previously described (Figure 5.4), the level of B3Z stimulation was lower when MDSC were used as APC, highlighting the fact that overall there were fewer SL8/H-2K^b complexes presented on their cell surface. Interestingly, this level of B3Z stimulation was dependent on the level of expression of H-2K^b molecules by MDSC. Indeed, MDSC expressing intermediate levels of MHC-I molecules generated a better activation of the B3Z hybridoma than H-2K$^{b\ low}$ MDSC. However, even with H-2K$^{b\ int}$, the B3Z response induced by MDSC was still about 2 fold lower than the B3Z response induced by BM-DC.

Overall, I could conclude that within the MDSC population, different subsets with different ability in presenting MHC-I restricted antigens could be distinguished on the basis of their level of expression of H-2K^b molecules. We could hypothesize that, while one subset expressing intermediate levels of H-2K^b molecules could be efficient in the presentation, those expressing low level of MHC-I molecules could be better at processing antigens. It could also be that one subset combines both antigen processing and presentation abilities while the other has no efficacy in any of these functions.

5.2.2.3 – The level of expression of MHC class I molecules is influenced by the inflammatory environment

I have previously described that the inflammatory environment present in TAZ10 mice has an effect on the accumulation of MDSC and is also associated with a gain of suppressive function (Figures 3.17 and 3.19). Indeed, I have shown that this inflammatory environment influenced the phenotype of MDSC as MDSC from TAZ10 mice expressed higher levels of CD11c, CD86 and MHC-II molecules compared to MDSC from WT mice (Figure 3.21). However, the pro-inflammatory cytokines IL-6 and IL-1β, present in the microenvironment of many tumours, significantly increase the rate of accumulation of MDSC while they dramatically enhance their suppressive activity on T cells (Bunt et al. 2006; Song et al. 2005).

In light of these previous observations, I decided to investigate the level of expression of MHC-I molecules (H-2K^b) of MDSC from TAZ10 and WT mice over time. Splenocytes from 2 and 6 months old TAZ10 and WT mice were analysed by flow cytometry for their expression of Gr1, CD11b and H-2K^b molecules (Figure 5.9).

As previously described in figure 5.7/A, the expression of MHC-I molecules was not homogenous within MDSC populations from both TAZ10 and WT mice. Two cell populations could again be distinguished: H-2K$^{b\ low}$ Gr1^{high} and H-2K$^{b\ int}$ Gr1^{low} MDSC. While the proportion of the different subsets of MDSC remained relatively stable over time in WT mice, a reduction in the number of MDSC in 6 months old TAZ10 mice was observed. Only 0.8% of those cells expressed low levels of H-2K^b molecules in 6 months old TAZ10 mice compared to 2.3% in 2 months old TAZ10 mice. Interestingly, we could also observe a substantial increase in the mean fluorescence intensity (MFI) of the CD11b$^+$ H-2K$^{b\ int}$ population of 2 months old compared to 6 months old mice highlighting the strong pro-inflammatory status of TAZ10 mice.

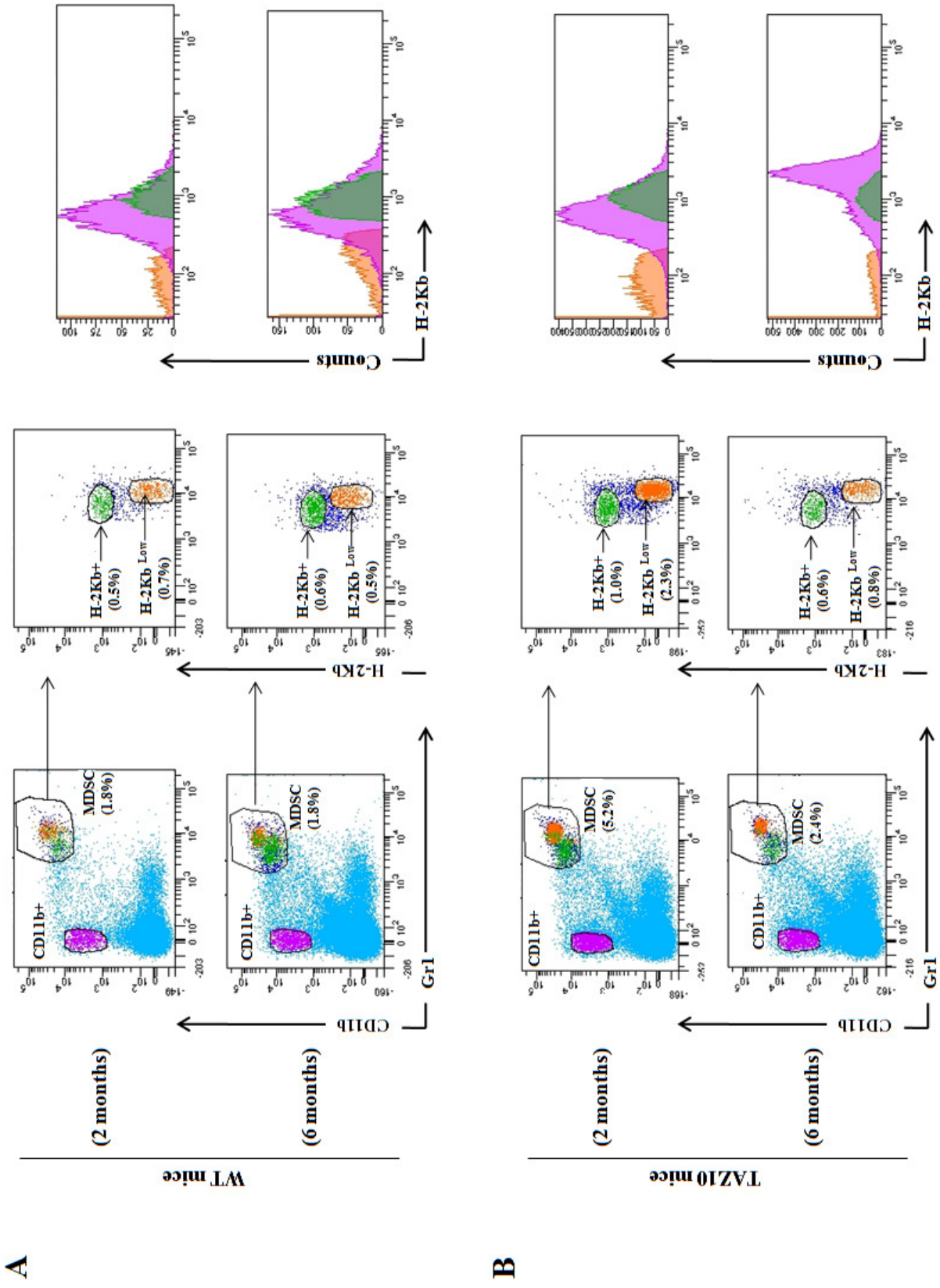

Figure 5.9: The level of expression of MHC class I molecules by MDSC is dependent on the inflammatory environment

Splenocytes from 2 and 6 months old WT and TAZ10 Rag$^{+/+}$ mice were stained for Gr1 and CD11b molecules. The Gr1^{+} CD11b^{+} MDSC and CD11b^{+} were further analysed for their expression of H-2K^{b} molecules. Data shown are representative of 3 different experiments.

These results suggest that the level of MHC-I expression of MDSC was associated with their differentiation/maturation state. When MDSC are differentiating, they can downregulate and/or lose the expression of Gr1 while upregulating the MHC-I expression (Figure 5.10). It has been shown that $Gr1^+$ $CD11b^+$ $F4/80^-$ MDSC can differentiate into tumour-associated macrophages and gain a $Gr1^-$ $CD11b^+$ $F4/80^+$ phenotype following their adoptive transfer into tumour-bearing mice (Kusmartsev et al. 2005). Also, high expression of Gr1 by MDSC correlates with high granularity and polymorphonuclear morphology while a lower Gr1 expression is associated with a lower granularity and a mononuclear profile (Movahedi et al. 2008).

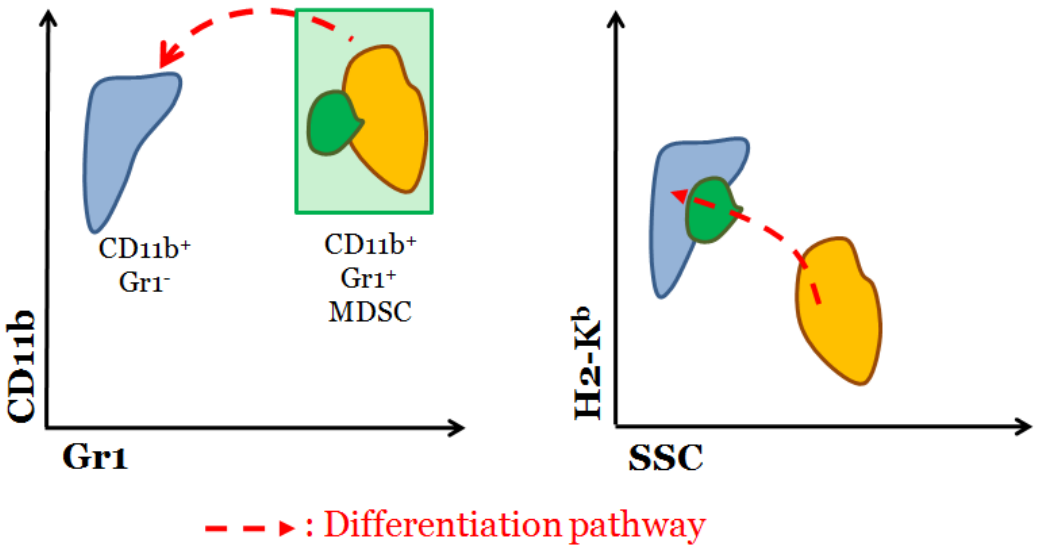

Figure 5.10: The level of MHC class I expression of MDSC is associated with their differentiation/maturation state
When $Gr1^+$ $CD11b^+$ MDSC start to differentiate, they lose the expression of Gr1 and display a lower granularity (SSC) while upregulating their expression of $H\text{-}2K^b$ MHC-I molecules.

5.2.3 – MDSC can endogenously process gp90 to generate GSW11 epitope

I have shown that MDSC can uptake and process OVA to present SL8 peptides in the context of MHC-I molecules. Because the initial aim was to investigate the role played by MDSC in the generation of tumour responses in the CT26 colon carcinoma model, I then decided to assess whether MDSC could process the endogenous gp90 protein and present the cross-protective epitope GSW11 in the context of MHC-I molecules.

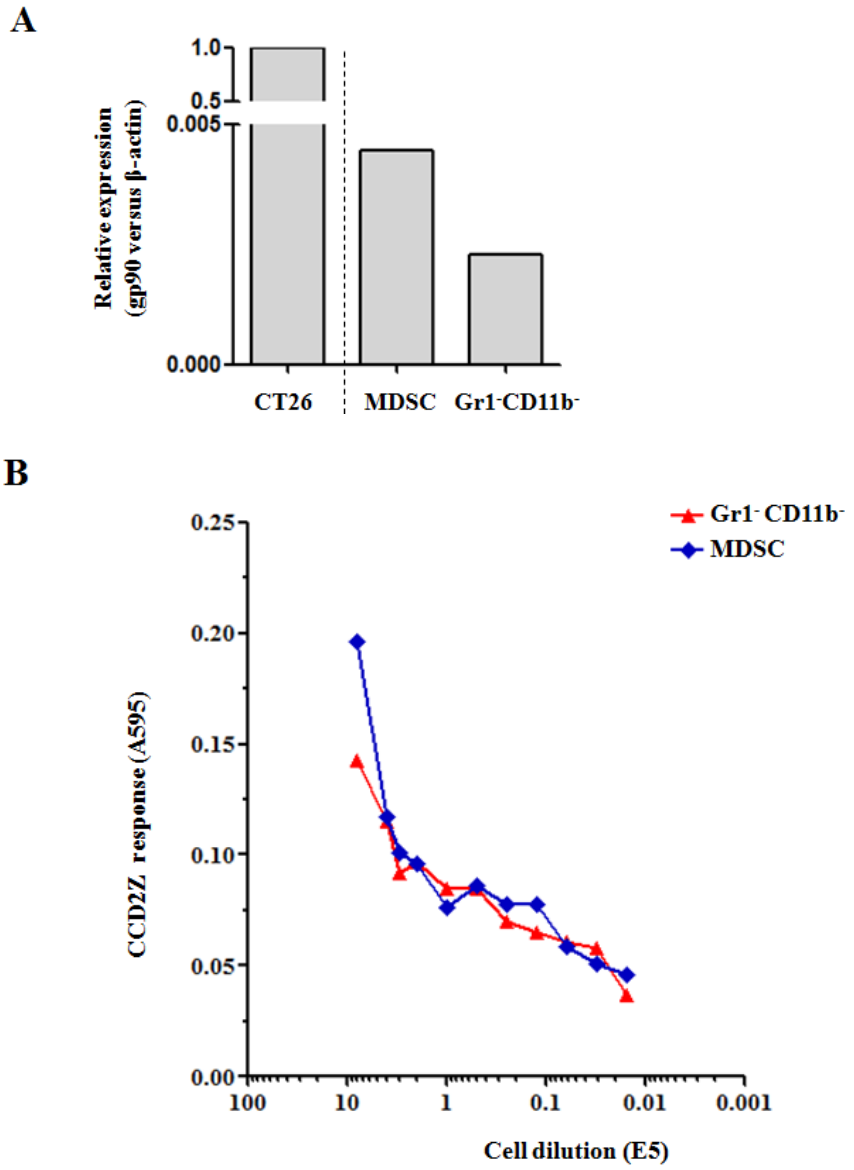

Figure 5.11: *Ex-vivo* Gr1$^+$ MDSC process gp90 protein to generate and present GSW11 peptides
(A) 1µg RNA extracted from CT26 cells, purified MDSC and Gr1$^-$CD11b$^-$ cells from the spleen of Balb/c mice was used to assess the level of expression of gp90 by semi-quantitative RT-PCR. Results were normalised against the housekeeping gene βactin. (B) The ability of MDSC and Gr1$^-$CD11b$^-$ cells to process gp90 and present GSW11 peptide to CCD2Z T cell hybridoma was assessed by measuring CCD2Z activation through IL-2 induced β-gal activity. Data shown are representative of 2 separate experiments.

I first investigated the level of expression of gp90 in MDSC. Total RNA was extracted from CT26 cells, MDSC and $Gr1^{-}CD11b^{-}$ cells purified from the spleen of Balb/c mice. The expression of gp90 was assessed by semi-quantitative RT-PCR and normalised against β-actin gene (Figure 5.11/A). While the level of expression of gp90 in CT26 tumour cells was very high, MDSC and $Gr1^{-}CD11b^{-}$ cells displayed a relatively low level of expression.
To investigate the endogenous processing of GSW11, MDSC and $Gr1^{-}CD11b^{-}$ cells purified from the spleen of Balb/c mice were used as APC in a T cell activation assay. Briefly, APC were incubated with a GSW11-specific T cell hybridoma (CCD2Z). Activation of CCD2Z cells was measured 24 hours later (Figure 5.11/B). A CCD2Z response was observed in all the various conditions meaning that $Gr1^{-}$ $CD11b^{-}$ and most importantly MDSC could process gp90 proteins to present the cross-protective epitope GSW11. Interestingly, although the expression of gp90 was slightly higher in MDSC, the level of stimulation of CCD2Z T cell hybridoma was similar compared to $Gr1^{-}CD11b^{-}$ cells. This reiterated the limited ability of MDSC to present peptides to T cells and could potentially be explained by the differential expression of MHC-I molecules we previously observed (Figure 5.7).

While I have described that MDSC could process OVA to generate and present SL8 peptides to T cells in the context of MHC-I molecules, I have also shown that MDSC were able to present the cross-protective tumour antigen GSW11 from the endogenous processing of gp90. This could suggest that MDSC could influence the generation of anti-tumour response in an antigen-dependent manner. I therefore decided to pursue the study and investigate the role played by MDSC in the generation of anti-tumour responses in the CT26 model.

5.3 – MDSC are critical in the initiation of anti-tumour responses in CT26 challenged mice

MDSC can mediate the suppression of tumour antigen-specific T cell response through the induction of T cell anergy. Indeed, MDSC have been shown to promote the induction of Tregs in tumour-bearing mice through the secretion of IL-10, TGFβ and NO (Huang et al. 2006) or by depleting L-arginine from the T cell microenvironment (Bronte et al. 2003). Moreover, they can achieve T cell tolerance through MHC-restricted presentation of antigen (Gabrilovich et al. 2001, Kusmartsev et al. 2005a) and by decreasing the binding of specific peptide: MHC complex to $CD8^+$ T cells (Nagaraj et al. 2007). Most importantly, MDSC can migrate to the tumour site where they induce the tolerance of antigen-specific T cell following the uptake, processing and presentation of tumour-associated antigens (TAA) (Kusmartsev et al. 2005a). I previously described that MDSC can endogenously process the gp90 protein to generate the cross-protective GSW11 epitope. I then decided to investigate whether MDSC would directly impact on the initiation of anti-tumour response.

5.3.1 – The removal of MDSC shortly before and after tumour challenge does not improve anti-tumour response

The potential impact of MDSC on anti-tumour responses in the CT26 mouse model was studied in the absence or presence of $Gr1^+$ cells under various experimental conditions (presence or absence of regulatory T cells). The first crucial step was to investigate the efficiency of the αGr1 antibody (clone RB6-8C5) in depleting $Gr1^+$ MDSC *in-vivo* and to confirm that the protocols for the subsequent *in-vivo* experiments were accurate. To this aim, Balb/c mice were injected intraperitoneally with αGr1 mAb 3 and 1 day prior to the considered day of CT26 challenge (day 0) and the proportion of $Gr1^+$ $CD11b^+$ MDSC in various tissues monitored daily over a period of 4 days (Figure 5.12/A).

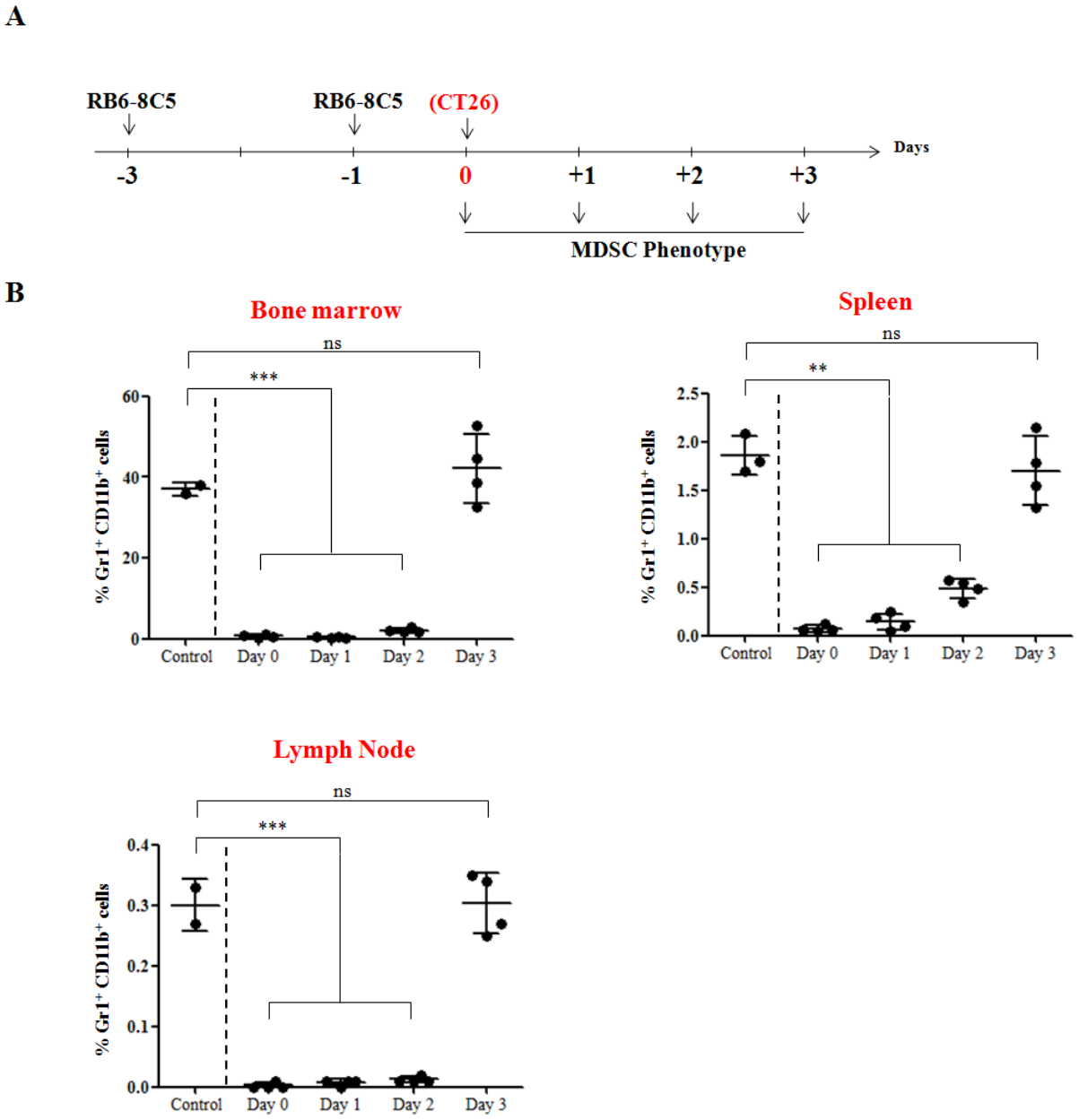

Figure 5.12: Treatment with αGr1 mAb allows the significant and lasting reduction of the number of $Gr1^+$ $CD11b^+$ cells in various tissues

(A) The αGr1 mAb (clone RB6-8C5) was administered to Balb/c mice intraperitoneally 3 and 1 day prior to the day mice would be challenged with CT26 tumour cells. The percentage of $Gr1^+$ $CD11b^+$ cells was then assessed daily by flow cytometry over a period of 4 days. **(B)** Cumulative results showing the percentage of $Gr1^+$ $CD11b^+$ cells in the bone marrow, the spleen and the lymph nodes of αGr1 treated Balb/c mice. Data shown are representative of three independent experiments. Statistics were performed using the unpaired Student's t-test.

I observed a significant reduction in the number of $Gr1^+$ $CD11b^+$ cells at day 0 (day when mice would have been challenged with CT26). Indeed, RB6-8C5 treatment decreased the proportion of $Gr1^+$ $CD11b^+$ cells from 36% to 0% in the bone marrow and from 2% to 0.1% in the spleen. The proportion of $Gr1^+$ $CD11b^+$ cells nearly reached 0% in all the studied

tissues of treated mice confirming that the antibody treatment efficiently promoted complete depletion of MDSC. This effect lasted for a further two days as the proportion of $Gr1^+$ $CD11b^+$ cells remained low. However, by day 3, the levels of MDSC in all the different tissues considered were restored back to control levels (Figure 5.12/B).

I was consequently confident that at the day of CT26 challenge, $Gr1^+$ cells were absent and remained absent for the first few days after tumour challenge when the anti-tumour immune response would be generated. The chosen experimental schedule therefore allowed the investigation of the role of $Gr1^+$ MDSC in the generation of anti-tumour responses.

It has long been described that MDSC are detrimental in anti-tumour immunity (Bronte et al. 1999; Gabrilovich et al. 2001; Melani et al. 2003) but the data only considered the role of MDSC once the tumour is already established i.e. a few weeks after tumour challenge. I therefore wanted to investigate whether MDSC displayed the same role and inhibitory functions at the onset of anti-tumour responses: Their depletion *in-vivo* would lift the suppression put on effector T cells thus promoting anti-tumour responses leading to tumour rejection.

To this aim, the impact of the *in-vivo* depletion of $Gr1^+$ cells shortly before or after tumour challenge on the ability of Balb/c mice to reject the tumour was studied. When the depletion is performed prior to the subcutaneous inoculation (D-3; D-1), MDSC are absent when the immune response is first primed by CT26 tumour antigens. On the contrary, if the depletion is carried out 1 and 3 days following CT26 challenge (D+1; D+3), MDSC are present at the generation of anti-tumour responses while absent the following days. Balb/c mice were administered αGr1 mAb (clone RB6-8C5) or αCD25 mAb (clone PC61) 1 and 3 days prior to CT26 challenge. A group of mice was left untreated while another received RB6-8C5 treatment 1 and 3 days after CT26 challenge. All mice were challenged with an equal number of CT26 tumour cells (1×10^5 cells) (Figure 5.13).

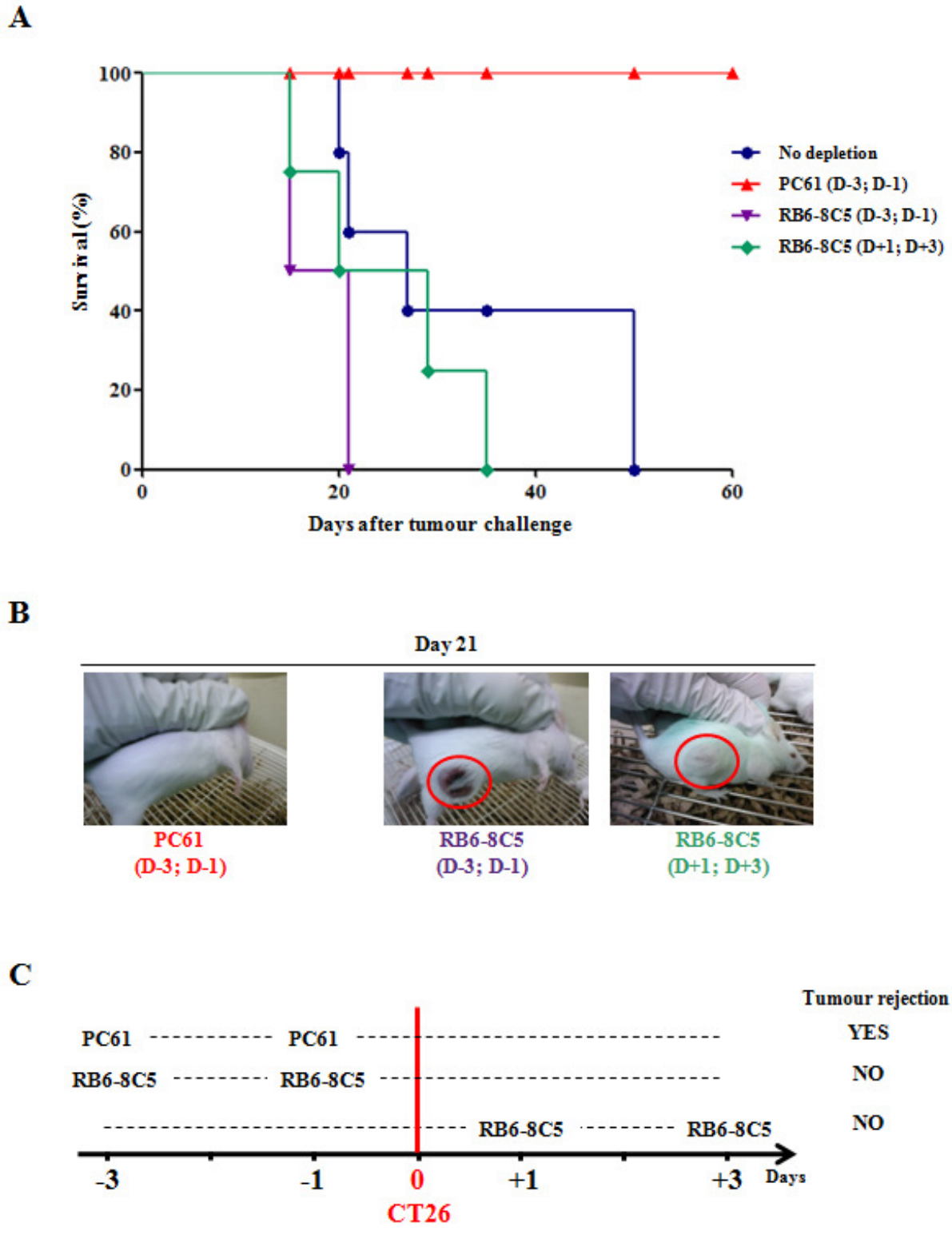

Figure 5.13: The depletion of Gr1$^+$ cells accelerates the death of CT26 challenged mice

(A) Balb/c mice were injected with αCD25 mAb (PC61, red line) or αGr1 mAb (RB6-8C5, purple line) 1 and 3 days prior (D-1; D-3) to subcutaneous inoculation of CT26 tumour cells. One group of mice was administered αGr1 mAb 1 and 3 days after CT26 challenge (D+1; D+3, green line). A control group of naive mice was also challenged with CT26 but did not receive any treatment (blue line). As the tumour reached end point, mice were culled and the overall survival monitored and recorded on a daily basis. **(B)** Pictures of αCD25 and αGr1 treated mice 21 days after CT26 challenge. **(C)** Schematic diagram representing the layout of the experiment and its outcome. Data shown are representative of two distinct experiments with 5 mice per group.

As previously reported, untreated challenged mice were unable to reject the tumour and died within 52 days after challenge (blue line, figure 5.13/A). The mice that had received the PC61 mAb and that had therefore been depleted in $CD25^+$ Tregs, survived the CT26 challenge and 100% of mice rejected the tumour (red line, figure 5.13/A). This is in line with previous observations showing that Tregs depletion of CT26 challenged mice allowed the generation of an efficient anti-tumour response (Golgher et al. 2002, James et al. 2010). Surprisingly and despite the fact that MDSC have been largely described as being detrimental in cancer, the groups of mice that were treated with RB6-8C5 mAb were unable to reject the CT26 tumour and died within 35 days, showing an even shorter survival rate than untreated CT26 challenged mice. Indeed, when $Gr1^+$ cells were depleted after CT26 challenge, all mice died within 35 days (green line, figure 5.13/A) while mice that had received the treatment before CT26 challenge all died within 21 days (purple line, Figure 5.13/A). While no tumour was visible in PC61 treated mice 21 days after CT26 challenge, RB6-8C5 treated mice had big tumour burdens at the site of CT26 challenge (Figure 5.13/B). Interestingly, mice that received RB6-8C5 treatment before CT26 challenge presented ulceration of the tumour, a sign of necrosis that could result from a lack of angiogenesis. This characteristic was not shared with the group of mice treated with RB6-8C5 mAb after tumour challenge.

These results showed that mice treated with RB6-8C5 could not mount an efficient anti-tumour response to reject the tumour whereas PC61 treated mice could (Figure 5.13/C). MDSC are therefore crucial at the onset of the generation of anti-tumour responses in the presence of Tregs as their removal at the time of challenge was detrimental. These observations also suggested that MDSC did not inhibit anti-tumour responses and therefore that their function at the onset of tumour immunity differed compared to when the tumour is established.

MDSC mediate their immunosuppressive activity in part via the induction of Tregs *in-vitro* and *in-vivo* in tumour-bearing mice (Huang et al. 2006; Serafini et al. 2008; Chapter 3). However, as $Gr1^+$ depleted mice were not immune to the tumour challenge in my experiments, I could hypothesize that these MDSC-induced Tregs did not have a strong impact on the inhibition of the anti-tumour response in the CT26 model.

5.3.2 – MDSC are crucial for the maintenance of the protective immune response generated after the *in-vivo* depletion/inhibition of Tregs

To further explore whether MDSC were beneficial at the onset of anti-tumour immunity, Balb/c mice were treated with αCD25 mAb (clone PC61) or a mix of αCD25-αGr1 mAbs (clones PC61 and RB6-8C5) 1 and 3 days prior to the CT26 subcutaneous challenge. A group of mice that did not receive any antibody treatement was used as control.

As observed in figure 5.14 (blue line), mice that did not receive any depleting treatment succumbed to the tumour and died within 30 days after tumour challenge. In comparison, six out of seven mice that had been depleted of Tregs were able to reject the tumour (red line, figure 5.14/A). Interestingly, mice that had been depleted of both Tregs and $Gr1^+$ MDSC could not reject the tumour and died within 28 days (orange line, figure 5.14/A). Pictures of mice from each group taken 21 days after CT26 challenge revealed that untreated and PC61/RB6-8C5 treated mice developed tumour burdens at the site of tumour challenge (Figure 5.14/B).

These results showed that the priming of an efficient anti-CT26 immune response required $Gr1^+$ MDSC as their removal abrogated the beneficial effect of PC61 therapy. They were indeed essential for the generation of the cross-protective immunity unravelled in the absence of Tregs (Figure 5.14/C).

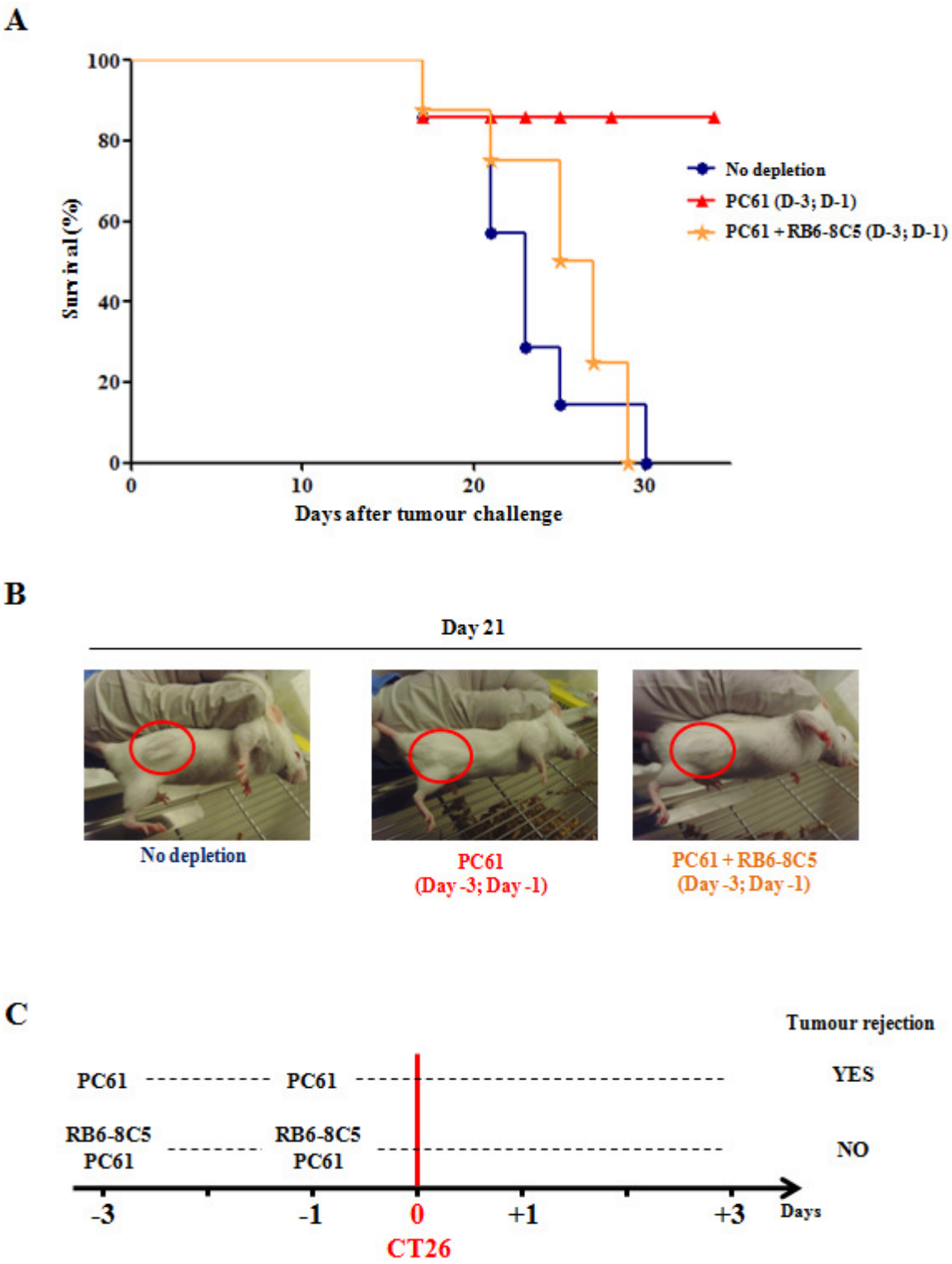

Figure 5.14: The removal of Gr1$^+$ cells abrogates the protective effect of the PC61 therapy

(A) Balb/c mice were administered αCD25 mAb (PC61, red line) or a mix of αCD25/αGr1 mAb (PC61 and RB6-8C5, orange line) 1 and 3 days prior to subcutaneous inoculation of CT26 tumour cells. A control group of naive mice did not receive any preliminary treatment but was challenged with CT26 tumour cells. The survival of mice was monitored and recorded daily over 35 days. **(B)** Pictures of untreated and αCD25, αGr1/αCD25 treated mice 21 days after CT26 challenge. Red circles indicate the site of the tumour burdens. **(C)** Schematic diagram representing the layout of the experiment and its outcome. Data are representative of two distinct experiments with 5 mice per group.

To further assess the impact of $Gr1^+$ MDSC on the generation of anti-CT26 tumour immune response upon the depletion of Tregs, I decided to investigate whether these observations would still be valid if the suppressive function of Treg was blocked *in-vivo* after tumour challenge rather than Tregs cells being depleted directly before tumour challenge. To this aim, I used an antibody that recognizes the glucocorticoid-induced TNF-receptor (GITR), a member of the TNF receptor superfamily. This molecule is expressed at high levels on Tregs and its ligation with a specific antibody has been shown to abrogate Tregs suppressive function *in-vivo* (Shimizu et al. 2002; Ji et al. 2004). Balb/c mice were injected with αCD25 mAb (clone PC61) 1 and 3 days prior to CT26 challenge while another group of mice was administered αGITR mAb (clone DTA.1) 1 and 3 days after CT26 challenge. An additional group received αGr1 mAb (clone RB6-8C5) 1 and 3 before CT26 challenge and αGITR mAb 1 and 3 days after this challenge. Finally, a group of mice that were only challenged with the tumour was used as a control.

Mice that did not receive any antibody treatment succumbed to the tumour within 30 days after CT26 challenge (dark blue line, figure 5.15/A) while PC61 treatment provided protection as all mice rejected the CT26 tumour (red line, figure 5.15/A). Interestingly, three out of four mice that had received αGITR mAb were able to reject the CT26 tumour (green line, figure 5.15/A). However, mice that had been depleted of $Gr1^+$ cells before receiving αGITR mAb had a poor survival rate as only one mouse was able to mount an efficient immune response and reject the CT26 tumour (pale blue line, figure 5.15/A).

These results confirmed previous observations where PC61 therapy conferred protection to CT26 challenged mice (Figures 5.13 and 5.14). Most importantly, treatment with aGITR mAb (DTA.1 therapy) provided a similar level of protection as PC61 treatment as only one mouse failed to reject the tumour (Figure 5.15/C). The abrogation of the suppression mediated by Tregs on T cells was therefore sufficient to the induction of an efficient anti-tumour immunity. Interestingly, these results also highlighted a potential "window of action" where the depletion/inhibition of Tregs could be performed after tumour challenge and still allow the generation of an efficient tumour response. It would be interesting to investigate the time scale where the generation of tumour immunity can be rescued by performing *in-vivo* inhibition of Tregs once the tumour is established.

A

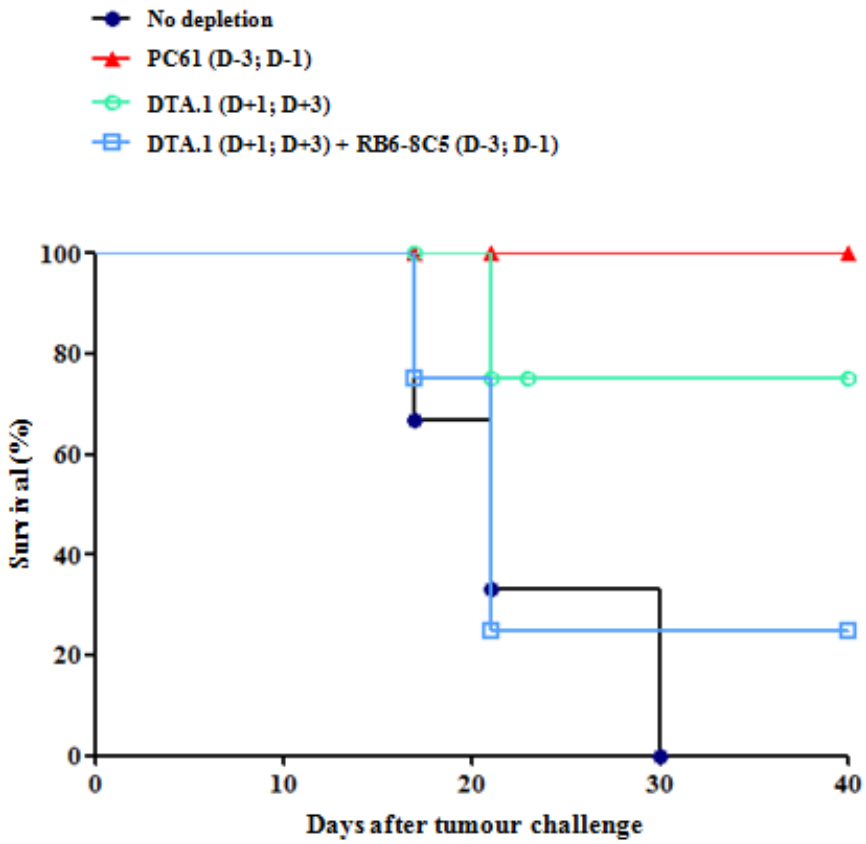

B

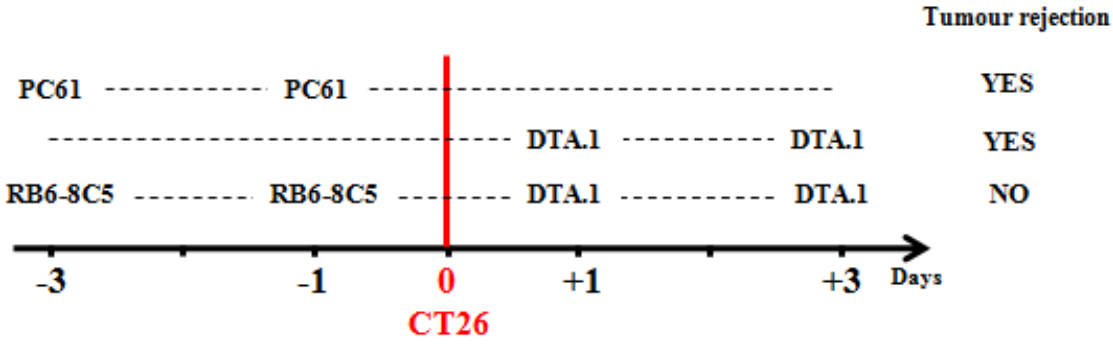

Figure 5.15: Treatment with αGITR mAb confers protection to CT26 challenged mice but its effect is abolished in the absence of Gr1$^+$ cells

(A) Balb/c mice were injected with αCD25 mAb (PC61, red line) 1 and 3 days prior to subcutaneous inoculation of CT26 tumour cells. One group of mice was administered αGITR mAb (DTA.1, green line) 1 and 3 days after CT26 challenge while an additional group received αGr1 mAb 1 and 3 days prior to CT26 inoculation and αGITR mAb 1 and 3 days after challenge (pale blue line). A control group of naive mice was also challenged with CT26 but did not receive any antibody treatment (blue line). As the tumour reached end point, mice were culled and the overall survival monitored and recorded daily. **(B)** Schematic diagram representing the layout of the experiment and its outcome. Data shown are representative of two distinct experiments with 4 mice per group.

This experiment reiterated the importance of $Gr1^+$ MDSC at the initiation of anti-tumour responses. Indeed, while mice treated with αGITR mAb developed a strong immune response to CT26 tumour cell in presence of $Gr1^+$ cells, this protective effect was abrogated by the use of RB6-8C5 mAb. MDSC were therefore crucial for the generation of the protective immunity.

Overall, all the previous results suggested that MDSC have an effect on anti-tumour responses and that they play a crucial role at their initiation.
In the absence of inflammation, MDSC are a heterogenous population of myeloid cells at various stages of differentiation that can give rise to monocytes/macrophages, granulocytes and dendritic cells. Some of these cells such as macrophages have a short half-life and their constant turnover means that the initial pool of cells needs to be frequently replenished. In the first few days after tumour challenge, the secretion of soluble factors by the tumour would still be insufficient to alter the ability of the immune system to generate an efficient anti-tumour response. MDSC can still naturally differentiate into immunostimulatory APC that are able to prime effector T cells in the lymph nodes draining the tumour site and promote anti-tumour responses. As a consequence, by depleting $Gr1^+$ MDSC, I would not only remove progenitors of cells of the myeloid origin but I would also prevent the replenishment of circulating/resident APC such as macrophages differentiating from MDSC. The removal of the suppressive activity on effector T cells promoted by the depletion of Tregs in absence of $Gr1^+$ cells is insufficient to efficiently prime effector T cells and promote tumour rejection. This shows that MDSC indirectly mediate the crucial priming of T cells, demonstrating their important role on the generation of anti-tumour responses.

5.3.3 – Simultaneous adoptive transfer of MDSC and tumour challenge does not promote a better immune response in CT26 challenged mice

I have previously investigated the potential use of MDSC *in-vivo* as a therapeutic tool to block the progression of AID in the TAZ10 mouse model of thyroiditis. Despite their strong inhibitory activity displayed *in-vitro* on T cells, MDSC could not prevent the development of the disease as they differentiated into immunostimulatory APC from the onset (Chapter 4.3) while the same phenomenom occurred when used as therapeutic agents

(Chapter 4.2). From these observations, I hypothesized that MDSC differentiating into immunostimulatory APC would favour the generation of anti-tumour responses. I therefore decided to investigate whether the AT of MDSC in CT26 challenged mice would promote tumour rejection and improve their survival. $Gr1^+$ MDSC were isolated from the spleen of naive or CT26 challenged mice and adoptively transferred into Balb/c mice at the day of CT26 inoculation (Figure 5.16/A).

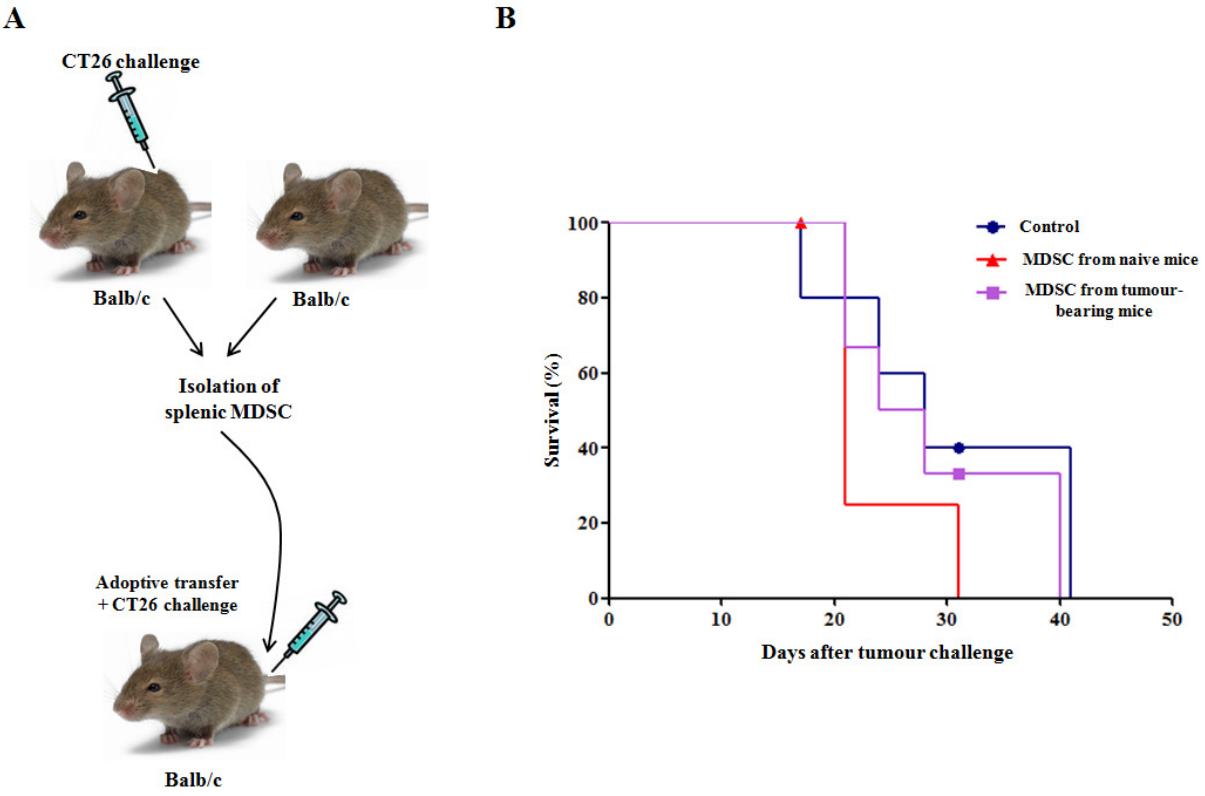

Figure 5.16: The adoptive transfer of $Gr1^+$ MDSC does not improve the survival of CT26 challenged mice
(A) Balb/c mice were challenged with CT26 tumour cells. 14 days after challenge, mice were culled and $Gr1^+$ cells were purified from the spleen. These cells, alongside $Gr1^+$ cells purified from naive Balb/c mice were adoptively transferred into Balb/c mice at the day of CT26 subcutaneous inoculation. **(B)** As the tumour size reached 15mm, mice were culled and their survival recorded on a daily basis. Data are representative of two experiments.

Balb/c mice inoculated with CT26 tumour cells all died 42 days after the challenge (blue line, figure 5.16/B). The groups of mice that had been adoptively transferred with MDSC from either naive mice (red line, figure 5.16/B) or tumour-bearing mice (purple line, figure 5.16/B) displayed a similar survival rate as mice died within 32 and 40 days respectively.

These results highlighted that the addition of $Gr1^+$ MDSC did not have an impact on the survival of CT26 challenged mice. Although MDSC have been shown to be crucial at the initiation of anti-tumour responses, they do not promote tumour rejection once the tumour is established. The impact of the tumour-derived factors on MDSC must be considered at this stage. As tumour grows, the secretion of several factors such as G-CSF, GM-CSF, IL-6, VEGF is increased and favours the accumulation of MDSC by promoting their recruitment while blocking their differentiation into APC (Gabrilovich et al. 1998; Bunt et al. 2007; Song et al. 2005). Upon activation by these different tumour-derived factors, MDSC display a strong inhibitory function on anti-CT26 responses promoting tumour growth. In this context, MDSC can also induce the generation of Tregs, which would in turn represent an additional suppression on effector T cells (Huang et al. 2006). Because tumours have a negative impact on MDSC by blocking their differentiation and promoting their activation, an adoptive transfer of MDSC at this stage is not beneficial to the generation of anti-tumour responses.

Overall, I have shown that MDSC are crucial at the initiation of anti-tumour responses. While still further work needs to be performed, we suggest that a "window of action" exists when the generation of efficient anti-tumour responses can be rescued as long as the tumour growth and consequent secretion of soluble factors do not have a detrimental impact on the immune response by promoting regulatory networks.

5.4 – Summary

I have previously shown that, despite their strong inhibitory activity displayed on T cell proliferation *in-vitro*, MDSC could not prevent the activation of self-reactive T cells and the occurence of autoimmune disease in TAZ10 mice. I described that from the onset of the disease, MDSC actually differentiate into immunostimulatory APC that promote the activation of self-reactive T cells and the inflammation (Chapter 4). While the role of MDSC has been extensively studied in tumour models when the tumour is already established, their role at the initiation of anti-tumour responses has never been adressed. Strong of the results I observed in TAZ10 mice, I decided to investigate the importance of MDSC in the first few days after tumour inoculation in the CT26 tumour model.

5.4.1 – MDSC can present endogenous antigen to $CD8^+$ T cells

Because, in the CT26 tumour model, tumour-specific T cell responses are restricted to the AH1 or GSW11 MHC-I restricted epitopes derived from the endogenous processing of gp70 and gp90 proteins respectively, I decided to assess whether MDSC could uptake, process and present antigens in the context of MHC-I molecules and therefore play a role in the initiation of anti-CT26 tumour responses. To this aim, I have used the widely known antigen presentation system using ovalbumin (OVA), which permitted the investigation of the ability of MDSC to cross-present OVA for the generation of the MHC-I restricted SL8 peptide.

Although MDSC were able to uptake exogenous OVA, their phagocytic ability was significantly reduced compared to professional APC as shown by the difference in the kinetic of internalization (Figure 5.2). The initial belief was that this limited efficiency would directly impact the ability of MDSC to process antigens. However, MDSC displayed a similar level of efficacy to BM-DC in processing OVA to produce the immunodominant SL8 peptide (Figure 5.3). Having demonstrated that MDSC could process exogenous antigens to generate immunogenic peptides, I then showed that they could present SL8 peptides to B3Z T cells in the context of MHC-I molecules (Figure 5.4). However, as the level of presentation

was significantly reduced when compared to the level of presentation achieved by BM-DC, several hypotheses were suggested to explain this discrepancy.

While I established that the inhibitory activity of MDSC was not responsible for the difference observed in the ability to present peptides (Figure 5.5), I showed that the level of expression of MHC-I molecules within MDSC population was heterogeneous. Indeed, two distinct populations could be distinguished (Figure 5.7). The first population displayed a low expression of MHC-I molecules, which was associated with a high expression of Gr1 and high granularity. By contrast, the second population expressed Gr1 at lower level and had a granularity and a level of expression of H-2K^b molecules comparable to any CD11b$^+$ macrophages. Interestingly, the level of expression of MHC-I molecules was dependent on the nature of the inflammatory environment, as more MDSC from 3 months old TAZ10 mice expressed an intermediate level of H-2K^b molecules (Figure 5.9). As a consequence, the inflammatory context also directly impacts on the ability of MDSC to present immunogenic peptides to T cells. MDSC expressing low level of H-2K^b molecules on their cell surface were less efficient in presenting SL8 peptides to B3Z T cells than MDSC expressing intermediate levels (Figure 5.8).

MDSC have been shown to be mobilised from hematopoietic sites (Gabrilovich et al. 2009) and driven by chemoattractant cytokines to invade the tumour microenvironment where they can uptake and present TAA to induce T cell anergy. Indeed, the ability of MDSC to capture and process antigens *in-vivo* has been shown in various tumour-bearing mice (Methylcholantrene-induced sarcoma and EL-4 lymphoma). MDSC can migrate to the tumour site where they uptake and present tumour-associated antigens (TAA) to promote the anergy of antigen-specific CD8$^+$ T cells (Kusmartsev et al. 2005a). Moreover in the A20 B cell lymphoma model, MDSC induced antigen-specific T cell tolerance through the cross-presentation of TAA and the expansion of pre-existing natural tumour-specific Tregs (Serafini et al. 2008).

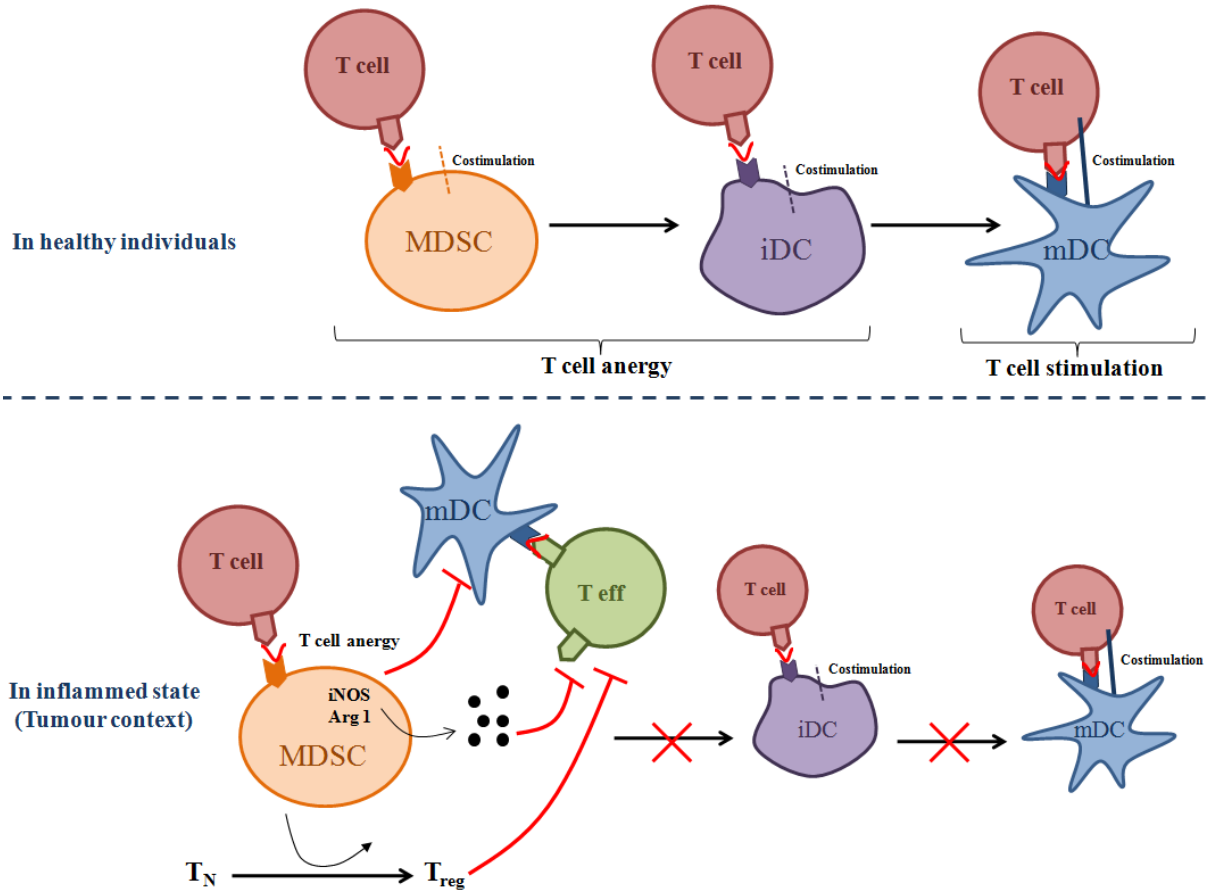

Figure 5.17: MDSC promote T cell tolerance by inducing T cell anergy and the generation of regulatory T cells

In steady state, MDSC and immature DC (iDC) induce T cell-anergy while mature DC (mDC) can promote T cell clonal expansion and differentiation. In a tumour environment, MDSC promote T cell tolerance by inducing T cell anergy through, for example an upregulation of Arg1 leading to L-arginine depletion from the microenvironment. They can also promote the differentiation of naive T cells (T_N) into regulatory T cells (Treg) and directly inhibit effector T cells (Teff) via the release of NO. Finally, MDSC can also suppress the activation of antigen-specific T cell activation by inhibiting the function of APC. The release of factors secreted by the tumour blocks the differentiation of MDSC into mature APC.

One interesting feature of the CT26 tumour model is that tumour-specific epitopes (AH1 and GSW11) are generated from the endogenous processing of gp70 and gp90 proteins. Therefore, the antigens shed while the tumour is growing are not crucial and would only have a minor impact at the initiation of anti-tumour responses. Because MDSC can endogenously process gp90 to generate the cross-protective epitope GSW11 (Figure 5.11), they could promote T cell tolerance through T cell anergy or induction of non-antigen specific regulatory T cells directly at the onset of anti-tumour responses (Figure 5.17). These observations therefore led to the hypothesis that the removal of MDSC would be beneficial to the generation of tumour immunity.

5.4.2 – MDSC are crucial at the initiation of anti-CT26 tumour responses

I therefore investigated the role played by MDSC in the generation of anti-tumour responses in the CT26 tumour model. Having demonstrated the efficiency of αGr1 mAb (clone RB6-8C5) in depleting $Gr1^+$ cells *in-vivo*, I first assessed the survival of CT26 challenged Balb/c mice in presence or absence of Tregs ($CD25^+$ cells) or MDSC ($Gr1^+$ cells).

As previously reported, mice that had been depleted of $CD25^+$ Tregs were able to reject the CT26 tumour (Figures 5.13, 5.14 and 5.15; Golgher et al. 2002). Indeed, the protective effect of PC61 therapy has been well documented. Because the removal of $CD25^+$ Tregs elicited autoimmunity and enhanced immune responses to non-self antigens such as allogeneic skin grafts (Sakagushi et al. 1995), it seemed likely that it could also break immunological unresponsiveness to tumour and actually provoke tumour immunity. Depletion of $CD25^+$ Tregs by PC61 treatment results in the generation of potent tumour-specific responses and the rejection of the tumour in Balb/c mice challenged with RL♂1 leukemia cells (Shimizu et al. 1999). It confers immunity to CT26 colon carcinoma as well as promoting the development of a long-lasting immunity since mice were able to reject a second challenge. A cross-protective immune response to other tumour cells of various histological origins is also generated (Golgher et al. 2002).

I have also described that treatment with agonistic αGITR antibody conferred protection to the mice (Figure 5.15). Indeed, similarly to PC61 treated mice, mice that had been injected with αGITR mAb were able to reject the tumour. GITR is a surface marker expressed at high levels on Tregs. Its ligation with a specific antibody abrogates the suppressive function of Tregs on effector T cells (Ji et al. 2004) and has been shown to induce effective tumour immunity in otherwise non-responding animals by enhancing tumour-killing activities of tumour-specific as well as non-specific effector cells (Shimizu et al. 1999, Ko et al. 2005). Our results demonstrated that the abolishment of Treg-mediated suppression was sufficient to promote the induction of anti-tumour responses and conferred protection to CT26 challenged mice. A complete removal of Tregs is therefore not necessary as long as their inhibitory function is abrogated. Interestingly, αGITR treatment performed up to 3 days after tumour challenge allowed the generation of the protective immunity. This highlights a potential "window of action" during which the generation of the anti-tumour response can still be rescued. Because PC61 do not only deplete Tregs but also effector T

cells, its use would be primarily limited to treatment before tumour challenge. In contrast, DTA.1 works after tumour challenge as it predominantly suppresses the function of Tregs *in-vivo*. Therefore, treatment with αGITR mAb is the most appropriate to investigate the time scale until which Tregs function needs to be abrogated to still promote the generation of an efficient immune response.

With regard to these results, the use of αGITR treatment as immunotherapy for cancer seems conceivable. However, this is not the only molecule related to regulatory T cells that could be targeted. The blockade of CTLA-4 has been shown to elicit autoimmunity and promote the generation of anti-tumour immunity *in-vivo*. Although the precise mechanism involved remains to be determined, it is likely to attenuate Treg-mediated suppression by blocking the activation of Tregs while enhancing the activity of effector T cells by preventing the binding of CTLA-4 and the generation of inhibitory signals altering the function of effector T cells (Takahashi et al. 2000). Combinations of αGITR mAb with antibodies specific for other members of TNF-TNFR family such as CD40, 4-1BB and OX40 could also prove to be an effective therapeutic strategy as they have been shown to enhance the activation of tumour-specific effector T cells (Sotomayor et al. 1999, Melero et al. 1997).

In contrast to mice that had been depleted of $CD25^+$ cells, mice depleted of $Gr1^+$ MDSC in the presence of Tregs were unable to mount an efficient immune response and succumbed to the tumour within days after tumour challenge (Figure 5.13). Most importantly, the removal of $Gr1^+$ cells abrogated the protective effect of both PC61 and DTA.1 therapies (Figures 5.14 and 5.15). Because MDSC promote T cell tolerance by inducing T cell anergy and the generation of Tregs from naive T cells, my initial belief was that their depletion would lift the suppression they exert on effector T cells thus promoting anti-tumour responses and tumour rejection. However, while this hypothesis is accurate when the tumour is established, the role of MDSC seemed to differ at the onset of anti-tumour responses i.e. within a few days after tumour inoculation. Indeed, these results showed that MDSC were crucial for the initiation of the protective anti-tumour responses unravelled in the absence of Tregs.

MDSC are cells of the myelomonocytic lineage that consist of myeloid progenitors and immature myeloid cells. In healthy individuals, MDSC, present in the bone marrow migrate to the secondary lymphoid organs where they differentiate into granulocytes, dendritic cells, macrophages and monocytes (Figure 5.18).

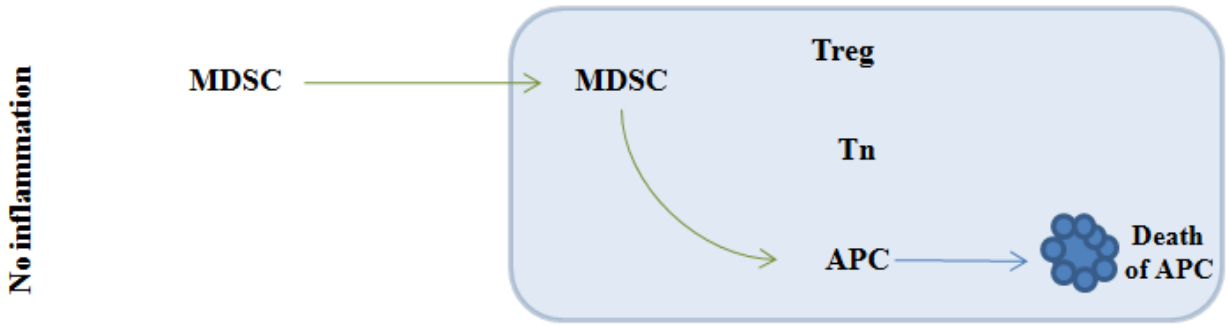

Figure 5.18: Under normal conditions, MDSC differentiate into APC such as dendritic cells or macrophages
MDSC is a heterogenous population of immature myeloid cells. They are generated in the bone marrow and then migrate to different peripheral organs where they differentiate into granulocytes, macrophages or dendritic cells. Because some of these cells have a short half-life, a constant turnover is necessary to assure the maintenance of the initial pool.

The ability of MDSC to differentiate into APC prompted the hypothesis that MDSC may play an indirect role on T cell priming. In the first few days after tumour challenge, when the level of inflammation is still moderate, MDSC naturally differentiate into APC that are able to prime AH1-specific effector T cells while inducing at the same time T cell anergy. The presentation of the AH1 epitope by APC can result from both the endogenous processing of the gp70 protein and the uptake and processing of necrotic CT26 cells. Nevertheless, the T cell priming is overcome by the suppression mediated by Tregs. Anti-tumour responses are therefore inhibited and the tumour allowed to grow, leading to the death of the mice (Figure 5.19/A).

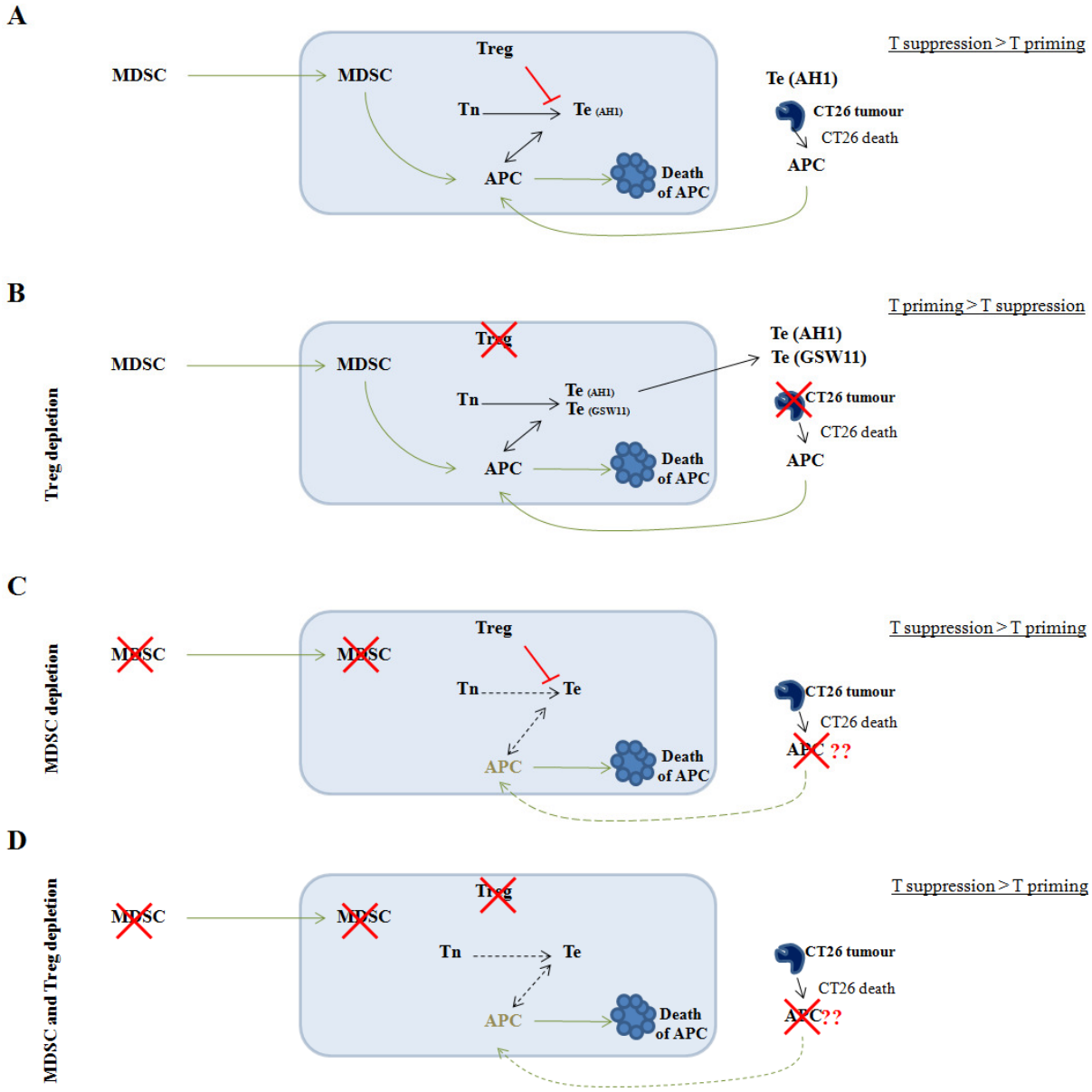

Figure 5.19: Summary of the role played by MDSC and Tregs in the generation of anti-tumour responses within a few days after tumour challenge

(A) In the presence of MDSC and Tregs, the priming of AH1-specific T cells, mediated in part through the differentiation of MDSC into APC, was unable to counteract the suppression mediated by Tregs, resulting in tumour growth. **(B)** In the absence of Tregs only, the tumour is eradicated by GSW11 and AH1 specific CTLs. **(C)** When $Gr1^+$ MDSC are depleted, the pool of APC is reduced and the priming of effector T cells is deficient. Therefore, the suppression mediated by Tregs overpowers this priming leading to tumour growth. **(D)** The lift of suppression on effector T cells induced by the absence of Tregs is not sufficient to promote tumour rejection. The priming of these effector T cells is reduced as MDSC are absent from the environment. Tn: Naive T cell; Te: Effector T cell; MDSC: Myeloid Derived Suppressor Cells; APC: Antigen Presenting Cells.

Interestingly, when the suppression mediated by Tregs is lifted by their *in-vivo* depletion or inhibition, tumour rejection is observed. T cell priming, still mediated in part by the differentiation of MDSC into APC, is no longer under suppression and effector T cells are

activated and able to eliminate tumour cells (Figure 5.19/B). CTLs responses observed in this case are both GSW11 and AH1-specific. Indeed, the response to the GSW11 epitope is only revealed in the absence of Tregs suggesting that GSW11-specific $CD8^+$ T cells are more sensitive to Treg suppression than AH1-specific $CD8^+$ T cell response. It has been described that GSW11-specific CTLs are actually more dependent on IL-2 for their activation and growth in culture than AH1-specific CTLs (James et al. 2010). As Tregs are well-known for their high consumption of IL-2 (Scheffold et al. 2005), this could explain why GSW11-specific responses are only revealed in the absence of Tregs.

The important role of MDSC at the initiation of anti-tumour responses really comes to light when tumour responses are studied in absence of $Gr1^+$ cells (Figures 5.19/C and 5.19/D). By depleting $Gr1^+$ cells, some progenitors of myeloid cells that can give rise to APC are removed. As a consequence, the pool of APC is decreased and the priming of effector T cells reduced. In these conditions, the Treg-mediated suppression is no longer an issue as both in the presence and absence of Tregs, mice could not reject the tumour. The key event is therefore the T cell priming that is mediated by APC coming from the naturally occurring differentiation of MDSC. Overall, these results taken together showed that MDSC play a crucial role in the initiation of anti-CT26 tumour responses by giving rise to APC that are key in promoting the priming of tumour-specific effector T cells.

Because MDSC differentiate into immunostimulatory APC at the onset of the disease in TAZ10 mice, I hypothesized that AT of MDSC in CT26 challenged mice would be beneficial as it would help promoting anti-tumour responses. However, the addition of $Gr1^+$ MDSC did not improve the survival of CT26 challenged mice (Figure 5.20).

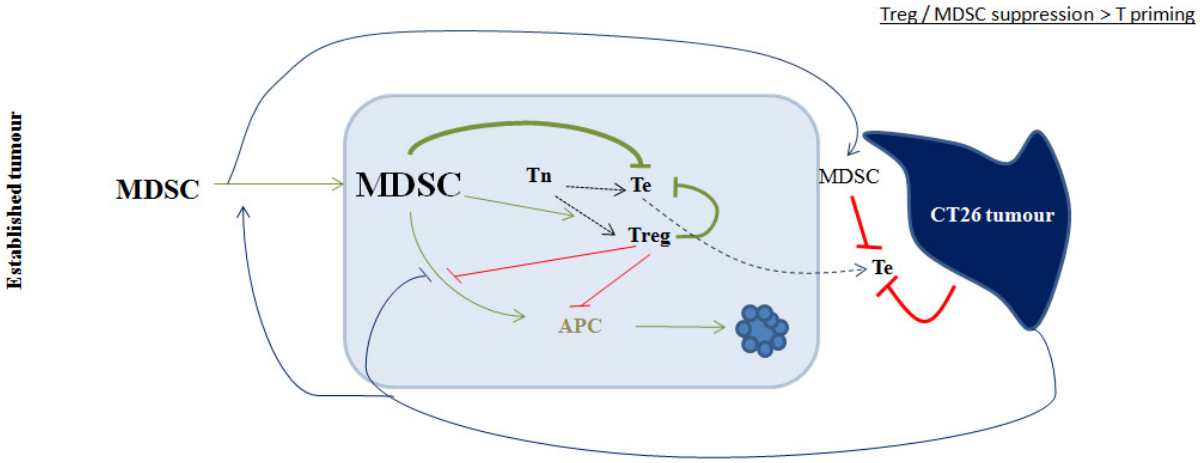

Figure 5.20: Once the tumour is established, MDSC become detrimental to tumour immunity
Factors that are produced in the tumour microenvironment promote the accumulation of MDSC, preventing their differentiation and inducing their activation. These cells exhibit immunosuppressive functions on effector T cells, promote the generation of Tregs, which in turn inhibit APC and put an additional suppression of effector T cells. All these conditions reunited favour the growth of the tumour.

While at the initiation of anti-tumour responses the factors secreted by the tumour are negligible, they play a major role on MDSC once the tumour is established. Those factors such as G-CSF, GM-CSF, IL-6, VEGF promote the accumulation of MDSC by favouring their recruitment while blocking their further differentiation into dendritic cells. As shown in the CT26 model (Figure 5.1), the subcutaneous inoculation of cancer cells has been shown to result in a profound expansion of splenic MDSC (Kusmartsev et al. 2005). MDSC are then activated and exhibit a strong suppressive activity on tumour-specific effector T cells. MDSC can also indirectly suppress antigen-specific T cell activation by inhibiting the function of APC. In this regard, a study has suggested the existence of a MDSC/macrophage cross-talk resulting in an increased IL-10 and decreased IL-12 production, thereby favouring tumour growth (Sinha et al. 2007). However, when studying MDSC, we must not neglect that they can give rise to immunostimulatory mature myeloid cells such as DC and macrophages that can have an important impact on the generation and the maintenance of a strong anti-tumour response. This ability to differentiate into immunostimulatory APC has been the target of tumours to evade the immune system by preventing MDSC from differentiating while favouring their accumulation. Moreover, the differentiation of MDSC into cell types with tumour-promoting effects can also be instigated. For example, they can be progenitors of

tumour-associated macrophages (TAMs) *in-vivo* which have been shown to inhibit T cell mediated immune response via the induction of T cell apoptosis (Kusmartsev et al. 2005).

As mentioned previously, MDSC mediate their immunosuppressive activity in part via the induction of Tregs. Indeed, $Gr1^+$ $CD115^+$ MDSC induced the development of $Foxp3^+$ Tregs in presence of IFNγ and IL-10 in tumour-bearing mice. Such induction also required the activation of tumour-specific T cells and was independent of NO (Huang et al. 2006). In a B cell lymphoma model (A20 cell-line), MDSC mediated the expansion of antigen-specific $Foxp3^+$ Tregs through arginase-1 activity while TGFβ was not required (Serafini et al. 2008). These *de-novo* induced Tregs put an additional suppression on effector T cells while they also have a negative impact on APC. Tregs directly inhibit the expression of MHC-II molecules and the secretion of proinflammatory cytokines (Onishi et al. 2008) while their secretion of IL-10 not only impact APC by maintaining them in an immature state but also inhibits the production of pro-inflammatory cytokines and expression of costimulatory factors required for the activation of NK cells (Tripp et al. 1993). Finally, Tregs controls DC/NK cross talk by preventing the DC exposure of IL-15Rα and interfering in the DC-mediated NK cell proliferation *in-vivo* (Terme et al. 2008).

While $Gr1^+$ MDSC are crucial at the initiation of anti-tumour responses, their presence in the tumour microenvironment, once the tumour is established, becomes detrimental. They can solely influence tumour immunity but their impact on different cell types present in this environment can dramatically affect the immune responses against the tumour.

6 - Summary

MDSC is a heterogenous population of cells of myelomonocytic lineage composed of myeloid progenitors and immature myeloid cells at various stages of differentiation that have the ability to differentiate into mature myeloid cells such as granulocytes, dendritic cells or macrophages depending on the microenvironment. Their physiological importance has been highlighted in recent studies showing that the replenishment of short-lived DC in lymphoid organs occurs from the differentiation of committed precursors (Geissman 2007). Contrary to the initial belief that DC are non-dividing cells (Kamath et al. 2000), about 5% of DC have a self-renewal ability and are in cell-cycle at any time (Kabashima et al. 2005). Their capacity to divide *in-situ* is however restricted to a limited number of divisions and the replenishment by blood-borne precursors migrating from the blood to peripheral tissues is crucial in order to maintain DC homeostasis. In this respect, it is estimated that about 71 precursors with short half-life enter the spleen from the blood every minute (Liu et al. 2007). Progenitors of the myelomonocytic lineage, MDSC play an important role in this replenishment and help to maintain the pool of APC. This was highlighted when the depletion of $Gr1^+$ MDSC prior to tumour challenge prevented the efficient priming of tumour-specific effector T cells (Chapter 5). It has been shown that the constant renewal of DC from progenitors is important in the establishment of immune surveillance as it allows the generation of an efficient adaptive immune response. Indeed, DC with a short self-renewal potential express a higher density of peptide/MHC (pMHC) complexes that favours the generation of effector $CD4^+$ T cells. By contrast, DC with increased self-renewal potential leading to a dilution in the level of expression of pMHC presented will favour the generation of Tregs (Kretschmer et al. 2005). This shows that the balance in lymphoid organs between the ability of MDSC to inhibit T cells and replenish the pool of APC with short half-life is crucial for the development and control of an efficient adaptive immune response.

The general aim of this work was to understand how MDSC fail to prevent and control the development of AID. This issue has been addressed using the humanised TAZ10 transgenic mouse model that spontaneously develops autoimmune thyroiditis (Quaratino et al. 2004).

T cells from TAZ10 transgenic mice express a human TCR specific for the cryptic epitope ($TPO_{524-535}$) generated upon endogenous processing of TPO by TEC and a naturally occurring antagonist peptide ($TPO_{525-536}$) presented by APC upon exogenous processing of TPO. DC uptaking dying TEC from the normal physiological turnover migrate to cervical

DLN where they present both the APL and the cryptic TPO epitopes. Mature DC (mDC) therefore allow for the anatomical spreading of TPO cryptic epitope from the thyroid to the DLN (Figure 6.1; **Point 1**). In WT mice, while MDSC naturally migrate from the blood to the DLN where they differentiate into APC, naive T cells are unable to recognise the cryptic epitope presented by mDC (Figure 6.1; **Point 2**). Thyroid specific T cells from TAZ10 mice recognise TPO cryptic epitope when presented by mDC in LN draining the thyroid. TAZ10-T_N cells are activated and proliferate within the first few days after AT in WT mice thus escaping the control of mechanisms of peripheral tolerance. While this activation promotes effector T cells, TPO specific regulatory T cells undergo antigen-induced cell death (AICD) upon encounter of the antagonist TPO epitope presented by mDC (Ester Badami's PhD Thesis – July 2007). Similarly to Tregs, I showed that MDSC could not control the activation of self-reactive TPO specific T cells. Indeed, the pro-inflammatory environment resulting from the sole activation of TAZ10-T_N favoured the differentiation of MDSC into immunostimulatory APC that would promote inflammation despite the increased ability of MDSC to inhibit T cell activation (Figure 6.1; **Point 3**).

Activated TPO specific $CD4^+$ T cells migrate to the thyroid and release cytokines such as IFNγ, TNFα and IL-1β that promote the death of TEC. Upon stimulation with inflammatory cytokines, TEC secrete nitric oxide and express Fas and FasL thus leading to their death by suicide or fratricide (Stassi et al. 2002; Olivier Cexus, 2009, University of Southampton - PhD thesis). While this study only focuses on $CD4^+$ T cells, $CD8^+$ T cells also recognise the TPO cryptic epitope in the context of MHC-II molecules and are therefore a key player in promoting the death of TEC (Quaratino et al. 2002)(Figure 6.1; **Points 4 and 5**).

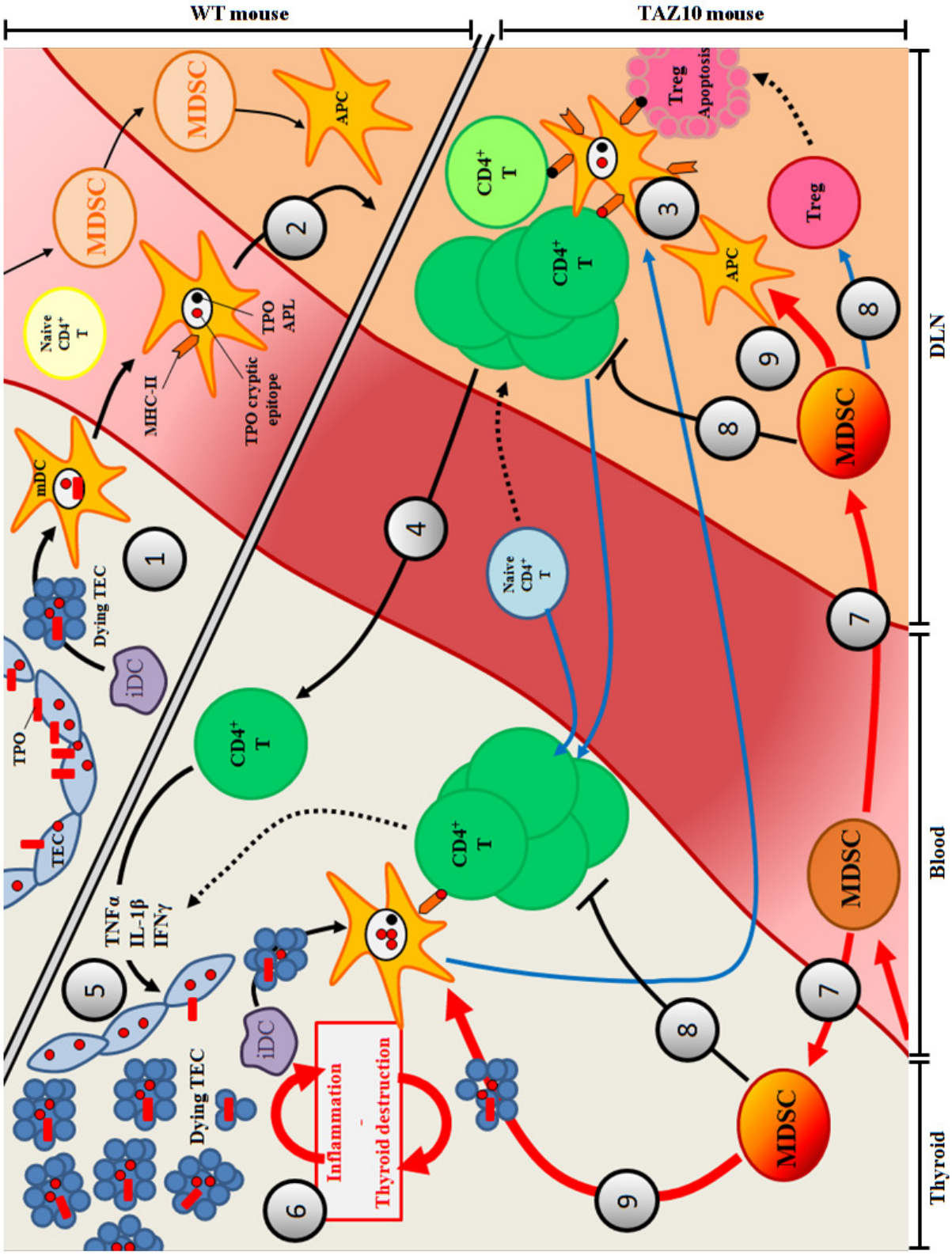

Figure 6.1: Suppressive Gr1$^+$ CD11b$^+$ MDSC fail to control the development of spontaneous autoimmunity in TAZ10 mice as they differentiate into immunostimulatory APC

Figure is detailed in the text of this chapter. **APC**: antigen presenting cells; **APL**: Altered peptide ligand; **DLN**: draining lymph nodes**; iDC**: Immature dendritic cells; **mDC**: mature dendritic cells; **MDSC**: myeloid derived suppressor cells; **TEC**: thyroid epithelial cells; **TPO**: thyroid peroxidase; **Treg**: regulatory T cells.

The increasing inflammation resulting from the release of pro-inflammatory cytokines and the death of TEC favours the recruitment of monocytic cells such as MDSC and lymphocytes. This leads to the amplification of the destruction of the thyroid and therefore of the inflammatory process (Figure 6.1; **Points 6**).

In parallel to the recruitment of transgenic T cells, the ongoing inflammation directly promotes the mobilization of MDSC in the blood from the bone marrow and their subsequent recruitment/accumulation to the thyroid and DLN (Figure 6.1; **Point 7**). As the inflammation is on-going, MDSC display stronger suppressive function on T cells mediated through the metabolism of L-arginine by iNOS and Arg-1 and the generation of Tregs (Figure 6.1; **Point 8**). Despite their gain of suppressive activity on T cells, MDSC cannot control the strong activation of self-reactive T cells as they differentiate into immunostimulatory APC that contribute to the exacerbation of autoimmune disease in TAZ10 mice. As MDSC and Tregs fail to prevent the progression of the disease, the inflammatory process further intensifies leading to an amplification of the naturally occurring differentiation of MDSC into immunostimulatory APC (Figure 6.1; **Point 9**)

From this study, a number of questions have emerged. Future work could investigate these questions as follow:

- I have shown that MDSC are recruited and differentiate into immunostimulatory APC at the onset of the disease in TAZ10 mice by performing adoptive transfers of MDSC from B6.eYFP mice into WT mice. The generation of bone marrow chimeric mice reconstituted with a mix of BM cells from B6.eYFP and TAZ10 mice would allow a more precise investigation of this process.

- I have suggested that the sole spontaneous activation of self-reactive T cells could be considered as a “Danger signal” promoting the recruitment and differentiation of MDSC at the onset of the disease. The adoptive transfer of varying numbers of TAZ10-T_N into WT mice would address the threshold of the number of T cells from which the inhibition provided by network of peripheral tolerance (such as MDSC and Tregs) becomes insufficient to control the activation of self-reactive T cells.

◆ Although I suggested that the activation of self-reactive T cells takes place in the DLN of TAZ10 mice, more work would be required to ascertain the impact of the sole activation of T cells on MDSC and exclude that initial T cell priming could also occur in the thyroid. To this aim, different strategies could be considered such as the use of Aly mice that do not have any LN, the drug FTY720 preventing the egress of lymphocytes from LN or the combination of αLFA.1 and αVLA.4 antibodies to prevent T cells from entering the thyroid.

◆ Considering the crucial role of MDSC at the initiation of anti-tumour responses and their contribution to the pathogenesis of the disease in TAZ10 mice through their differentiation into immunostimulatory APC, the impact of their depletion prior to the activation of self-reactive T cells at the onset of thyroiditis should be investigated.

7 - References

Afkarian, M., J. R. Sedy, et al. (2002). "T-bet is a STAT1-induced regulator of IL-12R expression in naive CD4+ T cells." Nat Immunol **3**(6): 549-57.

Akira, S., S. Uematsu, et al. (2006). "Pathogen recognition and innate immunity." Cell **124**(4): 783-801.

Alam, S. M., P. J. Travers, et al. (1996). "T-cell-receptor affinity and thymocyte positive selection." Nature **381**(6583): 616-20.

Allison, J. P. (1994). "CD28-B7 interactions in T-cell activation." Curr Opin Immunol **6**(3): 414-9.

Almand, B., J. I. Clark, et al. (2001). "Increased production of immature myeloid cells in cancer patients: a mechanism of immunosuppression in cancer." J Immunol **166**(1): 678-89.

Almand, B., J. R. Resser, et al. (2000). "Clinical significance of defective dendritic cell differentiation in cancer." Clin Cancer Res **6**(5): 1755-66.

Alterman, A. L., D. M. Fornabaio, et al. (1985). "Metastatic dissemination of B16 melanoma: pattern and sequence of metastasis." J Natl Cancer Inst **75**(4): 691-702.

Aly, T. A., A. Ide, et al. (2006). "Extreme genetic risk for type 1A diabetes." Proc Natl Acad Sci U S A **103**(38): 14074-9.

Anderson, H. A., D. T. Bergstralh, et al. (1999). "Phosphorylation of the invariant chain by protein kinase C regulates MHC class II trafficking to antigen-processing compartments." J Immunol **163**(10): 5435-43.

Anderson, M. S., E. S. Venanzi, et al. (2005). "The cellular mechanism of Aire control of T cell tolerance." Immunity **23**(2): 227-39.

Anderson, M. S., E. S. Venanzi, et al. (2002). "Projection of an immunological self shadow within the thymus by the aire protein." Science **298**(5597): 1395-401.

Anderton, S. M. and D. C. Wraith (2002). "Selection and fine-tuning of the autoimmune T-cell repertoire." Nat Rev Immunol **2**(7): 487-98.

Apetoh, L., F. Ghiringhelli, et al. (2007). "The interaction between HMGB1 and TLR4 dictates the outcome of anticancer chemotherapy and radiotherapy." Immunol Rev **220**: 47-59.

Banchereau, J., F. Briere, et al. (2000). "Immunobiology of dendritic cells." Annu Rev Immunol **18**: 767-811.

Banchereau, J. and R. M. Steinman (1998). "Dendritic cells and the control of immunity." Nature **392**(6673): 245-52.

Bangs, S. C., A. J. McMichael, et al. (2006). "Bystander T cell activation--implications for HIV infection and other diseases." Trends Immunol **27**(11): 518-24.

Bankovich, A. J., A. T. Girvin, et al. (2004). "Peptide register shifting within the MHC groove: theory becomes reality." Mol Immunol **40**(14-15): 1033-9.

Bartholomaus, I., N. Kawakami, et al. (2009). "Effector T cell interactions with meningeal vascular structures in nascent autoimmune CNS lesions." Nature **462**(7269): 94-8.

Battaglia, M., S. Gregori, et al. (2006). "Tr1 cells: from discovery to their clinical application." Semin Immunol **18**(2): 120-7.

Bettelli, E., Y. Carrier, et al. (2006). "Reciprocal developmental pathways for the generation of pathogenic effector TH17 and regulatory T cells." Nature **441**(7090): 235-8.

Betterle, C., N. A. Greggio, et al. (1998). "Clinical review 93: Autoimmune polyglandular syndrome type 1." J Clin Endocrinol Metab **83**(4): 1049-55.

Beutler, B. (2004). "Inferences, questions and possibilities in Toll-like receptor signalling." Nature **430**(6996): 257-63.

Bevan, M. J. (1976). "Cross-priming for a secondary cytotoxic response to minor H antigens with H-2 congenic cells which do not cross-react in the cytotoxic assay." J Exp Med **143**(5): 1283-8.

Bingisser, R. M., P. A. Tilbrook, et al. (1998). "Macrophage-derived nitric oxide regulates T cell activation via reversible disruption of the Jak3/STAT5 signaling pathway." J Immunol **160**(12): 5729-34.

Bliss, S. K., L. C. Gavrilescu, et al. (2001). "Neutrophil depletion during Toxoplasma gondii infection leads to impaired immunity and lethal systemic pathology." Infect Immun **69**(8): 4898-905.

Boehm, T., S. Scheu, et al. (2003). "Thymic medullary epithelial cell differentiation, thymocyte emigration, and the control of autoimmunity require lympho-epithelial cross talk via LTbetaR." J Exp Med **198**(5): 757-69.

Bonifaz, L., D. Bonnyay, et al. (2002). "Efficient targeting of protein antigen to the dendritic cell receptor DEC-205 in the steady state leads to antigen presentation on major histocompatibility complex class I products and peripheral CD8+ T cell tolerance." J Exp Med **196**(12): 1627-38.

Bronte, V., E. Apolloni, et al. (2000). "Identification of a CD11b(+)/Gr-1(+)/CD31(+) myeloid progenitor capable of activating or suppressing CD8(+) T cells." Blood **96**(12): 3838-46.

Bronte, V., D. B. Chappell, et al. (1999). "Unopposed production of granulocyte-macrophage colony-stimulating factor by tumors inhibits CD8+ T cell responses by dysregulating antigen-presenting cell maturation." J Immunol **162**(10): 5728-37.

Bronte, V., P. Serafini, et al. (2003). "IL-4-induced arginase 1 suppresses alloreactive T cells in tumor-bearing mice." J Immunol **170**(1): 270-8.

Bronte, V., M. Wang, et al. (1998). "Apoptotic death of CD8+ T lymphocytes after immunization: induction of a suppressive population of Mac-1+/Gr-1+ cells." J Immunol **161**(10): 5313-20.

Bronte, V. and P. Zanovello (2005). "Regulation of immune responses by L-arginine metabolism." Nat Rev Immunol **5**(8): 641-54.

Bunt, S. K., V. K. Clements, et al. (2009). "Inflammation enhances myeloid-derived suppressor cell cross-talk by signaling through Toll-like receptor 4." J Leukoc Biol **85**(6): 996-1004.

Bunt, S. K., P. Sinha, et al. (2006). "Inflammation induces myeloid-derived suppressor cells that facilitate tumor progression." J Immunol **176**(1): 284-90.

Bunt, S. K., L. Yang, et al. (2007). "Reduced inflammation in the tumor microenvironment delays the accumulation of myeloid-derived suppressor cells and limits tumor progression." Cancer Res **67**(20): 10019-26.

Burnet, F. M. (1961). "Immunological recognition of self." Science **133**: 307-11.

Burnet, F. M. (1976). "A modification of Jerne's theory of antibody production using the concept of clonal selection." CA Cancer J Clin **26**(2): 119-21.

Carrier, Y., J. Yuan, et al. (2007). "Th3 cells in peripheral tolerance. I. Induction of Foxp3-positive regulatory T cells by Th3 cells derived from TGF-beta T cell-transgenic mice." J Immunol **178**(1): 179-85.

Cavazzana-Calvo, M., S. Hacein-Bey, et al. (2000). "Gene therapy of human severe combined immunodeficiency (SCID)-X1 disease." Science **288**(5466): 669-72.

Chan, J. L., K. C. Tang, et al. (2006). "Antigen-presenting property of mesenchymal stem cells occurs during a narrow window at low levels of interferon-gamma." Blood **107**(12): 4817-24.

Chang, H. C., S. Sehra, et al. "The transcription factor PU.1 is required for the development of IL-9-producing T cells and allergic inflammation." Nat Immunol **11**(6): 527-34.

Chen, W., W. Jin, et al. (2003). "Conversion of peripheral CD4+CD25- naive T cells to CD4+CD25+ regulatory T cells by TGF-beta induction of transcription factor Foxp3." J Exp Med **198**(12): 1875-86.

Chin, R. K., J. C. Lo, et al. (2003). "Lymphotoxin pathway directs thymic Aire expression." Nat Immunol **4**(11): 1121-7.

Cresswell, P. (2005). "Antigen processing and presentation." Immunol Rev **207**: 5-7.

Curtsinger, J. M., D. C. Lins, et al. (2003). "Signal 3 determines tolerance versus full activation of naive CD8 T cells: dissociating proliferation and development of effector function." J Exp Med **197**(9): 1141-51.

Dani, A., A. Chaudhry, et al. (2004). "The pathway for MHCII-mediated presentation of endogenous proteins involves peptide transport to the endo-lysosomal compartment." J Cell Sci **117**(Pt 18): 4219-30.

Dardalhon, V., A. Awasthi, et al. (2008). "IL-4 inhibits TGF-beta-induced Foxp3+ T cells and, together with TGF-beta, generates IL-9+ IL-10+ Foxp3(-) effector T cells." Nat Immunol **9**(12): 1347-55.

De Santo, C., M. Salio, et al. (2008). "Invariant NKT cells reduce the immunosuppressive activity of influenza A virus-induced myeloid-derived suppressor cells in mice and humans." J Clin Invest.

Delano, M. J., P. O. Scumpia, et al. (2007). "MyD88-dependent expansion of an immature GR-1(+)CD11b(+) population induces T cell suppression and Th2 polarization in sepsis." J Exp Med **204**(6): 1463-74.

Derbinski, J., J. Gabler, et al. (2005). "Promiscuous gene expression in thymic epithelial cells is regulated at multiple levels." J Exp Med **202**(1): 33-45.

Dillon, S., A. Agrawal, et al. (2004). "A Toll-like receptor 2 ligand stimulates Th2 responses in vivo, via induction of extracellular signal-regulated kinase mitogen-activated protein kinase and c-Fos in dendritic cells." J Immunol **172**(8): 4733-43.

Dolcetti, L., I. Marigo, et al. (2008). "Myeloid-derived suppressor cell role in tumor-related inflammation." Cancer Lett **267**(2): 216-25.

Dong, C. (2006). "Diversification of T-helper-cell lineages: finding the family root of IL-17-producing cells." Nat Rev Immunol **6**(4): 329-33.

Doria, A., M. Canova, et al. (2008). "Infections as triggers and complications of systemic lupus erythematosus." Autoimmun Rev **8**(1): 24-8.

Dranoff, G., E. Jaffee, et al. (1993). "Vaccination with irradiated tumor cells engineered to secrete murine granulocyte-macrophage colony-stimulating factor stimulates potent, specific, and long-lasting anti-tumor immunity." Proc Natl Acad Sci U S A **90**(8): 3539-43.

Ehirchiou, D., Y. Xiong, et al. (2007). "CD11b facilitates the development of peripheral tolerance by suppressing Th17 differentiation." J Exp Med **204**(7): 1519-24.

Elias, K. M., A. Laurence, et al. (2008). "Retinoic acid inhibits Th17 polarization and enhances FoxP3 expression through a Stat-3/Stat-5 independent signaling pathway." Blood **111**(3): 1013-20.

Elliott, T. and A. Williams (2005). "The optimization of peptide cargo bound to MHC class I molecules by the peptide-loading complex." Immunol Rev **207**: 89-99.

Ernst, R. K., E. C. Yi, et al. (1999). "Specific lipopolysaccharide found in cystic fibrosis airway Pseudomonas aeruginosa." Science **286**(5444): 1561-5.

Faure-Andre, G., P. Vargas, et al. (2008). "Regulation of dendritic cell migration by CD74, the MHC class II-associated invariant chain." Science **322**(5908): 1705-10.

Fife, B. T. and J. A. Bluestone (2008). "Control of peripheral T-cell tolerance and autoimmunity via the CTLA-4 and PD-1 pathways." Immunol Rev **224**: 166-82.

Finlay, B. B. and G. McFadden (2006). "Anti-immunology: evasion of the host immune system by bacterial and viral pathogens." Cell **124**(4): 767-82.

Fischer, A. (2004). "Human primary immunodeficiency diseases: a perspective." Nat Immunol **5**(1): 23-30.

Fogg, D. K., C. Sibon, et al. (2006). "A clonogenic bone marrow progenitor specific for macrophages and dendritic cells." Science **311**(5757): 83-7.

Gabrilovich, D. (2004). "Mechanisms and functional significance of tumour-induced dendritic-cell defects." Nat Rev Immunol **4**(12): 941-52.

Gabrilovich, D., T. Ishida, et al. (1998). "Vascular endothelial growth factor inhibits the development of dendritic cells and dramatically affects the differentiation of multiple hematopoietic lineages in vivo." Blood **92**(11): 4150-66.

Gabrilovich, D. I. and S. Nagaraj (2009). "Myeloid-derived suppressor cells as regulators of the immune system." Nat Rev Immunol **9**(3): 162-74.

Gabrilovich, D. I., M. P. Velders, et al. (2001). "Mechanism of immune dysfunction in cancer mediated by immature Gr-1+ myeloid cells." J Immunol **166**(9): 5398-406.

Gaspar, H. B. and A. J. Thrasher (2005). "Gene therapy for severe combined immunodeficiencies." Expert Opin Biol Ther **5**(9): 1175-82.

Gautam, A. M., C. Pearson, et al. (1995). "Binding of an invariant-chain peptide, CLIP, to I-A major histocompatibility complex class II molecules." Proc Natl Acad Sci U S A **92**(1): 335-9.

Geissmann, F. (2007). "The origin of dendritic cells." Nat Immunol **8**(6): 558-60.

Germain, R. N. (2004). "An innately interesting decade of research in immunology." Nat Med **10**(12): 1307-20.

Ghiringhelli, F., P. E. Puig, et al. (2005). "Tumor cells convert immature myeloid dendritic cells into TGF-beta-secreting cells inducing CD4+CD25+ regulatory T cell proliferation." J Exp Med **202**(7): 919-29.

Golgher, D., E. Jones, et al. (2002). "Depletion of CD25+ regulatory cells uncovers immune responses to shared murine tumor rejection antigens." Eur J Immunol **32**(11): 3267-75.

Greenfield, E. A., K. A. Nguyen, et al. (1998). "CD28/B7 costimulation: a review." Crit Rev Immunol **18**(5): 389-418.

Greter, M., J. Hofmann, et al. (2009). "Neo-lymphoid aggregates in the adult liver can initiate potent cell-mediated immunity." PLoS Biol **7**(5): e1000109.

Guermonprez, P., L. Saveanu, et al. (2003). "ER-phagosome fusion defines an MHC class I cross-presentation compartment in dendritic cells." Nature **425**(6956): 397-402.

Guermonprez, P., J. Valladeau, et al. (2002). "Antigen presentation and T cell stimulation by dendritic cells." Annu Rev Immunol **20**: 621-67.

Hajjar, A. M., R. K. Ernst, et al. (2002). "Human Toll-like receptor 4 recognizes host-specific LPS modifications." Nat Immunol **3**(4): 354-9.

Hanson, E. M., V. K. Clements, et al. (2009). "Myeloid-derived suppressor cells down-regulate L-selectin expression on CD4+ and CD8+ T cells." J Immunol **183**(2): 937-44.

Harrington, L. E., R. D. Hatton, et al. (2005). "Interleukin 17-producing CD4+ effector T cells develop via a lineage distinct from the T helper type 1 and 2 lineages." Nat Immunol **6**(11): 1123-32.

Hartl, F. U. and M. Hayer-Hartl (2002). "Molecular chaperones in the cytosol: from nascent chain to folded protein." Science **295**(5561): 1852-8.

Heath, W. R. and F. R. Carbone (2001). "Cross-presentation in viral immunity and self-tolerance." Nat Rev Immunol **1**(2): 126-34.

Hirota, K., M. Hashimoto, et al. (2007). "T cell self-reactivity forms a cytokine milieu for spontaneous development of IL-17+ Th cells that cause autoimmune arthritis." J Exp Med **204**(1): 41-7.

Hogquist, K. A., T. A. Baldwin, et al. (2005). "Central tolerance: learning self-control in the thymus." Nat Rev Immunol **5**(10): 772-82.

Honey, K., K. Forbush, et al. (2004). "Effect of decreasing the affinity of the class II-associated invariant chain peptide on the MHC class II peptide repertoire in the presence or absence of H-2M." J Immunol **172**(7): 4142-50.

Hori, S., T. Nomura, et al. (2003). "Control of regulatory T cell development by the transcription factor Foxp3." Science **299**(5609): 1057-61.

Huang, A. Y., P. H. Gulden, et al. (1996). "The immunodominant major histocompatibility complex class I-restricted antigen of a murine colon tumor derives from an endogenous retroviral gene product." Proc Natl Acad Sci U S A **93**(18): 9730-5.

Huang, B., P. Y. Pan, et al. (2006). "Gr-1^{+}CD115^{+} immature myeloid suppressor cells mediate the development of tumor-induced T regulatory cells and T-cell anergy in tumor-bearing host." Cancer Res **66**(2): 1123-31.

Hugues, S., L. Fetler, et al. (2004). "Distinct T cell dynamics in lymph nodes during the induction of tolerance and immunity." Nat Immunol **5**(12): 1235-42.

James, E., A. Yeh, et al. (2010). "Differential suppression of tumor-specific CD8^{+} T cells by regulatory T cells." J Immunol **185**(9): 5048-55.

Janeway, C. A., Jr. and R. Medzhitov (2002). "Innate immune recognition." Annu Rev Immunol **20**: 197-216.

Jerne, N. K. (1955). "The Natural-Selection Theory of Antibody Formation." Proc Natl Acad Sci U S A **41**(11): 849-57.

Ji, H. B., G. Liao, et al. (2004). "Cutting edge: the natural ligand for glucocorticoid-induced TNF receptor-related protein abrogates regulatory T cell suppression." J Immunol **172**(10): 5823-7.

Kabashima, K., T. A. Banks, et al. (2005). "Intrinsic lymphotoxin-beta receptor requirement for homeostasis of lymphoid tissue dendritic cells." Immunity **22**(4): 439-50.

Kalinski, P., C. M. Hilkens, et al. (1999). "T-cell priming by type-1 and type-2 polarized dendritic cells: the concept of a third signal." Immunol Today **20**(12): 561-7.

Kamath, A. T., J. Pooley, et al. (2000). "The development, maturation, and turnover rate of mouse spleen dendritic cell populations." J Immunol **165**(12): 6762-70.

Kapsenberg, M. L. (2003). "Dendritic-cell control of pathogen-driven T-cell polarization." Nat Rev Immunol **3**(12): 984-93.

Kawai, T. and S. Akira (2005). "Pathogen recognition with Toll-like receptors." Curr Opin Immunol **17**(4): 338-44.

Kawai, T. and S. Akira (2010). "The role of pattern-recognition receptors in innate immunity: update on Toll-like receptors." Nat Immunol **11**(5): 373-84.

Kerr, E. C., B. J. Raveney, et al. (2008). "Analysis of retinal cellular infiltrate in experimental autoimmune uveoretinitis reveals multiple regulatory cell populations." J Autoimmun **31**(4): 354-61.

Kersh, G. J. and P. M. Allen (1996). "Structural basis for T cell recognition of altered peptide ligands: a single T cell receptor can productively recognize a large continuum of related ligands." J Exp Med **184**(4): 1259-68.

Kim, I., W. Xu, et al. (2008). "Cell death and endoplasmic reticulum stress: disease relevance and therapeutic opportunities." Nat Rev Drug Discov **7**(12): 1013-30.

King, I. L., T. L. Dickendesher, et al. (2009). "Circulating Ly-6C$^+$ myeloid precursors migrate to the CNS and play a pathogenic role during autoimmune demyelinating disease." Blood **113**(14): 3190-7.

Klein, L., M. Hinterberger, et al. (2009). "Antigen presentation in the thymus for positive selection and central tolerance induction." Nat Rev Immunol **9**(12): 833-44.

Ko, H. J., Y. J. Kim, et al. (2007). "A combination of chemoimmunotherapies can efficiently break self-tolerance and induce antitumor immunity in a tolerogenic murine tumor model." Cancer Res **67**(15): 7477-86.

Ko, K., S. Yamazaki, et al. (2005). "Treatment of advanced tumors with agonistic anti-GITR mAb and its effects on tumor-infiltrating Foxp3+CD25+CD4+ regulatory T cells." J Exp Med **202**(7): 885-91.

Kong, Y. C., J. C. Flynn, et al. (2003). "HLA and H2 class II transgenic mouse models to study susceptibility and protection in autoimmune thyroid disease." Autoimmunity **36**(6-7): 397-404.

Korn, T., M. Mitsdoerffer, et al. (2008). "IL-6 controls Th17 immunity in vivo by inhibiting the conversion of conventional T cells into Foxp3+ regulatory T cells." Proc Natl Acad Sci U S A **105**(47): 18460-5.

Korn, T., M. Oukka, et al. (2007). "Th17 cells: effector T cells with inflammatory properties." Semin Immunol **19**(6): 362-71.

Kovacsovics-Bankowski, M. and K. L. Rock (1995). "A phagosome-to-cytosol pathway for exogenous antigens presented on MHC class I molecules." Science **267**(5195): 243-6.

Kretschmer, K., I. Apostolou, et al. (2005). "Inducing and expanding regulatory T cell populations by foreign antigen." Nat Immunol **6**(12): 1219-27.

Kroenke, M. A., T. J. Carlson, et al. (2008). "IL-12- and IL-23-modulated T cells induce distinct types of EAE based on histology, CNS chemokine profile, and response to cytokine inhibition." J Exp Med **205**(7): 1535-41.

Kurts, C. (2000). "Cross-presentation: inducing CD8 T cell immunity and tolerance." J Mol Med **78**(6): 326-32.

Kusmartsev, S., F. Cheng, et al. (2003). "All-trans-retinoic acid eliminates immature myeloid cells from tumor-bearing mice and improves the effect of vaccination." Cancer Res **63**(15): 4441-9.

Kusmartsev, S. and D. I. Gabrilovich (2002). "Immature myeloid cells and cancer-associated immune suppression." Cancer Immunol Immunother **51**(6): 293-8.

Kusmartsev, S. and D. I. Gabrilovich (2003a). "Inhibition of myeloid cell differentiation in cancer: the role of reactive oxygen species." J Leukoc Biol **74**(2): 186-96.

Kusmartsev, S. and D. I. Gabrilovich (2005). "STAT1 signaling regulates tumor-associated macrophage-mediated T cell deletion." J Immunol **174**(8): 4880-91.

Kusmartsev, S., S. Nagaraj, et al. (2005a). "Tumor-associated CD8+ T cell tolerance induced by bone marrow-derived immature myeloid cells." J Immunol **175**(7): 4583-92.

Kusmartsev, S. A., Y. Li, et al. (2000). "Gr-1+ myeloid cells derived from tumor-bearing mice inhibit primary T cell activation induced through CD3/CD28 costimulation." J Immunol **165**(2): 779-85.

Kyewski, B. and J. Derbinski (2004). "Self-representation in the thymus: an extended view." Nat Rev Immunol **4**(9): 688-98.

Kyewski, B. and L. Klein (2006). "A central role for central tolerance." Annu Rev Immunol **24**: 571-606.

Ladi, E., X. Yin, et al. (2006). "Thymic microenvironments for T cell differentiation and selection." Nat Immunol **7**(4): 338-43.

Lang, H. L., H. Jacobsen, et al. (2002). "A functional and structural basis for TCR cross-reactivity in multiple sclerosis." Nat Immunol **3**(10): 940-3.

Lanier, L. L. and J. C. Sun (2009). "Do the terms innate and adaptive immunity create conceptual barriers?" Nat Rev Immunol **9**(5): 302-3.

Lanzavecchia, A. (1995). "How can cryptic epitopes trigger autoimmunity?" J Exp Med **181**(6): 1945-8.

Li, H., Y. Han, et al. (2009). "Cancer-expanded myeloid-derived suppressor cells induce anergy of NK cells through membrane-bound TGF-beta 1." J Immunol **182**(1): 240-9.

Liao, J. J., M. C. Huang, et al. (2007). "Cutting edge: Alternative signaling of Th17 cell development by sphingosine 1-phosphate." J Immunol **178**(9): 5425-8.

Liu, C., S. Yu, et al. (2007). "Expansion of spleen myeloid suppressor cells represses NK cell cytotoxicity in tumor-bearing host." Blood **109**(10): 4336-42.

Liu, K., C. Waskow, et al. (2007a). "Origin of dendritic cells in peripheral lymphoid organs of mice." Nat Immunol **8**(6): 578-83.

Lovitch, S. B., S. J. Petzold, et al. (2003). "Cutting edge: H-2DM is responsible for the large differences in presentation among peptides selected by I-Ak during antigen processing." J Immunol **171**(5): 2183-6.

Luger, D., P. B. Silver, et al. (2008). "Either a Th17 or a Th1 effector response can drive autoimmunity: conditions of disease induction affect dominant effector category." J Exp Med **205**(4): 799-810.

Luo, X., K. V. Tarbell, et al. (2007). "Dendritic cells with TGF-beta1 differentiate naive CD4+CD25- T cells into islet-protective Foxp3+ regulatory T cells." Proc Natl Acad Sci U S A **104**(8): 2821-6.

Lutz, M. B., N. Kukutsch, et al. (1999). "An advanced culture method for generating large quantities of highly pure dendritic cells from mouse bone marrow." J Immunol Methods **223**(1): 77-92.

Makarenkova, V. P., V. Bansal, et al. (2006). "CD11b+/Gr-1+ myeloid suppressor cells cause T cell dysfunction after traumatic stress." J Immunol **176**(4): 2085-94.

Marhaba, R., M. Vitacolonna, et al. (2007). "The importance of myeloid-derived suppressor cells in the regulation of autoimmune effector cells by a chronic contact eczema." J Immunol **179**(8): 5071-81.

Marigo, I., L. Dolcetti, et al. (2008). "Tumor-induced tolerance and immune suppression by myeloid derived suppressor cells." Immunol Rev **222**: 162-79.

Markiewski, M. M., R. A. DeAngelis, et al. (2008). "Modulation of the antitumor immune response by complement." Nat Immunol **9**(11): 1225-35.

Marks, D. J., M. W. Harbord, et al. (2006). "Defective acute inflammation in Crohn's disease: a clinical investigation." Lancet **367**(9511): 668-78.

Matloubian, M., C. G. Lo, et al. (2004). "Lymphocyte egress from thymus and peripheral lymphoid organs is dependent on S1P receptor 1." Nature **427**(6972): 355-60.

Matzinger, P. (2001). "Essay 1: the Danger model in its historical context." Scand J Immunol **54**(1-2): 4-9.

Matzinger, P. (2002). "The danger model: a renewed sense of self." Science **296**(5566): 301-5.

Matzinger, P. (2007). "Friendly and dangerous signals: is the tissue in control?" Nat Immunol **8**(1): 11-3.

Mauri, C., C. Q. Chu, et al. (1997). "Treatment of a newly established transgenic model of chronic arthritis with nondepleting anti-CD4 monoclonal antibody." J Immunol **159**(10): 5032-41.

Mazzoni, A., V. Bronte, et al. (2002). "Myeloid suppressor lines inhibit T cell responses by an NO-dependent mechanism." J Immunol **168**(2): 689-95.

McGeachy, M. J., K. S. Bak-Jensen, et al. (2007). "TGF-beta and IL-6 drive the production of IL-17 and IL-10 by T cells and restrain T(H)-17 cell-mediated pathology." Nat Immunol **8**(12): 1390-7.

Melani, C., C. Chiodoni, et al. (2003). "Myeloid cell expansion elicited by the progression of spontaneous mammary carcinomas in c-erbB-2 transgenic BALB/c mice suppresses immune reactivity." Blood **102**(6): 2138-45.

Melero, I., W. W. Shuford, et al. (1997). "Monoclonal antibodies against the 4-1BB T-cell activation molecule eradicate established tumors." Nat Med **3**(6): 682-5.

Merkenschlager, M., M. O. Power, et al. (1999). "Intrathymic deletion of MHC class I-restricted cytotoxic T cell precursors by constitutive cross-presentation of exogenous antigen." Eur J Immunol **29**(5): 1477-86.

Mirza, N., M. Fishman, et al. (2006). "All-trans-retinoic acid improves differentiation of myeloid cells and immune response in cancer patients." Cancer Res **66**(18): 9299-307.

Miyawaki, S., Y. Nakamura, et al. (1994). "A new mutation, aly, that induces a generalized lack of lymph nodes accompanied by immunodeficiency in mice." Eur J Immunol **24**(2): 429-34.

Mohammed, F., M. Cobbold, et al. (2008). "Phosphorylation-dependent interaction between antigenic peptides and MHC class I: a molecular basis for the presentation of transformed self." Nat Immunol **9**(11): 1236-43.

Morales, J. K., M. Kmieciak, et al. (2009). "Adoptive transfer of HER2/neu-specific T cells expanded with alternating gamma chain cytokines mediate tumor regression when combined with the depletion of myeloid-derived suppressor cells." Cancer Immunol Immunother **58**(6): 941-53.

Movahedi, K., M. Guilliams, et al. (2008). "Identification of discrete tumor-induced myeloid-derived suppressor cell subpopulations with distinct T cell-suppressive activity." Blood **111**(8): 4233-44.

Mucida, D., Y. Park, et al. (2007). "Reciprocal TH17 and regulatory T cell differentiation mediated by retinoic acid." Science **317**(5835): 256-60.

Mueller, D. L. and M. K. Jenkins (1995). "Molecular mechanisms underlying functional T-cell unresponsiveness." Curr Opin Immunol **7**(3): 375-81.

Murphy, E., K. Shibuya, et al. (1996). "Reversibility of T helper 1 and 2 populations is lost after long-term stimulation." J Exp Med **183**(3): 901-13.

Murphy, K. M. and S. L. Reiner (2002). "The lineage decisions of helper T cells." Nat Rev Immunol **2**(12): 933-44.

Nabors, G. S., L. C. Afonso, et al. (1995). "Switch from a type 2 to a type 1 T helper cell response and cure of established Leishmania major infection in mice is induced by combined therapy with interleukin 12 and Pentostam." Proc Natl Acad Sci U S A **92**(8): 3142-6.

Nagaraj, S., K. Gupta, et al. (2007). "Altered recognition of antigen is a mechanism of CD8+ T cell tolerance in cancer." Nat Med **13**(7): 828-35.

Nausch, N., I. E. Galani, et al. (2008). "Mononuclear myeloid-derived "suppressor" cells express RAE-1 and activate natural killer cells." Blood **112**(10): 4080-9.

Nefedova, Y., M. Fishman, et al. (2007). "Mechanism of all-trans retinoic acid effect on tumor-associated myeloid-derived suppressor cells." Cancer Res **67**(22): 11021-8.

Nefedova, Y., M. Huang, et al. (2004). "Hyperactivation of STAT3 is involved in abnormal differentiation of dendritic cells in cancer." J Immunol **172**(1): 464-74.

Netea, M. G., M. van Deuren, et al. (2002). "Does the shape of lipid A determine the interaction of LPS with Toll-like receptors?" Trends Immunol **23**(3): 135-9.

Ng, H. P., J. P. Banga, et al. (2004). "Development of a murine model of autoimmune thyroiditis induced with homologous mouse thyroid peroxidase." Endocrinology **145**(2): 809-16.

O'Garra, A. (1998). "Cytokines induce the development of functionally heterogeneous T helper cell subsets." Immunity **8**(3): 275-83.

Ogura, H., M. Murakami, et al. (2008). "Interleukin-17 promotes autoimmunity by triggering a positive-feedback loop via interleukin-6 induction." Immunity **29**(4): 628-36.

Onishi, Y., Z. Fehervari, et al. (2008). "Foxp3+ natural regulatory T cells preferentially form aggregates on dendritic cells in vitro and actively inhibit their maturation." Proc Natl Acad Sci U S A **105**(29): 10113-8.

Ostrand-Rosenberg, S. and P. Sinha (2009). "Myeloid-derived suppressor cells: linking inflammation and cancer." J Immunol **182**(8): 4499-506.

Ouyang, W., S. H. Ranganath, et al. (1998). "Inhibition of Th1 development mediated by GATA-3 through an IL-4-independent mechanism." Immunity **9**(5): 745-55.

Pak, A. S., M. A. Wright, et al. (1995). "Mechanisms of immune suppression in patients with head and neck cancer: presence of CD34(+) cells which suppress immune functions within cancers that secrete granulocyte-macrophage colony-stimulating factor." Clin Cancer Res **1**(1): 95-103.

Palmer, E. (2003). "Negative selection--clearing out the bad apples from the T-cell repertoire." Nat Rev Immunol **3**(5): 383-91.

Palucka, K. and J. Banchereau (2002). "How dendritic cells and microbes interact to elicit or subvert protective immune responses." Curr Opin Immunol **14**(4): 420-31.

Pandiyan, P., L. Zheng, et al. (2007). "CD4+CD25+Foxp3+ regulatory T cells induce cytokine deprivation-mediated apoptosis of effector CD4+ T cells." Nat Immunol **8**(12): 1353-62.

Peranzoni, E., S. Zilio, et al. (2010). "Myeloid-derived suppressor cell heterogeneity and subset definition." Curr Opin Immunol **22**(2): 238-44.

Perez, V. L., L. Van Parijs, et al. (1997). "Induction of peripheral T cell tolerance in vivo requires CTLA-4 engagement." Immunity **6**(4): 411-7.

Perona-Wright, G., S. M. Anderton, et al. (2007). "IL-10 permits transient activation of dendritic cells to tolerize T cells and protect from central nervous system autoimmune disease." Int Immunol **19**(9): 1123-34.

Peterson, P., K. Nagamine, et al. (1998). "APECED: a monogenic autoimmune disease providing new clues to self-tolerance." Immunol Today **19**(9): 384-6.

Priceman, S. J., J. L. Sung, et al. "Targeting distinct tumor-infiltrating myeloid cells by inhibiting CSF-1 receptor: combating tumor evasion of antiangiogenic therapy." Blood **115**(7): 1461-71.

Puccetti, P. and U. Grohmann (2007). "IDO and regulatory T cells: a role for reverse signalling and non-canonical NF-kappaB activation." Nat Rev Immunol **7**(10): 817-23.

Quaratino, S., E. Badami, et al. (2004). "Degenerate self-reactive human T-cell receptor causes spontaneous autoimmune disease in mice." Nat Med **10**(9): 920-6.

Quaratino, S., L. P. Duddy, et al. (2000). "Fully competent dendritic cells as inducers of T cell anergy in autoimmunity." Proc Natl Acad Sci U S A **97**(20): 10911-6.

Quaratino, S., C. J. Thorpe, et al. (1995). "Similar antigenic surfaces, rather than sequence homology, dictate T-cell epitope molecular mimicry." Proc Natl Acad Sci U S A **92**(22): 10398-402.

Reis e Sousa, C. (2004). "Activation of dendritic cells: translating innate into adaptive immunity." Curr Opin Immunol **16**(1): 21-5.

Roberts, C. G. and P. W. Ladenson (2004). "Hypothyroidism." Lancet **363**(9411): 793-803.

Robey, E. and J. P. Allison (1995). "T-cell activation: integration of signals from the antigen receptor and costimulatory molecules." Immunol Today **16**(7): 306-10.

Rodriguez, P. C. and A. C. Ochoa (2008). "Arginine regulation by myeloid derived suppressor cells and tolerance in cancer: mechanisms and therapeutic perspectives." Immunol Rev **222**: 180-91.

Rodriguez, P. C., D. G. Quiceno, et al. (2007). "L-arginine availability regulates T-lymphocyte cell-cycle progression." Blood **109**(4): 1568-73.

Rodriguez, P. C., D. G. Quiceno, et al. (2004). "Arginase I production in the tumor microenvironment by mature myeloid cells inhibits T-cell receptor expression and antigen-specific T-cell responses." Cancer Res **64**(16): 5839-49.

Rodriguez, P. C., A. H. Zea, et al. (2003). "L-arginine consumption by macrophages modulates the expression of CD3 zeta chain in T lymphocytes." J Immunol **171**(3): 1232-9.

Rossi, M. and J. W. Young (2005). "Human dendritic cells: potent antigen-presenting cells at the crossroads of innate and adaptive immunity." J Immunol **175**(3): 1373-81.

Rutella, S., S. Danese, et al. (2006). "Tolerogenic dendritic cells: cytokine modulation comes of age." Blood **108**(5): 1435-40.

Sakaguchi, S., M. Ono, et al. (2006). "Foxp3+ CD25+ CD4+ natural regulatory T cells in dominant self-tolerance and autoimmune disease." Immunol Rev **212**: 8-27.

Sakaguchi, S., N. Sakaguchi, et al. (1995). "Immunologic self-tolerance maintained by activated T cells expressing IL-2 receptor alpha-chains (CD25). Breakdown of a single mechanism of self-tolerance causes various autoimmune diseases." J Immunol **155**(3): 1151-64.

Sakaguchi, S., T. Yamaguchi, et al. (2008). "Regulatory T cells and immune tolerance." Cell **133**(5): 775-87.

Saveanu, L., D. Fruci, et al. (2002). "Beyond the proteasome: trimming, degradation and generation of MHC class I ligands by auxiliary proteases." Mol Immunol **39**(3-4): 203-15.

Scheffold, A., J. Huhn, et al. (2005). "Regulation of CD4+CD25+ regulatory T cell activity: it takes (IL-)two to tango." Eur J Immunol **35**(5): 1336-41.

Schmidt, C. S. and M. F. Mescher (2002). "Peptide antigen priming of naive, but not memory, CD8 T cells requires a third signal that can be provided by IL-12." J Immunol **168**(11): 5521-9.

Schubert, U., L. C. Anton, et al. (2000). "Rapid degradation of a large fraction of newly synthesized proteins by proteasomes." Nature **404**(6779): 770-4.

Schuurhuis, D. H., N. Fu, et al. (2006). "Ins and outs of dendritic cells." Int Arch Allergy Immunol **140**(1): 53-72.

Serafini, P., R. Carbley, et al. (2004). "High-dose granulocyte-macrophage colony-stimulating factor-producing vaccines impair the immune response through the recruitment of myeloid suppressor cells." Cancer Res **64**(17): 6337-43.

Serafini, P., K. Meckel, et al. (2006). "Phosphodiesterase-5 inhibition augments endogenous antitumor immunity by reducing myeloid-derived suppressor cell function." J Exp Med **203**(12): 2691-702.

Serafini, P., S. Mgebroff, et al. (2008). "Myeloid-derived suppressor cells promote cross-tolerance in B-cell lymphoma by expanding regulatory T cells." Cancer Res **68**(13): 5439-49.

Sercarz, E. E. (2000). "Driver clones and determinant spreading." J Autoimmun **14**(4): 275-7.

Shen, L. and K. L. Rock (2006). "Priming of T cells by exogenous antigen cross-presented on MHC class I molecules." Curr Opin Immunol **18**(1): 85-91.

Shimizu, J., S. Yamazaki, et al. (1999). "Induction of tumor immunity by removing CD25+CD4+ T cells: a common basis between tumor immunity and autoimmunity." J Immunol **163**(10): 5211-8.

Shimizu, J., S. Yamazaki, et al. (2002). "Stimulation of CD25(+)CD4(+) regulatory T cells through GITR breaks immunological self-tolerance." Nat Immunol **3**(2): 135-42.

Shojaei, F., X. Wu, et al. (2007). "Bv8 regulates myeloid-cell-dependent tumour angiogenesis." Nature **450**(7171): 825-31.

Sinha, P., V. K. Clements, et al. (2007). "Cross-talk between myeloid-derived suppressor cells and macrophages subverts tumor immunity toward a type 2 response." J Immunol **179**(2): 977-83.

Sinha, P., V. K. Clements, et al. (2007a). "Prostaglandin E2 promotes tumor progression by inducing myeloid-derived suppressor cells." Cancer Res **67**(9): 4507-13.

Sinha, P., V. K. Clements, et al. (2005). "Interleukin-13-regulated M2 macrophages in combination with myeloid suppressor cells block immune surveillance against metastasis." Cancer Res **65**(24): 11743-51.

Sinha, P., V. K. Clements, et al. (2005a). "Reduction of myeloid-derived suppressor cells and induction of M1 macrophages facilitate the rejection of established metastatic disease." J Immunol **174**(2): 636-45.

Sinha, P., C. Okoro, et al. (2008). "Proinflammatory S100 proteins regulate the accumulation of myeloid-derived suppressor cells." J Immunol **181**(7): 4666-75.

Song, X., Y. Krelin, et al. (2005). "CD11b+/Gr-1+ immature myeloid cells mediate suppression of T cells in mice bearing tumors of IL-1beta-secreting cells." J Immunol **175**(12): 8200-8.

Sotomayor, E. M., I. Borrello, et al. (1999). "Conversion of tumor-specific CD4+ T-cell tolerance to T-cell priming through in vivo ligation of CD40." Nat Med **5**(7): 780-7.

Sporri, R. and C. Reis e Sousa (2005). "Inflammatory mediators are insufficient for full dendritic cell activation and promote expansion of CD4+ T cell populations lacking helper function." Nat Immunol **6**(2): 163-70.

Srivastava, M. K., P. Sinha, et al. (2010). "Myeloid-derived suppressor cells inhibit T-cell activation by depleting cystine and cysteine." Cancer Res **70**(1): 68-77.

Stassi, G. and R. De Maria (2002). "Autoimmune thyroid disease: new models of cell death in autoimmunity." Nat Rev Immunol **2**(3): 195-204.

Steinbrink, K., M. Wolfl, et al. (1997). "Induction of tolerance by IL-10-treated dendritic cells." J Immunol **159**(10): 4772-80.

Steinman, L. (2008). "A rush to judgment on Th17." J Exp Med **205**(7): 1517-22.

Steinman, R. M., D. Hawiger, et al. (2003). "Tolerogenic dendritic cells." Annu Rev Immunol **21**: 685-711.

Steinman, R. M. and M. C. Nussenzweig (2002). "Avoiding horror autotoxicus: the importance of dendritic cells in peripheral T cell tolerance." Proc Natl Acad Sci U S A **99**(1): 351-8.

Steptoe, R. J., J. M. Ritchie, et al. (2005). "Autoimmune diabetes is suppressed by transfer of proinsulin-encoding Gr-1+ myeloid progenitor cells that differentiate in vivo into resting dendritic cells." Diabetes **54**(2): 434-42.

Strawbridge, A. B. and J. S. Blum (2007). "Autophagy in MHC class II antigen processing." Curr Opin Immunol **19**(1): 87-92.

Strober, S. (1984). "Natural suppressor (NS) cells, neonatal tolerance, and total lymphoid irradiation: exploring obscure relationships." Annu Rev Immunol **2**: 219-37.

Su, M. A. and M. S. Anderson (2004). "Aire: an update." Curr Opin Immunol **16**(6): 746-52.

Suri-Payer, E., A. Z. Amar, et al. (1998). "CD4+CD25+ T cells inhibit both the induction and effector function of autoreactive T cells and represent a unique lineage of immunoregulatory cells." J Immunol **160**(3): 1212-8.

Suzuki, E., V. Kapoor, et al. (2005). "Gemcitabine selectively eliminates splenic Gr-1+/CD11b+ myeloid suppressor cells in tumor-bearing animals and enhances antitumor immune activity." Clin Cancer Res **11**(18): 6713-21.

Szabo, S. J., N. G. Jacobson, et al. (1995). "Developmental commitment to the Th2 lineage by extinction of IL-12 signaling." Immunity **2**(6): 665-75.

Takahashi, T., T. Tagami, et al. (2000). "Immunologic self-tolerance maintained by CD25(+)CD4(+) regulatory T cells constitutively expressing cytotoxic T lymphocyte-associated antigen 4." J Exp Med **192**(2): 303-10.

Takeda, K., T. Kaisho, et al. (2003). "Toll-like receptors." Annu Rev Immunol **21**: 335-76.

Talmadge, J. E., K. C. Hood, et al. (2007). "Chemoprevention by cyclooxygenase-2 inhibition reduces immature myeloid suppressor cell expansion." Int Immunopharmacol **7**(2): 140-51.

Tarbell, K. V., S. Yamazaki, et al. (2004). "CD25+ CD4+ T cells, expanded with dendritic cells presenting a single autoantigenic peptide, suppress autoimmune diabetes." J Exp Med **199**(11): 1467-77.

Tato, C. M. and D. J. Cua (2008). "Alternative lifestyles of T cells." Nat Immunol **9**(12): 1323-5.

Terabe, M., S. Matsui, et al. (2003). "Transforming growth factor-beta production and myeloid cells are an effector mechanism through which CD1d-restricted T cells block cytotoxic T lymphocyte-mediated tumor immunosurveillance: abrogation prevents tumor recurrence." J Exp Med **198**(11): 1741-52.

Terabe, M., J. Swann, et al. (2005). "A nonclassical non-Valpha14Jalpha18 CD1d-restricted (type II) NKT cell is sufficient for down-regulation of tumor immunosurveillance." J Exp Med **202**(12): 1627-33.

Terme, M., N. Chaput, et al. (2008). "Regulatory T cells control dendritic cell/NK cell cross-talk in lymph nodes at the steady state by inhibiting CD4+ self-reactive T cells." J Immunol **180**(7): 4679-86.

Thornton, A. M. and E. M. Shevach (1998). "CD4+CD25+ immunoregulatory T cells suppress polyclonal T cell activation in vitro by inhibiting interleukin 2 production." J Exp Med **188**(2): 287-96.

Touret, N., P. Paroutis, et al. (2005). "Quantitative and dynamic assessment of the contribution of the ER to phagosome formation." Cell **123**(1): 157-70.

Tripp, C. S., S. F. Wolf, et al. (1993). "Interleukin 12 and tumor necrosis factor alpha are costimulators of interferon gamma production by natural killer cells in severe combined immunodeficiency mice with listeriosis, and interleukin 10 is a physiologic antagonist." Proc Natl Acad Sci U S A **90**(8): 3725-9.

Tu, S., G. Bhagat, et al. (2008). "Overexpression of interleukin-1beta induces gastric inflammation and cancer and mobilizes myeloid-derived suppressor cells in mice." Cancer Cell **14**(5): 408-19.

Ueda, H., J. M. Howson, et al. (2003). "Association of the T-cell regulatory gene CTLA4 with susceptibility to autoimmune disease." Nature **423**(6939): 506-11.

Umemura, N., M. Saio, et al. (2008). "Tumor-infiltrating myeloid-derived suppressor cells are pleiotropic-inflamed monocytes/macrophages that bear M1- and M2-type characteristics." J Leukoc Biol **83**(5): 1136-44.

van den Boorn, J. G., I. C. Le Poole, et al. (2006). "T-cell avidity and tuning: the flexible connection between tolerance and autoimmunity." Int Rev Immunol **25**(3-4): 235-58.

van der Kleij, D., E. Latz, et al. (2002). "A novel host-parasite lipid cross-talk. Schistosomal lyso-phosphatidylserine activates toll-like receptor 2 and affects immune polarization." J Biol Chem **277**(50): 48122-9.

van der Vliet, H. J., B. M. von Blomberg, et al. (2001). "Circulating V(alpha24+) Vbeta11+ NKT cell numbers are decreased in a wide variety of diseases that are characterized by autoreactive tissue damage." Clin Immunol **100**(2): 144-8.

Vanderlugt, C. L. and S. D. Miller (2002). "Epitope spreading in immune-mediated diseases: implications for immunotherapy." Nat Rev Immunol **2**(2): 85-95.

Veldhoen, M., C. Uyttenhove, et al. (2008). "Transforming growth factor-beta 'reprograms' the differentiation of T helper 2 cells and promotes an interleukin 9-producing subset." Nat Immunol **9**(12): 1341-6.

Venanzi, E. S., D. H. Gray, et al. (2007). "Lymphotoxin pathway and Aire influences on thymic medullary epithelial cells are unconnected." J Immunol **179**(9): 5693-700.

Vertuani, S., A. Sette, et al. (2004). "Improved immunogenicity of an immunodominant epitope of the HER-2/neu protooncogene by alterations of MHC contact residues." J Immunol **172**(6): 3501-8.

von Boehmer, H., I. Aifantis, et al. (2003). "Thymic selection revisited: how essential is it?" Immunol Rev **191**: 62-78.

Walker, L. S. and A. K. Abbas (2002). "The enemy within: keeping self-reactive T cells at bay in the periphery." Nat Rev Immunol **2**(1): 11-9.

Wan, Y., Y. Wu, et al. (2005). "Cross-presentation of phage particle antigen in MHC class II and endoplasmic reticulum marker-positive compartments." Eur J Immunol **35**(7): 2041-50.

Watanabe, S., K. Deguchi, et al. (2008). "Tumor-induced CD11b+Gr-1+ myeloid cells suppress T cell sensitization in tumor-draining lymph nodes." J Immunol **181**(5): 3291-300.

Watts, C. (2004). "The exogenous pathway for antigen presentation on major histocompatibility complex class II and CD1 molecules." Nat Immunol **5**(7): 685-92.

Yamazaki, S., T. Iyoda, et al. (2003). "Direct expansion of functional CD25+ CD4+ regulatory T cells by antigen-processing dendritic cells." J Exp Med **198**(2): 235-47.

Yamazaki, S., M. Patel, et al. (2006). "Effective expansion of alloantigen-specific Foxp3+ CD25+ CD4+ regulatory T cells by dendritic cells during the mixed leukocyte reaction." Proc Natl Acad Sci U S A **103**(8): 2758-63.

Yang, H. and K. J. Tracey (2009). "Targeting HMGB1 in inflammation." Biochim Biophys Acta **1799**(1-2): 149-56.

Yang, L., L. M. DeBusk, et al. (2004). "Expansion of myeloid immune suppressor Gr+CD11b+ cells in tumor-bearing host directly promotes tumor angiogenesis." Cancer Cell **6**(4): 409-21.

Yang, R., Z. Cai, et al. (2006). "CD80 in immune suppression by mouse ovarian carcinoma-associated Gr-1+CD11b+ myeloid cells." Cancer Res **66**(13): 6807-15.

Yee, C., J. A. Thompson, et al. (2000). "Melanocyte destruction after antigen-specific immunotherapy of melanoma: direct evidence of t cell-mediated vitiligo." J Exp Med **192**(11): 1637-44.

Yeramian, A., L. Martin, et al. (2006). "Arginine transport via cationic amino acid transporter 2 plays a critical regulatory role in classical or alternative activation of macrophages." J Immunol **176**(10): 5918-24.

Yewdell, J. W. and C. V. Nicchitta (2006). "The DRiP hypothesis decennial: support, controversy, refinement and extension." Trends Immunol **27**(8): 368-73.

Youn, J. I., S. Nagaraj, et al. (2008). "Subsets of myeloid-derived suppressor cells in tumor-bearing mice." J Immunol **181**(8): 5791-802.

Zhang, J., X. Xu, et al. (2004). "Activation-induced cell death in T cells and autoimmunity." Cell Mol Immunol **1**(3): 186-92.

Zhang, D., W. Yang, et al. (2007). "New differentiation pathway for double-negative regulatory T cells that regulates the magnitude of immune responses." Blood **109**(9): 4071-9.

Zhao, J., X. Yang, et al. (2009). "Do adaptive immune cells suppress or activate innate immunity?" Trends Immunol **30**(1): 8-12.

Zheng, S. G., J. Wang, et al. (2007). "IL-2 is essential for TGF-beta to convert naive CD4+CD25- cells to CD25+Foxp3+ regulatory T cells and for expansion of these cells." J Immunol **178**(4): 2018-27.

Zhou, L., J. E. Lopes, et al. (2008). "TGF-beta-induced Foxp3 inhibits T(H)17 cell differentiation by antagonizing RORgammat function." Nature **453**(7192): 236-40.

Zhu, B., Y. Bando, et al. (2007a). "CD11b+Ly-6C(hi) suppressive monocytes in experimental autoimmune encephalomyelitis." J Immunol **179**(8): 5228-37.

Zhu, J. and W. E. Paul (2008). "CD4 T cells: fates, functions, and faults." Blood **112**(5): 1557-69.

Zhu, M., R. K. Chin, et al. (2007). "Lymphotoxin beta receptor is required for the migration and selection of autoreactive T cells in thymic medulla." J Immunol **179**(12): 8069-75.

Zuniga-Pflucker, J. C. (2004). "T-cell development made simple." Nat Rev Immunol **4**(1): 67-72.

Where stated, the following theses have been used:

- Olivier CEXUS (2010) **– "Immunological mechanisms controlling Chronic Inflammatory Diseases",** University of Southampton, School of Medicine – PhD thesis
- Ester Badami (2007) – **"Mechanisms of activation and regulation in Autoimmunity"**, University of Southampton, School of Medicine – PhD thesis